Development of geochemical sensors for continuous, on-line monitoring and modelling of coastal groundwater aquifers

Thorn, Paul

Publication date:
2010

Document Version
Early version, also known as pre-print

Development of geochemical sensors for continuous, on-line monitoring and modelling of coastal groundwater aquifers

Ph.D. Thesis by:

Paul Thorn

Department of Environmental, Social and Spatial Changes,
&
Department of Science, Systems and Models
Roskilde University, Denmark

June 2010

Layout: Ritta Juel Bitsch
Front page: Paul Thorn and Ritta Juel Bitsch
Print: Prinfo Paritas Digital Service

Contents

Abstract

Continuous, on-line monitoring of groundwater salinity can be incorporated into real-time well-field management strategies in order maximize sustainable use of our near-coastal groundwater resources, while protecting the groundwater quality. This project looked to develop and test sensors for chloride, sodium and calcium for the continuous monitoring of groundwater salinity. The testing of the sensors was conducted both in the laboratory and in actual application in two monitoring wells, one in Greve, Denmark and the other in Wickford, Rhode Island, USA. In addition, a geological analysis and groundwater model of seawater intrusion and groundwater salinity for the Danish municipality of Greve, where there has been historically problems with groundwater salinity, was conducted with respect the integration of the sensor data to the groundwater model.

The results from the chloride sensor showed very good possibility for continual use. Laboratory tests showed very consistent response to changing chloride concentrations over longer periods. The signal was seen to be very stable, with regular drift. At the field test conducted in Wickford, where groundwater salinities changed diurnally, the chloride sensor successfully registered the changes at varying concentrations, with a low error of under 5% from the conductivity measurements. In fact, the chloride measurements responded to changes even at low concentrations where the conductivity measurements no longer showed changes in groundwater salinity. The chloride sensors were very inexpensive to produce, and had a long life-span. However, the test at the monitoring well in Greve showed that fouling of the sensor surface can degrade the quality of the signal, and affect the life-span of the sensor. This is not a factor in all cases, as seen at Wickford, where, fouling was not an issue.

The results of the sodium and calcium sensors were mixed. The development of a solid-state sodium sensor, both with the ionophore directly attached to a gold surface, and mixed into a PVC ion sensing film, showed good response to changing sodium concentrations in the laboratory. However, the life-span of the sensors was seen to be limited, where both in the laboratory and at the Greve and Rhode Island monitoring well sites, the sensors became unresponsive to changes in sodium concentrations after just a couple of days. Like the chloride sensors, the sodium sensors were also sensitive to fouling in the Greve monitoring well. The development of a calcium sensor, where the ionophore was polymerized on the

gold surface was unsuccessful. However, a calcium ionophore, when mixed in a PVC film showed a decent response, but only limited testing in the laboratory was conducted, and no testing was done in the field. Because of the short life-span of the sodium sensors and limited testing of the calcium sensor, more development and testing is required before they can be used for continuous monitoring.

The near-coastal zone in the municipality of Greve was used as a pilot project to determine how the developed sensors could be used in the groundwater management. This included creating an accurate geological and hydrogeological model for the area. The first step to fulfil this task was to produce an accurate geological map of the area using the high concentration of borehole data in Greve and the surrounding area. Thereafter, an evaluation of the source of salinity observed in the groundwater in Greve was conducted using bulk water samples taken at various intervals over the last 30-40 years. The evaluation showed that the salinity from northern two-thirds of the municipality was via diffusion from ancient pore waters in the chalk below the aquifer. In this case, thus the salinities are stable, restricted to the slow rate of diffusion from below. The southern third, however, showed a distinct signal for seawater intrusion from the Baltic Sea, likely through a sand and gravel layer which connects the sea to the primary groundwater aquifer in this region. However, the data also showed that over the last 10 years, salinities have not increased, and seawater intrusion has stabilized. The system was modelled with the groundwater transport and flow model FEFLOW. The model showed that with the reduction in groundwater abstraction over the last 15 years, the seawater intrusion into the aquifer has weakened, with groundwater salinities in the area stabilizing out, confirming the results from the geochemical analysis. From these results it was concluded that the sensors, though not used directly in an active well-field management system, could be used as a warning system in the southern third of the municipality, should the seawater intrusion begin again due to either increased abstraction in the immediate or upland area, or a reduction in the recharge to the aquifer.

Resumé

Konstant online monitering af salt i grundvandet kan inkorporeres i et kildepladsstyringssystem for at maksimere den bæredygtige udnyttelse af vores kystnære grundvandsressourcer, samt være med til at beskytte vandkvaliteten. I dette projekt er nye sensorer til klorid, natrium og kalcium blevet udviklet og testet til konstant brug i monitering af grundvandets saltindhold. Testning af sensorer er forgået både i laboratoriet og i to monitoreringsboringer, en i Greve, Danmark og den anden i Wickford, Rhode Island, USA. Moniteringsboringen i Greve, Danmark, som har et relativt højt saltindhold, blev brugt som en lokalitet hvor integrering af data fra sensorer i en hydrogeologisk model kunne forgå. Derfor var der også lavet en geologisk og hydrogeologisk, samt med grundvandsmodellering af Greve i projektet.

Resultaterne fra klorid sensorerne viste meget gode resultater med hensyn til konstant brug. Testning i laboratoriet viste meget stabil respons til skiftende klorid koncentrationer over længere perioder. Signalet var meget stabilt ved jævn drift. I Wickford testen, hvor grundvandets saltindhold har ændret sig to gange om dagen på grund af tidevand, kunne klorid sensorer registrere ændring i klorid med en fejl på mindre end 5 %. Især ved de lave koncentrationer var klorid sensorer meget følsomme over for klorid og kunne stadig måle ændringer i koncentrationer, hvor levningsevne sonde ikke længere kunne registrere det. Kloridsensorer var meget billige og nemme at producere, og havde en meget lang levetid. Men resultaterne fra Greve moniteringsboringer har vist, at klorid sensorer er sårbar overfor film (okker i dette tilfælde), der kan gro på sensoroverfladen og forstyrre signalet. Men det er ikke altid et problem, som testen i Wickford har vist.

Resultaterne fra natrium og kalcium sensorer vidste blandende resultater. To metoder blev brugt til at lave natrium sensorer: en hvor en ionofor specifik for natrium var pålagt direkte på en guldoverflade, og en hvor ionoforen var sat i en PVC film, som blev lagt på en guldoverflade. Begge metoder viste god respons til ændring i natriumkoncentrationer i laboratoriet. Men sensorernes levetid var meget lavt, hvor responsen forsvandt efter blot et par dage. Ligesom kloridsensorer var natriumsensorer også sårbare overfor okker. I forhold til kalciumsensorer var det ikke succesfuldt at pålægge ionoforen direkte på en guldoverflade, hvor der derefter var en respons til kalcium. Men der var delvis succes med en kalciumsensor, da kalcium ionoforen var inkorporeret i en PVC film, og lagt på en guldoverflade.

Men den kalcium sensor var ikke testet i moniteringsboringer i feltet. På grund af den korte levetid af natriumsensorer og manglende testning af kalciumsensor, er mere udvikling og testning af både sensorer nødvendigt, før de kan bruges til konstant monitering.

Det kystnære område i Greve blev brugt som et pilotprojekt, for at se hvordan sensorerne kunne bruges i grundvandsforvaltning. Dette indebærer udvikling af en præcis geologisk- og grundvandmodel for området. For at udføre dette, blev der produceret et detaljeret geologiske kort udfra fortolkning af de flere hundrede borehul logs i området. Dernæst blev der produceret en detaljeret undersøgelse af grundvandskemien fra grundvandskvalitetsprøver, som er blevet taget over det sidste 30-40 år. Denne undersøgelse viste, at det høje saltindhold i grundvandet i den nordlige del af Greve kommer fra diffusion op fra porevandet i skrivekridt. Men i den sydlige del af Greve, var det høje saltindhold fra saltvandsindtrængning i grundvandsmagasinet fra Køge Bugt, som kunne infiltrere ned til magasinet gennem et lokalt lag af smeltevands- sand og grus. Men prøverne viser, at saltindhold ikke er steget i de sidste 10 år, og at saltvandsindtrængning er stabiliseret. En grundvandsmodel til at modellere saltvandsindtrængning i Greve blev produceret med software FEFLOW. Modellen konfirmerer resultaterne fra grundvandsprøver, og viser også at saltvandsindtrængning er stabiliseret på grund af kraftig reducering af grundvandsindvinding over det sidste 15 år. Modellen også viser, at under nuværende indvinding er der meget lille fare for videre saltvandsindtrængning i området. Resultaterne fra modellerne viser, at i dette tilfælde er det ikke nødvendigt at bruge sensorerne i et kildepladsstyringssystem. Til gengæld kunne sensorer bruges i et alarmsystem i den sydlige del af Greve. Det kan give tidlig varsel af ny saltvandsindtrængning på grund af højere indvinding i enten de nuværende kildeplader eller i oplandet, eller mindre gendannelse af vandet til grundvandsmagasinet.

Acknowledgements

During the course of my Ph.d. studies, and even prior to even the start, there have been a large number of people who have helped me tremendously, both personally and professionally. Without this support, completion of my project would not have been possible.

I would like to begin by acknowledging the funding source – without this funding there simply would not have a Ph.d. project to begin with. The project was part of a larger project on "Well Field Optimisation", funded by the Danish Strategic Research Council, Programme Commission on Energy and Environment (grant nr. 5798000416635). My thanks go out to Henrik Madsen and the rest of my "Well Field" colleagues, who listened to my presentations and offered me excellent feed-back.

On the professional side, I need to start out by especially thanking my two advisors, John Mortensen and Niels Schrøder. John's teaching and guidance on electrochemistry, and Niels' experience and advice on groundwater were essential for completion of this project. Both advisers were always available when needed (with a smile none the less), no matter how busy they were. Appreciation also goes out to my ENSPAC Ph.d.colleagues, who provided me with excellent feedback and advice on my project when I just needed someone to discuss both the successes and failures in my research. This is also not to mention all the beers that we have shared along the way. They say that a Ph.d. student is often working in complete isolation from everyone else. With the support from both my advisors and Ph.d. colleagues, I can say that I never was working alone. Thanks also go out to Rita, Jacob, Eva and Annette in NSM for their help with my chemical preparations and analysis, as well as Ritta in ENSPAC for her help with numerous figures, well-logs and publication of this dissertation.

I am indebted to Prof. Dan Urish, who made the Wickford, Rhode Island monitoring well test happen. His help and advice in the location and establishment of the monitoring well, downloading my data when I could not, and discussing the results was essential in the successful completion of the test. You and your wife also made my visits to Wickford not only comfortable, but an outright pleasure – Dan, your hospitality is second to none. Thanks also goes out to your neighbor, Bruce, for use of his electricity to run my equipment for free.

I would like to thank Greve Water Works for providing me with free and easy access to all of their groundwater and well data as well as access to the Greve monitoring well in this study. Jakob Jakobsen and Henrik Lydersen were extremely helpful whenever I called and asked for access or assistance.

Finally, on the personal side, I would like to thank all of my friends, who have been there for me during the process. Particularly Thomas and Greg, who have always offered to help me out whenever I need it. Thanks to all of my family for their involvement and support from day 1. I owe my two boys, Benjamin and Bjørn, so much for their patience putting up with my long nights and weekends of working at home and in Roskilde – I will make it up to you! Last but not least, I owe more than thanks to my wife, Lotte. You truly know how to help me out the most – patiently listening, offering advice, correcting my mistakes, and most importantly feeding me with the world's best food. Thanks honey, and I look forward to returning the favor to you.

Introduction to the Ph.d. Project

1. PROBLEM FIELD

The steadily increasing pressure on freshwater resources and potential future climate change has put an increased focus on water resource management. Over-exploitation and inefficient management of groundwater resources has led to a number of water quality and related health problems worldwide. With a limited and shrinking supply of unpolluted groundwater resources, there is a growing need to develop techniques to maximize the available groundwater, while protecting it from contamination and preventing over-exploitation.

Seawater intrusion is a pressing threat to groundwater supplies in coastal regions – particularly those where there are not adequate freshwater resources to meet demand. In areas where saltwater intrusion has occurred, technical solutions, such as freshwater injection, have been employed to prevent the intrusion (Barlow 2003). Alternatively, the wells have been abandoned, forcing an alternative source of water such as surface water or even desalination plants. These solutions are often expensive and cannot be employed in every situation. In other cases, the fear of saltwater intrusion has led to groundwater abstraction being moved away from the coastal areas further inland. The movement of abstraction sites further inland has its problems, as it can result in a reduction of base flow to streams and wetlands, significantly affecting the fresh-water ecosystems.

Improvements in groundwater modelling technologies have allowed us to, at least in part, begin to tackle the problem of saltwater intrusion. However, many parameters in these models, such as recharge, are not constant and can vary both seasonally and annually. This leads to an uncertainty within these models, and often will force water managers to err on the side of caution and not utilize the full potential of the groundwater resources. If given the ability to collect real-time, in-situ monitoring data, a warning and response system could be employed to coastal groundwater abstraction sites to safely utilize the full potential – the benefit being an increased yield in fresh water.

The development of ion selective electrodes (ISE) could be used to fill this gap. Currently, ISEs are being used in industrial applications and in waste water monitoring. However, their application for groundwater quality monitoring has been limited. This is likely due to the high costs associated with the electrodes, as well as the frequent need for calibration and the physical durability of the electrodes. Overcoming these issues and employing ISEs in the well-field management framework could provide a higher sustainable groundwater yield in coastal regions.

The essence of this project is to look at the possibilities of using ISE's in active management of near-coastal well-fields, where seawater intrusion into the aquifer is a threat. This will consist of combining real-time, continuous data from the ISE's with a hydrogeological model in order to provide the best prediction of seawater intrusion under different groundwater abstraction rates. The real-time data can help to refine and make the predictive models more accurate, allowing a better protection for the well-field against seawater intrusion. The project is divided into two separate fields: the development and testing of sensors which can be used for continuous monitoring of groundwater salinity, and the hydrogeological modelling of coastal groundwater aquifers and seawater intrusion.

The Ph.d. project is part of a larger research project entitled "Integration of modelling, monitoring and optimisation technologies for real-time management of groundwater resources", partly funded by the Danish Strategic Research Council, under the program commission on energy and environment. The larger research group comprises of participants from six different institutions, including DHI, Technical University of Denmark, Copenhagen Energy A/S, Alectia A/S, Grundfos A/S and, of course, Roskilde University. The objectives of the overall project is to introduce mathematical modelling of well fields and combine with information from sensor networks within a management system to optimise pump scheduling and water withdrawal. This includes such parameters as protection of water quality and energy optimization in the well-fields. The specific role of this Ph.d. project is to develop groundwater sensors which can be used to continuously supply data that can be incorporated into the hydrogeological models for the well-fields in order to observe and protect the water quality.

This chapter provides the background information for the project as a whole. It begins with a description of the current management practices with respect to seawater intrusion. Then a description of the current available technologies and

use of ion selective electrodes will be provided. The chapter continues with a detailed description of the Ph.D. project as a whole, its objectives, execution and major obstacles encountered along the way. The chapter concludes with a summary description of the remaining chapters in the thesis.

2. MANAGEMENT RESPONSE TO SALTWATER INTRUSION

As the problem of saltwater intrusion into coastal aquifers is not new, the management responses have been numerous and varied. In a general sense, these responses can be put into four categories:

- Relocation of pumping wells,
- Actions over the demand (reduce pumping),
- Actions over recharge (artificial recharge), and
- Engineering solutions (seawater intrusion barriers).

The first two categories are generally passive management practices, where as the latter two categories include more proactive responses. In addition to these four categories, there has recently been a number of modelling efforts attempting optimize well location and pumping rates in order to reduce the risk of saltwater intrusion. This section will provide an overview of the management practices used to prevent and/or respond to saltwater intrusion into groundwater aquifers.

2.1 Passive Management Practices

Probably the most traditional management practice to deal with saltwater intrusion in the past has been to simply move the groundwater abstraction wells further inland, away from the coast (Barlow 2003). This has been the case in Denmark, where in general the groundwater wells are shut down when the chloride concentration reaches between 300 – 500 mg/l. This practice, of course, can only be done in regions where there is available groundwater supplies further inland (Barlow 2003). This is not possible in many regions, where the inland aquifer supplies are already fully exploited or do not exist due to the local geology, or on small islands or peninsulas where there simply is no inland area. In addition, moving the wells further inland can have a negative impact on the surface streams and wetlands

and subsequently the ecology, such has been observed in Denmark (Thorn and Conallin 2007), and can have implications in meeting the conditions of the EU Water Framework Directive.

A second passive management technique is to simply reduce the pumping rates (Barlow 2003). This, in theory, will reduce the pressure gradient between the well and the saltwater water source, with the saltwater interface moving away from the well. This management technique, however, results in a loss of production, which will have to be made up for elsewhere. In addition, when saltwater intrusion occurs, it is often a result of long-term negative mass-balance within the aquifer, and recovery from saltwater to fresh water can be a very slow process – even several years (Abarca et al. 2006).

When there are no other sources available, the third passive management practice is simply desalination of groundwater. This is, for example, currently being applied in Georgia, where brackish water of up to 2000 mg/l of salt is being desalinated (Barlow 2003). Improvements in desalination technologies and costs have made this option more attractive to many water stressed coastal areas. Current desalination costs range from approximately US$ 0.75 – 1.5 US$/m3 for pure seawater, and go even down to US$ 0.40 for brackish groundwater (Dale 2004, Dawoud 2005, Dreizin 2006). The decrease in costs has enticed some countries, such as Israel, to look more closely at this option (Dreizin 2006). It should be noted, however, that the desalination process is energy intensive, and costs are subject to swings in energy prices.

2.2 Proactive Management Techniques

Artificial recharge is a common proactive management technique. Also termed "aquifer storage and recovery", this technique is simply to inject, or artificially infiltrate, fresh water into an aquifer, store it for a period of time, and then abstracted out again. The injected water creates a zone around the well that pushes back the saltwater, and creating a positive mass balance. This technique is being used in Florida, New Jersey, Virginia and California (Barlow 2003, Reichard and Johnson 2005). The advantages of this technique is that it allows water to be stored safely, there is very little evapo-transpiration, the earth acts as a natural purifying filter, and it is inexpensive (Abarca et al. 2007). The disadvantages include: 1) the

need for a clean surface water supply to inject; 2) potential impacts on surface water systems, and 3) inefficient recovery – about a maximum of 70% (Abarca et al. 2006, Barlow 2003). However, with regard inefficiencies during recovery, the net loss is offset by the net gain from protection of further inland water resources (Abarca et al. 2006).

Intrusion barriers are a second proactive management technique. Here, surface water is injected into the aquifer between the source of the saline groundwater and the production wells (Fig. 1). This creates a positive hydraulic gradient, locally reversing the direction of flow and preventing saltwater from reaching the production wells (Barlow 2003). A series of injection wells can provide an effective "wall" against saltwater intrusion. This differs from artificial recharge, in that the water injected is not directly intended to be taken out. The injected water rather acts as a physical barrier, where as the water withdrawn is the natural recharge.

Pumping of brackish water is a final proactive management technique. Here, pumping of brackish groundwater will control the interface between the fresh and saline bodies (Sherif and Hamza 2001). This technique essentially creates a sink between the source of the saltwater and the production wells, preventing the saltwater from intruding further towards the production wells. In addition, the pumped brackish water, if held to a certain level, could also be used for other purposes, such as desalination (brackish groundwater has a lower desalination cost than water taken directly from the sea).

2.3 Well-field Optimization Modelling

By far, the most popular, and common approach for the prevention of saltwater intrusion, is management using well-field optimization models. In the most basic sense, these models look for the optimal well placement and pumping rates in order to maximize yield, while preventing saltwater intrusion into the field. Recent efforts have included (but not limited to) optimization of pumping rates using a response matrix approach (Zhou et al. 2003), optimization of both well placement and pumping rates (Park and Aral 2004), and optimizing flow rates using genetic algorithms (Katsifarakis and Petala 2006, Mantoglou et al. 2004). Studies have also combined an analysis of the optimization of both pumping rates and proactive management techniques including both artificial recharge and

intrusion barriers (Abarca et al. 2006, Reichard and Johnson 2005). One of the benefits of the modelling efforts is the ability for the modellers to assess which parameters affect the system the most. In general, the different studies found that the saltwater interface was most sensitive to recharge rates followed by pumping rates, sea level and water body salinity (Mantoglou 2003, Shoemaker 2004, Werner and Gallagher 2006).

The primary drawback with the models is that they represent simplifications of complex systems. The most common simplifications within the models deal with the interaction between salt and fresh water. Most models use the "sharp face" approximation, which assumes there is no mixing between the salt and fresh-water, and the Ghyben-Herzberg density relation, which assumes homogeneous, unconfined aquifers (Mantoglou 2003). Neither case is completely true, as there is generally a transition (mixing) zone between the fresh and saltwater bodies (Barlow 2003), and aquifers are rarely homogeneous and often not unconfined. In spite of these drawbacks, modelling can be very successful in providing managers with guidelines as to where and what to withdraw as well as most sensitive parameters affecting the state of the system.

2.4 Monitoring

The continual monitoring of water quality in coastal aquifers remains an essential part of any well management scheme employed. The coastal groundwater systems are rarely in equilibrium, and thus monitoring, which allows for model adjustments, is necessary (Werner and Gallagher 2006). Monitoring and control is also needed when employing proactive management schemes such as aquifer storage and recovery, where the salinity content of the water must be closely monitored due to the mixing of the injected water with the saline waters it is being injected into (Barlow 2003). Furthermore, Barlow (2003) points out that observation wells and monitoring networks are essential to keeping track of the location and movement saline water in coastal areas and for improving the understanding of the controls on saltwater occurrences and intrusion. The sensors being developed in this project can be a vital part of the monitoring for seawater intrusion.

2.5 Integration of sensors into real-time well-field management

The sensors developed in this project, by providing continuous, real-time data, can be a powerful tool in the management near-coastal groundwater resources. The information from the sensors can provide an early-warning for the encroachment of saltwater. When coupled to a groundwater abstraction site management system, it provides the water manager with the tools to make quick decisions and safely abstract the maximum amount of groundwater while maintaining the water quality.

Figure 1 illustrates an idealized model of a well-field management system. Here, you have a groundwater model determining the optimal operation of the well field. During operation, information on the well field, including water level, water quality, flow, power consumption, pressure, etc., is collected. The managers then process this information and make informed decisions to respond to changes within the system to maintain the optimal operation of the well field. Figure 2 illustrates a theoretical response to encroachment of saline waters into a well field.

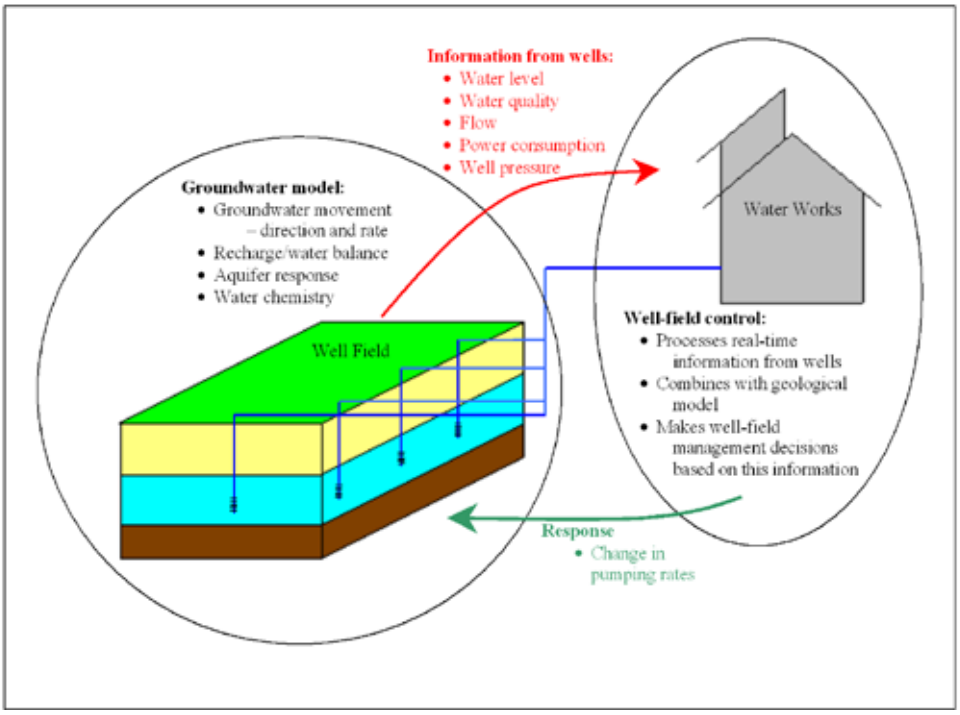

Figure 1. *Idealized model of a well-field management system.*

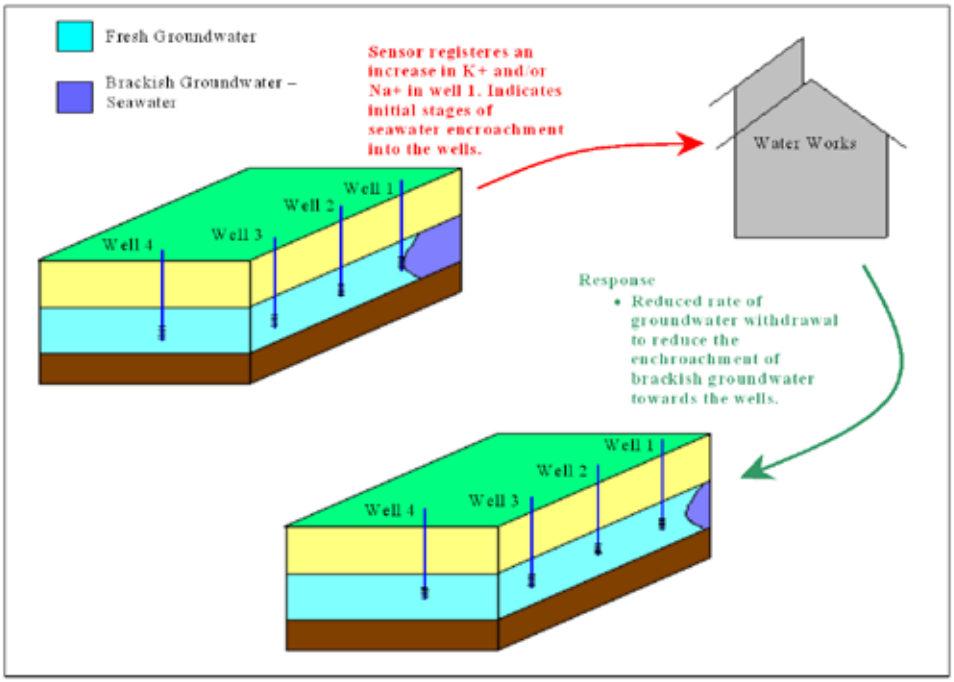

Figure 2. *Illustration of the sensor recognition/response process. The geochemical sensor in well one registers the initial encroachment of seawater into the well field. Using a response model developed for the well-field, a proper response is determined, and pumping rates are adjusted. The saltwater/fresh water interface subsequently moves away from the water wells.*

The true power of the continuous data provided by the sensors comes out when it is combined with well-field optimization techniques. Whenever an optimization model is developed for a well-field, it is inherently a simplification and has a degree of uncertainty (Dreizin 2006). However, with the potential of input of geochemical data, any changes not predicted by the model can be registered, allowing the model to be adjusted to the new data. Thus, a new, more effective optimization model can be applied to the well-field. For models optimizing coastal groundwater abstraction while protecting against saltwater intrusion, the refined models will enable managers to quickly and effectively respond to potential saline intrusion due to, for example, changes in precipitation.

In other proactive management techniques such as intrusion barriers and artificial storage and recovery, the sensors can also play an important role. In the case of intrusion barriers, the sensors could be used to confirm the effectiveness of the

barriers, and provide an early warning on the potential failure. In this way the sensors can be used to help optimize the system, signalling when water needs to be injected into the barrier, or when it is o.k., ultimately reducing the amount of water that will need to be injected to maintain the barrier. The sensors can also provide a benefit for aquifer storage and recovery systems. In this case, if there is a difference in the water quality between the infiltrated (clean) water and the aquifer (saline), the sensors can provide an immediate assessment as to when the infiltrated water has been used up, and the saline aquifer water is now approaching the well. This provides a safety feature, which will allow for the maximum recovery while still protecting the water quality. In both of these cases, the more water that needs to be injected into the aquifer, the higher costs will be for operating the system. The employment of sensors can reduce the amount of water infiltrated, while maintaining the safety and water quality, and thus ultimately result in lower operational costs.

3. CURRENT AVAILABLE GROUNDWATER SENSOR TECHNOLOGY

The technology of ion-selective electrodes (ISEs) is well known and has been available for some time. There have been a large number of ISE's developed used specifically for industrial purposes; however, use specifically for groundwater monitoring has been limited. There have been a number of sensors developed to monitor for specific pollutants within the groundwater, including heavy metals (Tercier-Waeber et al. 1999, Feeney and Kounaves 2002, Zou et al. 2008), arsenic (Chaniotakis and Sofikiti 2008), volatile organic chemicals (Groves et al. 2006, Morris et al. 2002), and per chlorate (Okeke et al. 2007, Parra et al. 2009). However, there have been few developed for the specific purpose of saltwater intrusion. One study developed a full array of non-specific chemical sensors, which included the determination of Ca2+, Mg2+, Na+, Cl-, and SO42-, which could be used to detect saltwater (Rudnitskaya et al. 2001). It remains unclear how successful the sensor array was, as the array was never tested in saline groundwater. A second, recent study used an array of 16 modified commercially available ion-selective electrodes in one tool that can be used for one-time measurements or for on-line measurements (Sotiropoulos et al. 2007). This array was successfully applied in mapping saltwater intrusion at a site in Greece, but there has not been an assessment on the stability and durability for constant, on-line measurements.

ISEs are widely used in industrial applications and readily available commercially. These sensors are available for a wide range of both cations and anions, including Ca2+, Mg2+, Na+, Cl-. However application in groundwater monitoring has been limited. This is likely due to a number of drawbacks with the sensors. First of all, the cost of the sensors – it is estimated that a two channel sensor will cost over US$7000 in initial investment, and a yearly operational cost of approximately US$1000 (Winkler et al. 2004). A quick search on the individual costs for an individual sensor shows a wide range, from US$100-1000, depending on the ion and the company. The second drawback is the calibration of the sensors. This needs to be done each time the sensors are used. For continuous measurement, the sensor membrane "ages" during use resulting in a drifting of signal. Subsequently, calibration has to be conducted periodically. The third (potential) drawback is the durability of the electrodes. There have been very few tests on ISEs conducted on the precision, stability and durability for in-situ, continuous groundwater monitoring. One test on chlorine, calcium, sodium and potassium sensors was conducted for in-situ measurements, where they generally showed good precision of between 8 and 10% (Timms et al. 2004). However, this study consisted of only one-time sample measurements, after the water was abstracted from the monitoring well; the sensors were not used for continuous monitoring over an extended period of time. One other study assessed the use of a nitrate sensor in the continuous monitoring in a river, which contained positive results with respect to both drift and stability over a 40-day period (Goff et al. 2003). However, there have not been any studies reported on application of sensors for monitoring of groundwater salinity.

In recent years, there have been a number of projects in which so called "electric tongue" sensor arrays have been developed for use in the production of wines (i.e. Esbensen et al. 2004, Parra et al. 2006, Wu et al. 2005). The electronic tongue sensor array is comprised of a number of different ion-selective electrodes, which, working together, are able to sense differences and/or changes in the chemical composition of the wines. Using these arrays, winemakers can accurately identify the type of wine and area of origin, or aid in evaluating the aging process and when the wine is ready for market. Because the sensors are based on solid-state technology, they offer the advantages of being more compact, less expensive to produce, and contain no electrolyte solutions which can leak into the test solutions. Although these electrodes have not been used in groundwater wells, there is potential application of this technology.

4. PROJECT DESCRIPTION, OBJECTIVES, EXECUTION AND OBSTACLES

4.1 Ph.d. Project Objectives

The overall objective of the Ph.D. project is the development and application of sensors for the monitoring of groundwater salinity and seawater intrusion. This can be divided into two separate parts: the development and testing of the geochemical sensors, and their application in groundwater modelling with respect to the protection of water quality. The first portion of the project involves the development of sensors that can be used in the observation and analysis of groundwater salinity. Si et al. (2007) developed a solid-state micro-sensor specifically for potassium by electrochemically polymerising an ion sensing film directly on to a gold electrode. It was observed that this same technology could potentially be applied to make sensors for sodium and calcium, both of which would be useful in monitoring of groundwater salinity. This is in addition to a simple technology for the development of a chloride sensor, which could also be used. None of these technologies have been tested for use in continuous application for groundwater monitoring.

In order to apply the sensors in a modelling program, the sensors need to be tested in a case-study. This will provide the information as to whether or not the developed sensor technologies can be used in an actual groundwater monitoring and well-field optimization program. Therefore, the second part of the project includes the identification and geological and groundwater modelling of an area which is being affected by seawater intrusion and elevated groundwater salinities. Here the sensors could be tested in an actual situation where the salinities are changing and incorporated into the understanding and groundwater modelling. The coastal area of Greve, Denmark has experienced elevated groundwater salinities, which were thought to be from seawater intrusion (Roskilde Amt 2004). Groundwater abstraction is still continuing in this area. After a discussion with Greve Water Works, where access to observation and production wells was provided, it was determined that Greve would provide a good opportunity to test the actual application of the developed sensors.

Given the two stages of the project, the initial objectives for the project include:

- Develop solid-state micro-sensors for calcium and sodium, using the technology developed by Si et al. (2004);
- Evaluate the sensors' ability to provide continuous data on the ion concentration in the controlled setting of the laboratory;
- Test the sensors in the field in monitoring and production wells to determine how the sensors perform in an actual situation;
- Develop a geological and groundwater model for the Greve pilot project area, and eventually incorporate the data from the field test monitoring in order to update and refine the groundwater model.

The sensor array employed in the tests will be backed up by using a conductivity probe, which provides a measure for the total dissolved solids in the groundwater. There are distinct advantages of using the sensors and conductivity measurements together. Conductivity measures the total dissolved solids in the water, and if the water is hard (which is not unusual in carbonate aquifers) the conductivity can be quite high due to the high concentration of calcium in the water. This presents a problem, as conductivity then will not be able to register the initial increase in sodium and chloride in the aquifer, as the seawater wedge reaches the wells. On the other hand, the chloride and sodium sensors will respond to this initial change, providing an early warning before the water quality is compromised. The second advantage is that, due to the log-linear response of the sensors, they are very sensitive to changes in lower concentrations, i.e. below 100mg/l, where as conductivity measurements, being linear, will have a much higher error in the lower concentrations and not be able to pick up on concentration changes in this area. Therefore, the sensors working together with the conductivity probe will be able to register the very initial stages of seawater intrusion before the groundwater salinity exceeds the water quality limit (in Denmark being 250mg/l), allowing for a reactive response from the well-field managers to be made.

4.2 Project execution plan

The project was executed in two stages. The first stage was the development and laboratory testing of the sensors. Here ionophores for calcium and sodium were derived though chemical reactions to allow for the electrochemical polymerization

directly on to a gold electrode. The success of the process was evaluated in the laboratory. The sensors which showed a successful response to sodium and calcium after polymerization were tested in the laboratory to provide an evaluation as to their performance, including the range and rate of sensitivity, as well as noise, stability and drift in continuous application under controlled conditions. The chloride sensor was also evaluated for these parameters.

The second stage of the project consisted of the field application of the sensors. Here the sensors were installed in actual monitoring wells, where they were exposed to uncontrolled environmental conditions, particularly with respect to temperature, as well as unknown and varying groundwater salinities. These were evaluated with respect to their performance in the field. This specifically includes the ability to effectively measure in groundwater and respond to changes in groundwater salinity. The sensors were evaluated with respect to drift and compared to the signal obtained from a commercial conductivity probe.

Concurrent with the extended laboratory testing of the sensors, a groundwater model for Greve was constructed. This was also done in two stages. The first stage involved the construction of a conceptual model of the groundwater salinity, utilizing the geological data obtained from over 100 boreholes as well as the water quality data of over 60 water wells. The purpose of the conceptual model was to develop an accurate geological model, as well as use the groundwater chemistry data in order to determine the source of groundwater salinity and extent of seawater intrusion in the area. Using the conceptual model as a starting point, a mathematical model (the groundwater variable flow and transport model, FEFLOW), was used to model the past and present conditions for seawater intrusion, as well as provide an assessment of the future risk. The model ideally would provide the basis for the incorporation of the data from the sensors in order to adjust the model, and allow for more accurate predictions and evaluation of different responses that could be made with respect to changing salinities.

4.3 Obstacles in the execution of the project

Section 4.2 states the ideal execution of the project. However, like any research project, there were significant difficulties that occurred during the execution of the project. In particular, there were two major obstacles that were encountered during the execution of the project that affected the timing and execution of the project.

The first problem was the development of the calcium sensor (described in detail in Chapter 5). The development of this sensor proved to be problematic. Though the theory behind the development of these sensors was sound, it proved to be very difficult to produce a sensor which worked. In the end, work on development of a calcium sensor took nearly a year. This caused a delay in the execution of the other parts of the project, particularly with respect to the long-term testing and field deployment of the sodium and chloride sensors. In addition, the final calcium sensor was developed so late; there was simply not enough time to test the calcium sensor in the field.

The second problem, with even further reaching consequences, was in the choice for Greve as a pilot project. Greve, as reported before, did have groundwater salinity problems, which was widely believed to be a result of seawater intrusion by both the water works and municipality. However, during the construction of the conceptual model for Greve (described in detail in Chapter 7), it became apparent that seawater was not the source of groundwater salinity for much of the municipality, including the groundwater wells which could be used for the testing of sensors. Close examination of the groundwater quality data revealed that the salinity in these wells, though elevated, was not changing with time. And in the part of the municipality where seawater intrusion was occurring, the groundwater quality data showed that over the last 10 years, a steady-state situation had formed, and even there, groundwater salinities were neither increasing nor decreasing with time. This created a problem because the sensors needed to be tested in a situation where groundwater salinities were in flux, allowing the incorporation of the sensor data into a well-field management model. Without temporal changes in the salinities, this would simply not be possible. This situation was confirmed when the sensors were installed and run in the Greve monitoring well, where groundwater salinity was seen to be constant during the entire 9 month period from which the groundwater was monitored. Therefore seeing how the sensors would respond to changing salinities, and incorporating the data into the groundwater model, was not possible for Greve. In addition, because the salinities were not changing, it was not possible to incorporate the monitoring data into the groundwater model for Greve.

4.4 Revised execution plan for the project

It was maintained that testing the sensors in changing groundwater salinities was essential in order to evaluate the ability for the sensors to be employed for continuous monitoring. In this way, a conclusion could be made as to whether or not the sensors did respond to changes in salinity in a manner that could be used in practice. By the time that it was confirmed that Greve could not fulfil this purpose, there was only one year left in the project. Therefore finding an appropriate partner at a water work to test the sensors, which would have had to be outside of Denmark, was not possible. However, an alternative possibility in the United States became available. In this case, it was possible to test the sensors in a monitoring well in the tidal zone at a site in Wickford, Rhode Island. Here, there was an unconfined aquifer, consisting of uniform sand, which was affected by the diurnal tidal fluctuations. During high tide, saline seawater entered into the aquifer, where as during low tide, the seawater is flushed out by the freshwater, creating a diurnal variation in groundwater salinity within the aquifer. It was possible to install a monitoring well by hand into the unconsolidated sediments and monitor the salinity. Although this was not a well-field, it did provide an excellent opportunity to test the sensors in changing salt concentrations.

Given the difficulties and new opportunities, the revised project consisted of the following:

- Development and evaluation of solid-state calcium and sodium sensors using electrochemical polymerisation procedures.
- Testing of the operational range, repetition, and continuous monitoring with respect to noise, stability and drift, for chloride and sodium sensors. The calcium sensor, with a working electrode developed late in the process, was only assessed on a limited basis.
- Testing of the sensor noise, stability, drift and life-span of the chloride and sodium sensors in the monitoring well in Greve. This provided a test in an uncontrolled environment and in reduced groundwater, while salinity remained stable.
- Testing of the sensor noise, stability, drift and life-span in the Wickford monitoring well. This provided a test in an uncontrolled environment with changing salinity.
- Development of a geological and conceptual model of groundwater salinity in

Greve. This study illustrates the possibility for making an accurate model for seawater intrusion in an coastal area with significant groundwater abstraction.
- Development of a groundwater model using FEFLOW in order to analyze the seawater intrusion which has occurred, and provide an assessment of the future sensitivity of the area to seawater intrusion under different groundwater abstraction scenarios.

In general, the execution was not changed with respect to the planned execution. The only real and significant differences were the addition of the Wickford monitoring test, and not being able to incorporate monitoring data from the sensors into a well-field model for Greve.

5. SUMMARY OF THE CHAPTERS

This thesis is written as a series of papers intended for individual publication. It does not follow a traditional format of Problem-Objectives-Methods-Results-Conclusion. The chapters which are not written as stand-alone papers are Chapters 2 and 9. Instead, they provide background information and general conclusions that cover the project as a whole. Because the chapters are written as individual papers, it is acknowledged that there will be some, albeit limited, repetition between the chapters. It was attempted to reduce this repetition, but for the flow of both the thesis and the individual chapters, it was not possible in every case. This section provides a description of the individual chapters, their status in publication, as well as the role of the author in the research conducted in the paper.

Chapter Two provides and introduction to the use of ion selective electrode (ISE) technology and saltwater intrusion. Since this is a multi-disciplinary study, this chapter provides the reader with a background in these areas in which he or she may not be familiar with. Furthermore it centralizes important detailed information, specifically the governing equations for ISE's and the signal corrections used, which apply to Chapters 3, 4 and 5. The chapter also provides detailed descriptions of the two monitoring well sites used in the study. This chapter is not meant for publication.

Chapters Three, Four and Five present the results of the testing of the chloride, sodium and calcium sensors, respectively. This covers the tests from the laboratory,

Greve monitoring well, and Wickford monitoring well for chloride and sodium, and the laboratory tests for calcium. The calcium sensor was not tested in the field. None of these chapters to date have been submitted for publication. It is anticipated that Chapter Three on chloride will be submitted to a journal, with Sensors and Actuators B, Water Science and Technology and Ground Water Monitoring & Remediation considered as the most applicable journals for submission. It is uncertain whether or not the results from Chapter Four and Five warrant publication. The most likely case, the results will be published after further research in the sodium and calcium sensors. In all three cases, project co-supervisor John Mortensen has had a significant contribution, particularly with respect to the theory behind the development and ideas for improvement of the sensors, and will be listed as a second author for any papers submitted. However, the bulk of the research, analysis and writing was carried out by the author.

Chapter Six provides the results of the geological investigation of Greve and the surrounding area from the numerous boreholes in the region. In this study the borehole logs were analyzed and evaluated, with the geological structure of the pre-quaternary sediments as well as the pre-quaternary elevation mapped out. This is part of a larger investigation comprising of nearly the entire eastern half of the island of Zealand in Denmark. This chapter will be included in a publication on the larger investigation, which will be submitted to the Bulletin of the Geological Association of Denmark. The author's role in this was the analysis of the wells in Greve and it's surrounding area. Therefore I will be listed as third author on this publication with Niels Schrøder and Ritta Juel Bitsch being the primary authors, as they were responsible for the analysis for the remaining coverage, which is more than 75% of the total area. However, the author was the primus motor for the geological analysis for the Greve area as written in this thesis.

Chapter Seven consists of a conceptual model for the salinity observed in the water wells in Greve. The geochemistry of bulk water samples from the groundwater wells was analyzed to determine the source for the salinity and the risk for seawater intrusion. This chapter has been submitted to Hydrogeology Journal, and accepted for publication after moderate revisions. The suggested revisions are currently being addressed, and will be resubmitted before August, 2010. There are no co-authors on this paper.

Chapter Eight is the FEFLOW variable transport and flow model for Greve. The chapter discusses the model set-up and effectiveness of simulating seawater intrusion in Greve, as well as providing an analysis of the sensitivity of the study area to seawater intrusion under differing groundwater abstraction scenarios. This chapter will be submitted for publication, with Hydrogeology Research, Ground Water or Hydrogeology Journal considered the most appropriate journals for publication. There are no co-authors for this paper.

Chapter Nine simply provides the over-all conclusions from the project as a whole. This chapter will not be published.

6. APPENDIX A AND B

There are two appendices associated with the dissertation. Appendix A provides the data from all of the tested chloride sensors. Appendix B provides the NMR and Infrared scanning data for the development of the sodium ionophores and polymerization on to the gold electrode. In addition, Appendix B provides all of the data from the sodium sensor tests. The information included in the appendices is considered as documentation for the data that is summarized in the tables and text. Therefore, it is not provided in printed version in the dissertation. The appendices are available by request to Paul Thorn via e-mail (pthorn@ruc.dk) or can be downloaded from the Roskilde Univsersity Library at http://diggy.ruc.dk:8080/retrieve/17768 .

Overview of Ion Selective Electrode Technology, Saltwater Intrusion and the Study Sites

1. INTRODUCTION

The purpose of this chapter is to give a general background of concepts and theory, which provides the academic foundation for the remaining chapters in the thesis. This is important because it is a multi-disciplinary project, combining both electrochemistry and hydrogeology (groundwater), and one may not be familiar with both topics. The chapter will start out with a description of ion selective electrodes, how they work, and the governing Nernst equation. The chapter will then continue with a description of electrical conductivity in solutions. The theoretical discussion will then proceed with a description of the problem of groundwater salinity and seawater intrusion. The chapter will conclude with a full description of the two test sites used in the study, Greve, Denmark, and Wickford, Rhode Island, USA. This will include a detailed description of the well and groundwater monitoring set-up.

2. ION SELECTIVE ELECTRODES

2.1 How Ion Selective Electrodes work

In its basic sense, an ion selective electrode (ISE) is a sensor that converts the activity of a specific ion, dissolved in a solution, into an electrical potential, which then can be measured by a voltmeter (Cammann and Schroeder 1979). A typical ISE contains a membrane containing contain an ionophore, which selectively binds to a specific ion (Bühlmann et al. 1998). When the membrane is submerged in a solution, the ions will selectively bind to the ionophore in the membrane, with the amount dependent upon the activity of the ions in the

solution. The ISE is used with a reference electrode with a constant potential, which creates a potential difference between the two electrodes, which can be measured with a volt meter (Fig. 1) (Cammann and Schroeder 1979, Harris 1996). As only the working electrode will change potential with increasing ion activity, the potential difference is a direct measurement of increasing ion activity in the measured solution. The response of the sensing electrodes to ion activity is log-linear, with an ideal response of 59.1 mV/decade concentration change for ions with an ionic charge of 1, and 29.5mV/decade for ions with an ionic charge of 2, at an ideal temperature of 25°C (Cammann and Schroeder 1979).

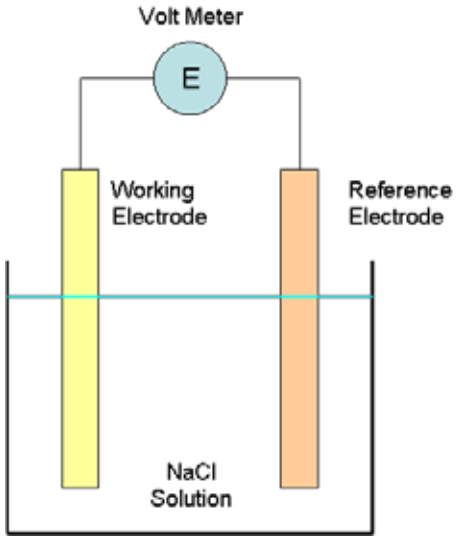

Figure 1. *Electrochemical cell with an ion-selective electrode as the working electrode, and a standard reference electrode in a NaCl solution. The working electrode will change potential depending on the NaCl concentration, where as the reference electrode maintains a constant potential regardless of solution concentration. The volt meter registers the potential difference between the two electrodes.*

As described above, the potential of ISE's is related to the activity of an ion in solution. The activity of an ion is simply a relative measurement of an ions ability to chemically interact with its surroundings. Although activity is influenced by temperature, pressure, and composition of the mixture, it is generally seen to be directly proportional to the concentration of the ion, and thus is a measure of the effective concentration (Cammann and Schroeder 1979, Levine 1995). Even though ISE's measure the activity of an ion, because the activity is related to the concentration, the potential measured is also a function of concentration. However, when concentrations become high enough, the ions start interfering

with each other. From this point, the activity of the ions no longer responds proportionally to the increase in concentration (Levine 1995). The log-linear response from the ISE's will no longer be valid once this concentration is reached, creating a theoretical upper concentration limit for ISE's.

A reference electrode is an electrode which maintains a virtually constant potential, regardless of the concentration of the solution being measured (Buck and Lindner 1994). It acts as the control point for the measurement electrode, allowing for observation of the potential difference, which is related to the ion concentration in the solution. A typical example of a reference electrode is an Ag/AgCl rod in a glass tube submersed in a saturated KCl solution, and a semi-permeable membrane maintaining contact with the measuring solution. Since the reference electrode is continuously in contact with a constant, saturated solution, the potential will not vary, and theoretically measure the same potential regardless of the ion concentration in the measured solution (Buck and Lindner 1994). There are generally two structural types of reference electrodes: single and double junction. Single junction reference electrode is constructed with a single tube containing one filling solution. A double junction reference electrode contains both an inner tube with a filling solution and electrode, and an outer tube surrounding the inner tube with a second, inert filling solution. The double junction electrode will prevent contamination of the measured solution from the inner filling solution. The type of reference electrode used is determined by the ion being measured for. For example, if one is measuring for potassium, then using a Ag/AgCl electrode with a KCl solution, there is the chance for cross-contamination. Therefore in this case a double junction reference electrode should be used. However, if one is measuring for calcium, then the single junction electrode can be used.

2.2 Theory behind ISE measurements: Nernst Equation

Potentiometry, in its basic sense, is the measurement of voltage between two electrodes in an electrochemical cell, in order to measure concentrations of dissolved ions in a solution (Harris 1996, Manahan 2001). The Nernst equation is used to account for the effect of the different ion activity in this electrochemical cell. Since activity is essentially equivalent to ion concentration, the Nernst equation states:

$$E = Eo - \frac{2.303RT}{nF}\log[a] \quad (1)$$

where E is the measured potential, Eo is the standard electrode potential, both measured in volts, R is the molar gas constant, T is the absolute temperature, n is the ion valence, F is the Faraday constant and [a] is the concentration of the ion. Using a standard reference temperature of 25°C, the Nernst equation simplifies to:

$$E = Eo - \frac{0.059}{n}\log[a] \quad (2)$$

From this equation, it is apparent that the potential is proportional to the log of the concentration for the measured ion. Therefore, under ideal conditions, there is expected a change of 59 mV per every decade (10-fold) increase in concentration for sodium and potassium (+1 valence), 30mV for calcium (+2 valence), and -59mV for Cl (-1 valence). This slope, of course is an ideal "Nernstian" slope. When dealing with ion-selective electrodes, the actual response of the electrodes will often be less than that of the ideal Nernstian slope (Brown et al. 1976, Bühlmann et al. 1998, Hobby et al. 1983, Sutter et al. 2004). This can be accommodated through calibration of the electrode through standards of changing ionic concentrations. For example, a typical sensor calibration will plot E (mV) vs. ion concentration, ranging from 10^{-5} to 1Molar concentration (Fig. 2). Through the calibration of the sensor using known concentrations, both the slope and Eo can then be calculated for the ISE. Thus, the calibrated slope can be used in place of the ideal slope, and the ISE can then be used to calculate the concentrations in unknown samples.

In the case where temperature varies from the ideal 25°C, such as applications of the ISEs out in the field, there must also be a correction made for the Nernst equation. Equation 2 is based upon a reference temperature of 25°C, however, it can be seen from Equation 1, that any deviation from this temperature will affect the response slope. Correction of the slope can be easily made using the following equation:

$$S(corr) = \frac{S(cal) * (T + 273)}{298} \quad (3)$$

Where S(corr) is the temperature corrected slope, S(cal) is the calibrated slope, and T is the temperature (ºC). The temperature corrected slope is then used in the Nernst equation in order to calculate the ion concentration from the ISE.

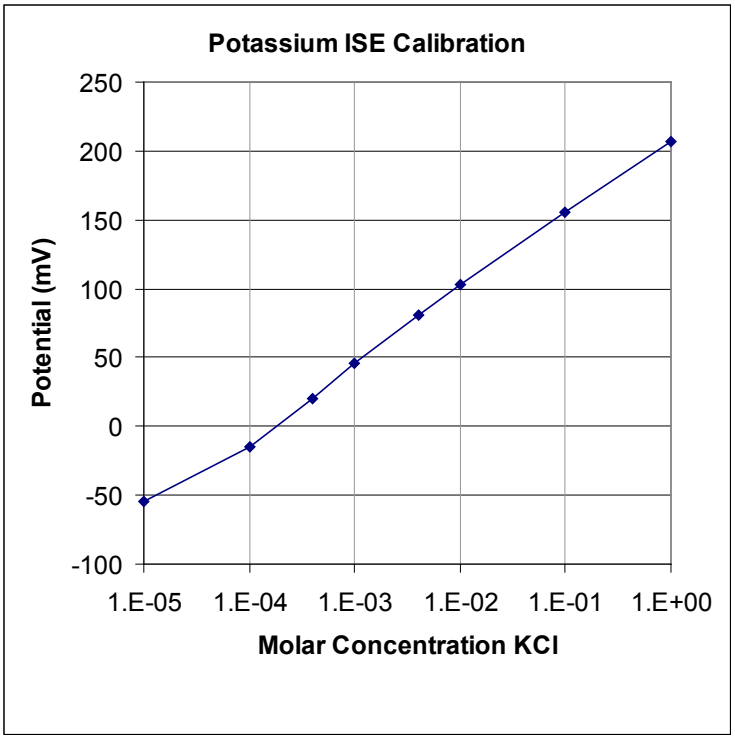

Figure 2. *Standard calibration curve for a commercial ISE for potassium. The calibrated response rate is 52mV, with a calculated Eo value of 204mV.*

2.4 Potential problems for ISE measurements

In spite of the advantages for ISE's, there are a number of potential problems when using ion-selective electrodes to measure ion concentration. The first of these problems is interference from other ions, also referred to as ion selectivity. Although ionophores are selective towards a specific ion, there is often cross-sensitivities to with other ions (Buck and Lindner 1994, Bühlmann et al. 1998, Winkler et al. 2004). Thus, the interfering ion will also contribute to the potential measurement in an ISE, but to a lesser extent than the intended ion. This rate can be measured and is represented as the selectivity coefficient (Buck and Lindner 1994). The selectivity coefficient is defined as "the ability for an ISE to distinguish a specific ion from the others" (Buck and Lindner 1994).

It is expressed as a ratio of the selectivity of the interfering ion to the selective ion. Thus, if an ISE for potassium has a selectivity coefficient of 0.1 towards sodium, that would mean that the ISE is ten times more sensitive towards potassium than sodium. It also shows that a 10mg/l change in sodium concentration would be registered as a 1mg/l concentration change by the potassium ISE. Therefore, when using ISE's for a specific measuring or monitoring purpose, cross-sensitivities to potential interfering ions must be considered.

A second problem with using ISE's for concentration measurements is that, in higher concentrations, ionic activity does not increase at the same rate as concentration. In lower concentrations, ionic activity roughly is equivalent to ion concentration. However, as the concentrations increase, the activity decreases, creating an error within the reading of an ISE, particularly at concentrations over 0.1M (Cammann and Schroeder 1979). Thus, the ISE will tend to underestimate the actual values at higher concentrations.

A third problem with ISE's is drift. Drift is defined as "the slow, non-random change with time in the potential of an ion-selective electrode cell assembly maintained in a solution of constant composition and temperature" (Buck and Lindner 1994). Drift is measured by the submersion of the ISE in a solution with a constant concentration and temperature over an extended period of time. There are many possible reasons for drift in the measurements, but it is often not possible to determine what the actual cause of the drift is. Possibilities include drift in the ISE itself, drift within the reference electrode (particularly if the liquid junction of the reference electrode is not constant), or even with the volt meter itself (Cammann and Schroeder 1979). Drift in ISE's has been reported by a number of studies, ranging from virtually no recorded drift (Goff et al. 2003) (Pawlak et al. 2008), to as high as 12mV/day (Noh and Coetzee 2007), with average drifts usually between 1-3 mV/day (Parra et al. 2009). The drift can be corrected for, particularly if it is steady. However, periodic calibration is required for continuous measurements (Winkler et al. 2004).

The final potential problem in the use of ISE's, particularly when used in the field for continuous monitoring, is fouling of the sensing membrane. Fouling is defined as any outside material that accumulates on the sensing surface during the measurement process. This is often a biological growth or a chemical film such as ocher, which forms from the oxidation of iron in the water. It has

been observed that fouling will cause the sensor to loose its responsiveness over time (Winkler et al. 2004). Therefore, any application of ISE's in longer-term monitoring programs, issues with respect to fouling need to be considered.

3. CONDUCTIVITY MEASUREMENTS

Conductivity in solutions is simply the ability for an electrical current to be transmitted through the solution. In water, it is the dissolved ions which facilitate the conductance of the electrical current, and thus measured conductivity is proportional to the concentration of all of the dissolved ions in solution (Appelo and Postma 2005). Conductivity is measured in Siemens per cm, with the most common measurements for water quality expressed in either milli-Siemens (mS/cm) or micro-Siemens (μS/cm). The measurements are usually standardized to a temperature of 25°C. Conductivity is seen to vary depending on the ions present in the solution, and their individual ability to transmit the current; thus the conductance of sodium is not the same for potassium (Appelo and Postma 2005). However, a general conversion of conductivity (μS/cm) to the total dissolved solids (mg/l) in water can be made using a 1:0.67 ratio.

Conductivity measurements are temperature dependent. As temperature increases, the solvents viscosity decreases. Conductivity is related to the ion mobility, which is seen to increase with lower viscosities, and therefore, as temperature increases, so does conductivity (Levine 1995). The degree to which temperature affects conductivity varies, depending on the dissolved constituents in the solution. However, the effect can be calculated using the following formula:

$$(4) \qquad Kt = Kt_{cal}\,(1+\alpha(T-T_{cal})$$

where Kt is conductivity at a given temperature, Kt_{cal} is the conductivity at calibration temperature, T_{cal} is the calibration temperature, T is temperature, and α is the temperature coefficient of the solution. The temperature coefficient is seen to vary from solution to solution, dependent upon the constituents. According to documentation from Topac, Inc. (the producer of the conductivity probe used in this study), and backed by documentation obtained on the internet from other producers of conductivity probes, the general rule of thumb is that the temperature coefficient is around 0.02 for most studies, but varies

from, for example 0.0188 in KCl to 0.0214 in NaCl. However, the temperature coefficient can be simply measured in the laboratory by measuring how conductivity changes in a solution under different temperatures. As the temperature of 25 ºC is generally used as the standard temperature for conductivity, the measurements should be corrected to this temperature.

4. GROUNDWATER AND SALINITY

The overall goal of this study is to develop sensors which can be used for the monitoring of groundwater salinity for the management of groundwater resources. There are a wide range of possible sources for elevated salinity in groundwater aquifers. In the case of the two study sites for this project, the sources include seawater intrusion, pollution from road salt, or upward diffusion from ancient pore waters. This section provides a brief description of these sources for groundwater salinity. There are, of course other sources for groundwater salinity, including infiltration from salts in the soils and sediments above the water table, or even direct contact with rock salt deposits (sylvite and halite deposits) in the underground. However, because these sources are not applicable at the two study sites, they will not be discussed here.

4.1 Seawater intrusion

Seawater is probably the best known source for groundwater salinity in aquifers near the coast. The theoretical basis for seawater intrusion starts with the density difference between seawater and freshwater. Average seawater, with a 3.5% salinity, has a density of 1025 kg/m3, where as pure freshwater has a density of 1000 kg/m3. Because of this density difference, the heavier seawater sinks below the freshwater, with seawater extending further inland, below the freshwater (Hiscock 2005). In the late 1800's the density relationship between the heavier seawater and fresh groundwater in coastal zones was defined, now commonly termed the Ghyben-Herzberg relation (Drabbe and Badon-Ghyben 1888-1889, Herzberg 1901). This predicts that, in aquifers flowing towards the sea, the depth to the saltwater/freshwater interface will be 40 times the height of the freshwater table above sea level (Fig. 3). This relationship is calculated as a sharp boundary. However, the boundary in reality is not seen to be sharp,

but rather have a transition zone between the high saline sea water and the fresh water (Hiscock 2005). The thickness of the transition zone is variable, and dependent upon both diffusion and advective dispersion. Groundwater abstraction near the coast will cause a reduction in the groundwater head (height of the groundwater table). This in turn, will cause upconing of the seawater (Fig. 3). If the well is deep enough, or the groundwater head is reduced to below sea-level, seawater will begin to intrude into the well.

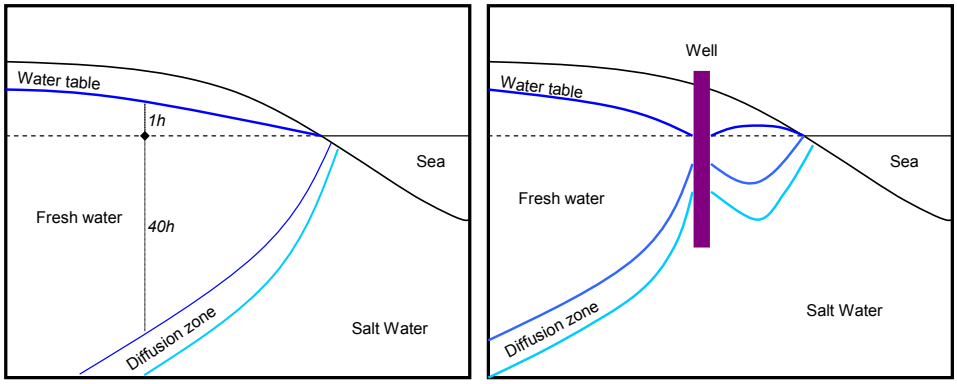

Figure 3. *Diagram of the freshwater/seawater interface according to the Gyben-Herzberg relation. The left diagram shows the freshwater/saltwater interface under steady-state conditions, with the 1:40 Ghyben-Herzberg relation. The right diagram shows the situation, as altered from pumping. Here pumping from the well has induced saltwater to enter into the well.*

The relationship described above is for unconfined aquifers, where there are permeable sediments from the water table to the ground surface. In confined aquifers, however, there is an impermeable layer on top of the groundwater aquifer, preventing infiltration of surface waters to the aquifer (Hiscock 2005). In this case, water pressures in the aquifer rise above the physical boundary of the aquifer, creating a potentiometric surface. If a well is drilled into the aquifer, the water will rise to the level of the potentiometric surface. In confined aquifers, the Ghyben-Herzberg relation also applies, with the potentiometric surface representing the water table (Fig. 4). Groundwater abstraction will reduce this pressures in the groundwater aquifer from it's steady-state levels. If the pressure is lowered to below sea-level, seawater will start moving into the confined aquifer towards the well (Fig. 4). If abstraction continues over a long enough time period, the seawater will eventually reach the well.

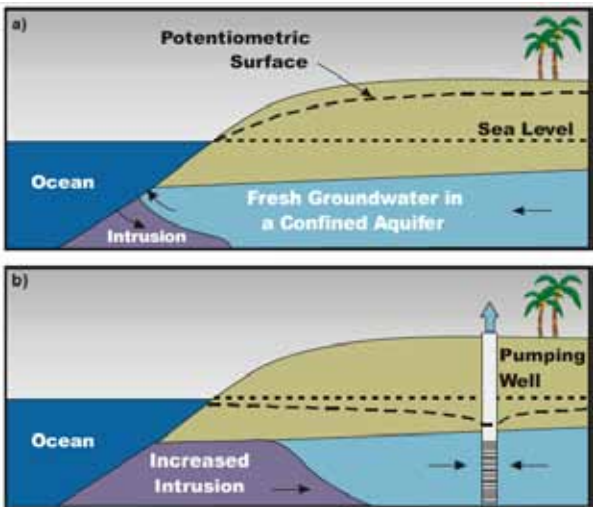

Figure 4. *Seawater intrusion into a confined aquifer. The top diagram shows a steady-state situation, with submarine groundwater discharge, and a Ghyben-Herzberg relation at the contact between the ocean and the aquifer. The bottom diagram shows the intrusion of seawater into the aquifer as groundwater abstraction through the well commences. Diagram is modified from (Edwards and Evans 2005).*

In unconfined aquifers, tides can also have an effect on the seawater interface in the immediate tidal zone. During high tide, seawater extends the furthest in-land, where it then infiltrates down through the sediments to the water table. This saline water will form a lens on top of the fresh water, where it mixes with the fresh water below (Michael et al. 2005, Urish and McKenna 2004). As the tide retreats, the saline water gradually is washed out from the aquifer. Then when the tides rise again, the process is repeated. In the events of spring tides, storm surges, or even tsunamis, the saltwater can be pushed even further inland, depending on the local geography, creating a potential source salt intruding into the groundwater aquifer (Kume et al. 2009, Violette et al. 2009).

4.2 Road salt

In colder climates, such as Denmark, salt is often used on the roads in order to prevent snow and ice from accumulating on the roads. As the snow and ice melts, the salt is carried off to the sides of the roads into the drains and the ditches beside the road. If the water is not removed away through the drain or sewer system, the salt can then infiltrated down into the aquifer system. In a recent report conducted in by the Geological Survey of Denmark and Green-

land, it was estimated that as much as 10-20% of the salt applied to roads in urban areas, and up to 50% in rural areas, can infiltrate into the soil and groundwater (Kristiansen et al. 2010). There have already been wells observed to have been polluted by road salt in the Copenhagen metropolitan area, the geological survey estimates that the problem will become even worse over the next two decades (Kristiansen et al. 2010).

4.3 Formational pore waters

Upwards diffusion of salts from pore waters in low permeable sedimentary rocks can also be a significant source for salts in groundwater (Appelo and Postma 2005). This is not an uncommon phenomenon in, particularly marine deposits. The most common scenario for this is through the salt entering into the pore spaces of the low permeable geological unit, either because the rock was formed in marine water, or submerged beneath saline water for an extended period of time – often millions of years. Then later, there was a local fall in sea-level (caused either by uplift or global sea-level change), resulting in a fresh water aquifer forming on top of the low permeable unit. The low permeability of the unit prevents the salts from being removed via advective groundwater flow, where as in the high permeable aquifer directly above, fresh water is circulating through quickly taking the formational salts with it. Therefore, at the border between the low permeable saline units and the high permeable fresh water aquifer, creates a concentration gradient, where the ions move upwards via diffusion, from high salinity to low salinity (Appelo and Postma 2005). Here, the ions then enter into the advective groundwater system. This situation has been observed, for example, in both England and Denmark, where diffusion from Cretaceous chalk deposits below a fractured aquifer has resulted in groundwater well chloride levels as high as 300-500 mg/l (Appelo and Postma 2005, Bonnesen et al. 2009). However, because of the slow process of diffusion across this boundary, there is a upper limit to the salinity that the groundwater can achieve, depending on the depth of the aquifer and the concentration gradient.

5. DESCRIPTION OF THE GREVE MONITORING WELL SITE

5.1 Monitoring well history and set-up

In order to test the sensors developed in this project, a monitoring well, owned by Greve Water Works, was used. The well (Danish Geological Survey – DGU - number 207.2500) originated as a groundwater abstraction well, being drilled in 1971. The well is located in a park area in the middle of a residential section in Greve, Denmark, approximately 25km to the SW of Copenhagen (Fig. 5).

Figure 5. *Location and picture of the Greve monitoring well (shown on the left by the red star). The sensors and data logger were kept inside of the concrete casing with a metal lid, shown right, which could be locked for security purposes.*

According to the drillers report, the well was drilled to a depth of 60m, and had an elevation of 4.5m above mean sea-level (GEUS 2010). The well penetrated only two different geological units: clayey till from the surface down to a depth of 19.2m (elevation of -14.7m), with the remainder consisting of Maastrictian age chalk deposits. The well is screened from a depth of 23.1 m (elevation of -18.6m) to the base of the well. The screen occurs only in the Maastrictian chalk. According to documents from Greve Water Works, in 1982 the well was filled in to a level of 27.5m below the surface (an elevation of -23m), leaving an open screen interval of 4.4m. The well is screened in the lower confined

aquifer, which consists of the fractured chalk. Transmissivity for the well is not reported, however, is estimated to be in the range of 4x10-4 m2/sec, based on other studies (Larsen et al. 2006, Roskilde Amt 2004). The glacial clayey till has a very low permeability, with conductivity estimated at under 1x10-9m/s (McKay et al. 1999, Nilsson et al. 2001), and acts as a confining unit. Groundwater level in the well was measured in May, 2009 to be at an elevation of 0.5m (4.0m below ground surface).

Groundwater abstraction began in 1975, and continued until 1989. Afterwards, the well was kept open and used as a monitoring well by the water works. While the well was in operation, chloride levels were seen to vary between 289 and 421 mg/l. Groundwater abstraction was ultimately discontinued from this well because the chloride levels continuously exceeded the 250mg/l water quality limit for chloride.

5.2 Experimental set-up

The testing of the sensors in the Greve monitoring well was conducted in an above ground installation. The sensors were mounted in a clear plastic block (Fig. 6), which was then set in a metal box. The metal box was used in order to create a Faraday cage, which limits electrical noise from outside sources. The block was connected to tubing which brought water from the well, by the sensors, and through a pump, and then to an outlet (Fig. 7). The sensors were

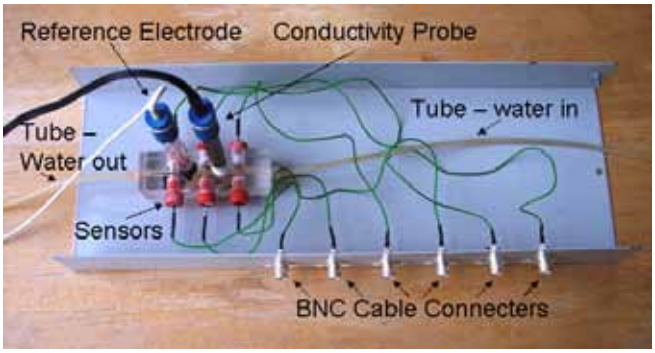

Figure 6. *Picture of the sensor system used in the in-situ monitoring tests. The sensors are mounted in the clear plastic block, which is encased in a metal box (lower half shown in picture). The conductivity probe and double junction reference electrode are sitting vertically in the block. Silicone tubing is connected to the block, which allows water to be pumped across the sensors, conductivity probe and the reference electrode. The system was used in both the Greve and Wickford monitoring well.*

connected to a multi-channel electrochemistry meter (Fig. 7). The meter was fromConsort nv (Turnhout, Belgium), model number C864. BNC cables were used for the connection in order maintain the quality of the signal.

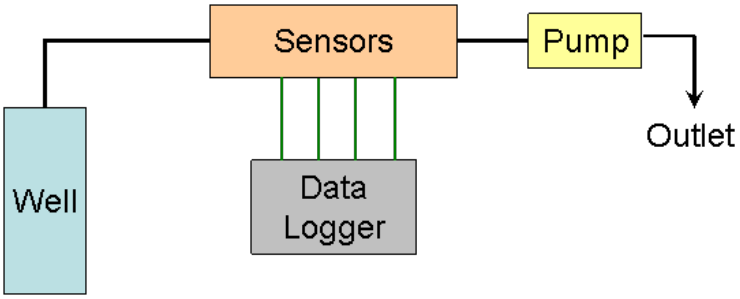

Figure 7. *Diagram illustrating the monitoring setup. The silicone tubing (shown in black) extends from the well (intake) to the sensors, and then to the pump and finally the outlet. The sensors, in a metal box, are then connected to the data logger via BNC cables (shown in green). This set-up was used in both the Greve and Wickford monitoring well.*

The Greve monitoring well is a non-pumping well. The well was flushed before the tests that began in December 2008, and in June 2009. In both cases, the well was flushed at a rate of 9.5m3/hour for 24 hours. The well was allowed to recover for over 24 hours before the testing began. In order to abstract water from the well for the monitoring test, a thin silicone tube was lowered down into the well and connected to the sensor mount. A laboratory pump was attached to the system. Water was pumped from the well through the system at a rate of 1-2ml/min. All air was removed from the system, and thus the sensors remained in contact with the flowing water for the entire test.

Water from the Greve monitoring well was taken at two different depths. For the tests conducted in December 2008, January-February 2009, and June/July 2009, the water was taken from a depth of 4m below the water level in the well (an elevation of -3.5m). In these tests, a total 10m of silicone tubing was used from the abstraction point in the well to the sensors. The tubing used had a diameter of 2mm, giving a total volume in the system of 35 ml, including the mounting block. Thus, the time delay between the intake of the water to reaching the sensors was between 18 and 35 minutes. Water samples collected after passing by the sensors during these tests were analyzed for sodium (using atomic absorption) and chloride (titrating with AgNO3). Sodium concentrations ranged from 110mg/l (Dec. 6, 2008) to 118mg/l (July 26, 2009), and

chloride concentrations ranged from 195mg/l (Dec. 6, 2008) to 186mg/l (July 26, 2009). Conductivity measurements were also constant during the tests. Thus, it can be seen that the salinity of the water taken from this level remained at a constant rate throughout the testing period.

For the August and September 2009 tests, the tubing was switched to non-air permeable tubing in order to prevent oxygen from permeating through the tubing and oxidizing the groundwater in the system. The intake was also lowered 8m to a depth of 12m below the water level (elevation of -11.5m). A total of 18m of tubing was used in this test, yielding a volume of 59 ml in the system. Thus there was between a 30 and 60 minute delay from the intake of the water to reaching the sensors. Water samples collected during these tests showed a much lower salinity, with sodium levels ranging between 37mg/l (August 17, 2009) and 41mg/l (September 24, 2009), and chloride levels ranging between 44 (August 17, 2009) and 51 (September 24, 2009). Like the shallower groundwater, conductivity was also constant, and thus salinity is seen to be constant throughout the testing period.

The test set-up was above ground, and thus temperature varied. Thus, the sensor signals needed to be corrected, using equation 3 (discussed above). In addition, the system was also susceptible to freezing when temperatures dropped below 0^{o}C for an extended period of time. This was seen to be a problem in the January 2009 test, where the system froze up for two periods of time, between January 2-4 and 6-12. During these periods, water was not able to be pumped through the system, and thus no measurements were taken during this time.

6. DESCRIPTION OF THE WICKFORD MONITORING WELL TEST SITE

6.1 Monitoring well location and set-up

The sensors were also tested at a site in Wickford Cove, Rhode Island, USA, just off of Narragansett Bay (Fig. 8). One monitoring well was used near the top of the tidal zone on the beach front (Fig. 9 and Fig. 10). The well is constructed of a steel tubing 10cm in diameter, and was manually pounded down into the

unconsolidated sediments. The well was installed to a depth of 3.28m below the surface, with an elevation of -2.82m (mean lower low water (MLLW) from 1929NGVD). The lowest 10cm of the well was screened and open to the aquifer.

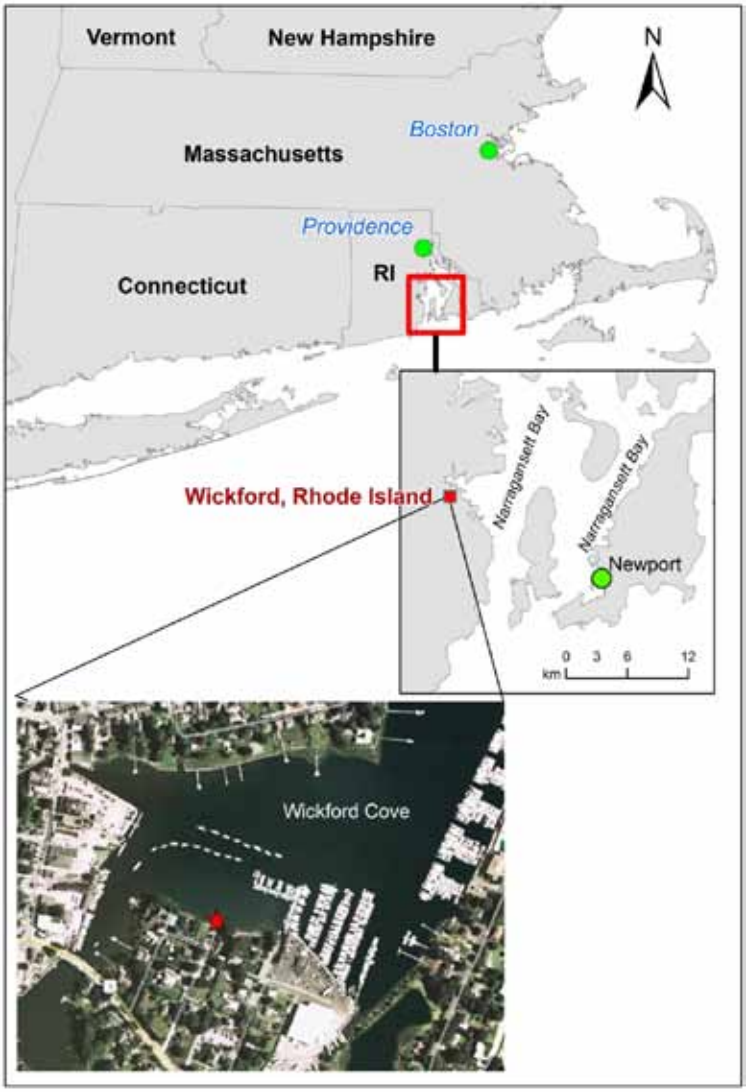

Figure 8. *Location of the Wickford monitoring well site, at Wickford Cove, Rhode Island. The red star marks location of the monitoring well.*

The monitoring well lies in an unconfined aquifer consisting of unconsolidated fine to medium grained sands. The sands were deposited as glacial outwash sands and are reported to be in a thickness of approximately 10m in the Wickford Cove area (Johnson and Marks 1959). Samples taken from the well show the sands to be well sorted fine grained, with a median size of 0.4mm. Porosity was

measured at 40% using the simple formula (wet weight – dry weight)/volume. Hydraulic conductivity was measured at 2.2x10-4 m/sec, using the falling head permeameter (Urish 2009).

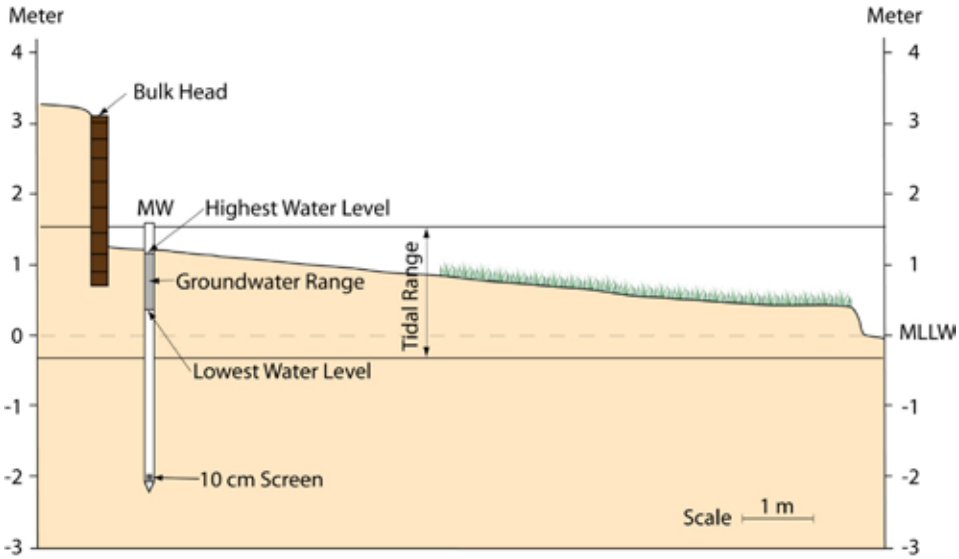

Figure 9. *Diagram of the beach front with the monitoring well at Wickford. Elevations are taken from mean lower low water, from 1929 datum. The lines show the tidal range during the test, as well as the difference in the water level measured in the well. Note the screen is located in the lowest 10cm of the well.*

Figure 10. *Pictures of the monitoring well and beach front. The left picture shows the beach front profile, with the monitoring well directly beneath the person. The right picture shows a close-up of the well with the clear thin tubing seen extending down from the bulk head and into the well.*

The approximate tidal range at the site is illustrated on Figure 9. The tides were seen to rise to as high as approximately 20cm on the bulk head. The seawater came close, within 2-3cm, but never reached the top of the monitoring well. The tides were not recorded in Wickford Cove, however, the U.S. National Oceanic and Atmospheric Administration (NOAA) has a constant record of the tides at their Newport monitoring station, which lies approximately 12km to the SE of Wickford Cove on the southern end of Narragansett Bay (Fig. 8). Here, the tidal range was from -0.3m below MLLW to as high as 1.6m above MLLW. As this is the closest station to Wickford Cove, it is assumed that the height and timing of the tides from the Newport station is the closest approximation. Groundwater level was monitored in the well using a down-hole water level sensor, CTD-Diver by Schlumberger Water Services. The in-well water level was seen to respond to the diurnal tidal variations with an approximately 2-hour delay from the monitored tides (Fig. 11). The water level in the well ranged from as low as 0.25m to as high as 1.12m in the well. The variations diurnal variations in the water level in the well ensured that water was in and out of the well, providing a natural flushing of the well.

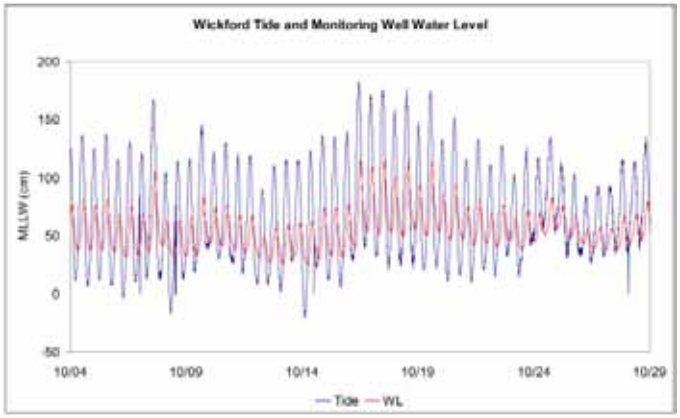

Figure 11. *Recorded tide levels (as recorded from NOAA's Newport station) and water level in the monitoring well. Note the 2-hour delay between high tide and the high water level in the well.*

6.2 Experimental set-up

The sensor set-up used at the Wickford monitoring well test was similar to that of the Greve monitoring well test (Figs. 6 and 7). Four sensors were used, two chloride and two sodium, as well as a conductivity probe (by Topac) and a double

junction reference electrode – all installed in the clear plastic mounting block. The sensors were encased in the metal box, and connected to the data-logger via BNC cables. The sensors and data-logger, together with the water pump, were set in an insulated plastic container, located at the top of the bulkhead (Fig. 12). The sensor mounting block was connected to the well via a 10m long silicone tube. The intake of the tube was lowered to the bottom of the well, at the screened interval, to ensure that the water samples were coming from the water flowing in and out of the well through the well screen. The water was pumped at a rate of between 1-2ml/minute. Given the length (10m) and diameter (2mm) of the tubing, the total volume of water in the system was 31ml, and thus the time delay from the sample to reaching the sensors was a maximum of 31 minutes. A temperature logger, from Schlumberger Water Service, was located in the white box. This provided the temperature data needed to correct the signals for chloride, sodium and conductivity.

Figure 12. *The container holding the sensors, pump and data-logger (on top). The container was located on top of the bulk head, just above and approximately 2m to the north of the monitoring well.*

The testing of the sensors was conducted over 30 days, beginning on September 30, 2009 and ending on October 29, 2009. Measurements were taken at 6-minute intervals for the entire period. The data was downloaded off of the data-logger once a week. During the test, there was a short power outage, from 03:55 – 05:10 on October 25. No data was recorded during this period; however the system was seen to function properly both before and after the power outage.

6.3 Conductivity temperature correction

Conductivity measurements are used in this study as the control measurements for both the chloride and sodium sensors. As described in section 3, conductivity measurements can be converted to actual total dissolved solid concentrations, and further to sodium and chloride concentrations. However, as equation 4 shows, conductivity is sensitive to temperature and must be corrected for. Given that the temperature coefficient in equation 4 varies depending on the constituents in the water, the coefficient specifically for the Wickford monitoring well was calculated. This was conducted using a sample collected from the monitoring well. The conductivity of the sample was measured in the laboratory at differing temperatures. Using equation 4, the temperature coefficient (α) could then be calculated. Table 1 shows the data collected from the laboratory conductivity tests on the Wickford monitoring well sample. From this, a temperature coefficient of 0.0199 was calculated. This was subsequently used in equation 4 to correct the conductivity measurements for temperature.

Table 1. *Laboratory conductivity measurements conducted on a sample from the Wickford monitoring well taken on September 30, 2009.*

Measured Conductivity (μS/cm)	**Temperature** (^{o}C)	**Actual Conductivity** (μS/cm)	**Temperature coefficient** (α)
3416	23	3560	0.0202
3560	25	3560	0.0199
3773	28	3560	0.0197
3910	30	3560	0.0198
4054	32	3560	0.0200
4272	35	3560	0.0199
4412	37	3560	0.0198
4480	38	3560	0.0199

Testing of Chloride Sensors for Continuous Groundwater Monitoring

1. INTRODUCTION

Saltwater intrusion is a pressing threat to groundwater supplies in coastal regions – particularly those where there is not adequate freshwater resources to meet demand. In areas where saltwater intrusion has occurred, technical solutions, such as freshwater injection, have been employed to prevent the intrusion (Barlow 2003). Alternatively, the wells have been abandoned, forcing an alternative source of water such as surface water or even desalination plants. These solutions are often expensive and cannot be used in every situation. In other cases, the fear of saltwater intrusion has led to groundwater abstraction being moved away from the coastal areas further inland. The movement of abstraction sites further inland has its problems, as it can result in a reduction of baseflow to streams and wetlands, significantly affecting the fresh-water ecosystems.

Improvements in groundwater modeling technologies have allowed us to, at least in part, begin to tackle the problem of saltwater intrusion. However, many parameters in these models, such as recharge, are not constant and can vary both seasonally and annually. This leads to an uncertainty within these models, and often will force water managers to err on the side of caution and not utilize the full potential of the groundwater resources. If given the ability to collect real-time, in-situ monitoring data, a warning and response system could be employed to coastal groundwater abstraction sites to safely utilize the full potential – the benefit being a increased yield in fresh water.

A chloride electrode that can be used for continuous, on-line monitoring, could be used for this purpose. Chloride is commonly used as the primary indicator for the detection of seawater intrusion into an aquifer. This is due to the fact that

chloride represents approximately 55% of all of the dissolved solids in seawater, and is a conservative ion, not subject to ion exchange in the sediments. Often water quality standards for groundwater salinity are set with respect to chloride concentrations, with WHO recommending a limit of 250mg/l chloride in drinking water. However, in order for practical use, the chloride electrode would have to provide a reliable signal, have a long life-span, easy to employ and inexpensive.

A simple technology offers a potential solution for a chloride electrode. The use of a small, oxidized silver rod encased in a plastic housing, could in fact be used for this purpose. In fact, the total cost of such a sensor would be less than $10 per piece, and could be continually refurbished for a fraction of that cost. The theory behind this is extremely simple. The sensor is created by taking one end of the silver rod, which is the sensing surface, and electrochemically oxidizing it in a salt solution of either NaCl or KCl. The sensor then can indirectly measure chloride concentrations in solutions, with an ideal Nernstian response of -59mV/decade change in concentration. The application of such a chloride electrode has not previously been tested for continuous application in groundwater. Potential limitations in the practical application of the sensor could be drift and noise in the sensor signal, sensor fouling and a limited life-span of the sensor.

The purpose of this study is to test a chloride electrode produced using the described technique, for application in continuous monitoring. The electrode will be evaluated based on calibration responses to determine the operational range of chloride concentrations and assess its response with respect to the -59mV/decade response predicted by the Nernst equation. Long-term continuous testing will be conducted in the laboratory to look at sensor noise and drift in continuous application. Finally, the electrode will be applied in two different groundwater wells in order to see how the sensor responds in application in the field.

2. METHODOLOGY

The testing of the sensors was conducted to provide an evaluation of the selectivity of the developed sensors towards chloride and its response in seawater. The tests conducted provide an evaluation of the effectiveness of its monitoring for chloride, the durability of the sensors, as well as drift and noise in the continuous signals. The tests were conducted in different environments to determine how the

sensors would perform in practice. The sensors were tested in the laboratory, where conditions, both solution concentration and temperature, could be controlled. Two field tests were conducted in order to test the practical application of the sensors. First, a monitoring well in Greve, Denmark provided a test in reduced groundwater under stable chloride levels. The second test was conducted in a monitoring well in the tidal zone at Wickford, Rhode Island, USA, and provided a test in an unconfined aquifer with groundwater salinity changing with the tidal fluctuations. A description of both study sites is provided in Chapter 2.

2.1 Construction of the sensors

The chloride sensors were constructed using silver rods, 2.5mm in diameter and 2.5cm long. They were encased in customized plastic housing for installation, with one end of the rod flush with the end of the plastic housing (Fig. 1). The other end was attached to a BNC cable, which is connected with the data logger. The end flush with the plastic housing was oxidized using cyclic voltemmetry in 1M NaCl solution, using the silver rod as the working electrode, a platinum counter electrode and a Ag/AgCl reference electrode. One cycle was used, with the potential varying from 0-1000mV at 20mV/sec. This produced a thick oxidized silver surface with an initially light gray in colour, but turning to dark gray to black with time (Fig. 1). After the sensor was rinsed with de-ionized water, it was ready for use.

2.2 Chloride sensor calibration

Calibration of the sensors was conducted in either KCl or NaCl solutions ranging from 10^{-5}M to 1M in concentration. The potential (in millivolts or mV) was measured using a standard laboratory pH/mV meter. Measurements were conducted with a double junction reference electrode, consisting of Ag/AgCl inner electrode in a saturated KCl solution, with an outer solution of ammonium nitrate. The potential curves were plotted on a semi-logarithmic scale, with potential (mV) vs. log concentration of chloride. The curves were then analyzed to determine the electrodes range of operation and response slope (compared to the ideal Nernst slope of -59.1 mV/decade concentration change).

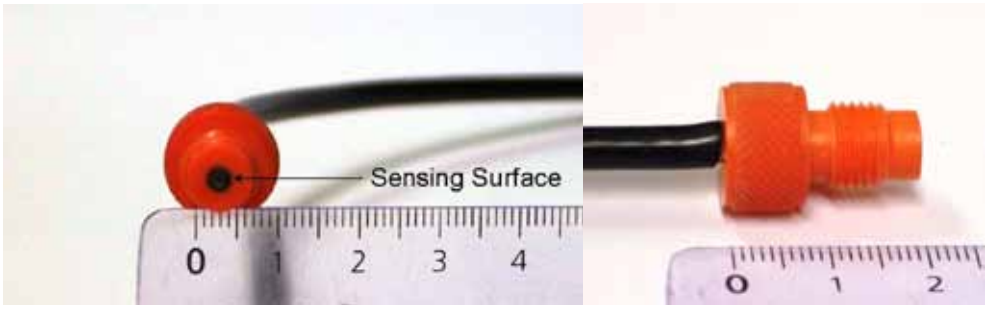

Figure 1. *Chloride sensors used in the study. The sensor consists of a silver rod, 2.5mm in diameter, encased in a plastic housing. The sensing surface is flush with the housing, and oxidized forming a dark gray to black layer. The other end of the silver rod is connected to a BNC cable, which is connected to the data-logger*

2.3 Response to seawater

The chloride sensors were tested to determine whether or not they responded to changes in seawater concentration. Seawater from Køge Bay of the Baltic Sea, with a salinity of 12,000 mg/l total dissolved solids (TDS) (determined from conductivity measurements) was used for the tests. For the tests, the seawater was diluted with de-ionized water to concentrations ranging from 2 to 12,000mg/l TDS.

2.4 Laboratory stabilization and long-term drift analysis

The sensors were tested in the laboratory to determine the length of time for signal stabilization and signal noise and drift analysis. The tests were conducted at varying time lengths from 3 to 30 days. In these tests, water was pumped at slow rates (1-2ml/min) across the sensing membrane of the sensors. The sensing surface remained completely immersed in the solutions for the entire duration of the tests. The tests were conducted in both at stable and varying NaCl concentrations. The stable concentrations were set at $4x10^{-3}$ M NaCl (140 mg/l Cl^-). Stable tests were conducted to evaluate the extent of signal noise and drift. Varying concentration tests were conducted using either NaCl (concentrations varying from $1x10^{-3}$ to $1x10^{-1}$M) or varying concentrations of seawater. These were conducted to determine whether or not the sensors respond to changes in chloride concentrations, and how long it takes for the sensors to respond. The tests were analyzed using a multichannel data logger taking measurements at 1 to 6 minute intervals, depending on the length of the tests.

2.5 Greve monitoring well tests

The sensors were tested in groundwater from a monitoring well (Danish Geological Survey nr. 207.2500) in Greve, Denmark. A description of the location, geological setting and experimental set-up is provided in Chapter 1. The signal was recorded using a multi-channel data logger, with measurements taken at 6 minute intervals. Drift and signal quality were calculated using regression on the raw (uncorrected) data, and through the potential drift (measured from changes in the reference potential, Eo) calculated through the Nernst equation using the technique outlined in Chapter II, which also corrects for temperature. The purpose was to see how the sensors would respond in an actual deployment situation, particularly with respect to the testing in the reduced groundwater in the Greve monitoring well. The test will also provide an evaluation of signal noise and drift in an actual application of the sensors.

For the Greve monitoring well tests, three separate tests were conducted: one for 31 days in June/July 2009, one for 17 days in August 2009, and one for 14 days in September 2009. The July test was conducted in water from the well taken at a depth of 4m below the static water level, and had measured chloride concentrations of 188mg/l at the start of the test (June 26) and 186mg/l at the end of the of the test (July 26). The August and September tests were taken from water at a depth of 12m below the static water level, and had measured chloride concentrations of 44mg/l (August 17) and 51mg/l (September 24). The concentrations were measured from samples collected from the water flowing through the system over an hour, and concentrations were measured through titration of 100ml of the sample in 0.1M $AgNO_3$. Due to the lack of chloride concentration change between the beginning and end of the tests, it is assumed that the concentration in the wells did not change during the tests. This makes it possible to analyze the drift and stability both with the uncorrected data and with the temperature corrected Eo calculations. Different tubing, used to abstract the water from the well, was used in the August and September tests. Standard silicon tubing was used in the June/July test. This tubing has the advantage of being more robust, but is permeable to oxygen, which allows for the oxidation of the reduced groundwater in the system. For the August and September tests, the tubing was switched to low air-permeable tubing in order to prevent oxygen coming in contact with, and thus oxidizing the sample water. During the June/July test, there were problems with the data recorder, where two separate time periods, where data was not logged.

2.6 Wickford, Rhode Island test

Two chloride sensors were tested at the Wickford, Rhode Island site. A description of the location, geological setting and experimental set-up is provided in Chapter 2. The measurements were taken using a multi-channel data logger, recording the measurements at 6-minute intervals. The purpose of this test is to see how the sensors will react in an unconfined aquifer with changing salinity resulting from tidal fluctuations. This provided a test where the sensors were exposed to natural variations of chloride concentrations.

Chloride values from the sensor were calculated using the Nernst equation for the effect of ionic activities on electrode potential, ***E=Eo-59.1 * Log[Cl]*** (as outlined in Chapter 2), where ***E*** is the measured potential, ***Eo*** is the reference potential for the sensor, ***-59.1*** is the ideal response slope for chloride and ***Log[Cl]*** is the chloride concentration. A sample from the well was taken at the beginning of the test, was titrated in $AgNO_3$ and yielded a chloride concentration of 808mg/l. This concentration was used to set the Eo value at the beginning of the monitoring, from which the chloride values for the remainder of the test were calculated. For the calculation of chloride concentrations, both an ideal response slope of -59.1mV/decade and the slope from pre-test calibration were used in the analysis. Noise was filtered out from the signal using a simple algorithm, where any measured difference of over 3mV from the previous measurement was considered noise, and removed from the data set.

The chloride sensors were used in conjunction with a conductivity probe (manufactured by Topac Inc., Cohasset, MA, USA) and newly developed sodium sensors, which were also being tested (described in Chapter 4). Chloride concentrations calculated by the sensors were compared with concentration determined from the temperature corrected conductivity probe values (described in Chapter 2) using a conversion factor of 0.67 times conductivity (μS/cm) to obtain TDS, and multiplying that by 55% (the percent of sodium in seawater) (DOE 1994). It needs to be noted that, according to the manufacturer of conductivity probe, the error of the readings is <5%. Thus there is already a built in error in the conversion from conductivity to chloride concentration. Accuracy, drift, and durability of the sensors were evaluated from the data gathered.

2.7 Nomenclature for the produced sensors

For each produced sensor, a specific nomenclature was used, describing the type of sensor and when it was made. Cl was used to indicate that the sensor is for chloride. The following three numbers show the month and year in which the sensor was produced (i.e. 408 represents April 2008). The numbers are followed by a small letter a, b or c in order to differentiate between the sensors which were produced in the same month.

3. RESULTS

The following section outlines the results from the testing of the chloride sensor. Please note that not all the calibration and long-term tests are shown for the individual sensors, but the data is represented in the tables. These calibration curves and long term tests can be seen in Appendix A.

3.1 Chloride sensor response and calibration

A total of ten chloride sensors were constructed and tested. Overall, the chloride sensors showed a very good response to changing chloride concentrations in solutions of both KCl and NaCl. The response rate varied from -56mV/decade to -44mV/decade, with the average response rate being -50mV/decade (Fig. 2; Table 1).The lower limit of the sensor response was between 3.5mg/l and 35mg/l, with the upper limit being above 35,000 mg/l (Fig.2; Table 1). The chloride sensor is also seen to have a similar response when tested in different concentrations from the seawater collected from the Baltic Sea, where Cl308 was seen to have a 47mV/decade response from a concentration of 30mg/l chloride and above (Fig. 3).

3.2 Continuous laboratory tests

Continuous tests in the laboratory were conducted to determine the noise, stability and drift of the chloride sensors in constant and varying concentrations in a controlled environment. The tests tended to show a steady signal with a stable (negative) drift (Fig. 4) when conducted in steady concentrations of NaCl or KCl.

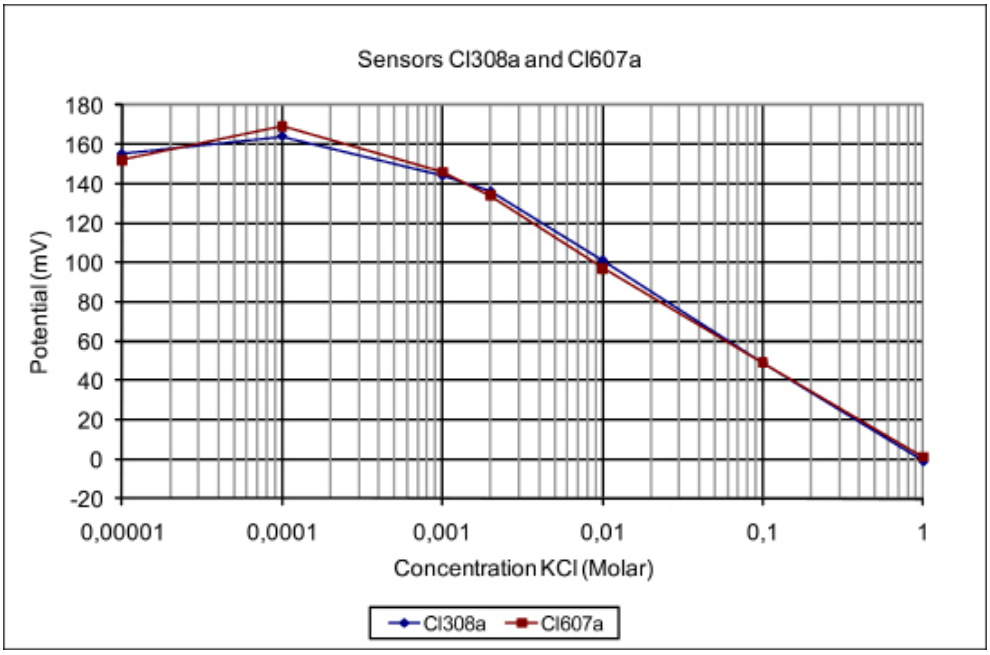

Figure 2. *Calibration curves for two of the chloride sensors tested. All of the other sensors tested showed a similar response to the one showed in this graph*

Table 1. *Calibration statistics for chloride sensors used in the tests.*

	First		Last		Difference		
Sensor	Rate (mV/dec)	Lower Limit (mg/l)	Rate (mV/dec)	Lower Limit (mg/l)	Rate (mV/dec)	Lower Limit (mg/l)	Last measurement
Cl607a	-54	3.5	-49	35	-5	-31.5	Mar-08
Cl308a	-52	35	-51	3.5	-1	31.5	Jun-08
Cl608a	-53	14	-40	35	-13	-21	Nov-08
Cl509a	-52	35	-50	14	-2	21	Jun-09
Cl609a^	-56	35					Aug-09
Cl609b^	-49	35					Aug-09
Cl809a^	-44	35					Sept-09
Cl809b^	-44	35					Sept-09
Cl909a*	-45	35	-43	35	-2	0	Dec-09
Cl909b*	-51	14	-49	14	-2	0	Dec-09
Ave:	-50	25.8	-48.3	22.7	-3.1	3.1	

^ Used in the Greve well tests

* Used in the Wickford tests, September and October 2009

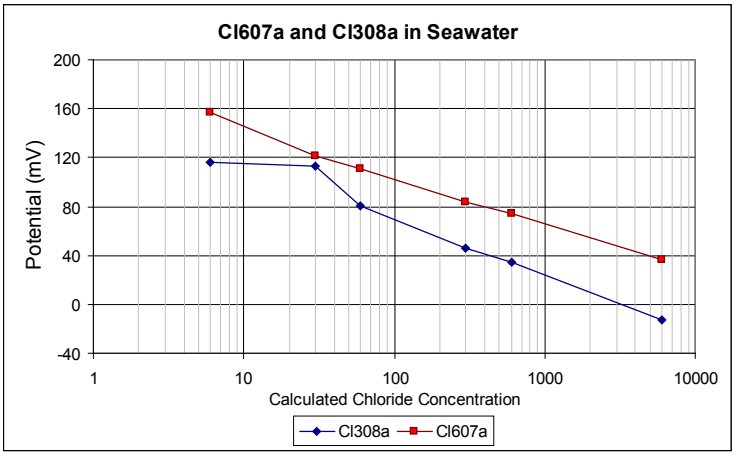

Figure 3. *Response of sensors Cl607a and Cl308a in changing seawater concentrations. The chloride concentrations were calculated from conductivity measurements on the solution.*

The same trend was also observed in the laboratory test conducted in a steady concentration of seawater (Fig. 5).

The observed drift varied from sensor to sensor with Cl607a showing high drift of -2.7mV/day, and a low of -0.5m/day for Cl909a (Table 2). The drift also varied from test to test, where Cl608a showed a variation from -2.2mV/day to -0.6mV/day. Signal noise and stability was measured with respect to the variation from the trend of the drift. The signal was, in general, seen to be stable where the R^2 cor-

Table 2. *Analysis of drift, stability and noise for chloride sensor tests conducted in the laboratory. SD gives the standard deviation from the calculated drift (in mV), the 95% column shows the deviation (in mV) with a 95% confidence interval and n gives the number of measurements in the analysis.*

		Unfiltered Data				Filtered (moving average over 10 measurement periods)					
Sensor Nr.	Test nr.	Drift (mV/day)	R^2	SD	95%	Drift (mV/day)	R^2	SD	95%	Test length (days)	n
Cl607a	1	-2.4	0.97	0.69	1.4	-2.4	0.98	0.57	1.1	6	908
Cl607a	2	-2.7	0.98	0.73	1.4	-2.7	0.99	0.57	1.1	6	998
Cl308a	1	-1.4	0.99	0.14	0.3	-1.4	0.99	0.07	0.14	5	2545
Cl608a	1	-2.2	0.98	0.71	1.4	-2.2	0.98	0.64	1.3	8	895
Cl608a	2	-0.6	0.97	0.41	0.8	-0.6	0.98	0.31	0.6	15	1662
Cl608a	3	-0.7	0.66	0.44	0.9	-0.7	0.7	0.39	0.8	3.5	1119
Cl509a	1	-0.5	0.94	0.1	0.2	-0.5	0.95	0.08	0.2	3	234
Cl909a	1	-0.5	0.48	0.5	1	-0.5	0.48	0.5	1	4	5394
Average		-1.4	0.87	0.46	0.92	-1.375	0.88	0.39	0.78		

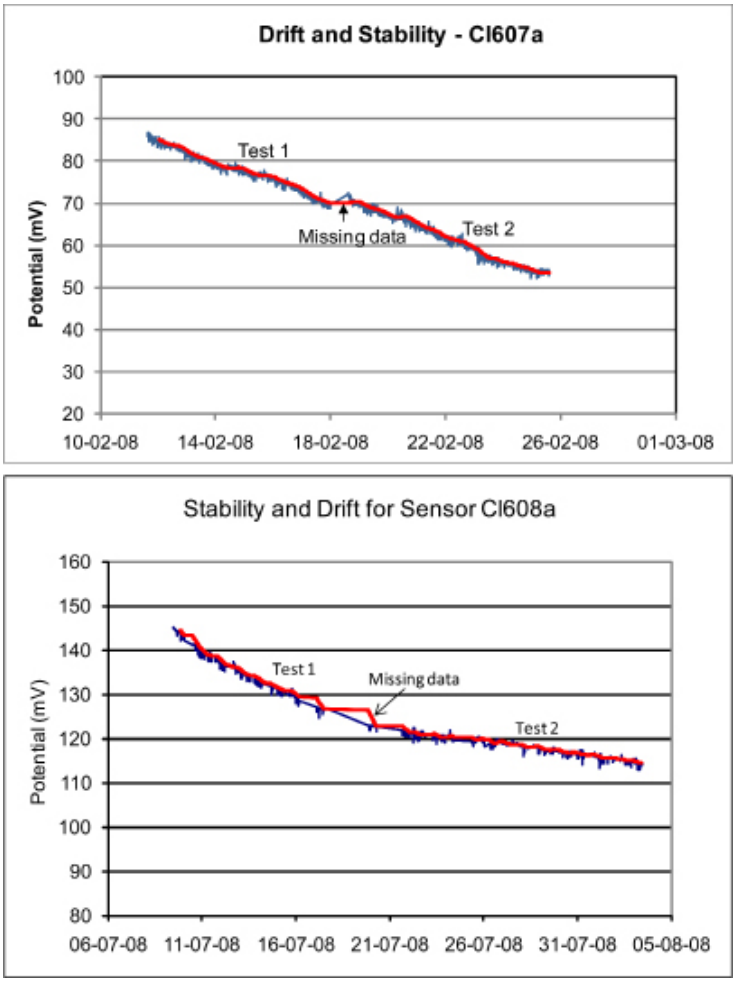

Figure 4. *Drift and stability of continuous measurements for two chloride electrodes. The red lines show the moving average for each test. The plots show a relatively stable signal with a negative drift.*

relation values were over 0.94 in six of eight tests (Table 2). The worst performing sensor, Cl909a, had an R^2 value of 0.48 over a 4-day test (Fig. 6). Signal noise can be quantified by looking at the standard deviation and the 95% confidence interval from the signal trend. The signal noise was seen to be small, with the standard deviation varying from as little a 0.1mV in Cl509a to 0.7mVin Cl607a, test 2 (Table 2). The 95% confidence interval ranged from 0.2mV to 1.4mV, with an average of 0.9mV for all of these sensors. Given an average calibration rate of 50mV/decade, the laboratory tests show that the sensors have a standard error of 4% from the signal drift trend. Even in the worst performing sensor, Cl909a, there was only a 1mV deviance from the trend (Table 2).

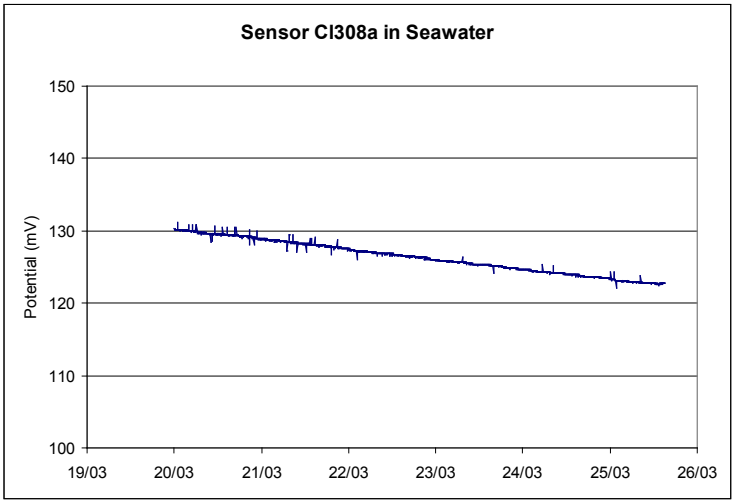

Figure 5. *Drift and stability of Cl308a conducted in a steady concentration of seawater collected from the Baltic Sea.*

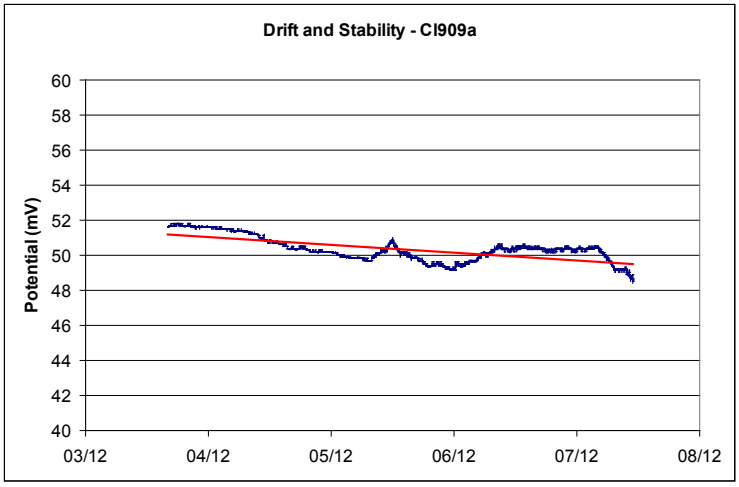

Figure 6. *Drift of sensor Cl909a. The red line shows the trend of the drift and the blue line shows the actual signal from the sensor.*

Simple data filtering processes were used to reduce the noise even further. Using a 20-step (one to two hour) moving average, much of the short term noise can be removed (Fig. 4). The moving average had no effect on the drift or the stability of the sensors, with the drift and correlation data virtually the same as the unfiltered data (Table 2). However, there was a noticeable improvement, as expected, in the signal noise, lowering the average standard error to 0.78 mV, or an error of about 3%.

In the laboratory test with changing NaCl concentrations, the chloride sensor responded very well, reacting immediately to the changes in concentration (Fig. 7). However, the signal, response was seen to be an average of -41mV/decade concentration, which was 10mV less than the calibration of the sensor, which was -51mV/decade. Drift in the signal during this test was seen to be a relatively constant -1.6mV/day, as calculated on from the periods during the test with high chloride concentrations. This is similar to what was observed in the stable concentration tests.

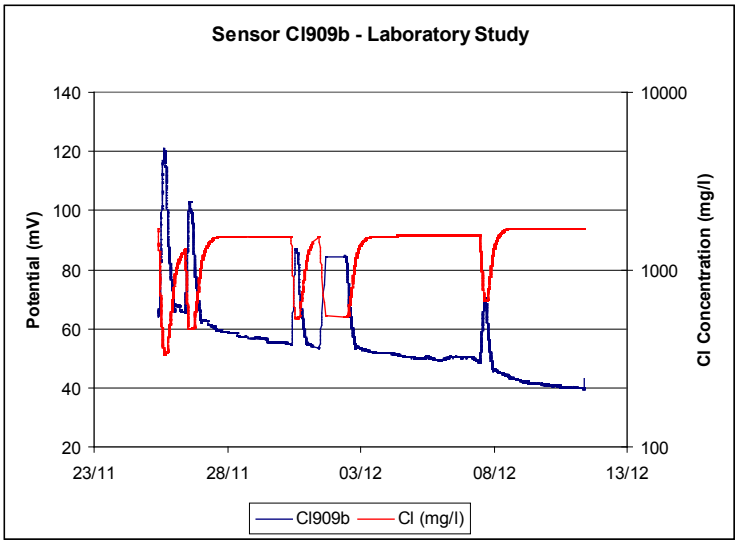

Figure 7. *Sensor test with changing NaCl concentrations. The blue line shows the sensor signal (left-hand axis), where as the red line shows the chloride concentrations (right-hand axis). Note that the sensor reacted immediately after changes in concentration. A sensor drift of 1.6mV/day can also be observed from the plot.*

3.3 Greve monitoring well test results

Three separate monitoring well tests were conducted in Greve. For the June/July test, conducted in the shallower groundwater from the well, one sensor, Cl609b was used. Initial calibration of the electrode showed a response of -49mV/decade from 35mg/l and higher (Table 1). During this test, there were three disturbances observed in the data collection: two periods where data was missing, and a significant 15mV jump in potential during the downloading of the data from the data logger (Fig. 8). Because of these disturbances, the analysis of the data was

divided into two different time periods – the 6 days, spanning from the just after the first period of missing data to the data download, and the next 10 days after the data download to the second period of missing data.

The uncorrected results from the June/July test show a sensor response with more noise and less stability than that measured in the laboratory (Fig. 8). It took the sensor nearly 48 hours to stabilize, where the potential is seen to decrease by 25mV; this was not observed for the sensors used in the laboratory tests. Drift calculated from the sensor's uncorrected data showed an average rate of -0.58mV/day, with

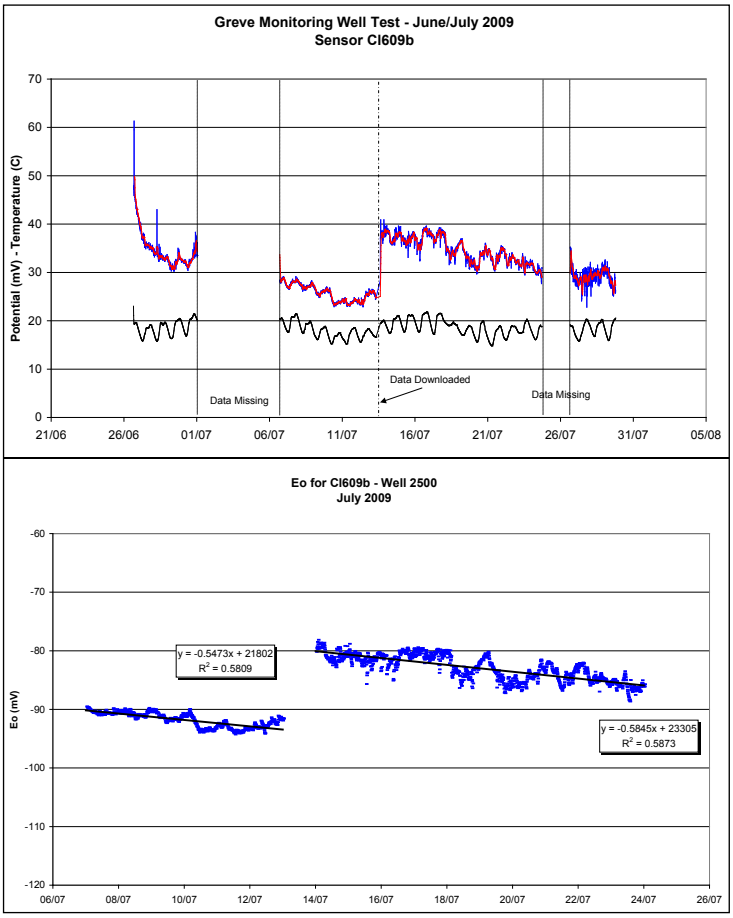

Figure 8. *The upper graph shows the response of sensor Cl609b in the Greve monitoring well. The blue line represents the raw data, where as the red line shows the 1-hour moving average. The solid black line shows the temperature for the measurement period. Note the two periods where data from the sensor is missing. The lower graph shows the calculation of Eo for Cl609b. The y values show the drift, with the R^2 representing the sensor stability.*

less than a 0.1mV/day difference between the two measuring periods (Table 3). However, the stability of this signal was seen to be less, with R^2 values of 0.52 and 0.66 (Table 3). Standard deviation from drift trend is an average of 1.3mV, with a 95% confidence interval of +/-2.5 mV. Given the calibration rate of 49mV/decade for the sensor, this gives a signal error of approximately 10%. When the signal is corrected for temperature, through the calculations of Eo, drift changed only slightly to -0.56mV/day, with an R^2 value of 0.58 and 0.59 (Table 3). There was a slight difference in the standard deviation in both tests (Table 3), decreasing the signal error to 9%. Much of the data noise can be reduced by simply using an hourly moving average (Fig. 8). However, when the drift, stability and standard deviation from the drift were analyzed, the results were nearly identical, with only a slight improvement observed in the stability, with the R^2 value improved by less than 0.05 in both cases. By the end of the test period, it was seen that fouling of the sensors was an issue during this test; the sensors were covered with a thick layer of bright orange ochre from the oxidation of the groundwater moving through the tubing and by the sensors. Subsequent post-test sensor calibration showed no response in changing chloride concentrations.

Table 3. *Analysis of drift, stability and noise for the chloride sensors used in the Greve monitoring well tests. Uncorrected data shows the analysis of the raw signal, where as the drift of Eo incorporates the correction for temperature in the analysis of the drift and stability of the sensor.*

	Uncorrected Data					Drift of Eo					
Sensor Nr.	Test	Drift (mV/day)	R^2	SD	95%	Drift (mV/day)	R^2	SD	95%	Test length (days)	n
Cl609b	Jul1	-0.64	0.52	1.1	2.0	-0.55	0.58	0.9	1.8	6	869
Cl609b	Jul2	-0.71	0.66	1.5	3.0	-0.58	0.59	1.4	2.8	10	1425
Cl809a	Aug	-0.59	0.89	1.0	2.0	-0.59	0.89	1.0	2.0	17	1236
Cl809a	Sept	0.79	0.23	3.4	6.8	0.96	0.31	3.4	6.8	8	596
Cl809b	Aug	-0.72	0.92	1.0	2.0	-0.73	0.93	1.0	2.0	17	1236
Cl809b	Sept	1.6	0.57	3.3	6.6	1.7	0.62	3.3	6.6	8	596

Two sensors, Cl809a and Cl809b were used in the August test (Fig. 9). Both sensors showed an identical -44mV/decade calibration rate, from 35mg/l and higher. The sensors during this test showed a much better response. Uncorrected linear drift was measured at -0.59 and -0.72 mV/day respectively, with very good signal stability (R^2 values of 0.89 and 0.92) (Table 3). Standard deviation was lower, at 1mV in both cases, yielding a 95% confidence interval of +/-2mV. Thus the

uncorrected signal error was 9% based upon the sensor calibration. When the signal is corrected for temperature through the calculation of Eo, no difference in drift or improvement in signal quality was observed (Table 3). However, drift is seen not to be linear in this case, but rather curved, with a higher drift rate in the beginning, the gradually decreasing as the test continues. When the sensors are evaluated with respect to the polynomial curve, they are even more stable, with R^2 values of 0.98 and 0.99 (Fig. 9), and standard deviation of +/- 0.5mV, with a 95% confidence interval of slightly less than +/- 1.0mV for both sensors. This significantly reduced the error for the chloride sensor to just under 5%. In well calibration showed that the sensors were still responsive at the end of the

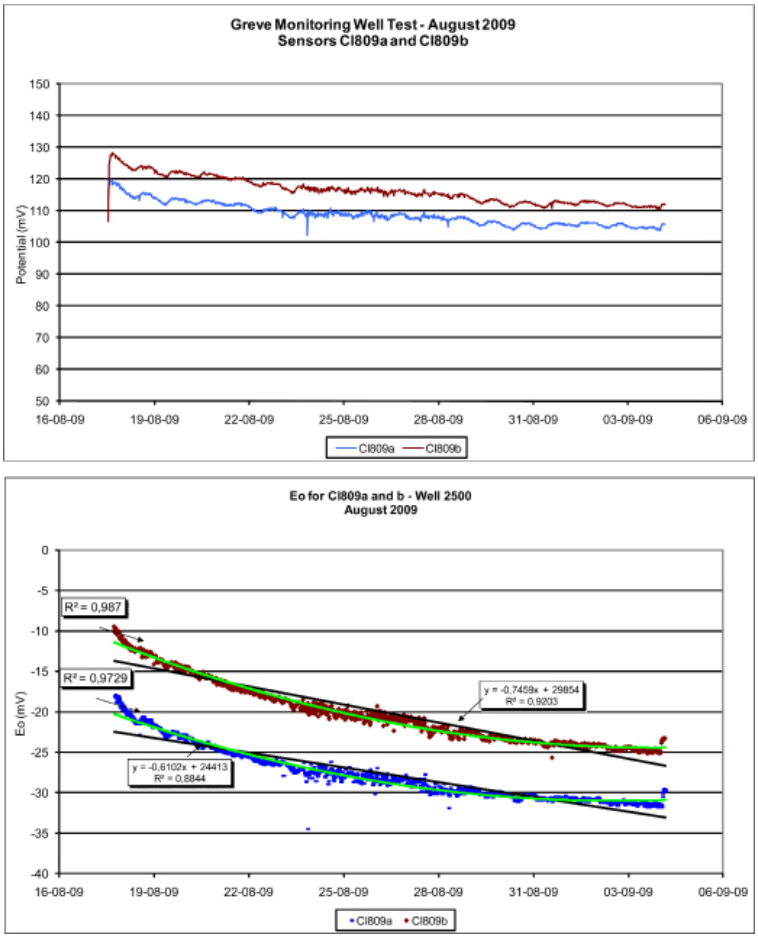

Figure 9. *The upper plot shows the response of the two chloride sensors, Cl809a and b for the August test. The lower plot shows the calculated Eo values. The y values are the linear trend in the drift, shown by the black line. Because the line has a curved shape, the trend is seen to be polynomial, which is shown by the light green line.*

August test, with -45mV/decade (Cl809a) and -46mV/decade (Cl809b) response when tested with prepared NaCl solutions with concentrations from 35mg/l to 3500mg/l chloride.

Because there was no noticeable deterioration in the sensor signal, the testing of both Cl809a and Cl809b was continued in September. However, the sensors for this test did not have nearly as good of a response as in the August test, with the signal being very irregular and having three significantly disruptive events, where there was an immediate jump of 10mV or more in the signal (Fig. 10). The overall drift of both sensors was also significantly different from all other previous tests, now being positive, at 0.79 and 1.6mV/day (Table 3). Standard deviation from the drift was also high, at +/- 3.3 and 3.4mV. The signal error is thus as high as

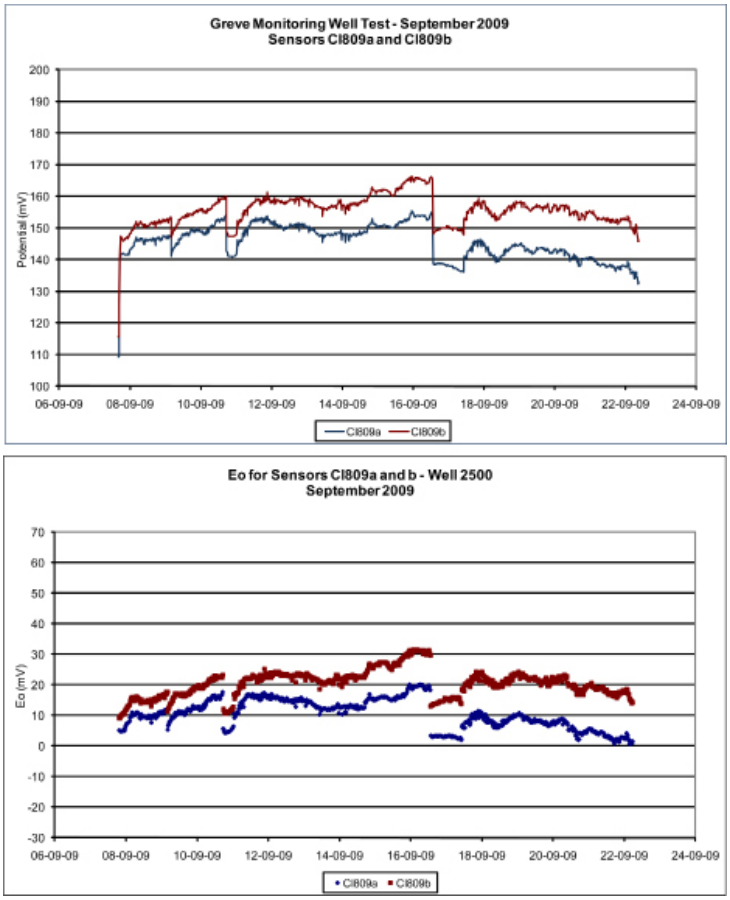

Figure 10. *The upper plot shows the September monitoring well test for sensors Cl809a and b. The lower plot shows the Eo calculations for sensor drift. Note that there were three different signal disturbance events, at 09/09, 11/09 and 16/09.*

30% from the calculated drift in both sensors. Correcting for temperature in the Eo drift calculations did not improve the signal at all (Fig. 10; Table 3). Post-test sensor calibration, however, showed that there was still a good response to changing chloride concentrations, with responses of -42 and -50mV/decade (Fig. 11). Examination of the sensors after the test showed that there was a slight build up of orange ochre on the sensors. This is less than what was observed in the June/July monitoring tests in spite of being in use twice as long. This is likely due to the switch to low air permeable tubing for the collection of the sample water from the well.

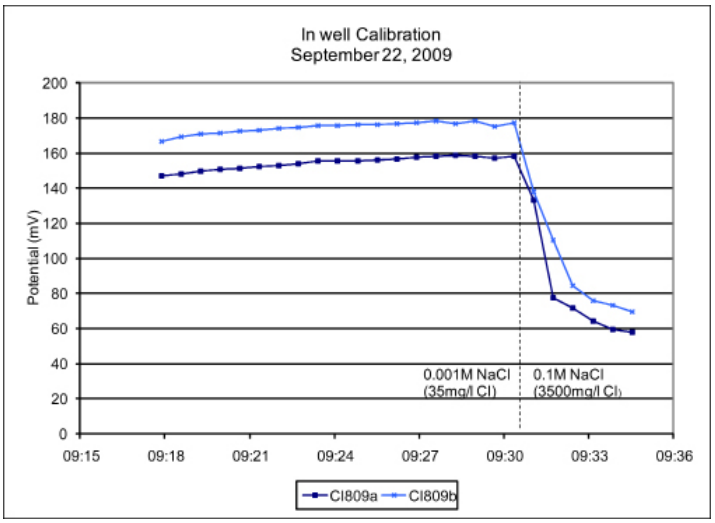

Figure 11. *In well calibration of Cl809a and b after the September monitoring well test. From the graph it can be seen that the sensors still responded quite well to concentration changes*

3.4 Wickford, Rhode Island test results

Two chloride sensors, Cl909a and Cl909b, were used in the Wickford monitoring well test. Sensor Cl909a was operational for the entire test period, and had a very good signal (Fig. 12). The sensor recorded the changes in salinity in tact with the conductivity and the diurnal tidal changes (Fig. 12). The sensor also showed very good correlation to the longer term changes in salinity levels. The raw data from the senor did exhibit a high amount of noise in the signal, particularly around Oct. 9, Oct. 15 and Oct. 19 (Fig. 12). However, this noise could be removed by using a simple algorithm, where any reading with a change of over 3mV from the previous reading was considered incorrect and removed from the dataset.

The result was a much cleaner signal for the entire monitoring period (Fig. 12). There were 3442 original measurements, where 401 measurements (11.6%) were removed as noise during the filtering process.

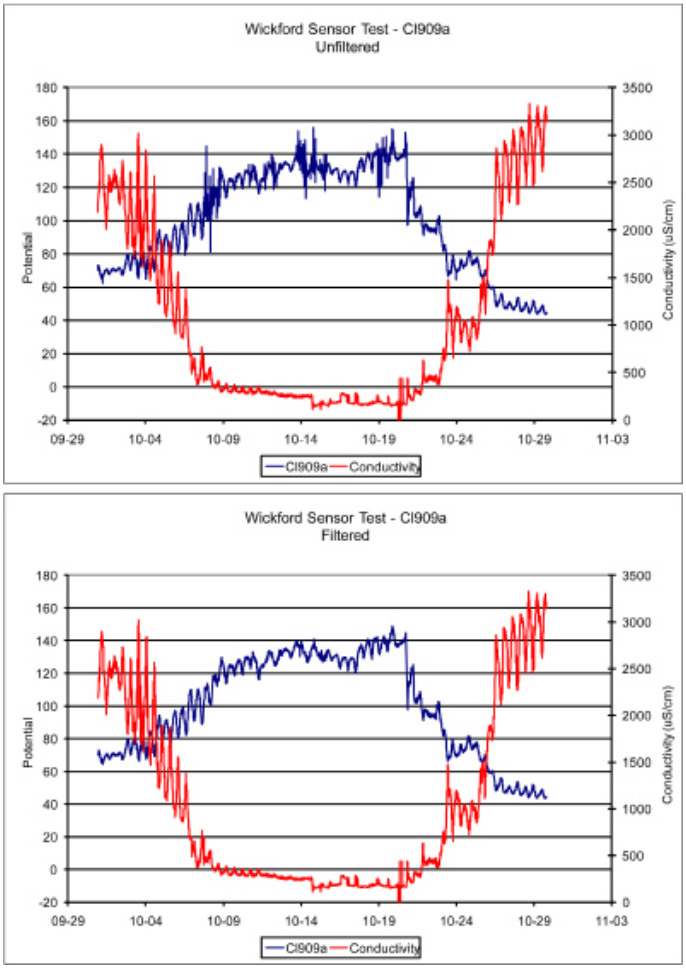

Figure 12. *Response of Cl909a in the Wickford monitoring well. The upper chart shows the unfiltered data together with the conductivity measured at the site. The lower chart shows data filtered, with changes of over 2mV from the previous reading removed. The diurnal tidal levels, as recorded by NOAA at the Newport Rhode Island tide monitoring station, and given in cm from the mean lower low water (MLLW).*

Electrical connection problems in sensor Cl909b made the data for the response of this sensor unusable (Fig. 13). However, there were periods where the sensor did show stability, particularly October 6-7, October 10, and October 15-19. The presumed reason for the fluctuation is a loose wiring contact between the sensor and the data logger, which was observed when the monitoring system was

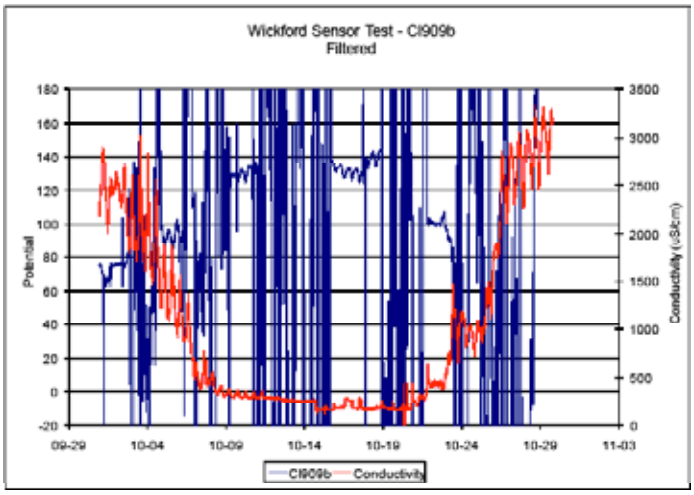

Figure 13. *Results of the Wickford monitoring well test for sensor Cl909b. The sensor was extremely unstable for most of the test, likely resulting from connection problems with the data logger. There were, however, some periods (i.e. from 10/15-10/18) where there was a stable response from the sensor.*

dismantled. Why the sensor turned off and on during the test is not known, but the test did show a response of the sensor to changing chloride concentrations when the sensor was operational. A comparison of the two chloride sensors from October 15 to October 18 (the period with the longest operation for Cl909b) shows that there is almost a perfect match in response between the two sensors (Fig. 14). Therefore, it is presumed that when the connection between the data logger and the sensor was in tact, Cl909b performed as well as Cl909a.

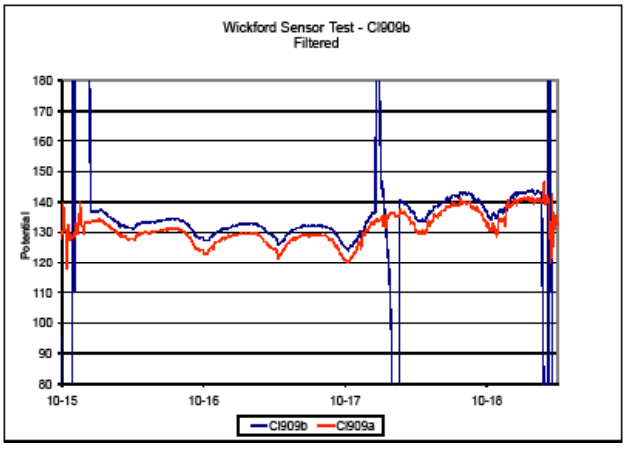

Figure 14. *Comparison of the two chloride sensors in the Wickford monitoring well test for the period between October 15 and October 18.*

Using the equation ***E=Eo-59.1 *Log[Cl]***, Eo for Cl909a was calculated at the start of the test. At the time of the collection of the water sample (September 30), E was measured at 72.8mV, and a temperature corrected slope of -57.5mV/decade was calculated. The concentration of chloride from the sample was measured at 808mg/l. This provides a starting Eo value for Cl909a of -21.3mV.

Chloride values for the duration of the test were first calculated using the pre-test sensor calibration rate of -45mV/decade for Cl909a (Table 1; Fig. 15). When compared with the calculated chloride values from the conductivity probe, there is a greater difference in the two measurements as time goes on (Fig. 15). The correlation between the conductivity and Cl909a measurements is very good, with an R^2 of 0.96; however, the trend is seen to be curved, which suggests either that the calibrated slope was incorrect, or that there is non-linear drift in the sensors. When a ideal Nernstian slope of -59mV/decade was used for the chloride calculations, the correlation was closer to linear, with an R^2 of 0.98 (Fig. 16).

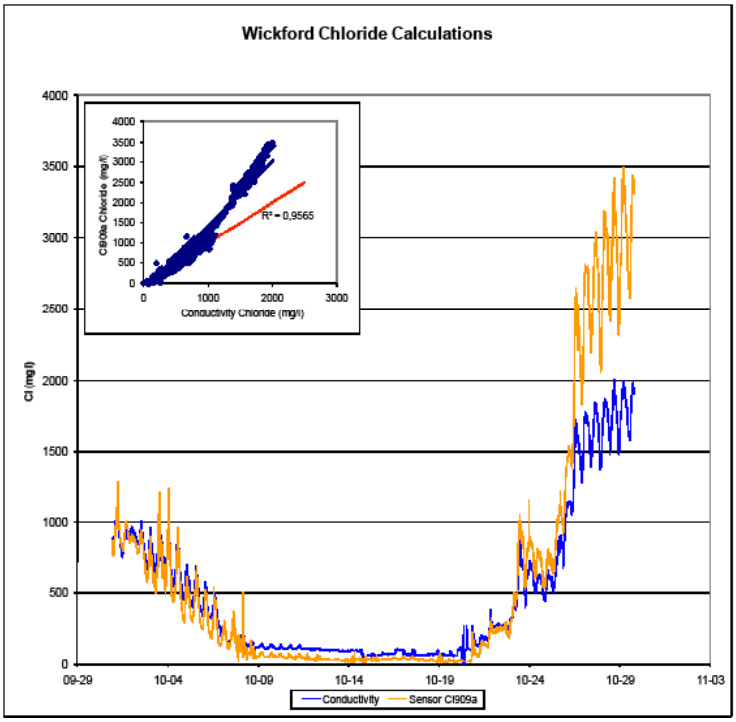

Figure 15. *Calculation of chloride from conductivity and Cl909a. The calculated concentrations from Cl909a were calculated using the temperature corrected calibrated slope of -45mV/decade. The inset plot shows the relationship between the two calculated chloride values. The red line shows the 1:1 correlation. Note the over-estimation of the chloride level by the Cl909a sensor, particularly toward the end of the test.*

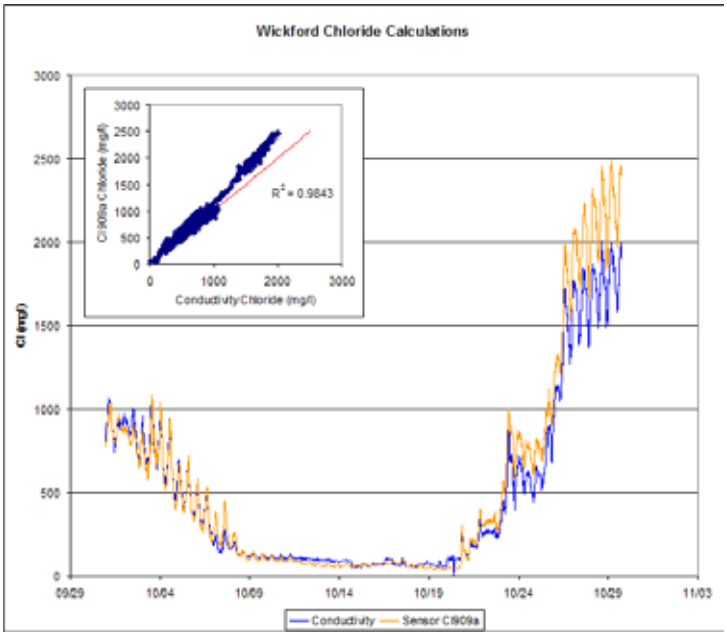

Figure 16. *Calculated chloride values from conductivity and Cl909a, with the signal filtered to remove noise and using an ideal slope of -59.1 mV/decade. The inset plot shows that the sensor and conductivity values are much closer in correlation, with the red line being 1:1. Note the drift affecting the signal particularly at the end of the test.*

There was, however, significant drift in the sensor observed in the later part of the test, from approximately October 20 and on (Fig. 16). In addition, there was observed a disturbance in the signal on October 8, where there was a period with a high amount of noise in the signal (Fig. 12). In the disturbance on October 8, the data indicated that there was an Eo jump of 2.3mV to -19mV. Therefore, the Eo value used after the October 8 disturbance was adjusted to match this level. In addition, the drift of the signal after October 20 was corrected using a steady rate of -0.3mV/day. This resulted in a very good linear correlation between the conductivity and Cl909a measurements, with an R^2 value of 0.996 at a 1:1 ratio (Fig. 17). The standard deviation of the correlation between the chloride measured from the conductivity probe and Cl909a was 34.5mg/l, with a 95% confidence interval of +/-70mg/l.

Between October 12 and 21, the salinity in the groundwater was so low that the conductivity probe used in the study was no longer effective. During that time, the chloride electrode still recorded changes in salinity in tact with the tidal variations, indicating that tides were still influencing the salinities in the well in spite of the

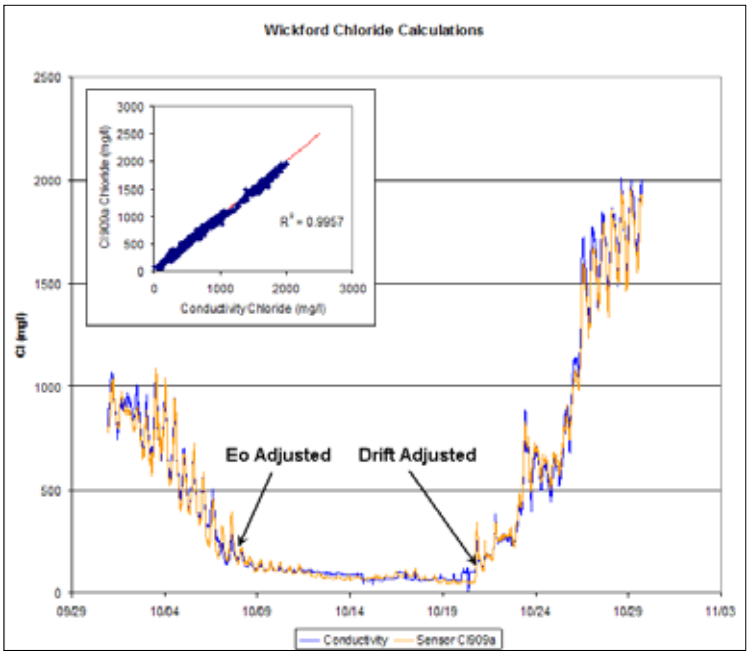

Figure 17. *Calculated chloride levels for sensor Cl909a, drift adjusted on October 8, after a period of a noisy signal (note Figure 15), and adjusted for a drift of -0.25mV/day after October 20. The inset plot shows very good correlation between the sensor and conductivity readings, with the red line showing a 1:1 correlation.*

low overall salinities (Fig. 18). With the conductivity probe no longer responding, the chloride concentration could only be measured using the Cl909a sensor. This showed changes of chloride concentrations of between 20-40mg/l between low and high tide, and an overall concentration range of between 50-100mg/l (Fig. 18). When the conductivity measurements from this period are removed from the overall analysis, the results are virtually the same, with an R^2 of 0.995 and a standard deviation of 39mg/l (Fig. 19).

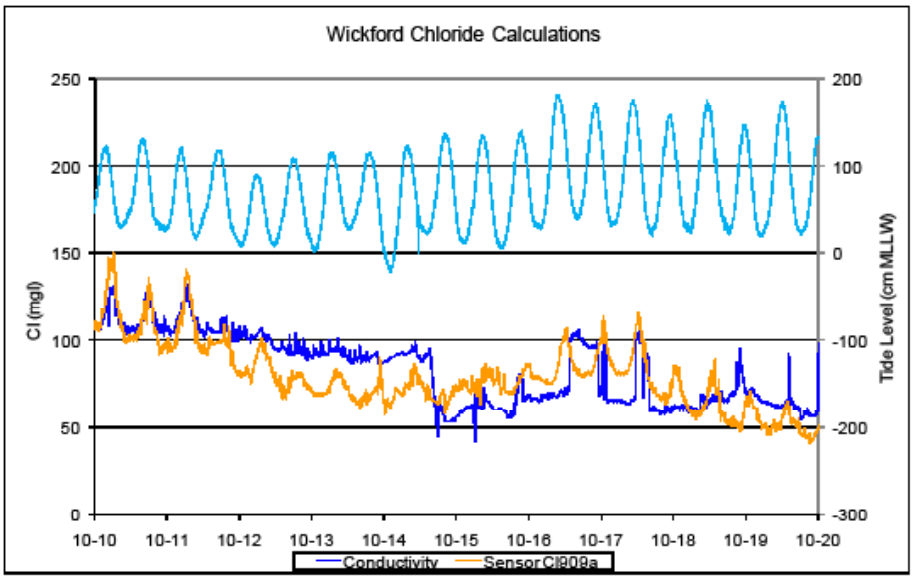

Figure 18. *Conductivity and Sensor Cl909a chloride levels for the period of low conductivity from October 10 to 21. Note how, after October 12 the conductivity sensor fails to respond to the fluctuations in salinity with the tide, where as sensor Cl909a still is sensitive to the tidally induced salinity changes of 20-50mg/l per cycle.*

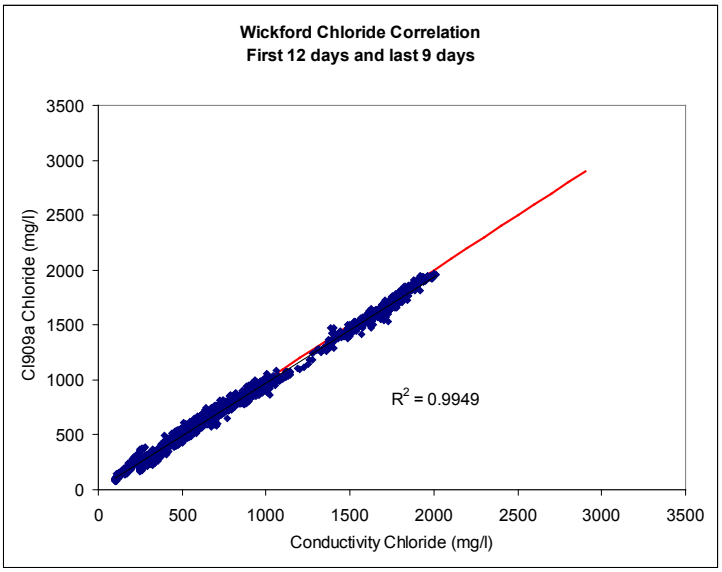

Figure 19. *Chloride comparison between the conductivity and sensor Cl909a. The data between October 12 and 20 are not included in this plot due to the lack of response by the conductivity probe. The red line represents a 1:1 relationship*

4. DISCUSSION

The ultimate purpose of this project is to test a chloride sensor which can be used in continuous monitoring of chloride in groundwater. The relative simple technology of using a small, oxidized silver surface together with a reference electrode provides an interesting possibility. The cost for the development of the sensor – all you need is a small silver rod – is very low, and it is extremely simple to produce. Therefore, this becomes an interesting prospect for application in both research projects and in active monitoring of groundwater quality at, for example, water works. This would be particularly useful in the study and monitoring of seawater intrusion. In order to employ this sensor in a situation for continuous monitoring, both sensor performance and life-span must be considered.

The laboratory tests conducted in this study showed very good promise for the chloride sensor technology. Laboratory calibration tests on the sensor showed a very good and consistent response to changes in chloride. The average response of -50mV/decade response from the chloride sensors is on par with the sensors available on market. This is admittedly lower than the ideal Nernstian response of -59mV/decade. This decrease is most likely due to a combination of signal deterioration and loss through the cables between the sensor and the data logger as well as inefficiencies with respect to the reference electrodes. However, these inefficiencies are common for all ion selective electrodes. The chloride sensors also performed very well with respect to its life-span, where it was shown to be very durable. Apart from the one Greve monitoring well test, the sensors never lost responsiveness during application, and even lasted over a year, though not in constant use. Not surprisingly, fouling is an issue, as was seen in the Greve monitoring well tests, where the sensor became non-responsive due to a thick layer of ochre which covered the sensing surface. Therefore, any employment of the chloride sensor for continuous monitoring, the potential for sensor fouling must be considered, and reduced or eliminated when possible.

Sensor drift is one of the primary obstacles to overcome in the use of ion selective electrodes for continuous monitoring. Studies have shown a wide range of drift, from as much as 12mV/day (Noh and Coetzee 2007) and 5 mV/day (Parra et al. 2009), to as low as 0.2 mV/day (Pawlak et al. 2008), or even no discernable drift (Goff et al. 2003). High sensor drift rates quickly deteriorate the accuracy of the sensor reading, and will require regular and frequent re-calibration; the higher the

drift rates, the more often re-calibration is required. However, if the drift is regular and predictable, drift can be accommodated for automatically without the need for recalibration, through relatively simple mathematical algorithms. The laboratory tests conducted on the chloride sensors did show reasonable drift rates, averaging -1.3mV/day, with standard deviations from the drift at +/- 0.4mV. These trends were seen to be regular and relatively linear, suggesting that there may be the possibility for accommodating the drift automatically through the use of algorithms.

The changes in both the slope and the lower limit provide information on the drift and degradation of the sensor itself. This can be observed changes in slope and lower measurement limit. If drift was the only parameter influencing the signal, then the first and last calibration would remain parallel, with the offset of the measured potential being the drift. As Table 1 shows, there were two sensors which had a significant difference in rate, Cl607a andCl608a as well as lower limit. These differences are likely due to build-up of film, restricting the sensing capabilities, or a physical degrading of the sensor surface. However, the other 5 sensors from which this comparison was possible showed only negligible differences in the response rate and lower limit, and in some cases even improved with the lower limit. This is particularly evident in the sensors used in the Wickford tests, where there was very little degradation observed, in spite of over a month of application in the field. This suggests that the sensors are robust, as long as build-up of films can be avoided.

The application of the sensors in the Greve monitoring well showed mixed results. In the June/July and August tests, with the stable chloride concentrations, showed very good drift correlation. When the signal was corrected for the drift, it gave an error rate of 9% for the 17-days analyzed in the June/July test. The August test performed even better, and when a polynomial drift trend was used for the correction, the signal error was less than 5% over the course of the 18-day test. This is considered very acceptable for use in continuous monitoring. Unfortunately, the well tests also showed that this was not the case for all tests. The September test, using the same sensors as in the August test showed a very unstable signal. When the drift was assessed, the standard deviation from the drift was very high, at +/- 3.4mV, resulting in a signal error of up to 30%. Error of this magnitude would not be acceptable for most applications of the sensors.

The reason for the difference in the quality of the sensor response in the August and September tests is unknown. The sensors were not disturbed in the transition

between the August and September test, with only in-well calibration conducted in between the two tests. The data-logger was turned off for two days between the tests, in order analyze the data to determine whether or not the sensors needed to be replaced. However, replacement was not necessary, so the system was started again without any disruptions. Sensor fouling could play a role for the degradation of the sensor response. However, the September sensor signal was of poor quality from the start. In addition, the in-well calibration conducted at the end of the test showed that the sensors remained responsive at a better rate than the initial calibration. If fouling of the sensors was to be a problem for this test, one would expect gradual signal degradation along with a lack of sensor response to the post-test calibration. The two sensors in the September test did move in tact with each other (Fig. 10), including having the same response to the three major disturbances observed in the signal. This suggests that the answer to the degradation of the signal is not with the sensors themselves. Possibilities include potential problems with the data-logger or even electrical disturbances, possibly via the power supply, affecting the data logger. The sensors themselves were located in a metal box, shielding them from outside electrical disturbances, and shielded BNC cables were used to connect the sensors to the data logger. Thus both the sensors and connection between the sensors and the data logger should have been completely isolated. The reason for the disturbance in the signal remains unknown; however, it does illustrate potential problems which may be encountered when applying the sensors for continuous monitoring.

The Wickford tests provided a good test for the chloride sensors in a natural situation where groundwater salinities change quite rapidly. The overall results showed a very good response of the chloride sensors to the changes in groundwater salinity. The sensor Cl909a, once the noise was removed, showed a very good, clean signal that responded in tact with the tidal fluctuations throughout the entire monitoring period. In spite of the connection problems experienced with sensor Cl909b, when this sensor worked, it showed an almost identical response to that recorded with Cl909a, with the only difference being the sensors reference potential (Eo). This provides a good indication that the response measured in Cl909a is representative for the chloride sensors in general.

Comparison with the conductivity measurements also showed a very good result for calculation of actual chloride values from the sensor. Once the proper adjustments to signal drift and the one disturbance was made, the response from the chloride

sensor was very similar to that of the conductivity probe. The actual response of the chloride sensor would likely be even better than the stated +/-70mg/l when compared to the conductivity probe, due to the fact that the conductivity measurements already have an up to 5% error. Considering the semi-logarithmic response of the chloride sensor compared to the linear response of the conductivity probe, much of the error measured in the lower concentrations will be from the conductivity probe, where as in the higher concentrations, the error will be higher with the chloride sensor. If one assumes that all of the error for the concentrations measured at 2000mg/l in this study came from the chloride sensor, there is only an error of 7% for the chloride sensor, which is on-line with the results from the August test at the Greve monitoring well.

The Wickford test also showed some difficulties in the use of the chloride sensors. The first is the jump in the reference potential Eo on October 8, which corresponded with a period of relatively high noise. In this case the event was easily identified because of the noise in the raw signal. However, in future applications, these jumps may occur without any noise at all, such as those which were observed in the June/July Greve monitoring well test. This could make identifying the timing of the disturbance more difficult. The second problem is the drift associated with the sensor. Drift was not observed in the first 21 days of the test, where after there was observed a relatively stable -0.3mV/day. The linear nature of the drift made it easily correctable, but this might not be the case every time. Both the problem of the signal jump and drift can be corrected for by regular sampling of the water for chloride levels. One of the drawbacks of this study was that only one sample, at the beginning of the test, was obtained. Regular sampling was not taken, as it was assumed that the conductivity measurements would provide the needed chloride concentrations, which it did to some degree. However, more sampling would provide more precise measurements from which the chloride sensor could be adjusted to. Regardless, in studies without conductivity, or other proxy measurements, regular sampling will be needed in order to maintain signal accuracy from the sensors, and correct for the sharp disruptions and signal drift.

There were a number of advantages in the use of the chloride sensor in the monitoring for groundwater salinity. First of all, it provided a very inexpensive alternative, with total costs under $10 per sensor. This is compared with other ion selective electrodes which can cost as much as $1000/per unit. This is also much less expensive than a conductivity probe, where the cheapest start at about $100.

They are also very easy to make, with only a silver rod and a means to oxidize the sensing surface needed. The sensors are very small, and solid-state, making them very easy to use in tight fittings and in custom design settings. The chloride sensors also showed to be responsive even at low salinities, where the conductivity measurements failed. This can have a very practical application for the monitoring of seawater intrusion in coastal groundwater abstraction. The chloride sensors have shown that they respond to concentrations low enough that one can detect very first encroachment of a seawater intrusion wedge towards the well field. This would be the case where groundwater chloride values change from 50mg/l to 100mg/l. This fact, combined with the long durability and stability of the signal, makes the use of the chloride sensors for continuous monitoring of groundwater salinity a possibility. Thus, the sensors could be used to provide well field managers with the needed warning in order to protect the well field and prevent the salinity from contaminating the wells before the salinity exceeds the health limits. The sensors could also be used in pure research projects, such as monitoring the low salinity concentration changes in order to quantify the impact of tides on the groundwater salinity in the coastal zone. These are just two examples where the chloride sensors would be effective, where as the conductivity measurements may be more problematic.

5. CONCLUSION

Over all, the chloride sensors showed promise in the application for continuous monitoring, both in practical situations such as monitoring in well-fields and for research projects. The sensors are very inexpensive and easy to produce, and the small size makes them very flexible in their application. Calibration of all of the sensors showed good and consistent responses in concentrations from 35mg/l and higher. The sensors also showed promise in the use for continuous monitoring, where laboratory testing showed stable sensor signals. However, like most of the ion selective electrodes, drift was an issue and needs to be compensated for. In most of the tests it was seen to be regular, but the drift rate varied from electrode to electrode and from test to test. In all of the laboratory tests, the chloride sensors had an error of less than 5% after compensation for drift. The sensors used in the laboratory tests were seen to be extremely robust, with no sensor seen to become unresponsive, even after over a year of testing, storage and re-calibration.

In the field application of the chloride sensors, the chloride sensors were also seen to be very robust, with only fouling of the sensor surface influencing the sensors longevity. The tests from the Greve monitoring well showed that when fouling was an issue, the signal was a lot more unstable and eventually the sensors became non-responsive. However, when the sensors were not yet compromised by fouling, the signal was very stable, and had a predictive drift, which could be corrected for. The sensors performed very well in groundwater with rapidly changing chloride concentrations. The Wickford test showed a very stable signal, and remained responsive even in the lower chloride concentrations when the conductivity probe was unresponsive. The test also showed that it is possible to correct the signal for disruptions and drift in order to maintain a reliable measurement and conversion to an absolute concentration value for chloride. The with long life-spans in tests in both the laboratory and in the field, with fouling of the surface being the only real threat to the sensor.

In order for the sensors to be applied in a continuous monitoring program, they should have a reliable signal, long life-span, easy to install and preferably inexpensive. The sensors tested in this study showed that they meet all four of these criteria. Combined with a regular groundwater sampling program in order to correct for drift and disruptions in the signal, the sensors could be a very inexpensive and reliable method for conducting continuous monitoring for chloride in both practical applications, such as monitoring for seawater intrusion in operational well fields, or for research projects where continuous data is needed.

Construction and Testing of Sodium Sensors

1. INTRODUCTION

The focus of this chapter is on using two new techniques to develop a sodium sensor for continuous, on-line measurements. Such sensors could provide well-field managers with important information in areas where there is a risk of salinity intruding into the groundwater aquifer. This includes salt from seawater intrusion, road salt, or mobilization of salts from changing in groundwater levels. Chloride, being a conservative ion, is seen as the classic indicator for groundwater salinity. However, the ability to monitor for sodium in tandem with chloride offers a couple of advantages when monitoring for groundwater salinity; namely quality control for the sensors and determination of the source for salinity.

In stead of just relying on one ion, using the sodium and chloride together will give a direct indication on if the sensors are working properly, and provide a warning as to when they might need to be looked at closer. This is possible because these two ions are the predominate constituents in saline groundwater. In the utilization of ion selective electrodes (ISEs), significant signal change can be a result of a malfunction in the sensor itself, malfunction of the reference electrode or a disruption in the monitoring system. Cat ions, such as sodium, have higher electrochemical potential with increasing concentration, and anions, such as chloride have a lower potential. This fact allows the two to work together to provide quality control for the groundwater monitoring. For example, if there is an increasing potential for sodium, and a lower potential for chloride, it will indicate that there is an increasing salt concentration in the water. However, if only one sensor has a signal increase/decrease, where as the other senor remains the same, it suggests that one of the sensors is failing, and should be checked out. If the potential for both sensors move in the same direction, this indicates that there has been a disruption in the system, or drift with respect to the reference electrode. In contrast, if multiple sensors of, for example chloride, were used alone, only the

functioning of the individual sensor could be accounted for, where as drift from the reference or disruption of the system, may not be able to be differentiated from a real signal, and give a false positive.

Monitoring for both sodium and chloride also will provide information on determining and registering changes in the source for salinity. This can be done in the monitoring of changes in the sodium to chloride ratios. Chloride is, as mentioned before, a relatively conservative ion in groundwater. This is in contrast to sodium, which is an active participant in ion exchange with the sediments (Appelo and Postma 2005). For example, under seawater intrusion conditions, sodium is preferentially held back by the sediments, yielding a lower sodium to chloride molecular ratio (in pure seawater, the molecular ratio is close to 1:1). However, when the salt is being washed out, and the aquifer is being freshened, sodium is preferentially released, yielding higher sodium to chloride ratio (Appelo and Postma 2005). Thus, if the monitoring shows that the sodium to chloride ratio is decreasing, this shows that the aquifer is undergoing saline intrusion. When looking at the source for salinity, different sources, such as seawater vs. road salt, will have a different chemical fingerprint. The information on sodium and chloride could provide important information as to whether the salinity in an aquifer is primarily from seawater intrusion or road salt, and provide an indication on when this situation might change with time.

A number of previous studies have shown that it is possible to electrochemically attach different types of thiophene directly on to a gold surface due to the interaction of thiophene's sulphur with the gold surface (Sakaguchi et al. 2005, Sutter et al. 2004, Tran et al. 2008). The direct contact between the gold and thiophene allows for a direct electrical contact the ionophore and the data logger. Two recent studies utilized this possibility by attaching a thin layer of octylthiophene to a gold surface using cyclic voltammetry, then applying a PVC membrane with an ionophore on top of the octylthiophene (Guo and Amemiya 2006, Kim and Amemiya 2008). Here, octylthiophene was the material that could bind with the PVC membrane, allowing conductuctance between the two. However, Si et al. (2007) went one step further by attaching an ionophore directly to the gold surface, rather than using a PVC membrane. The novelty of this study was the ability to successfully attach a thiophene group (3-thiophenecarboxaldehyde) on a 4-benzeno-15-crown-5, which is an ionophore specifically for potassium (Gokel et al. 2004)(Si et al. 2007). The result was a solid-state electrode for potassium, with a near-Nernstian response of

50 mV/decade from a concentration of 4 mg/l and above (Si et al. 2007). According to Nernst's Law, ideal response for sodium and potassium is 59mV/decade at 25°C. This study illustrated the possibility of, if a thiophene group can be successfully attached to an ionophore, electrochemically polymerizing it on to a conducting surface, such as gold, to produce a solid-state electrode.

The crown ether rings are well known to be ionophores for the alkali metals, lithium, sodium and potassium (Bühlmann et al. 1998, Gokel et al. 2004). The different crown rings, 12-crown-4, 15-crown-5, and 18-crown-6, have a specific radius to preferentially bind lithium, sodium and potassium, respectively, in within the crown ether matrix (Fig.1)(Gokel et al. 2004). The potassium electrode developed by Si et al. (2007) used a 4-benzeno-15-crown-5 for its ion selective ionophore. In this case, the addition of the benzene ring on the 15-crown-5 ring changed it properties enough so that the 15-crown-5 ring became more selective to potassium. However, the sensor still registered a cross-sensitivity towards sodium of approximately one order of magnitude less than that of potassium (Si et al. 2007). As seawater contains approximately 45 times more sodium than potassium, when using this sensor for monitoring of seawater intrusion, the sensor would be responding to the sodium concentrations in the water rather than potassium. Thus, it may be possible to use this sensor directly for the monitoring of groundwater salinity.

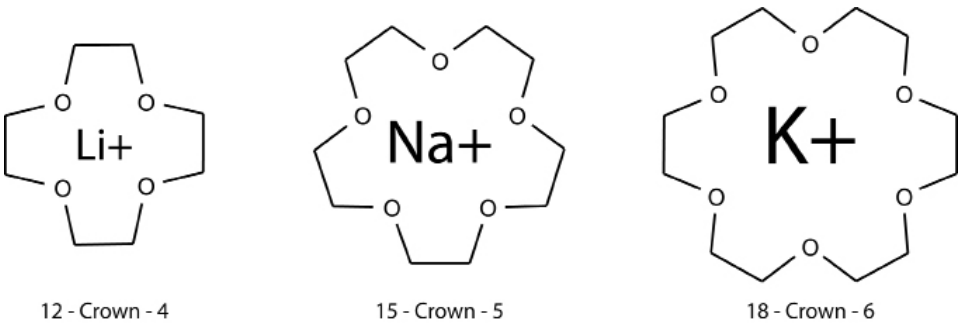

Figure 1. *Drawing illustrating the primary crown ether ionophores. The ring of oxygen atoms in each of the crown ether: Lithium in the 12-crown-4 ring, the larger sodium ion in 15-crown-5 ring, and the even larger potassium ion in the 18-crown-6 ring. Note that potassium will also bind in the 15-crown-5, but to a lesser extent to that of sodium.*

Other 15-crown-5 ionophores used in a sensor could provide a higher selectivity to sodium over potassium (Gokel et al. 2004). However, in order to develop a solid-state electrode, the ionophore must also contain a thiophene group, to allow the

polymerization of thiophene on to the gold surface. Si et al. (2007) showed that, in the development of the potassium electrode described above, it was possible to attach thiophenecarboxaldehyde on to an amine group, utilizing the technique outlined by Patra and Goldberg (2003). It could therefore be possible, using the same technique to attach a thiophene group to a 2-aminomethyl-15-crown-5 ionophore, and subsequently polymerized onto a gold surface. However, the synthesis of this ionophore has not previously been attempted.

Another option to producing a solid-state sodium sensor is through the attachment of a thin PVC membrane containing an ionophore on to a conducting surface. The difficulty in this, however, is that the PVC membrane does not produce an electrical contact with the gold surface directly, and thus no signal is conducted from the membrane to the gold electrode. This problem can be fixed by attaching an intermediary membrane, for example 3-octylthiophene, to the gold surface first, and then apply the PVC membrane with the ionophore. This has most recently been successful in the development of a sensor to monitor perchlorate in drinking water (Guo and Amemiya 2006; Kim and Amemiya 2008). The basis behind this theory is that when octylthiophene is polymerized on to the gold surface, the PVC film surrounds the arms of the octylthiophene molecule, providing an avenue of conductance between the PVC film and the gold electrode (Fig. 2). If a pure ionophore for sodium, such as 15-crown-5, is added to the PVC film, the result should be a sodium specific ISE. However, using this technique to produce a sodium electrode in this manner has not been previously attempted.

These three techniques provide different possibilities for the development of a solid state, on-line sensor for sodium. All three provide the possibility to produce a flexible, low-cost alternative to the commercially available electrodes. This chapter outlines the development and testing of a sodium sensor using these three techniques. First, the potential use of the potassium sensor developed by Si et al. (2007) for monitoring for sodium will be tested and evaluated. Second, the synthesis of a new ionophore with thiophene from 2-aminomethyl-15-crown-5 will be conducted. This will be polymerized on to a gold electrode and tested. Finally, development and testing of a PVC based film containing a 15-crown-5 ionophore attached to a gold electrode will be described. These three different sensors will be evaluated with respect to their success, in terms of accuracy and stability, to conduct continuous, on-line measurements for sodium in changing concentrations of seawater.

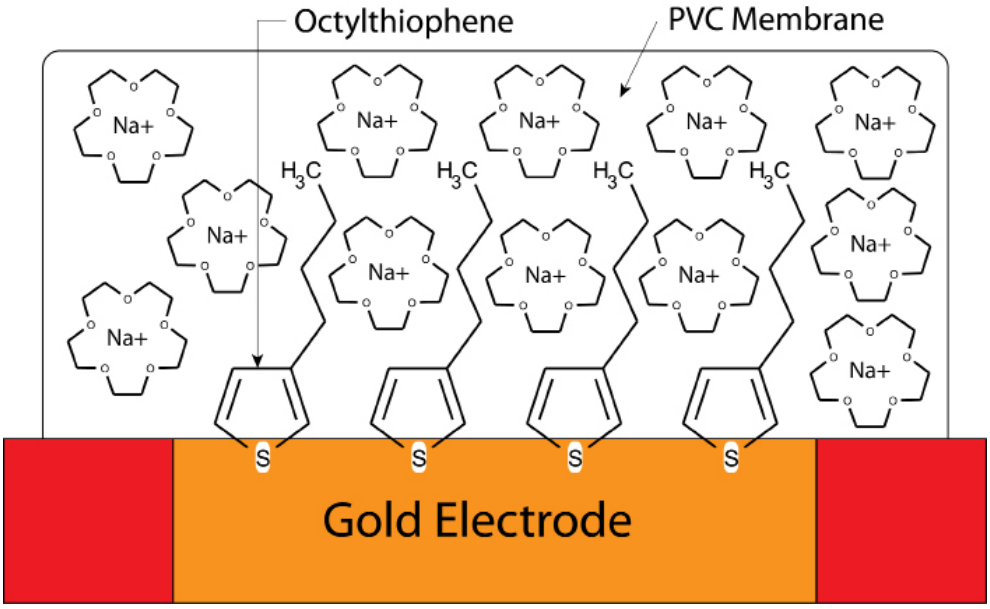

Figure 2. *Diagram showing the construction of the PVC based electrodes. First is a layer of octylthiophene, where the sulfur atoms from the thiophene are polymerized on to the gold electrode surface. A plasticized PVC membrane containing the sodium ionophore 15-crown-5 is applied on top of the octylthiophene layer. The plasticized PVC is permeable in water and the sodium ions to diffuse into and be bound by the 15-crown-5. The potential charge from the ionophore is then transferred through the octylthiophene to the gold electrode.*

2. MATERIALS AND METHODS

2.1 Development of the three sensors

The Potassium Sensor (BTA): The development of the potassium sensor follows the procedure outlined by Si et al. (2007), and is a two step process. The first step includes the cobbling of a thiophene group on to the 4′-Aminobenzo-15crown-5 ionophore for potassium to form a (4-benzeno-15-crown-5) – thiophene-3-methylene-amine (BTA for short). The second step involves the electrochemical co-polymerization of BTA with thiophene on to a polished gold electrode encased in a plastic housing (Fig. 3).

The Sodium Sensor (MTA): The development of the sodium sensor follows the same procedure as for the BTA, except substituting 2-aminomethyl-15-crown-5 for the 4′-Aminobenzo-15crown-5. After the cobbling of the 2-aminomethyl-

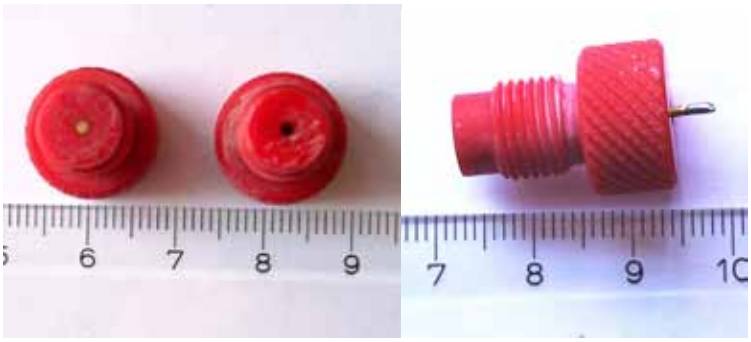

Figure 3. *Photograph of the electrodes used for polymerization. The electrode on the left shows the gold surface before polymerization, and the electrode in the center shows the surface after polymerization. The side view shows the plastic casing with the gold rod extending out. The extension is connected to copper wire, which is then connected to the data logger.*

15-crown-5 to the thiophene group, the ionophore (2-aminomethyl-15-crown-5) thiophene-3-methylene-amine (MTA for short) is produced. This is also co-polymerized on to a gold electrode.

The PVC Sensor (Na): This sensor is developed through a two step process as outlined by Kim and Amemiya (2008). The first step consists of the polymerization of a layer of 3-octylthiophene on to a gold electrode. Then a mixture of poly(vinyl chloride)(PVC), the plasticizer 2-nitrophenyl octyl ether (NPOE) and 15-crown-5 ionophore was dissolved in tetrahydrofuran (THF). A thin coat was applied to on top of the coated gold electrode. The THF was allowed to evaporate, leaving a thin membrane attached to the electrode.

The following subsection provides the specific details of the materials and procedures used to produce the three different sensors for sodium. NMR, IR spectra data, and cyclic voltammograms used to control that the synthesis and polymerization was completed, is provided in Appendix B.

2.1.1 Reagents and materials used

Reagents used include 4′-Aminobenzo-15crown-5 (≥97%, GC), poly(vinyl chloride), and 2-nitrophenyl octyl ether from Fluka; 2-aminomethyl 15-crown-5 (95%), thiophene (≥99%), 15-crown-5 (99%), 3-octylthiophene (99%) and 3-thiophenecarboxaldehyde (≥98%) from Aldrich; methanol (99.9%, GC), dichloromethane (HPLC, 99.8%) and acetonitrile (HPLC, 99.9%), from Labscan Ltd; and tetrahydrofuran (99.5%) and Lithium Perchlorate (≥99%) from Merck. All reagents were used as received.

Gold electrodes for polymerization were produced from pure gold, stretched into thin rods to 1.0mm in diameter. The rods were cut into 25mm lengths and set into a plastic housing, 15mm long. One end of the gold rod sat flush with the plastic housing (Fig. 3), and was polished using a 2μm diamond polishing paste. This polished surface was used for the polymerization of the sensing film. The other end of the gold rod was connected to copper wiring, which was connected to the data logger.

2.1.2 Development of the BTA sensor

The synthesis of BTA was carried out using the procedure attaching an amine to an aldehyde, as outlined by Patra and Goldberg (2003). 4′-aminobenzo-15-crown-5 (2mmol), and 3- thiophenecarboxyldehyde (3mmol) were refluxed in 6ml of anhydrous methanol in a nitrogen atmosphere for 18 hours at a constant temperature of 55°C. The methanol was evaporated off, leaving a cream coloured waxy substance. The product was then purified using TLC plates with an 8:2 mixture of dichloromethane and methanol. The separated bands on the plates, one being the reactant and the other being the product, were scraped off separately, and filtered through methanol to dissolve the product from the TLC plate film. The methanol was then evaporated, leaving again a light brown substance. The structure and purity of the resultant compound was confirmed by 1H NMR (CDCl3, 300Mhz).

Polymerization of BTA on to the gold electrode (described in 2.1.1) was conducted using cyclic voltemmetry. This was carried out at room temperature (23 +/- 2 °C) with a three-electrode standard system consisting of a Pt counter electrode, an Ag/AgCl reference electrode, and an Au working electrode. For the polymerization, 30 mg of BTA, 20μl of thiophene and 100mg of lithium perchlorate were dissolved in 10ml of Acetonitrile. The voltemmetric scans were conducted at potential from 1000 – 2500mV at a rate of 10mV/sec. A minimum of five scans were completed in order to obtain a good, dark brown coating on the gold surface. The presence of BTA on the gold electrode was confirmed medium range IR conducted on an FT-IR spectrometer, Spectrum 2000, using a Pike Technologies Miracle ATR with a diamond crystal plate.

2.1.3 Development of the MTA sensor

The synthesis of MTA, illustrated in Figure 4, used the exact procedure as for the synthesis of the BTA, with the only difference being the substitution of 2-aminomethyl 15-crown-5 in place of 4-benzeno-15-crown-5. The polymerization on to the gold electrode was also conducted in the same manner, with the MTA ionophore substituting for the BTA.

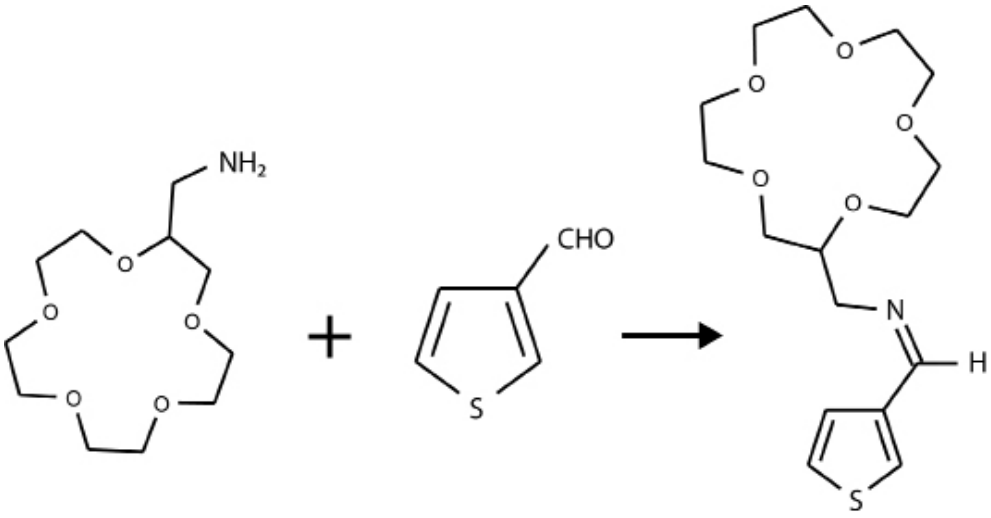

Figure 4. *Synthesis of the MTA ionophore. 2-aminomethyl 15-crown-5 (left) is reacted with 3-thiophenecarboxaldehyde (center). The sulfur on the thiophene can then be polymerized directly on to a gold surface.*

2.1.4 Development of the PVC (Na) sensor

The development of the PVC sodium sensor is based off of the procedure developed by Guo et al. (2006) and Kim and Amemiya (2008). The first step includes polymerization of 3-octylthiophene on to the prepared gold electrode. This was carried out at room temperature (23 +/- 2 °C) with a three-electrode standard system consisting of a Pt counter electrode, an Ag/AgCl reference electrode, and an Au working electrode. For the polymerization, 30µl 3-octylthiophene and 100mg of lithium perchlorate were dissolved in 10ml of acetonitrile. The voltemmetric scans were conducted at potential from 0 – 1900mV at a rate of 10mV/sec. Four cycles were completed in order to obtain a good, dark brown coating on the gold surface. The electrode was rinsed with acetonitrile and then soaked in THF, dissolving the octylthiophene not directly attached to the gold surface. The remaining coat of octylthiophene had a lighter, golden brown colour.

For the PVC film, a mixture of 8mg PVC, 30µl (32mg) NPOE (as a plasticizer), and 3.6µl (4mg) was dissolved in 2ml THF. A thin layer, containing 30-40µl of the mixture was applied on top of the polymerized electrode. The THF was allowed to evaporate off overnight, leaving a thin, clear plasticized PVC membrane containing the sodium ionophore on top of the octylthiophene coated gold electrode.

2.2 Testing of the three sensors

The testing of the sensors was conducted to provide an evaluation of the selectivity of the developed sensors towards sodium and its response in seawater. The tests conducted provide an evaluation of the effectiveness of their monitoring for sodium, the durability of the sensors, as well as drift and noise in the continuous signals. Two commercial sensors, one for potassium from Radiometer Analytical, and one for sodium from Terramentor, were purchased and tested for comparison with the developed solid-state electrodes. The potassium ISE consists of a PVC based membrane with an inner electrolyte solution. The sodium ISE is a glass electrode, also with an inner electrolyte solution.

The tests were conducted in different environments to determine how the sensors would perform in practice. The sensors were tested in the laboratory, where conditions could be controlled both in sodium concentration in the test solutions as well as temperature (which remained relatively constant between 23° +/- 2°C). In the Greve well test, temperature and groundwater chemistry could not be controlled, with the signal needed to be corrected for temperature (see Chapter 2 for explanation on the temperature correction procedure). Because the Greve well was a non-pumping monitoring well, the salinity concentration was stable throughout the monitoring period (see the description in Chapter 2).

2.2.1 Sensor conditioning and calibration

Before use, all of the sensors were conditioned in a NaCl solution, ranging between 0.02 – 1M in concentration. The NaCl concentration in the conditioning had no impact on the subsequent performance of the sensors. Conditioning allowed the Na+ ions to diffuse into the sensing film on the electrodes. Initial conditioning was done for 24hours before the first use. Conditioning of 1-2 hours was sufficient for electrodes taken out of storage. Calibration of the sensors was conducted in NaCl solutions ranging in concentrations from 10-5M to 1M. The potential (in

mV) was measured using a standard laboratory pH/mV meter. Measurements were conducted with a double junction reference electrode. The potential curves were plotted on semi-logarithmic scale, potential (mV) vs. log concentration of NaCl. The curves were then analyzed to determine the electrodes range of operation and response slope (compared to the ideal Nernst slope of +59mV/decade concentration change). Calibration was also conducted in solutions of KCl to provide an indication of the cross-selectivity towards potassium, which has a strong affinity towards the 15-crown-5 ionophores used for the all three ISE's (Gokel et al. 2004). However, the calibration in KCl was not conducted on the PVC sensors.

2.2.2 Response to seawater

The sensors were tested to determine whether or not they responded to changes in seawater concentration. Seawater from Køge Bay of the Baltic Sea, with a salinity of 12,000 mg/l total dissolved solids (TDS), as determined from conductivity measurements, was used for the tests. For the tests, the seawater was diluted with de-ionized water to concentrations ranging from 2 – 12,000mg/l TDS.

2.2.3 Laboratory stabilization and long-term drift analysis

The sensors were tested in the laboratory to determine the length of time for signal stabilization and signal noise and drift analysis. The tests were conducted at varying time lengths from 3 to 30 days. In these tests, water was pumped at slow rates (1-2ml/min) across the sensing membrane of the sensors. The membranes remained completely immersed in the solutions for the entire duration of the tests. The tests were conducted in both at stable and varying NaCl concentrations. When stable concentrations were set at 4*10-3 M NaCl (92 mg/l Na+). Stable tests were conducted to evaluate the extent of signal noise and drift. Varying concentration tests were conducted using either NaCl (concentrations from 10-3 to 10-1M) or varying concentrations of seawater. These were conducted to determine whether or not the sensors respond to changes in sodium concentrations, and how long it takes for the sensors to respond. The tests were analyzed using a multichannel data logger taking measurements at 1 to 6 minute intervals, depending on the length of the tests.

2.2.4 Greve monitoring well tests

The sensors were tested in groundwater from a monitoring well (Danish Geological Survey nr. 207.2500) in Greve, Denmark. A description of the location, geological setting and experimental set-up is provided in Chapter 2. The signal was recorded

using a multi-channel data logger, with measurements taken at 6 minute intervals. The signal was corrected for temperature. For the PVC sensors, drift and signal quality were calculated using regression on the raw data, and through the potential drift calculated through Nernsts equation using the technique outlined in Chapter 2. The purpose was to see how the sensors would respond in an actual deployment situation, particularly with respect to the testing in the reduced groundwater in the Greve monitoring well. The test will also provide an evaluation of signal noise and drift in an actual application of the sensors.

2.2.5 Wickford, Rhode Island test

Two of the PVC sodium sensors were tested at the Wickford, Rhode Island site. A description of the location, geological setting and experimental set-up is provided in Chapter 2. The measurements were taken using a multi-channel data logger, recording the measurements at 6-minute intervals. The purpose of this test is to see how the sensors will react in an unconfined aquifer which is influenced by salt water intrusion as a result from the changing in tide levels. Therefore the sensors were exposed to natural variations of sodium concentrations. Combined with data from the chloride sensors and conductivity measurements, this provided the means to evaluate the effectiveness for the sensors in monitoring for changes in the sodium levels over a month long period. Sodium concentrations for the sensors were calculated from the Nernst equation, as described in Chapter 2, and compared with sodium concentrations determined from conductivity using a conversion factor of 0.67*conductivity (μS/cm) to obtain TDS, and multiplying that by 30% (the percent of sodium in seawater) (DOE 1994). It needs to be noted that, according to the Topac, Inc. (manufacturer of conductivity probe), the error of the readings is <5%. Thus there is already a built in error in the conductivity derived sodium concentrations used in the comparison. Accuracy, drift, and durability of the sensors were evaluated from the data gathered.

2.2.6 Nomenclature for the produced sensors

For each produced sensor, a specific nomenclature was used, describing the type of sensor and when it was made. For each sensor, the first two-three letters in the sensor name indicate the type of sensor: BTA represents the potassium sensors which are tested to determine their applicability for sodium (as described in section 2.1.2); MTA represents the sodium sensor that was polymerised directly on the gold electrode (as described in section 2.1.3); and Na represents the PVC based sensors (as described in section 2.1.4). The following four numbers show

the month and year in which the sensor was produced (i.e. 0408 represents April 2008). The numbers are followed by a small letter a, b or c in order to differentiate between the sensors which were produced in the same month.

3. RESULTS

The following section outlines the results from the sensor tests. The results are presented for each sensor individually. Calibration and stabilization data for the sensors not presented in this chapter is available in Appendix B.

3.1 Results for the BTA sensors

3.1.1 Ionophore synthesis and polymerization results

Initial results indicate success in reproducing the techniques from Si et al. (2007) in the synthesis of the BTA ionophore. NMR results show a shift in 1H peaks along as was expected. The NMR also shows that purification of the BTA ionophore was also successful. Cyclic voltammograms show irreversible co-polymerization of BTA to thiophene during polymerization process. IR spectra data shows that co-polymerization on the gold electrode was successful. Results are shown in Appendix B.

3.1.2 BTA sensor response and calibration

The first sensor polymerized in this test (BTA0707a) showed a very good correlation to potassium of 50mV/decade, from 4 mg/l to above 40,000mg/l (Fig.5). This was along the same lines as in the original study(Si et al. 2007). The BTA sensors were less responsive to sodium, with a correlation of 25mV/decade, from 23 to 2300 mg/l. Subsequent sensors produced later could not duplicate the response for either potassium or sodium (Table 1). The response of the sensors for potassium ranged from as low as 25mV/decade to as high as 50mV/decade (Table 1). The response for sodium was worse, ranging from 25mV/decade to as high as 35 mV/decade (Table 1). As expected, the operational range for potassium was better than for sodium. The operational range for potassium was from 4 to 40,000 mg/l. In contrast, the operational range for sodium was from 2 to 2300 mg/l (Table 1). The best sensor response recorded for sodium was sensor BTA0209b, with a respectable response of 35 mV/decade, with an operational

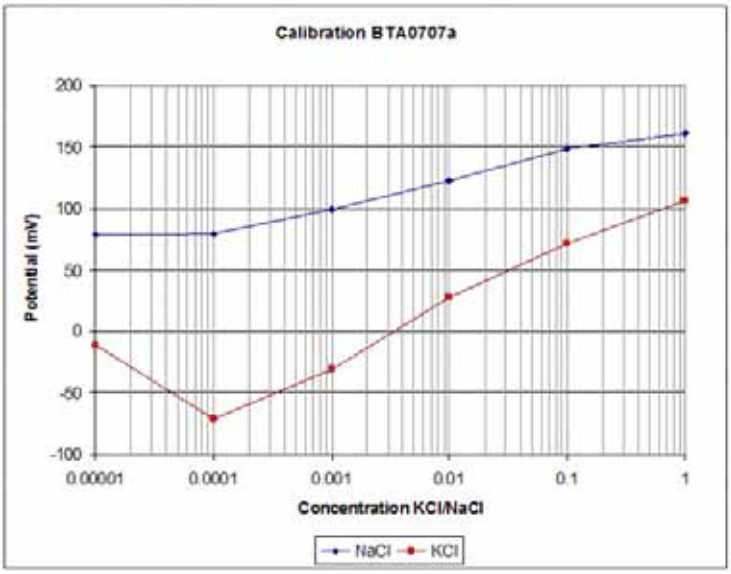

Figure 5. *Calibration curve for sensor BTA0707a. This is an example of a typical calibration curve for the BTA sensor series. Note that the sensor responds better to potassium (KCl) then to sodium (NaCl).*

Table 1. *Calibration data for the BTA sensors.*

Sensor	KCl Calibration			NaCl Calibration			Sensor Life Span	Reason for lack of response
	Rate (mV/dec)	Lower Limit (mg/l)	Upper Limit (mg/l)	Rate (mV/dec)	Lower Limit (mg/l)	Upper Limit (mg/l)		
BTA0707a	50	4	40,000	25	23	2300	6 months	S
BTA0408a	33	4	40,000	-	-	-	7 days	S
BTA0408b	38	4	40,000	-	-	-	2 months	S
BTA0608a	42	4	40,000	32	2	1000	2 months	S
BTA0808a	30	16	40,000	35	23	2300	1 month	S
BTA0808b	32	16	40,000	28	2	2300	1 month	S
BTA1008a	25	16	4000	25	9	2300	NU	IR
BTA0209a	28	4	40,000	27	2	230	2 months	T
BTA0209b	39	4	40,000	35	2	23,000	4 months	T
BTA0909a	-	-	-	30	2	23,000	1 week	S
Commercial K	52	4	40,000	NR	NR	NR	Still Operable	-
Commercial Na	NR	NR	NR	50	2	23,000	Still Operable	-

Sensors that did not work: BTA-0508a and b, 0608b, 0808c, 0908a and b

Note: dashes indicate that tests were not conducted. NR indicates that no response was recorded. NU= sensor not used, S=storage/ conditioning, T=during a stabilization test, IR=irregular/not acceptable response

range from 2 to 23,000 mg/l sodium concentrations, which was comparable to its response to potassium (Table 1). In total, polymerisation of 15 BTA sensors were attempted, with 9 showing some response to polymerization, and 6 failing to show any response altogether (Table 1).

3.1.3 BTA sensor response in seawater

The BTA sensors showed a fairly good response when calibrated in different concentrations of seawater (gradually changing from 12mg/l TDS to 12,000mg/l TDS). The response range of 40mV/decade was observed from concentrations of 12mg/l TDS and above (Fig. 6). A short test in gradually changing seawater

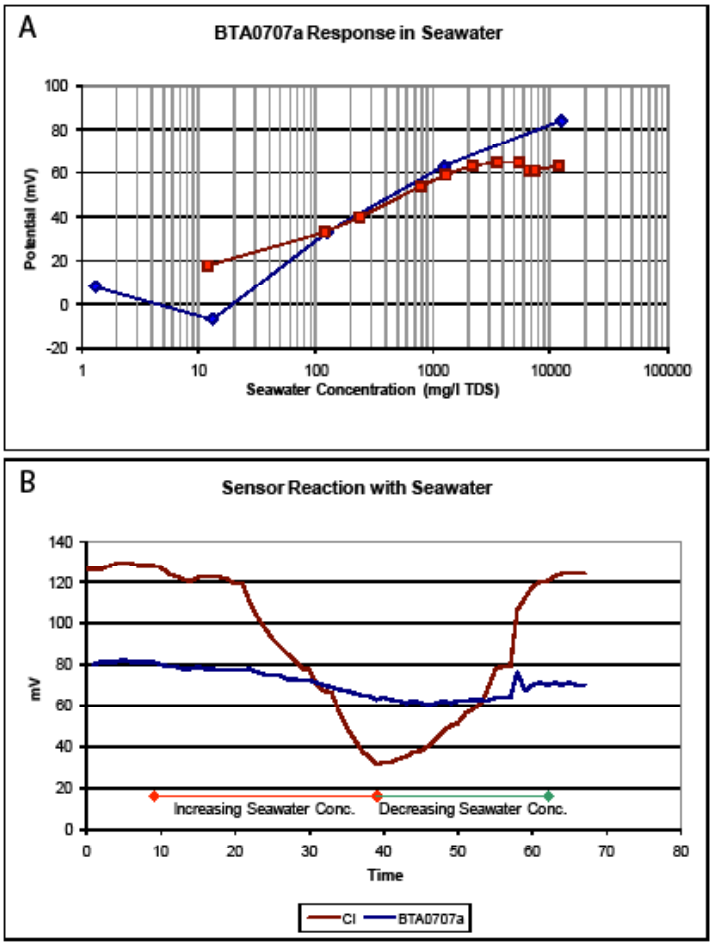

Figure 6. *Response of BTA0707a in saltwater. The upper graph (A) shows the calibration response before and after the test with changing seawater concentrations. The lower graph (B) shows the response under gradual change in seawater concentration. Note that, while the chloride electrode responded to the changes in concentration, BTA0707a did not respond at all.*

concentrations was conducted on BTA0707a. During this test, the sensor signal did not respond to changing seawater concentrations (which is in contrast to the chloride sensor used on the same test) (Fig. 6). However, calibration in seawater afterwards again showed a response in changing seawater, though the signal had deteriorated to 27mV/decade from 10 – 3000mg/l TDS. Connections between the data logger and sensor were not altered between the test with changing seawater concentrations and the subsequent calibration afterwards. It is not known why there was not at least a partial response of the BTA0707a sensor to the changing concentrations during this test.

3.1.4 BTA laboratory test results

Figure 7 illustrates a typical curve obtained from the BTA sensor series when continuously monitoring in a constant sodium concentration. The first 24 hours typically has a significant change in signal until it stabilizes out. The amount that the potential changed before relative stabilization varied from sensor to sensor, as much as 180mV in BTA0808b to as little as 15mV in BTA0608a. Once stabilized, drift was typically recorded to be between 2 mV/day (BTA0808a) and -8mV/day (BTA0408b). In the case of BTA0808a, the drift after stabilization was 3mV/day (Fig. 7). In the laboratory, the signal tended to be steady and clean, with noise being only, +/- 0.5mV. This noise could be easily filtered out by simply using an hourly moving average, or a Fourier transformation. These initial stabilization tests showed promise for longer continuous monitoring tests.

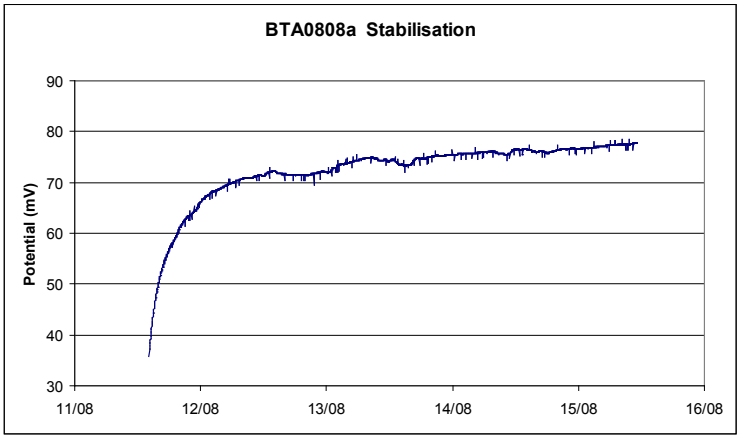

Figure 7. *Example of stabilization of the BTA sensors. Note how there is a sharp rise in potential over the first 24 hours, where after the signal stabilizes out into a more stable drift.*

The laboratory tests with changing concentrations show mixed results. For example, BTA0209a, in spite of a relatively good calibration in NaCl, showed a less than stable signal, and no response to a change in concentration from 230mg/l to 23mg/l Na, which should have been within the response range according to the calibration curve (Fig. 8a). Even more perplexing was a test with BTA0209b. This test varied the concentration from 92mg/l Na in the beginning to 2300mg/l Na, then stepping down to 23mg/l (Fig. 8b). The sensor responded to the first and

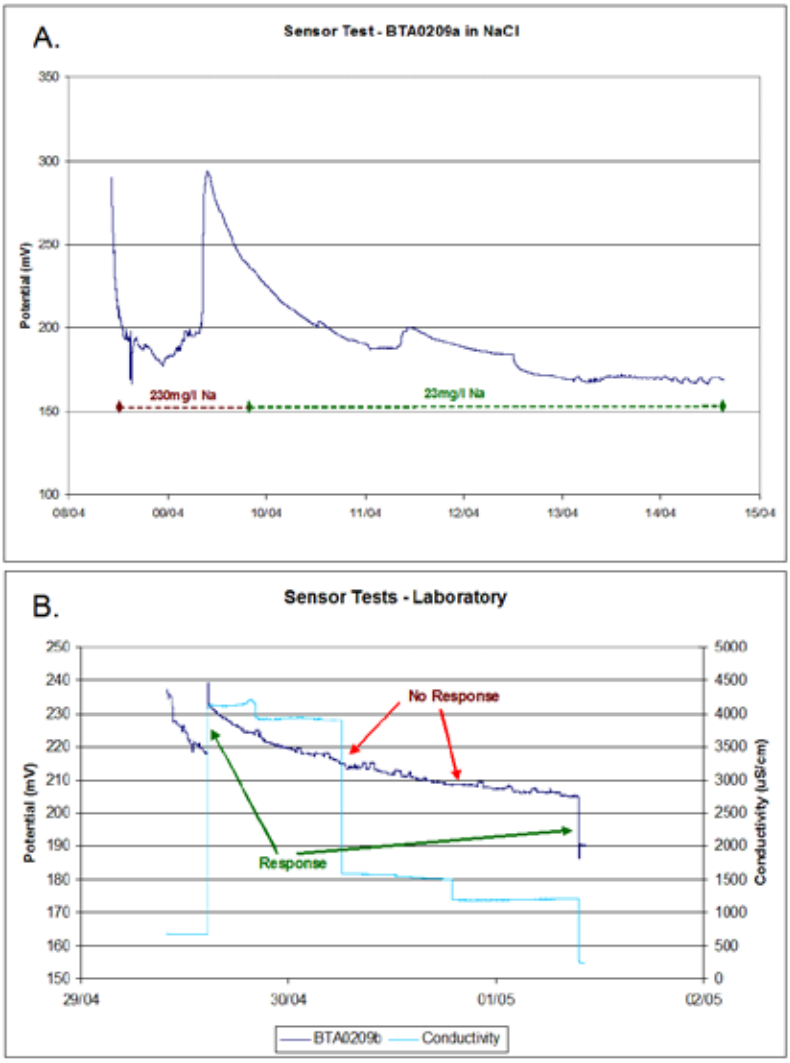

Figure 8. *BTA response in laboratory tests with changing NaCl concentrations. Fig. 8A shows the unstable response from BTA0209a, in which it did not respond at all to the change in NaCl concentration. Fig. 8B shows the response of BTA0209b to the first and last change in NaCl concentration, but not the second and third change.*

last step, but was completely unresponsive in the intermediary steps. According to the calibration of the sensor (Table 1), the changing concentrations fall entirely within its operational range, so there should have been a response.

3.1.5 Greve monitoring well test

Only one sensor, BTA0209b, was tested outside of the laboratory. This sensor had the best response to NaCl of all of the BTA series sensors. In fact, pre-test calibration of the sensor, conducted in June, 2009, showed a response of 35mV/decade Na, from concentrations of 2mg/l and above (Fig. 9a). The application in the well, however, showed less than stable results (Fig.9b). The sensor never really stabilized during the month that the test was conducted. The signal changed

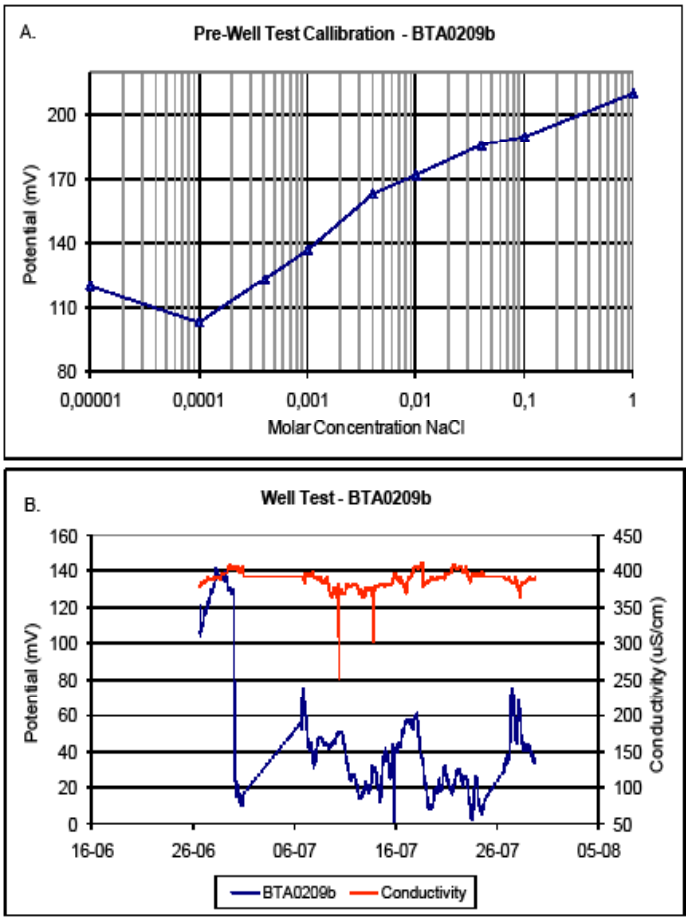

Figure 9. *Results of BTA0209b in the Greve monitoring well test. Fig. 9A shows the pre-test calibration of the sensor. Fig. 9B shows the unstable response of the sensor during the well test. The dashed lines show the periods where data was not recorded by the data-logger.*

rapidly up and down, with swings as high as 40mV within a one-hour period. Conductivity during the same period remained stable at between 350-400μS/cm (Fig. 9b). If the signal was real, the conductivity should have also increased or decreased by a factor of 10. A post-test, in-well calibration of the sensor showed only a 7mV/decade response to NaCl. The sensor was also covered by a red ochre film from the oxidation of iron in the groundwater.

3.1.6 Life span of the BTA sensors

The life span observed for the BTA sensors varied considerably, from a matter of days to 6 months (Table 1). It needs to be noted that the life span of the sensors is determined simply by the length of time between when the sensor was polymerized to when no response was observed during calibration. During this time, the sensors were not used continuously. When the sensors were not in use, they were rinsed off and put into dry storage. In most of the cases, when the sensors became unresponsive, it was when coming out of dry storage. However, most of the sensors with a lifespan of over 1 week were put into dry storage at one time or another, and successfully re-conditioned and calibrated. The most notable is BTA0707a, which was in dry storage, and successfully re-calibrated several times. Sensor BTA0209b was also put into dry storage on three different occasions, where after it was successfully re-calibrated.

3.2 Results for the MTA sensors

3.2.1 MTA ionophore synthesis and polymerization results

Initial results indicate success in using the techniques from Si et al. (2007) in the synthesis of the MTA ionophore. NMR results (shown in Appendix B) show a shift in 1H peaks from the reactants, showing that the reaction did take place. The NMR also shows that purification of the MTA ionophore was also success-ful. Like the BTA sensors, Cyclic Voltammograms and IR spectra data (shown in Appendix B) also show that co-polymerization on to the gold electrode was successful.

3.2.2 MTA sensor response and calibration

The results of the calibration of the different MTA sensors showed variable response. Responses in NaCl calibration solutions ranged from a very respectable 53mV/decade down to as low as 18mV/decade (Table 2). The range of response also varied, with the lower limits between 2mg/l and 23mg/l, with the upper limits

Table 2. *Calibration data for the MTA sensors.*

Sensor	NaCl Calibration			KCl Calibration			Sensor Life Span	Reason for lack of response
	Rate (mV/dec)	Lower Limit (mg/l)	Upper Limit (mg/l)	Rate (mV/dec)	Lower Limit (mg/l)	Upper Limit (mg/l)		
MTA0608a	43	2.3	23,000	40	4	40,000	3 months	S
MTA0808a	25	23	2300	-	-	-	7 days	T – IR
MTA0808b	18	8	23,000	-	-	-	1 month	S
MTA0908a	39	8	23,000	40	40	40,000	2 weeks	S
MTA0908b	30	23	2300	15	40	4000	NU	IR
MTA1008a	55	8	230	-	-	-	1 month	T – IR
MTA1008b	25	8	2300	-	-	-	1.5 months	T
MTA1008c	53	8	23,000	-	-	-	2 months	T
MTA1108a	31	8	23,000	-	-	-	2 months	T
MTA0109a	25	8	2300	-	-	-	4 days	S - IR
MTA0209a	25	2	2300	25	40	4000	2.5 months	T - IR
Commercial Na	50	2	23,000	NR	NR	NR	Still Operable	-
Commercial K	NR	NR	NR	52	4	40,000	Still Operable	-

Sensors that did not work: MTA-0808c, 0209b and c.

Note: dashes indicate that tests were not conducted. NR indicates that no response was recorded. NU= not used, S=storage/ conditioning, T=during a stabilization test, IR=irregular/not acceptable response.

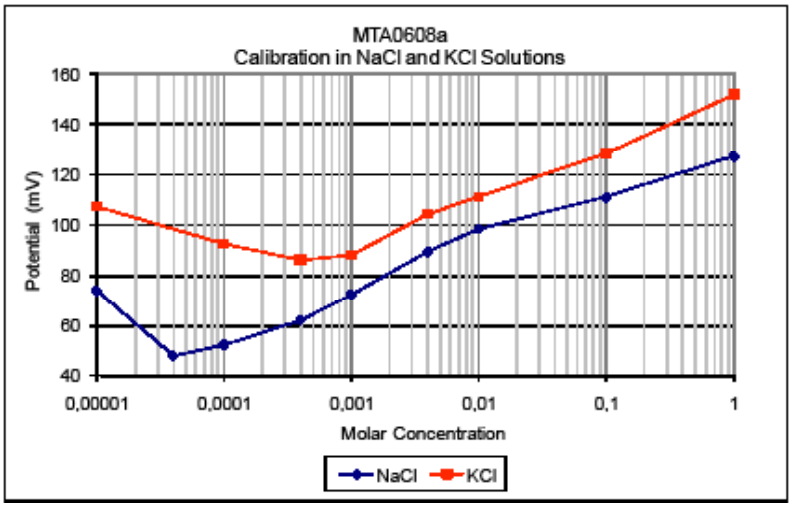

Figure 10. *Calibration curve for MTA0608a in NaCl and KCl solutions. Note how the sensor responded slightly better to sodium than potassium.*

between 2300 and 23,000mg/l (with the exception of MTA1008a). MTA0608a (Fig. 10) and MTA1008c showed the best responses of all the MTA sensors. There was also observed a strong response to potassium by the sensors tested in KCl solution, however, this response was either nearly equal or worse than the response to sodium (Table 2). This, however, is expected, as the 15-crown-5 ionophores are known to have a high cross-selectivity to potassium (Gokel et al. 2004). The sensors showed a good response to seawater as well, equalling their response to Na+. In fact, one sensor, MTA0608a actually performed better in saltwater, with a near Nernstian change of 60mV/decade change in concentration (Fig. 11). In total, 14 sensors were co-polymerized with MTA, with 11 showing a response, and 3 failing to show any response after polymerization.

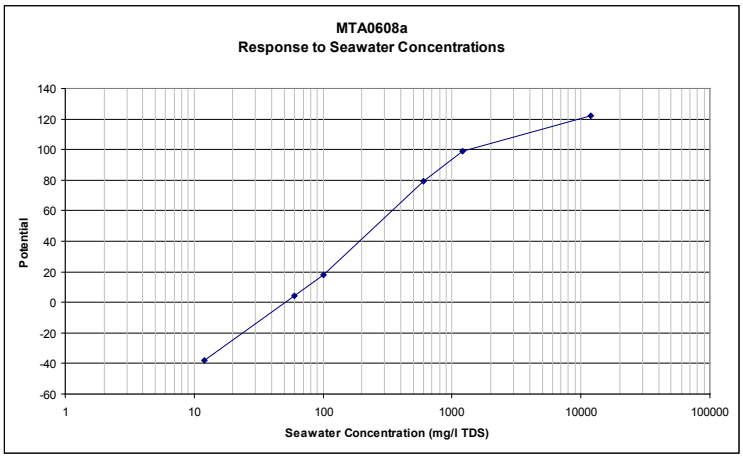

Figure 11. *Calibration of MTA0608a in changing seawater concentrations.*

3.2.3 MTA laboratory test results

The laboratory tests for the MTA sensor series proved to be problematic. Figure 12 shows the stabilization results for the first three MTA sensors produced. MTA0608a and MTA0808b both show similar stabilization pattern to that observed in the BTA sensors, with an initial jump in potential within the first 24hours, then a gradual smoothing of the curve afterwards. The curve is also very smooth, with little noise – +/-0.5mV (Fig. 12). However, MTA0808a showed a much different response, with a very irregular and noisier signal (Fig. 12c). The first two mentioned sensors could not be re-calibrated after put in dry storage for one month, and thus no further tests could be conducted. With respect to the other sensors, MTA0908a could not be tested, as it did not respond after being

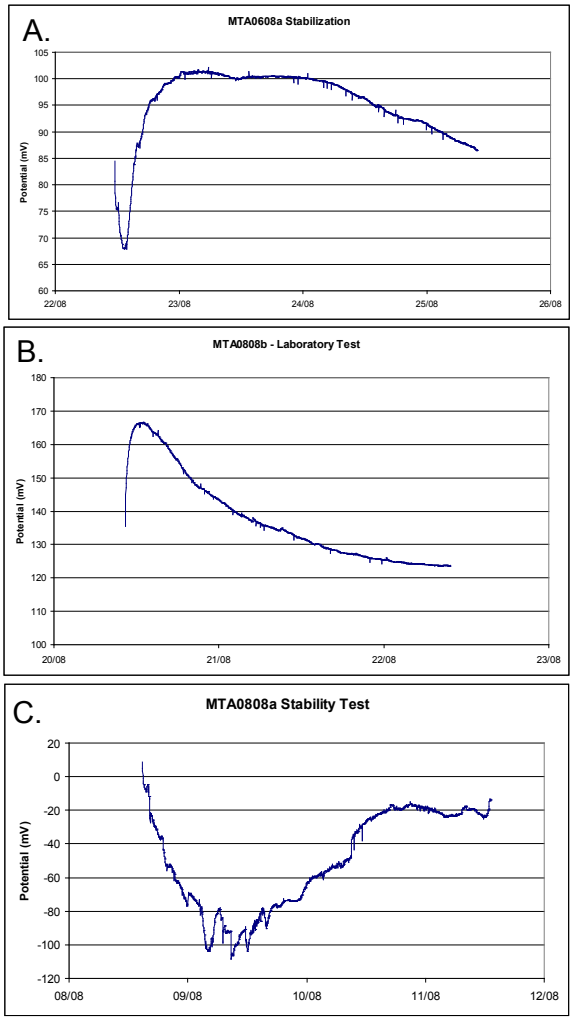

Figure 12. *Signal stabilization for MTA sensors. Note that the first two (A. and B.) stabilize smoothly, with rapid changes over the first 24 hours, then the signal smoothing out, where as MTA0808c (C.) had a much more irregular signal during the test.*

put in storage for the two weeks after the initial calibration. Sensor MTA1008a did not respond at all during its stabilization test in spite of successful calibration after 2 weeks in dry storage. Thus, the first two stabilization tests showed promise for longer term tests, but the overall use of several other sensors subsequently proved to be unreliable.

Laboratory tests with changing concentrations were conducted on sensors MTA1008b and MTA0209a with mixed results (Fig. 13). Both sensors appear to respond in signal when the sodium concentration was changed. However, the

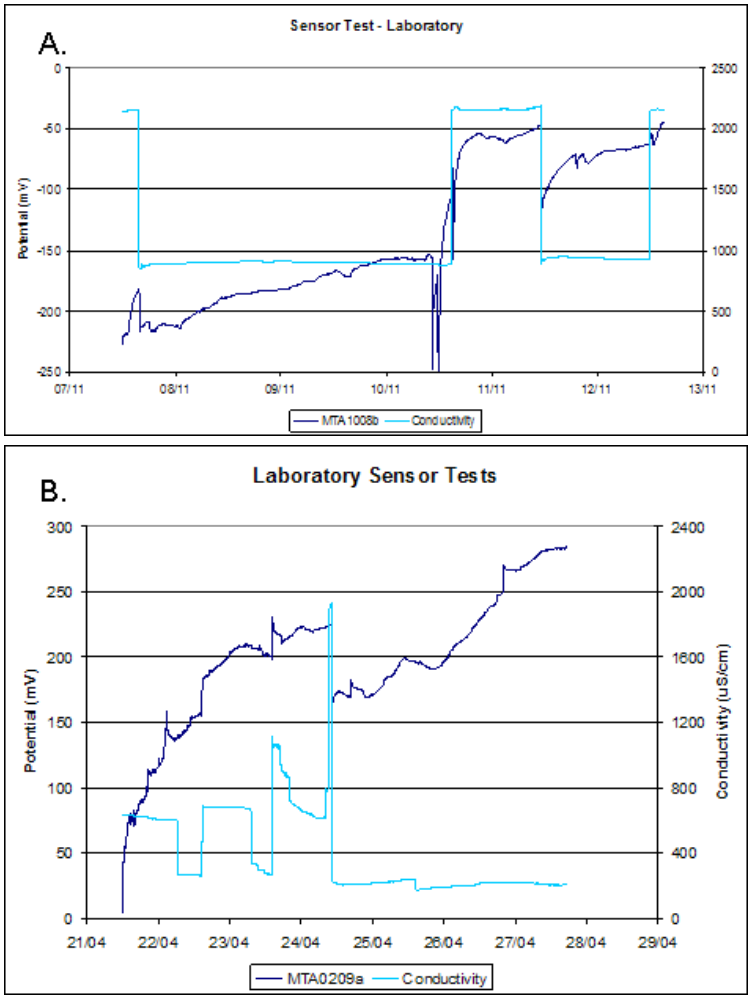

Figure 13. *Laboratory tests on MTA sensors with changing concentrations of NaCl solutions. Response is to the concentration changes is often recorded by the sensors, but is drown out by the unstable signal and high rate of drift observed in the tests.*

signal in between the concentration changes was anything but stable. For example, MTA1008b, from 8/11 to 10/11 measured a continuous concentration, but had an unsteady drift of over 60mV – a rate of 30mV/day (Fig. 13a). This pattern was repeated over the two subsequent concentration changes. MTA0209a appears to respond to the changes when concentration is increased, however there is often no observable response to decreases in concentration change (Fig. 13b). This sensor also had a very poor response with regard to drift, with a very high and unsteady drift rate observed between the concentration changes. Most apparent is the last 3 days of the test, where there was a constant sodium concentration, but there was observed a very unsteady positive drift of over 100mV – again a rate of over 30mV/day (Fig. 13b).

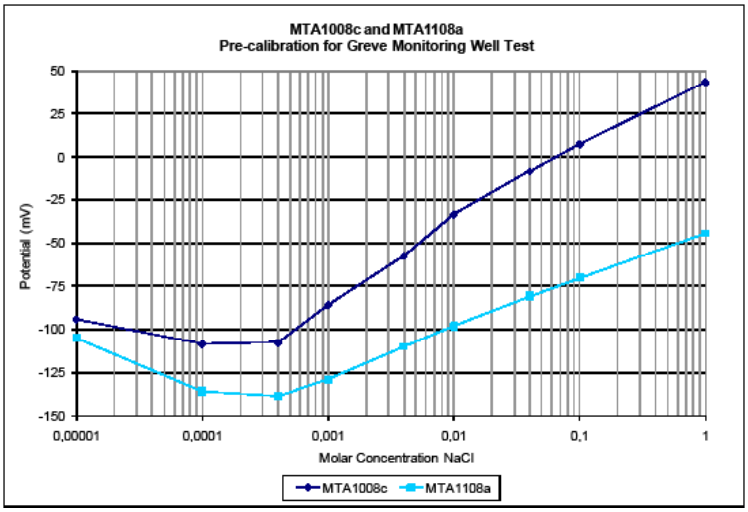

Figure 14. *Pre-Greve monitoring well test sensor calibration. Note that both sensors had relatively good calibration in NaCl solutions*

3.2.4 MTA Greve monitoring well test results

Two MTA sensors were tested in the Greve monitoring well: MTA1008c and MTA1108a. Both sensors showed a good pre-test calibration, with MTA1008c responding at a rate of 53mV/decade, and MTA1108a responding at 31mV/decade (Fig. 14). For MTA1008c, the signal from the sensor was relatively stable but noisy (Fig. 15a). In the relatively constant salinity in the water (measured at 117mg/l from samples taken from the well), the signal moved continuously from -25 to -35 mV, although there is no apparent drift in the signal (Fig. 15a). Upon completion of the test, the sensor was not responsive to post-test calibrations, after less than a week in continuous use. Only slight fouling from ochre was observed on the sensor. MTA1108a was installed in the monitoring well for nearly two months. The observed signal was even worse, with the signal moving up down between -75 and -50 mV for the first 15 days of the test (Fig. 15b). Difficulties were encountered in the middle of this test when the system literally froze on three separate occasions, when temperatures fell below 0°C over extended periods. However, the system stabilized out after 12/01, as can be seen by the conductivity readings (Fig. 15b). After about 5 days of relatively stable behaviour by the sensor, the signal started to degrade, with the signal going completely haywire by 27/01 (Fig. 15b). Upon post-test calibration, MTA1108a had no response, and was coated by a thick orange coat of ochre from the oxidized iron.

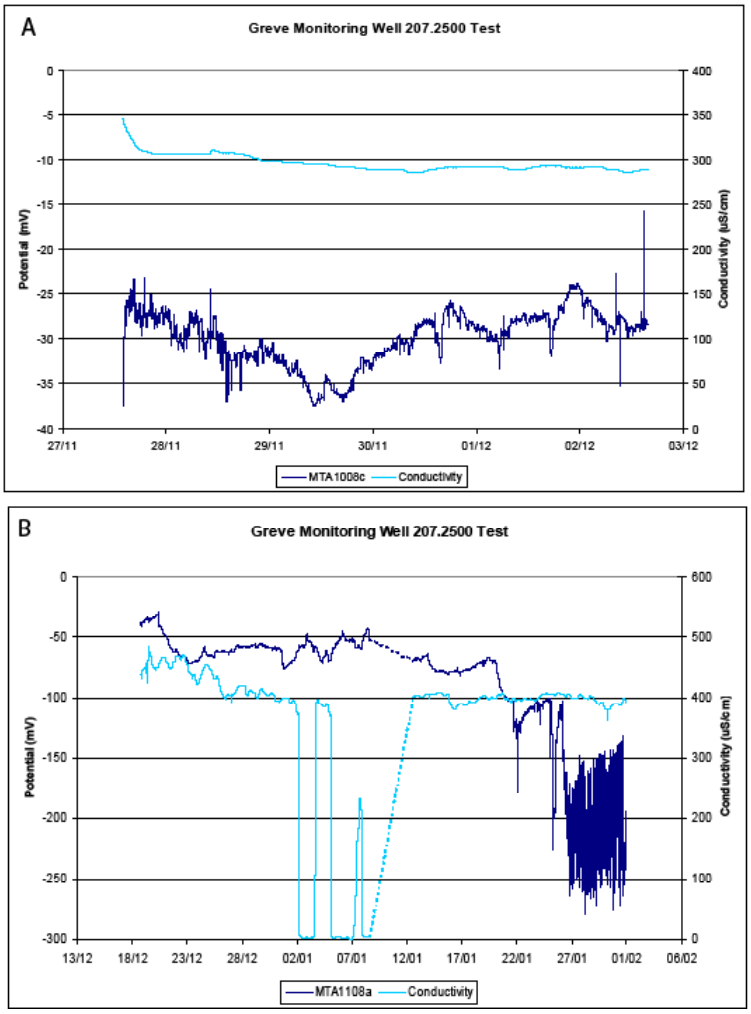

***Figure 15**. Response of the MTA sensors in the Greve monitoring well test. Fig. 15A shows a very noisy, unstable response during the test, in spite of the conductivity remaining stable at approximately 300uS/cm. Fig. 15B shows a similar response for MTA1108a until January 25, where the signal goes completely haywire. In this test, there were three periods where the system froze, which is indicated by the periods where conductivity dropped down to 0uS/cm.*

3.2.5 Life span of the MTA sensor

The life span of the MTA sensors, like the BTA sensors, was variable, lasting from 4 days to as long as 3 months (Table 2). Four of the sensors died in dry storage, where it was not possible to calibrate them coming out of storage. The other sensors had either no, or only irregular response in calibrations conducted after the continuous monitoring tests.

3.3 Results from the PVC sensors

3.3.1 Polymerization and sensing membrane results

In the case of the PVC sensors, no synthesis of new ionophores was necessary, with the 15-crown-5 ionophore readily available commercially. Polymerization of octylthiophene on to the gold electrode was successful, leaving a think dark-brown coat. After soaking in THF, the excess octylthiophene was removed from the surface, leaving a much thinner, golden brown membrane. Application of the PVC membrane was successful, with no problems of the membrane falling off the electrode. IR data for the success of the membrane application was not possible. The plasticizer, NPOE, being the predominant component in the membrane, dominated the signal, with no other components observed in the IR data. The results outlined below, however, confirm the success of the application of the membrane.

3.3.2 PVC Sensor response and calibration

A total of 11 PVC sensors were produced. The observed response in the sensors ranged from 28mV/decade to as high as 45mV/decade (Table 3; Fig. 16). This is much lower than the ideal Nernstian respose of 59mV/decade, but the response was consistent where seven sensors had responses in the upper 30's or lower 40's.

Table 3. *Calibration results for the PVC sensor series. All sensors developed were used in extended tests, and the pre- and post test calibrations are listed in the table.*

Sensor	Pre-test			Post-test			Stability Test Used	Test length
	Rate (mV/dec)	Lower Limit (mg/l)	Upper Limit (mg/l)	Rate (mV/dec)	Lower Limit (mg/l)	Upper Limit (mg/l)		
Na309a	28	10	2300	50	23	2300	Laboratory test	4 days
Na309b	30	2.3	920	X	X	X	Laboratory test	9 days
Na409a	34	10	2300	X	X	X	Laboratory test	14 days
Na509a	44	10	23,000	X	X	X	Laboratory test	12 days
Na609a	44	10	23,000	X	X	X	Greve well test	32 days
Na609b	45	23	23,000	X	X	X	Greve well test	32 days
Na809a	41	23	23,000	X	X	X	Greve well test	30 days
Na809b	31	23	23,000	X	X	X	Greve well test	30 days
Na909a	41	10	23,000	X	X	X	Wickford test	28 days
Na909b	38	23	23,000	5	23	23,000	Wickford test	28 days
Na1109a	37	10	23,000	X	X	X	Laboratory test	30 days

X indicates no response to the sensor in the post-test calibration.

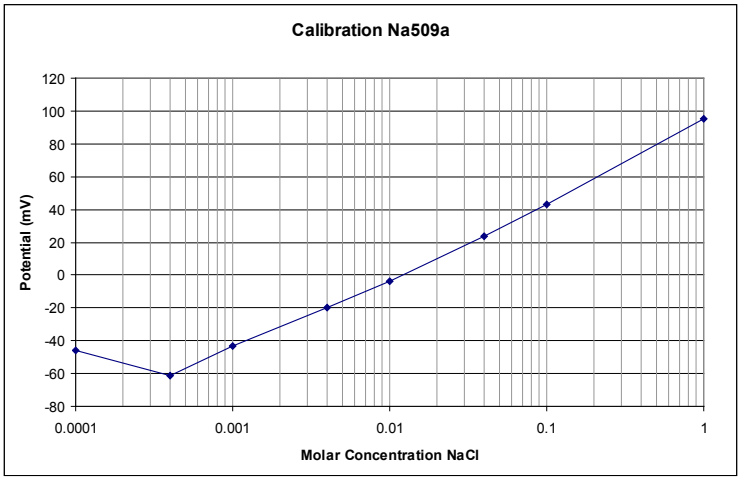

Figure 16. *Calibration curve for PVC sensor Na509a. This sensor shows a very good calibration of 44mV/decade, with the response beginning at a concentration of 10mg/l.*

The range of response was typically between 10 and 23mg/l Na to 23,000, with a notable exception of the first three produced sensors, where the upper limit was lower (Table 3). The production of the PVC sensors proved to be reliable, where all the sensors produced were responsive during calibration. Tests on the sensor response to changing pH concentrations were also conducted for sensor Na1109a. The sensor showed no variation in its potential when the pH was varied from as low as 3 to as high as 9 – the range in which nearly all groundwater falls.

3.3.3 PVC laboratory test results

The laboratory tests on sensor stabilization conducted on Na309a and Na409a

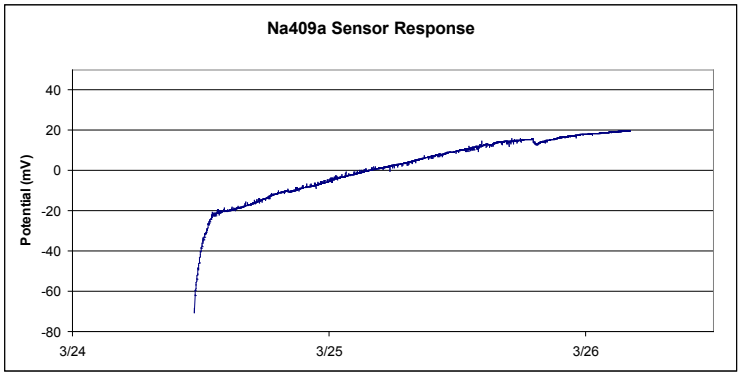

Figure 17. *Sensor stabilization for PVC sensor Na409a. This shows a typical response, with an initial swift rise in potential in the initial stages of the test, with the signal stabilizing out to a more consistent drift.*

reveal a similar response to that of both the BTA and MTA sensors. There was observed an initial stabilization period of about 12-24 hours, with an initial shift of 20 mV in Na309a and 40mV in Na409a where after the stabilized, with gradually less drift in the signal (Fig. 17). The signal for Na309a was seen to be fairly noisy, +/- 3mV, where as the signal from Na409a was very clean, +/-0.5 mV (Fig. 17).

In the laboratory tests with changing concentrations, the PVC sensors showed a good response to changing concentrations over the first few days, with the signal degenerating thereafter. Figure 18 shows the response of Na0509a to changing concentrations. The sensor responded to the first three changes in concentration during the first three days of the test. However, at the fourth change in concentration, the sensor started to react, but then reverted back to its pre-change potential, where after the sensor was no longer responsive to changes in sodium content (Fig. 18). The signal between the concentration changes also degraded during the test, starting out fairly stable with a drift of about 3mV between the first and second change, becoming more unstable between the second and third change, and third and fourth change (Fig. 18). Other sensors tested were also observed to become non-responsive after a few days in continuous monitoring. Na309b, Na409b and Na1109b all lost responsiveness within a week of continuous application (Table 3). Only Na309 survived a 4-day test, where the response rate improving to 50mV/decade from 23mg/l to 2300mg/l. However, in four of the five laboratory tests, the sensor failed to survive more than seven days of testing.

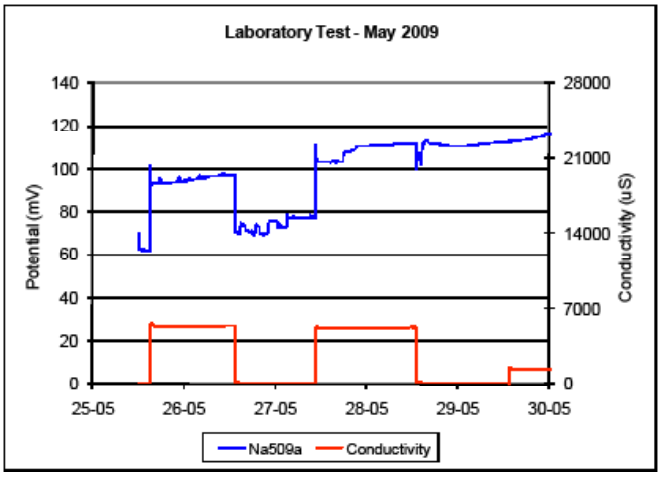

Figure 18. *The response from Na509a tested in the laboratory with changing sodium concentrations. The sensor responded as expected in the first 2-3 days of operation. Although the sensor began to react to the concentration change on May 28, in the end, no change was recorded, and the sensor did not respond to any subsequent changes in sodium concentration.*

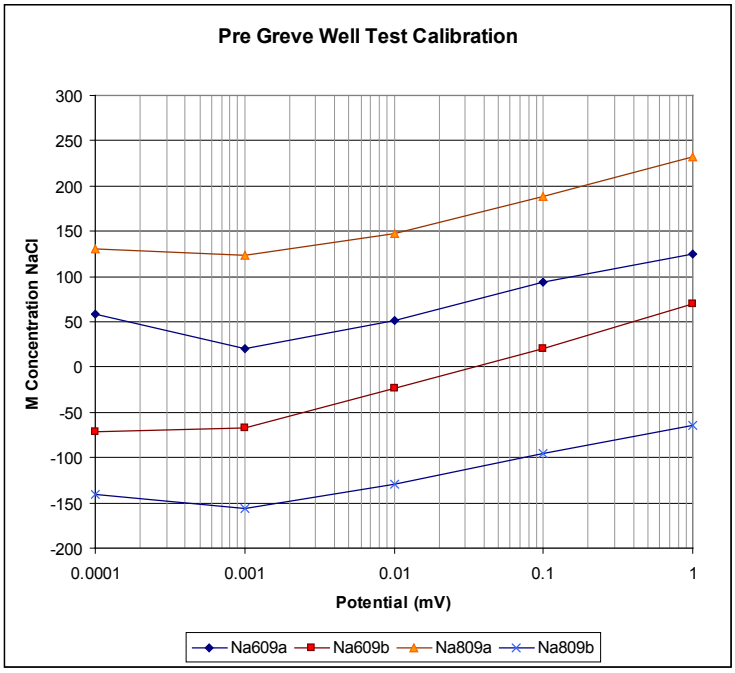

Figure 19. *Calibration curves for the four PVC sensors tested in the Greve monitoring well. All four sensors had good calibration before the test*

3.3.4 PVC Greve monitoring well results

Four PVC sensors were tested in the monitoring well at Greve. The first two sensors, Na609a and Na609b, were tested in waters taken from a depth of 4m below the water level in the well. The second two sensors, Na809a and Na809b, were tested in waters taken from a depth of 12m below the water level in the well. All four sensors had very good initial calibration responses to changes in NaCl concentrations prior to deployment in the monitoring well (Fig. 19).

During the monitoring well tests, the sodium remained constant at 117mg/l in the June/July test conducted in the shallower groundwater, and at 37mg/l in the August/September test conducted in the deeper groundwater. The sodium content was analyzed using Atomic Absorption from water samples collected during the test. The constant concentrations provided the opportunity to assess the quality of the signal (noise) and the observed drift, as well as the durability of the sensors. It needs to be noted that during the July test, data is missing from the data logger for two periods, one in early July and one in late July (Fig. 20a).

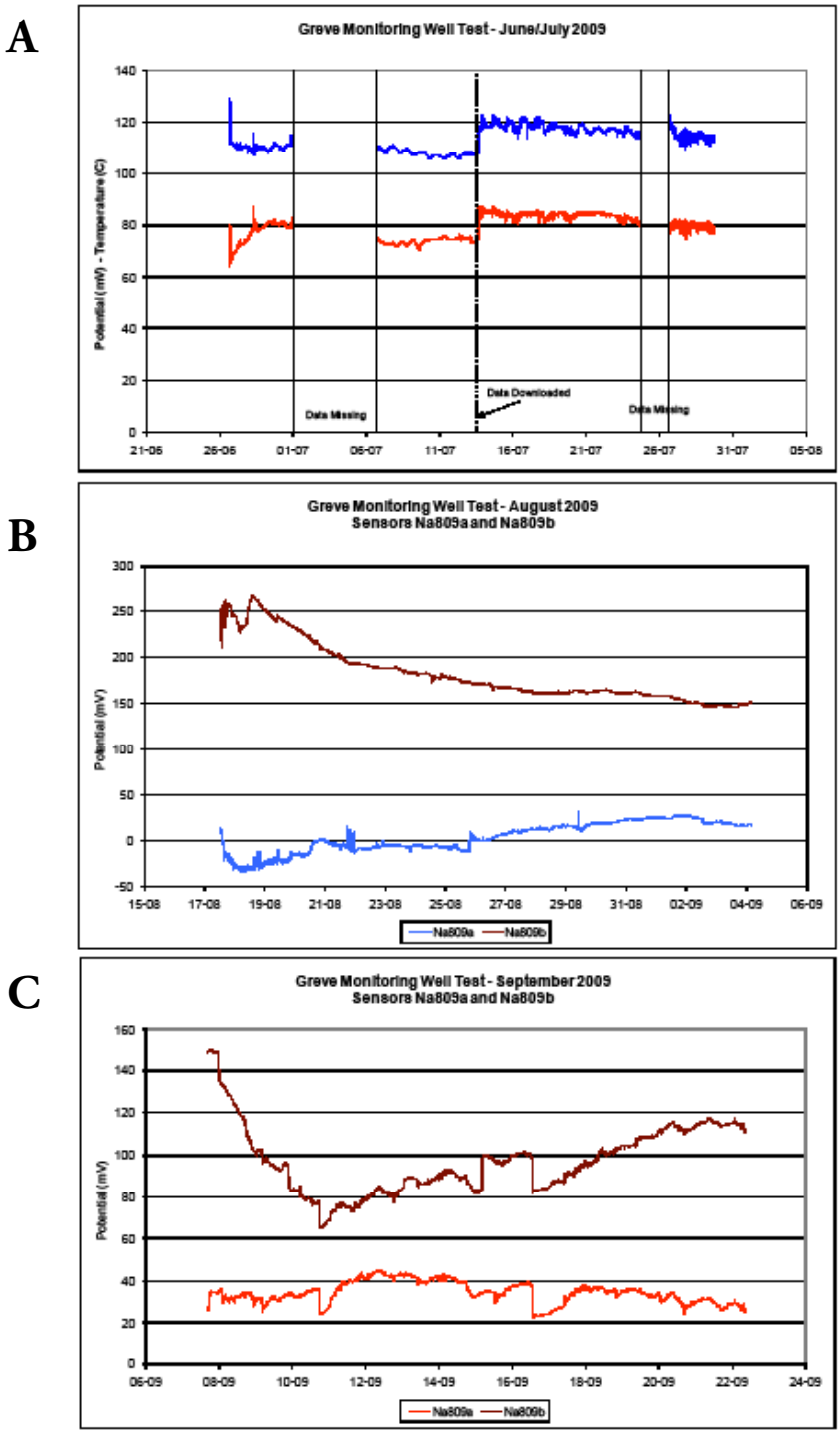

Figure 20. *Response of the PVC sensors in the July, August and Sepember 2009 Greve monitoring well test. Note that there were two time periods in the July test where data is missing due to the malfunctioning of the data logger.*

In the July test, the signal from the sensors took approximately 24hours to stabilize, with both sensors moving approximately 20mV during this time. This corresponds with the results observed in the laboratory. The signal remained fairly stable until the data was downloaded on July 14. There was an unexplained jump in the signal after downloading, where after the quality of the signal degraded (Fig. 20a). Drift, as calculated in the regression of the signal vs. time, was seen to be under 0.5mV/day (Table 4). Na609b performed slightly better than Na609a with respect to the standard deviation from the drift trend and the 95% confidence interval (Table 4). The error from the drift calculated from Nernst's equation, correcting for temperature, was higher than that for the uncorrected data (Table 4). Using the 95% confidence interval of +/-2.1mV for Na609a and +/-1.65mV for Na609b, and based upon the pre-test calibration curves, the accuracy of the drift corrected signal was +/-29mg/l for Na609a and +/-22mg/l - an error of 25% and 19%, respectively, from the observed 117mg/l concentration.

Table 4. *Analysis of drift and noise for the PVC sensors in the Greve monitoring well test.*

		Uncorrected Data - Regression				Drift of Eo					
Sensor Nr.	Test	Drift (mV/day)	R^2	SD	95%	Drift (mV/day)	R^2	SD	95%	Test length (days)	n
Na609a	Jul 1	-0.43	0.46	0.8	1.6	-0.67	0.46	1.2	2.4	6	869
Na609a	Jul 2	-0.34	0.40	1.3	2.5	-0.42	0.34	1.7	3.4	10	1425
	Ave	-0.38	0.43	1.05	2.1	-0.55	0.40	1.4	2.9		
Na609b	Jul 1	0.44	0.54	0.74	1.4	0.30	0.39	0.7	1.3	6	869
Na609b	Jul 2	-0.13	0.15	0.96	1.9	-0.18	0.22	1.0	1.9	10	1425
	Ave	0.16	0.34	0.85	1.65	0.06	0.30	0.8	1.6		
Na809a	Aug	3.0	0.85	6.0	12	3.0	0.85	6.3	12.6	17	1236
Na809a	Sept	0.99	0.22	4.4	8.8	0.85	0.18	4.3	8.6	8	596
Na809b	Aug	-5.5	0.82	12	24	-5.5	0.83	12	24	17	1236
Na809b	Sept	-3.5	0.21	16	32	-3.6	0.22	16	32	8	596

SD gives the standard deviation from the calculated drift (in mV), the 95% column shows the deviation (in mV) with a 95% confidence interval and n gives the number of measurements in the analysis.

The August and September tests on sensors Na809a and Na809b faired much worse for both of the tests (Fig. 20b and c). Drift on both of the sensors was much higher, ranging from 1mV/day to 5.5mV/day (Table 4). On top of the much higher drift rates, the signal was also much noisier and more unstable. This can be seen directly in the analysis of the 95% confidence interval, where the best

performance was +/-8.8mV, but as bad as 32mV (Table 4). Even when calculating the best responding sensor, Na809a, the drift corrected signal yielded a 95% confidence interval range of concentrations between 15mg/l and 115mg/l, and a standard deviation range of 27-75mg/l – an error of 78% from the measured 32mg/l concentration.

Upon completion of the tests, all four sensors were covered with ochre. On Na609a and Na609b, the layer was so thick that brown electrode surface could not be seen through the bright orange layer. The ochre layer on Na809a and Na809b was thinner, where the electrode surface could still be observed. In the post-test calibration of the sensors, not one of the sensors showed any response to changing sodium concentrations in the NaCl calibration solutions. From the signal, it was not possible to determine exactly when, during the tests, that the sensors became unresponsive.

3.3.5 Wickford monitoring well test

Two sensors, Na909a and Na909b were tested in the Wickford monitoring well for a one month period. Both sensors showed very good pre-test calibration with rates of 41 and 38mV/decade (Table 3). The diurnal changes in groundwater salinity from tidal pumping allowed an analysis of the sensors performance in conditions of changing groundwater salinities.

Figure 21 shows the raw, non-temperature corrected response of the sensors during the test. The two sensors show a differing response during the same test. Na909a appears to respond to the larger trend in the changes of sodium concentration, where as Na909b shows a much higher response to the diurnal changes in sodium, represented by the wave-like peaks and valleys (Fig. 21). Both sensors show periods of greater stability and periods of increased noise. For sensor Na909a, it took two days, from 09/30 – 10/01 for the signal to stabilize out.

Sodium concentrations were calculated from the sodium sensors, using the pre-test calibration response rates, corrected for temperature. The results were evaluated with respect to the calculated concentrations from the conductivity probe. The calculations were conducted after the noise was removed from signal. The analysis on the sensors began on October 2, as it took two days for the sensor signal to stabilize. There was not a water sample taken from the monitoring well at this point. Therefore the conductivity measurement was used as the initial concentration

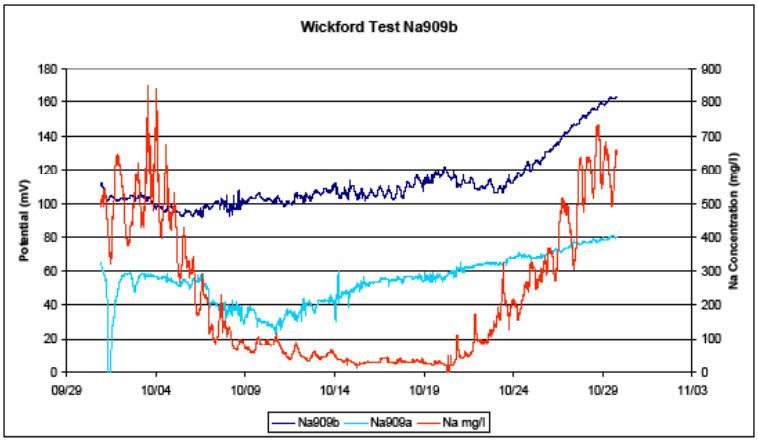

Figure 21. *Response of the PVC sensors used at the Wickford, Rhode Island test. The sodium level was calculated from conductivity measurements taken at the site. Note that the diurnal variations in the sodium signal in Na909b, illustrating the effect of tides on groundwater salinity in the well.*

from which the signal for both sensors was calibrated to. The results show that the sensors followed the general trend of the changing sodium concentrations in the beginning, but after about 4 days, on October 6, the signal diverged significantly from the sodium concentrations calculated from the conductivity measurements (Fig. 22a). It is also observed that during the first four days, in spite of following the general trend, the sensors showed an opposite response to the diurnal highs and lows (from the tides) than that of the conductivity (Fig. 22b). Analysing the correlation between the sensors and the conductivity measurement over the 4 days of the best fit, Na909a had an R2 value of 0.41 and a standard deviation of 55mg/l with a 95% confidence interval of +/-110mg/l. Na909b had an R2 value of 0.40 with a standard deviation of 65mg/l, with a 95% confidence interval of +/-130mg/l. Assuming concentrations below 500mg/l, the sensors had a standard error from the 95% confidence interval of greater than 40% for Na909a and 50% for Na909b. It is apparent that much of this error is a result of sodium sensors being out of phase with the conductivity on the diurnal variations of the sodium concentrations.

It is apparent that both of the sodium sensors were not stable and that there was drift, jumps in the reference potential during the test and possibly even changes in the response rate of the sensors. An attempt to correct for these issues was made in order to attempt to get the best fit for the sodium sensors to the sodium concentrations as calculated by the conductivity probe. During the course of the test, four adjustments were made on each sensor, which are listed in Table 5. The

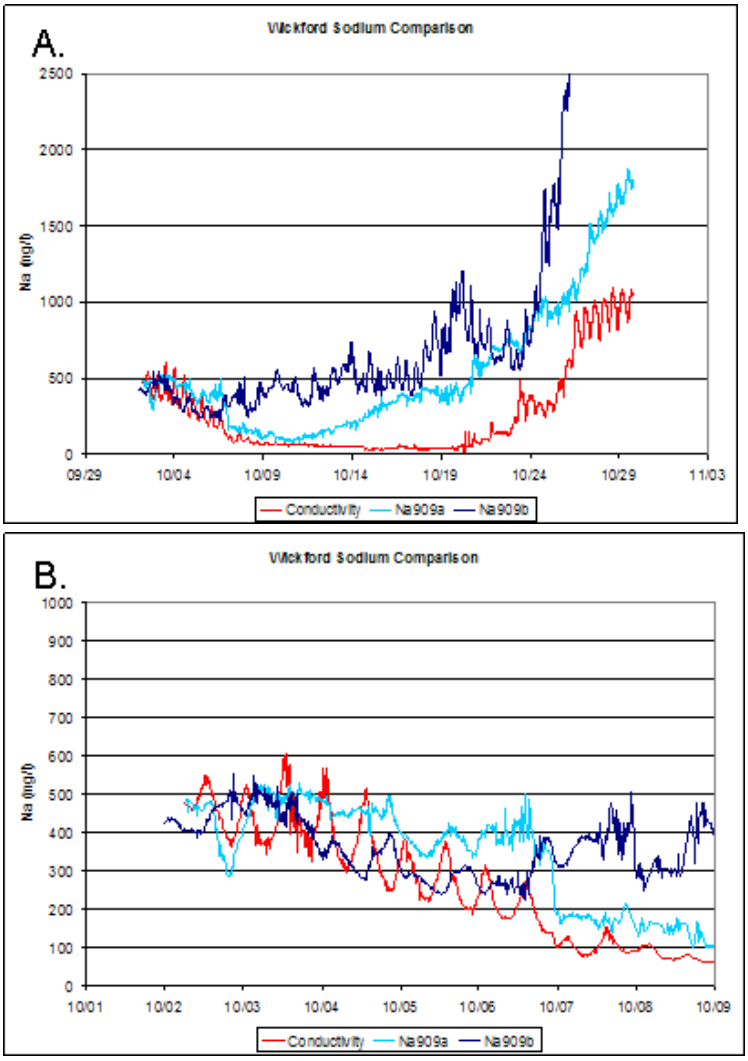

Figure 22. *Wickford sodium calculations with starting sodium levels calibrated to the measured conductivity. The plots show that both sensors follow the general trend of the concentrations from the conductivity probe until about October 6, where as afterwards there is significant deviation from the signal. The plots also show an opposite response to the diurnal tidally induced sodium concentration changes, as measured by the conductivity probe.*

results were a closer fit to that of the conductivity probe, however, there were still some large discrepancies (Fig. 23). More adjustments on the signals could have been made, however, for each adjustment made, the more the difference is from the original data. Detailed analysis of the sensor signal reveals a mixed result. During the period of low groundwater salinity where the conductivity probe was not responsive, sensor Na909b showed a fairly good response, moving in tact with the chloride sensor Cl909a (as described in Chapter 3) with respect to the diurnal

Table 5. *Signal corrections performed on sensors Na909a and Na909b for the Wickford monitoring well test. The sensors were corrected at different stages during the monitoring period for drift, recalibration to conductivity, and changes in the response (mV/decade concentration change).*

Correction Time	Sensor	Correction Type
Oct. 7, 00:00	Na909a	Sensor recalibrated to conductivity concentrations.
Oct. 7, 00:00	Na909b	Sensor recalibrated to conductivity concentrations.
Oct. 9, 07:02	Na909b	Sensor recalibrated to conductivity concentrations, sensor drift adjusted to 1mV/day.
Oct. 11, 10:46	Na909a	Drift adjusted to -6mV/day.
Oct. 19, 09:40	Na909a	Drift adjusted to 6mV/day.
Oct. 20, 07:16	Na909b	Drift removed, and a new response rate of 30mV/decade.
Oct. 26, 12:21	Na909a	Drift adjusted to 1.5mV/day.
Oct. 26, 12:21	Na909b	Drift corrected to 3mV/day.

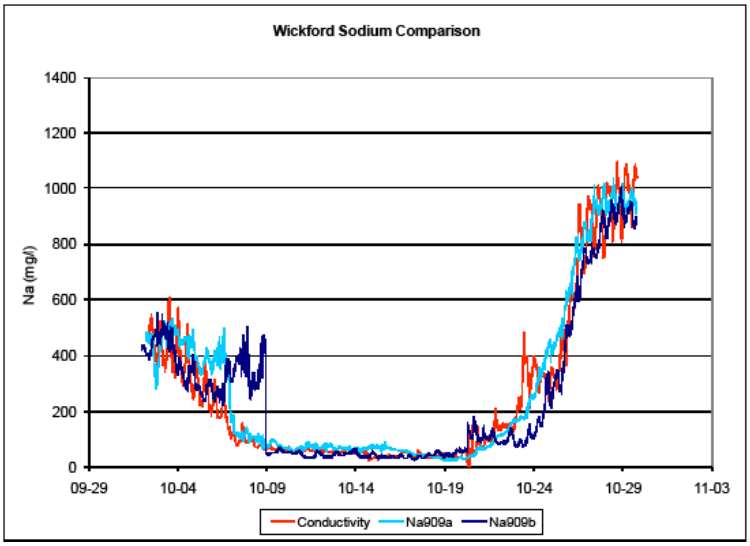

Figure 23*. Wickford sodium calculations with adjustments made to the signals. The adjustments that were made are listed in Table 5.*

salinity variations from October 9 to October 20 (Fig. 24). However, there remains a discrepancy between the actual concentrations, which should be at an approximate 5:3 chloride to sodium ratio. This ratio is more or less maintained from Oct. 9-11 and 16-18, but otherwise is too low (Fig. 24). During this period, sensor Na909a is adjusted to approximately the correct salinity level, but does not respond to the diurnal changes in sodium in the same manner that Na909b does (Fig. 24).

At the end of the period, both sensors are able to be adjusted to the long-term sodium concentration trend of the conductivity probe (Fig. 25). However, now

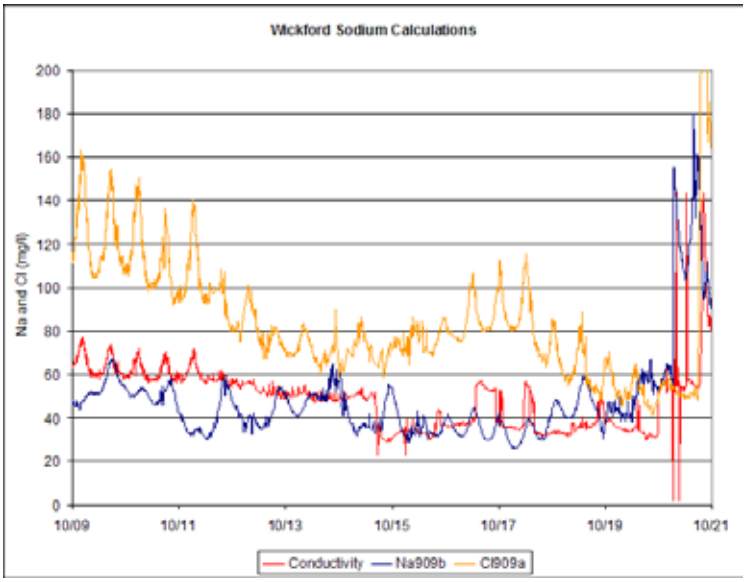

Figure 24. *Sodium calculations for Na909b in the middle period where conductivity probe was not responsive. The signal shows that Na909b sensor was fairly responsive to the changes in salinity, responding in tact with the chloride sensor for the diurnal variations. However, there remain discrepancies between the sodium and chloride sensors in the larger scale salinity changes (over several days).*

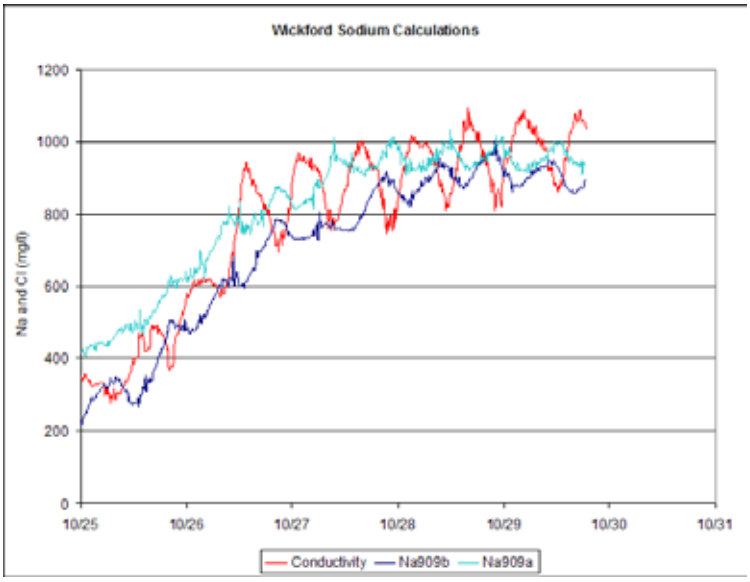

Figure 25. *Wickford sodium calculations for the end of the test period. During this time, the general trend in increasing sodium is observed, however, peaks and valleys with respect to the tidal variations is opposite to the conductivity sensor measurements.*

both sensors are seen to again respond opposite to that of conductivity with respect to the diurnal changes in the sodium concentrations. Water samples were taken at different times during the tidal cycle in early November. These samples showed that sodium and chloride levels remained at a constant ratio, and moved in tact with the conductivity measurements (Fig. 26). This indicates a possible delay in the response of four hours in the sodium sensors, or that they are not functioning properly. In spite of the question of the performance of the sodium sensors, the overall performance of the sensors for the last 9 days of the test was evaluated. Sensor Na909a showed a relatively good correlation, with an R2 value of 0.88. Standard deviation was seen to be fairly high, however, at 105mg/l, yielding a +/-210mg/l confidence interval. Sensor Na909b also had a relatively good overall correlation, with an R2 value of 0.90, with a standard deviation of 100mg/l, and a 95% confidence level of 200mg/l. Assuming concentrations below 1000mg/l over this analysis period, the sensors again showed standard error from the 95% confidence interval of greater than 40%.

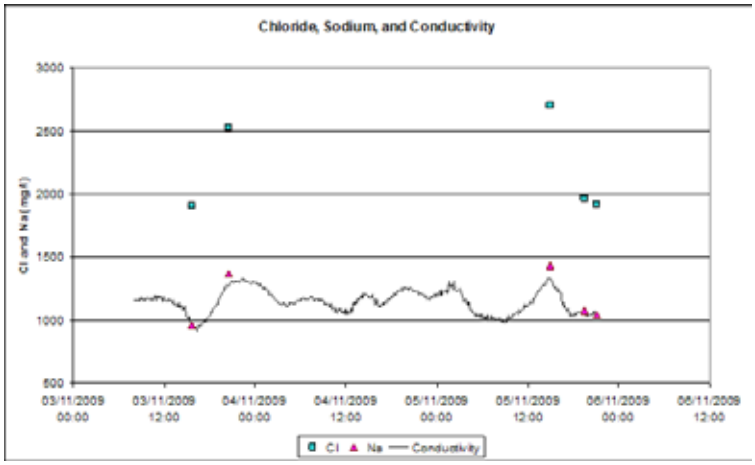

Figure 26. *Post-test water sample analysis from the Wickford monitoring well. Note how both sodium and chloride respond in-tact with conductivity with respect to the diurnal tidal variations. The sodium-chloride ratio also remains the same in all of the collected samples.*

3.4 Performance of commercial sodium and potassium ISE

The performance of a readily available commercial sensor for sodium and were tested against the response to sodium and potassium, as well as their performance for continuous measurements. It needs to be noted that only one ISE for each ion was tested. It was not within the scope of this project to do extensive testing

on different commercially available ISEs. The tests were conducted in order to provide a basic comparison on the effectiveness of the sensors developed and tested in this project.

The response and operational ranges for the commercial sensors was 50mV/decade from 2 to 23,000 mg/l for sodium and 52mV/decade from 4 to 40,000mg/l for potassium (Table 1, Fig. 27). Neither electrode responded to the other ion, thus cross-sensitivity was not a large issue (Fig. 27). The drift on the sodium electrode was very low, being -0.07mV/day over the 23 day test in the laboratory. The signal, however, was not as stable (Fig. 28). The standard deviation from the drift was +/-

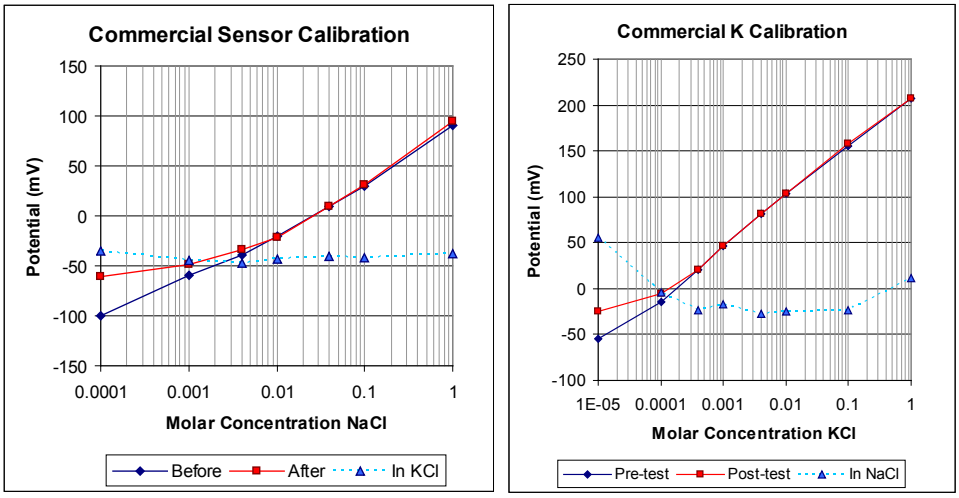

Figure 27. *Calibration curves for the commercial sodium (left) and potassium (right) electrodes. Note that the response for both electrodes was not as good after the continuous monitoring tests conducted on the sensors.*

1.6mV, with a 95% confidence interval at +/-3.2mV. The drift for the potassium electrode was higher at 0.6mV/day, but remained consistent over the 8 day test (Fig. 28). The signal from the potassium electrode was slightly more stable than the sodium, with a standard deviation from the drift at +/-1.4mV, with a 95% confidence interval at 2.7mV. Given the calibration curves, this shows a signal accuracy of 13% for the sodium electrode and 11% for the potassium electrode. Post-test calibrations on both electrodes showed very good responses, with slight signal degradation of the signal below 0.004 M concentrations (10mg/l and 16mg/l for sodium and potassium respectively).

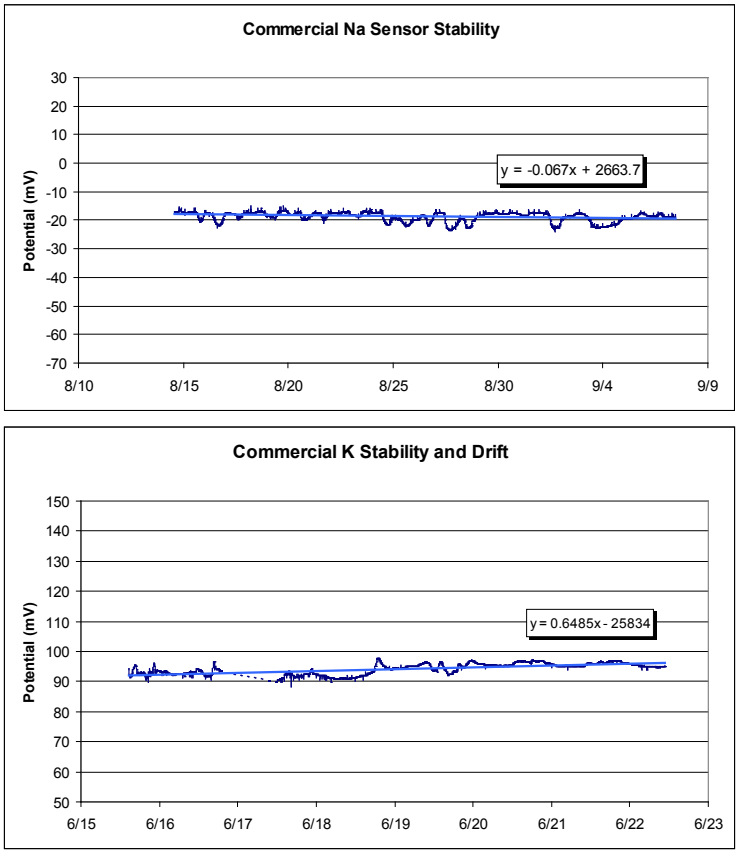

Figure 28. *Continuous laboratory tests of the commercial sodium (A) and potassium (B) electrodes. The slopes of each trend show the drift per day for each sensor.*

4. DISCUSSION

4. 1 Performance of the BTA sensor

The initial tests on the BTA sensors showed promise for continuous monitoring of sodium in groundwater. The BTA ionophore is recognized to be selective primarily for potassium, but the calibration tests in NaCl solutions showed a decent response to sodium as well. The tests conducted in changing seawater concentrations showed that the sensor responded to seawater concentration changes above 100mg/l TDS (30mg/l sodium). Although there are no specific drinking water quality standards or recommendations for sodium by the World Health Organization (WHO), sodium can be used as a measurement of salinity in the water. Chloride is used as the standard measure for salinity for which WHO has set the limit to 250mg/l. Given the approximate sodium to chloride ratio of 3:5 in seawater, the limit for salinity, as measured with sodium would be 150mg/l. Given this cut-off concentration, the BTA sensor responded in saltwater well within this range of operation, and therefore could be of interest to water works for use in monitoring changes in groundwater salinity.

In spite of the initial promise that the sensor showed in the calibration tests, the BTA sensors did not perform well in the continuous tests. The signal was seen to be unstable and drift irregular. Particularly the irregular drift is problematic, as it makes it difficult to differentiate between drift and real concentration changes. If drift is observed to be constant, then it can be accounted for quite simply during the processing of the sensor data, as well as in real-time. However, if the drift changes slope, then any signal corrections based upon the previous drift slope will be incorrect. The problem of drift alone will make it difficult to use the BTA sensors for continuous monitoring.

The sensors also were not stable in their responses to changing sodium concentrations during continuous monitoring in the laboratories. In one test, the sensor responded to two concentration changes, where as did not for two other. The concentration of the sodium in the solutions was within the sensor's pre-test calibration range, so there should have been responses for all concentration changes. When the sensor did respond to the concentration change, it did so within a matter of minutes (Fig. 8a). Since there were several hours between concentration changes, a lack of time for the sensors to respond could not have been a reason

for the lack of response. In two other continuous monitoring tests, one conducted in seawater (Fig. 6c) and one in NaCl solution (Fig. 8b), the sensor did not respond at all. Even more perplexing is the fact that, after the seawater test, the sensor responded again to changes in seawater concentrations during the post-test calibration (Fig. 6b). This fact suggests that the sensor may not be able to measure the sodium concentrations in water moving across the sensing membrane even at the slow rates used in the test. However, in order to measure changes in the sodium concentrations, a continuous circulation of water must occur. If this is the case, then use in continuous monitoring of groundwater becomes problematic.

The life-span of the sensors was also extremely variable. While it was possible to recalibrate some of the sensors multiple times after being in dry storage (BTA0707a, for example), other sensors died after being in dry storage just one time. The sensors lasted everywhere from a couple of days, to as long as 6 months. This fact makes it difficult to use the sensors in a real monitoring program. Before employment in the field, all sensors will have to be tested coming out of dry storage. As a large number of the sensors ceased to function while in storage, several BTA sensors will have to be ready and hopefully at least one of them will function coming out of storage. This is illustrated in the Wickford monitoring well test, where BTA0909a was calibrated at Roskilde University before travelling to Rhode Island. Upon arrival in Rhode Island, and before installation in the Wickford monitoring well, BTA0909a did not respond to pre-installation calibration attempts; the sensor simply did not survive the dry storage during transportation.

When the BTA sensors are compared to the commercial sensors, both for sodium and potassium tested in this study, there is no operational advantage. The commercial sensors showed only slight, but even drift that could be corrected for. The commercial sodium error of 13% is also fairly respectable. The commercial sensors did show a tendency of signal degredation after 2-4 weeks of continuous operation. This fact combined with the price of the commercial sensors, as well as size and flexibility in use, could remain a restricting factor in their use for continual monitoring.

In the Greve monitoring well test, the groundwater tested was transforming from reduced to oxidized conditions, with a relatively high concentration of reduced iron and manganese in the water. Oxidation of the iron led to the situation where ochre build-up on the sensor membranes became a problem. All of the BTA sensors used

in the monitoring well tests worked prior to installation, but not after. Given the instability of the results from the laboratory tests, it can not be said with certainty that the ochre affected the BTA sensor signal, but it is likely that it did. Thus, any employment of these sensors must take oxidizing and reducing conditions in mind, and develop a system which can prevent or hinder the build-up of fouling films, such as ochre on the sensor surface.

4.2 Performance of the MTA sensors

The first concern in the analysis of the MTA sensors is whether or not there was success in the synthesis of the MTA ionophore prior to polymerization – in other words, the cobbling of the thiophene group on to the 2-Aminomethyl 15-crown-5 ionophore (Fig. 4). The results from this study indicate that the synthesis of the MTA ionophore was indeed successful – as indicated from NMR and IR data collected. This, of course, is confirmed through the testing and calibration of the MTA sensors, which did show fairly good response in changing NaCl concentrations (Table 2). With this success, it opens up the possibility of directly polymerizing the ionophore directly to the gold electrode surface.

As to the performance of the MTA sensors in the continuous tests, much of the same argumentation stated for the BTA sensors applies to the MTA sensors as well. The response of the MTA sensors in general had a slightly better response to sodium than the BTA sensors. This is likely due to the fact that the crown ether in MTA has a purer selectivity towards sodium. However, the MTA sensor had almost as strong cross-selectivity to potassium, so it was by no means a pure electrode for sodium. Good responses to changes in seawater concentrations were observed, showing the potential for the MTA sensors to be used in the monitoring for groundwater salinity.

Along the same lines as the BTA sensors, the MTA sensors were also observed to be unstable in their application. This includes an inconsistency in whether or not they respond to concentration changes during the continuous tests in the laboratory. This includes problems with drift, where in one test there was a drift observed of over 30mV/day, which is completely unacceptable. In the Greve monitoring well tests, the sensors were successfully calibrated before the test, but died during the test. MTA1008c, used during the first monitoring well test showed very little drift

(Fig. 15a), however the signal was +/- 7mV, which leads to an error of about 50% from the measured signal. For applicability in a monitoring system, this error is considered too high for monitoring purposes – any signal would simply be lost in the noise. In the second monitoring well test, MTA1108a showed an even more unstable response in the signal (Fig.16b). Furthermore, the life span of the MTA sensors was highly variable, with several sensors failing to be reactivated coming out of dry storage. Thus it can be seen that actual application of the MTA sensors are not reliable enough, either in signal or life span, to be applied in continuous groundwater monitoring.

4.3 Performance of the PVC sensors

Of the three sodium sensor types tested in this study, the PVC sensor proved to be the most stable. Initial calibrations of these sensors were more consistent, and tended to be better, with responses generally in between 35mV/decade to 45mV/decade. The detection limits of the sensors also fell well within the range of interest (above 20mg/l) when monitoring for changes in groundwater salinity. The construction of the sensors was also simple and successful, with every attempt to develop a sensor succeeding. There were also no problems experienced in the storage of the PVC sensors; all sensors which were put into dry storage after successful calibration were able to be conditioned and re-calibrated coming out of storage. The stability of calibration and consistent ability for storage gives more confidence in the field application of the sensors when compared to the BTA and MTA counterparts.

The continuous laboratory tests also show, initially, a good response. It takes the PVC sensors about 24 hours to stabilize, where after the signal tends to settle down into more regular drift. The sensors also have shown good initial response to concentration changes. However, on the two longer-term laboratory tests, the signal is observed to gradually degrade, with responses to sodium concentration changes ceasing after 3-5 days. The reason for this short operational period could be due to the construction of the sensor. The 15-crown-5 ionophore sits loosely within the plasticised PVC membrane; it is not chemically attached to the gold surface like the BTA and MTA ionophores are. Thus, when the sensor is applied in continuous monitoring, and continually under saturation, it could be susceptible to diffusion of the ionophore out of the PVC membrane. As the ionophore

slowly diffuses out of the membrane, the signal would likely become weaker and eventually lost all together. This will restrict the life span of the sensor in continuous application. From the two laboratory tests, it appears that this life span is around 5 days. The lack of response in the sensors could also be due to build-up of film on the sensor, but in the tests pure solutions of NaCl were used, and no film build-up was observed on the sensors after the tests.

Analysis of the performance of the PVC sensors in the Greve monitoring well is problematic due to the ochre build-up that occurred on the sensors. Looking at the data, it is not possible to determine when the sensors stopped operation. In any event, none of the four sensors employed survived the 15-30 day applications in Greve, and it is apparent that fouling of the sensors during continuous monitoring will have to be prevented, or in the least, hindered.

The Wickford monitoring well test provided a very good testing ground for the PVC sensors with diurnal variations in salinity and an environment where fouling of the sensor surface was not a problem. The results, however, were mixed. After correction to the sodium concentrations from the PVC sensors to the conductivity probe, both sensors responded to some degree to the general trend over the first four days, where after, the signal significantly diverged. As the conductivity measurements were controlled at different times throughout the test, it is presumed that the conductivity measurements are accurate, and thus the error rests with the sodium sensors. The sensor signals were subsequently adjusted to attempt to match the concentrations from the conductivity probe. The adjustments were limited to only four for each sensor. Of course, more adjustments could have been made, in which the signal for each sensor would become better. However, the more adjustments that are made, the further away one strays from the original signal, and it becomes an issue as to whether the sensor is responding to changes in sodium, or if the adjustments are being made to make an artificial response. In addition, if the sensors are to be applied in a seawater monitoring program, the number of adjustments needed have to be kept to a minimum. Even with the adjustments made from the Wickford test, the sensors gave over a 40% error, which is not acceptable.

Sensor Na909b appeared to work better than Na909a during the test, where it appears to respond to the diurnal variations in sodium caused by the tides. Only at the very end of the test did Na909a show diurnal fluctuations, where as Na909b

did, more or less, throughout the entire test period. However, upon close examination, it is seen that the diurnal variations in both of the sodium sensors was opposite that recorded in both the conductivity and the chloride sensor (evaluated in Chapter 3) during part of the test. In the middle of the test, when sodium was below 80mg/l, Na909b started to respond in tact with both the conductivity (when it worked) and the chloride sensor (as illustrated in Fig. 24). Then when the salinity increased, the sensor went again out of sync with the conductivity and chloride. Tests on groundwater samples taken from the well after the test showed that sodium, chloride and conductivity always moved in tact with each other, with sodium and chloride maintaining a constant molecular ratio. The author has no explanation for why this switch from being in sync to out of sync with the chloride and conductivity. Since the conductivity and chloride responded in tact with each other throughout the test, and the measured chloride and sodium from the water samples responded in tact with conductivity, it is assumed that there is a problem with the sodium sensor which is creating an artificial signal. It is possible that the sodium sensor became responsive during the period of low sodium concentration, where as it was not as responsive during the remainder of the test. If the sensor did not respond to sodium for the remainder of the test, it is not known what could cause its inverse response to chloride and conductivity. The sodium sensor potential is not affected by pH, as the laboratory test showed, and thus even if pH in the groundwater changed with the salinity, it should not have affected the sensor reading. In the end, the cause of the diurnal variation opposite to that of the conductivity remains unknown.

Overall, however, there are several concerns with respect to the PVC sensors, which will need to be sorted out before the sensors can be employed for continuous monitoring. First of all, it is a concern that in the laboratory tests, the sensors stopped responding after only 5 days, where as in the Wickford test, they were possibly operational after 30 days. This discrepancy needs to be investigated even further. Being able to secure the membrane so that the ionophore can not diffuse out of the membrane with time may help to both stabilize the signal and increase the life-span of the PVC sensors. These sensors, in the end, did show promise for application in the measurement for sodium, however more work still needs to be done in order to apply the PVC based sodium sensors in a continuous monitoring program.

5. CONCLUSION

The possibility of creating a solid-state ion selective electrode for sodium provides a good opportunity for the monitoring of groundwater salinity. Working together with chloride and conductivity, the sensors could provide well-field operators and groundwater managers with important information on groundwater salinity and the opportunity to react quickly to changes in groundwater salinity. Both the BTA and MTA sensors showed initial promise in the use of the solid-state electrode. However, the sensors showed problems during the continuous monitoring tests. The sensor signal was relatively unstable and the sensors did not respond regularly to changes in salinity during the tests. In addition, there were problems with the storage and inconsistent life-span of the sensors. The inconsistent results for the BTA and MTA sensors do not allow for the application of the sensors in a continuous monitoring program.

The PVC sensors show some promise in the application. These sensors had a consistent response to sodium and were able to go in and out of dry storage. However, there were still difficulties in the application of these sensors for use in continuous monitoring. There was significant differences in the response slope of the sensors in application and calibration. There was also a significant difference in the life-span of the sensors during the monitoring tests. The results from the Wickford test showed that, though the appeared to show a response, that it was inconsistent, and there is more work in the development needed before they can be used for continuous monitoring.

Construction and Testing of Calcium Sensors

1. INTRODUCTION

The primary goal of this study is to develop a calcium sensor that could accurately provide real-time, continuous measurements. Successful development would give well-field managers the ability to monitor changes in calcium during groundwater abstraction. Should changes occur, it would provide a warning that the groundwater being delivered to the wells is coming from a different source and should be further investigated. Changes could be, for example, the draining of a secondary aquifer (which could be polluted) or seawater intrusion into the aquifer. In order to be used for this purpose, it is vital that the sensor be developed to provide continuous data over longer period of time.

A number of previous studies have recently shown that it is possible to develop solid-state sensors by electrochemically attaching different types of thiophene directly on to a gold surface. This is possible due to the interaction of thiophene's sulfur with the gold surface, Which was described in Chapter 4. These studies illustrated the possibility of electrochemically polymerizing a calcium ionophore to a conducting surface, such as gold, if a thiophene group can be successfully attached to the ionophore. If successful, this would produce a solid-state sensor for calcium.

Phosphoric acid esters have been long known as very good ionophores for Ca^{2+}, with the calcium ion preferentially attaching to the phosphate group on the organic molecules (Bühlmann et al. 1998). In fact, these were some of the very first ionophores used in ion selective electrodes (ISE's). A specific group, phenyl phosphates, has been very well studied for their selectivity to calcium (Ruzicka et al. 1973, Keil et al. 1978, Hobby et al. 1983, Khalil et al. 1985, Bühlmann et al. 1998). Several different forms of phenyl phosphates have been shown to provide good selectivity to Ca^{2+}, while providing a near Nernstian response (Khalil et al.

1985). The calcium ionophores were shown to be responsive in pH's between 4 and 9.5, showing applicability for measuring ground water in most circumstances (Keil et al. 1978, Ruzicka et al. 1973). Thus, if an ionophore from this group could be connected to a thiophene group, it could be polymerized on to a gold surface to produce a solid-state calcium ISE.

Si et al. (2007) showed that it was possible to attach thiophenecarboxaldehyde on to an amine group, utilizing the technique outlined by (Patra and Goldberg 2003). Takakusa et al. (2002) successfully synthesized Bis(4-aminophenyl) phosphoric acid through the reduction of the commercially available compound of Bis(4-nitrophenyl) phosphoric acid. Therefore with the synthesis of the Bis(4-aminophenyl) phosphoric acid, which is within the group of proven calcium ionophores (as described above), it should be possible to attach a thiophene group to the amine, and subsequently allow for the polymerization of the molecule on to a gold surface. Therefore, this study will attempt to produce a solid-state calcium sensor utilizing a three step process (outlined in Figure 1), which includes 1) the reduction of Bis(4-nitrophenyl) phosphoric acid to produce Bis(4-aminophenyl) phosphoric acid; 2) attachment of a thiophene group to Bis(4-aminophenyl) phosphoric acid to produce Bis(3-thiophene-P-phenyl amide) phosphate; and 3) copolymerization of the Bis(3-thiophene-P-phenyl amide) phosphate on to the gold surface. The success of the sensor will be tested and evaluated.

Although the focus of the study is to develop this technique to polymerize a calcium ionophore directly on to the gold electrode, the technique used to develop a PVC-based sodium sensor (described in Chapter 4) was also used to develop a PVC-based sensor for calcium. This was conducted only as a first attempt to determine whether or not a PVC-based calcium sensor would be possible.

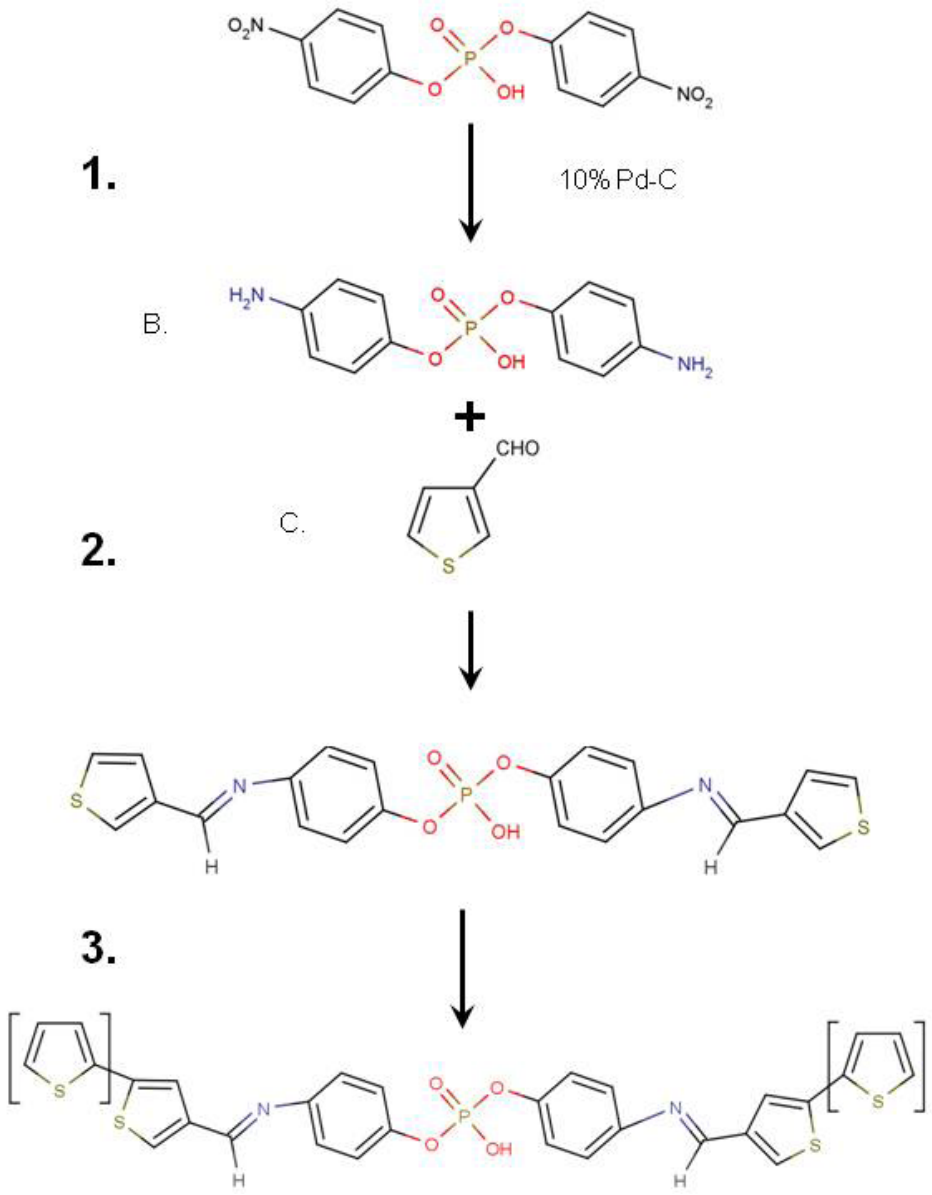

Figure 1. *Illustration of the process to derive the calcium ionophore. Step one consists of the reduction of Bis(4-nitrophenyl)phosphate (A) in an hydrogen atmosphere to produce Bis(4-aminophenyl)phosphate(B). Step two includes the reaction of B with 3-thiophenecarboxaldehyde (C) to form Bis(3-thiophene-P-phenyl amide) phosphate (D). Step three includes the electrochemical polymerization of thiophene to the thiophene ring on D.*

2. MATERIALS AND METHODS

2.1 Reagents and Materials

The reagents used in the study include Bis(4-nitrophenyl)phosphoric acid (>99%), thiophene (>99%), and 3-thiophenecarboxyldehyde (>98%) from Sigma-Aldrich, 10% Pd-C from Fluca, ethanol (HPLC, 99.9%), anhydrous methanol (HPLC, 99.9%), dichloromethane (HPLC, 99.8%) and acetonitrile (HPLC, 99.9%) from Labscan Lid, and lithium perchlorate from Merck. These materials were used as received. For the construction of the calcium PVC electrode, the Calcium Ionophore from Sigma-Aldrich was used.

Gold conducting surfaces were produced from pure Au, stretched into thin rods to 1.0mm in diameter. The rods were cut into 25mm lengths and set into a plastic housing, 22mm long. One end of the gold rod sat flush with the plastic housing (Fig. 2), and was polished using a 2μm diamond polishing paste. This polished surface was used for the polymerization of the sensing film. The other end of the gold rod was connected to copper wiring, which was connected to the data logger.

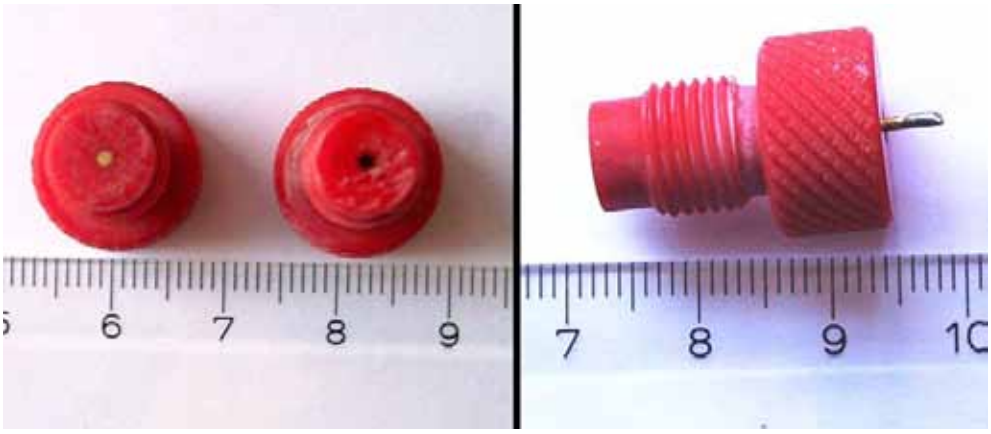

Figure 2. *Photograph of the electrodes used for polymerization. The electrode on the left shows the gold surface before polymerization, and the electrode in the center shows the surface after polymerization. The side view shows the plastic casing with the gold rod extending out. The extension is connected to copper wire, which is then connected to the data logger.*

2.2 Synthesis of Bis(4-aminophenyl)phosphate (BAP)

BAP was synthesized using a procedure outlined by Takukusa et al. (2002). Bis(4-aminophenyl)phosphate (1.0g, 2.9mmol) was dissolved in a 30ml mixture of ethanol and water (2:1). 300mg of 10% Pd-C was added to the mixture under a H_2 atmosphere and stirred vigorously for 15 hours to assure that the reaction goes to completion. The Pd-C was filtered off and washed with de-ionized water. The mixture was evaporated off to dryness. The structure and purity of the resultant compound (B in Fig. 1) was confirmed by ^{1}H NMR ($CDCl_3$, 300Mhz).

2.3 Synthesis of Bis(3-thiophene-P-phenyl amide) phosphate (TPA)

The synthesis of TPA was carried out using the procedure attaching an amine to an aldehyde, as outlined by Patra and Goldberg (2003). BAP, as synthesized in 2.2 (544mg, 2mmol), and 3- thiophenecarboxyldehyde (263µl, 3mmol) were refluxed in 6ml of anhydrous methanol in a nitrogen atmosphere for 18 hours at a constant temperature of 55°C. The methanol was evaporated off, leaving a cream colored waxy substance. The product was then purified using TLC plates with an 8:2 mixture of dichloromethane and methanol. The separated bands on the plates, one being the reactant and the other being the product, were scraped off separately, and filtered through methanol to dissolve the product from the TLC plate film. The methanol was then evaporated, leaving again a cream colored waxy substance. The structure and purity of the resultant compound (D in Fig. 1) was confirmed by ^{1}H NMR ($CDCl_3$, 300Mhz).

2.4 Binding Ca^{2+} to TPA

Due to the fact that the TPA is such a large molecule, after attachment to a gold surface (described in section 2.5), Ca^{2+} ion may not be able to penetrate in be bound to the ionophore. Therefore it may be required to bind this prior to electrochemical polymerization. This was conducted by dissolving the TPA product in 0.5M solution of sodium hydroxide and 0.5M solution of $CaNO_3$, buffered to a pH of 9 using a borax buffer. The product slowly crystallized, and the solid product, TPA with bound Ca^{2+} ions incorporated into the structure, was filtered off from the solution.

2.5 Electrochemical polymerization of TPA

Polymerisation of TPA from steps 2.3 and 2.4 (separately) on to the gold electrode was carried out using cyclic voltemmetry at room temperature (23 +/- 2 °C) with a three-electrode standard system consisting of a Pt counter electrode, an Ag/AgCl reference electrode, and a gold working electrode. For the polymerization, 30 mg of TPA, 20µl of thiophene and 100mg of lithium perchlorate were dissolved in 10ml of Acetonitrile. The voltemmetric scans were conducted at potential from 1000 – 2900mV at a rate of 10mV/sec. A minimum of five scans were completed in order to obtain a good, dark brown coating on the gold surface. The presence of TPA on the gold electrode was confirmed using a medium range IR conducted on an FT-IR spectrometer, Spectrum 2000, using a Pike Technologies Miracle ATR with a diamond crystal plate.

2.6 PVC based calcium sensor

The development of the calcium PVC based sensor was conducted using the same reagents and technique as described for the sodium sensor in Chapter IV, section 2.1.4. The only difference is that 4.0µl of Calcium Ionophore was used in place of the 15-crown-5 ionophore. As this is only an initial trial for this study, only two sensors were produced.

2.7 Testing of the sensors

Prior to testing, the calcium electrodes were conditioned in 0.01M or 0.1M calcium nitrate ($Ca(NO_3)_2$) solution initially for a period of 24hours. In subsequent tests, this time was varied from 1 hour to as long as 3 days. This is to allow the Ca^{2+} ion to be incorporated into the film on the sensors. The electrodes were then tested in solutions of calcium nitrate $Ca(NO_3)_2$prepared from de-ionized water and from $Ca(NO_3)_2$prepared in a borax buffer solution with a pH of 8.0. The $Ca(NO_3)_2$concentrations in the solutions ranged from 10^{-4} to 1M, with measurements taken at each decade step (5 steps in total). The results were plotted on semi-logarithmic scale to determine whether the sensors responded at or near the predictions of Nernst's law (+30mV/decade concentration change at 25°C), as well as to evaluate the upper and lower limits for the response of the electrode.

3. RESULTS

3.1 Synthesis of BAP

The synthesis consists of the reduction of the nitro group on the Bis(4-nitrophenyl) phosphoric acid to an amino group through the replacement of the oxygen atoms with hydrogen (Fig.1, step 1). The reaction took place in a hydrogen atmosphere, using 10% palladium on charcoal as the catalyst for the reaction. The reaction was completed over 18 hours in order to assure that it went to completion. A comparison of the NMR between the starting materials and the product, BAP, show that the reduction did take place. This is shown through the shift of the hydrogen peaks from 8.25, 8.22 and 7.42, 7.39 in the starting materials to 7.06, 7.02 and 6.90 and 6.87 in the reactants (Fig. 3). In addition, the NMR of the product is very clean, showing that only BAP is present.

3.2 Synthesis of TPA

The synthesis consists of the attaching of the thiophene group on to the amine group on the BAP (Fig. 1, step 2). Excess BAP was used in the reaction to assure that all of the 3-carboxaldehyde monomers were attached. TLC plates were used in a bath of 80% dichloromethane and 20% methanol in order to separate the BAP (starting reagent) from TPA (the product). A comparison of the NMR of the reactants and the product also shows a successful reaction and purification. Firstly, there is a shift of the hydrogen peaks from the BAP to 7.63, 7.61 and 7.17, 7.15, in addition to new peaks at 8.6 and four close peaks between 8.13 and 8.12 (Fig. 3). None of the major peaks of the reactants were present on the product NMR, indicating a clean purification of the product. NMR of the TPA after binding with the Ca^{2+} ion was exactly the same. Therefore it was not possible to determine whether or not calcium was indeed incorporated into the ionophore prior to polymerization.

3.3 Electrochemical Polymerization of TPA

Cyclic voltammetry was used to follow electrochemically induced polymerization of the TPA on the gold electrode surface. Figure 4 shows the cyclic voltammogram

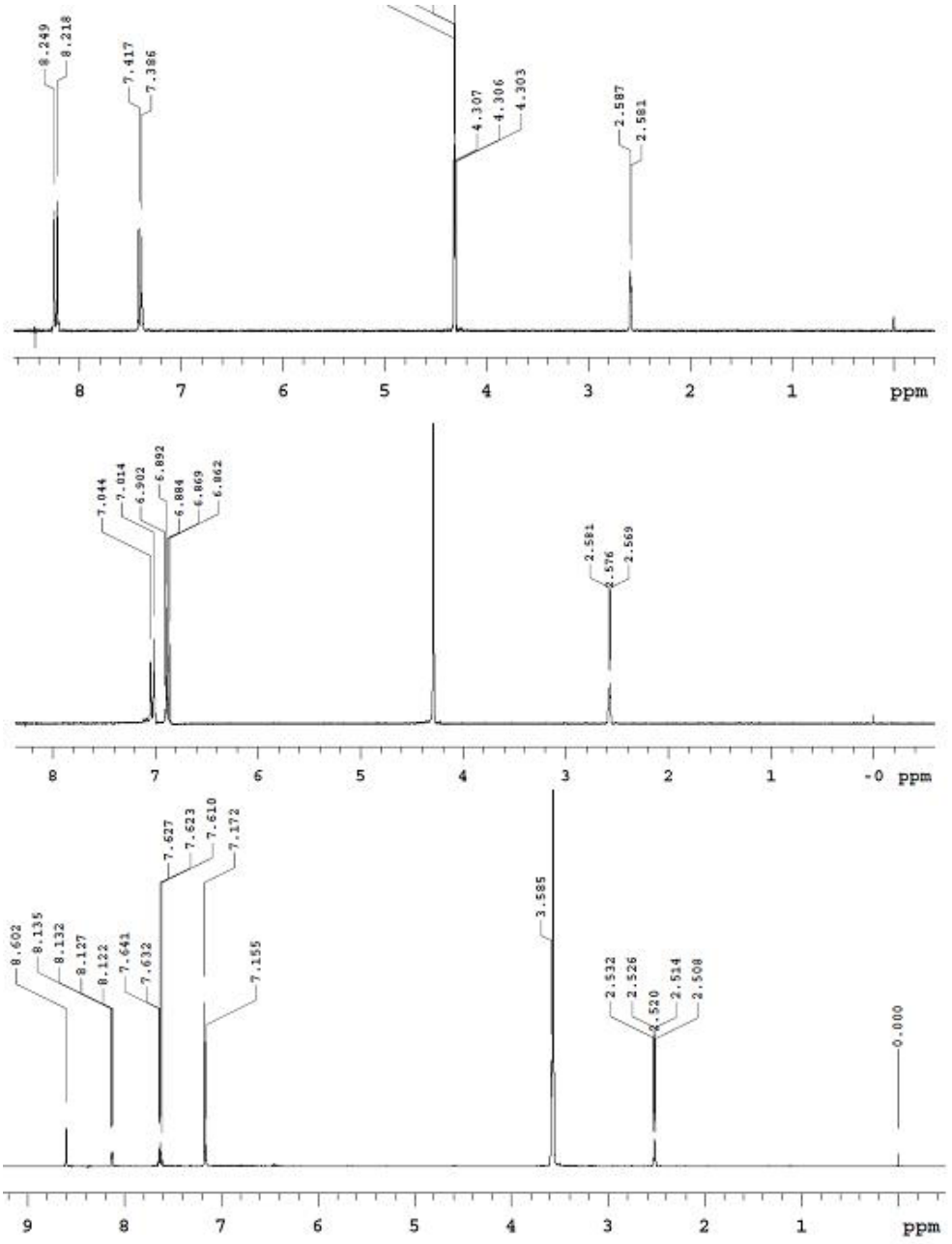

Figure 3. *NMR results of the chemical reactions. The top spectra shows a spectra of the unreduced phosphate ionophore (A in Fig. 1). The middle spectra shows the reduced ionophore (B in Fig. 1). Note the shift of the peaks from 8.2 and 7.4 to 7.1 and 6.9. The lower plot shows the spectra after the reaction of "B" with thiophenecarboxaldehyde (D in Fig. 1).*

for the five scans of the polymerization process. The plot shows that initial rise in current at potential of about 1500mV, indicating the development of thiophene-thiophene copolymers. The second and largest, and dominant peak at 2800mV represents the polymerization of the thiophene to the TPA ionophore (shown in step 3, Fig. 1). For each subsequent scan, the current was lower, indicating decreasing polymerization, as the film on the gold surface continues to grow (Fig. 4). It is important to note that the TPA polymer was not fully soluble in the acetonitrile and lithium perchlorate solution used for polymerization.

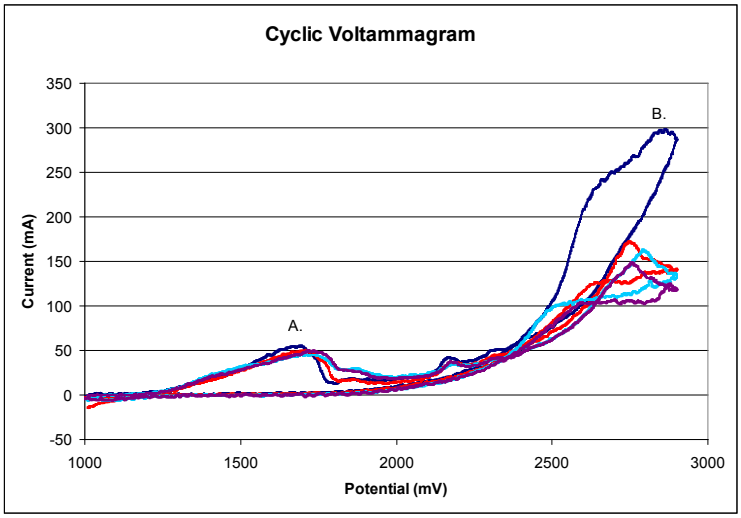

Figure 4. *Voltammogram of the first four scans from the electrical polymerization of the gold electrode. The first scan is shown in dark blue, followed by red, light blue and finally violet. The first peak (at A) represents the co-polymerization of thiophene to thiophene. The second, and largest peak (B) represents the co-polymerization of thiophene to PTA (step four in Fig. 1). Note that, as expected, the current falls with each progressive scan, indicating that co-polymerization has taken place.*

The presence of the TPA ionophore on the gold surface was confirmed by IR scans conducted after polymerization. Figure 5 shows the IR signal of TPA and thiophene alone, and the signal from the polymerized calcium sensor. The peaks from the pure TPA ionophore correspond with the peaks seen on the calcium sensor scan (Fig. 5). On the other hand, the peaks from thiophene are not present on the calcium sensor scan, indicating that no thiophene was directly polymerized directly on to the gold surface. The changes between the calcium sensor IR scan and the TPA IR scan suggests that there was a formation of a thiophene-TPA copolymer (Fig. 5).

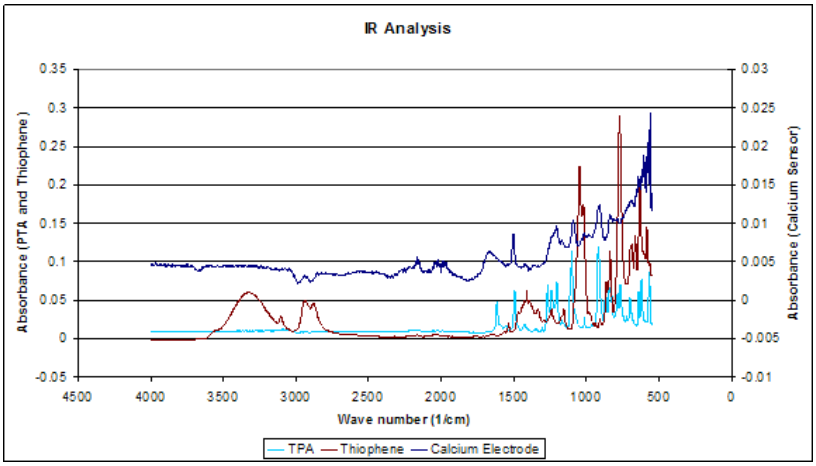

Figure 5. *IR scan of the calcium electrode after polymerization and the TPA ionophore and thiophene before polymerization. Note that the peaks from the calcium electrode match closely to TPA, where as have no relation to thiophene. This indicates that the TPA has dominated the polymerization onto the gold surface, illustrating the success of the polymerization process onto the gold electrode.*

The electrochemical polymerization process produced a dark brown film on the gold surface (Fig. 2). Through the experiments, it was noted that the TPA ionophore attached best when five cycles were used. However, this coating was seen to be relatively unstable, with a tendency of falling off of the gold surface, particularly after the conditioning of the sensors. The coating after 5 cycles tended to be more stable, rarely falling off during the conditioning period.

3.4 Testing of the electrodes

The tests of the electrodes polymerized using the TPA from step 2.3 show no response to the calcium ions in either the buffered or non-buffered $CaNO_3$ solutions (Fig. 6). A total of 11 electrodes were polymerized and tested multiple times, all with the same results. The electrodes produced using the TPA from step 2.4, with the Ca^{2+} bounded to the TPA prior to electrochemical polymerization, also showed no response (Fig. 6). As stated in section 2.6, the length of time the electrode was conditioned for was also varied – from 1 hour to 3 days. The results from this were the same, with no response recorded. Table 1 shows the details of the developed sensors. From this data it is apparent that, utilizing the techniques described above, the development of the ISE for calcium did not succeed.

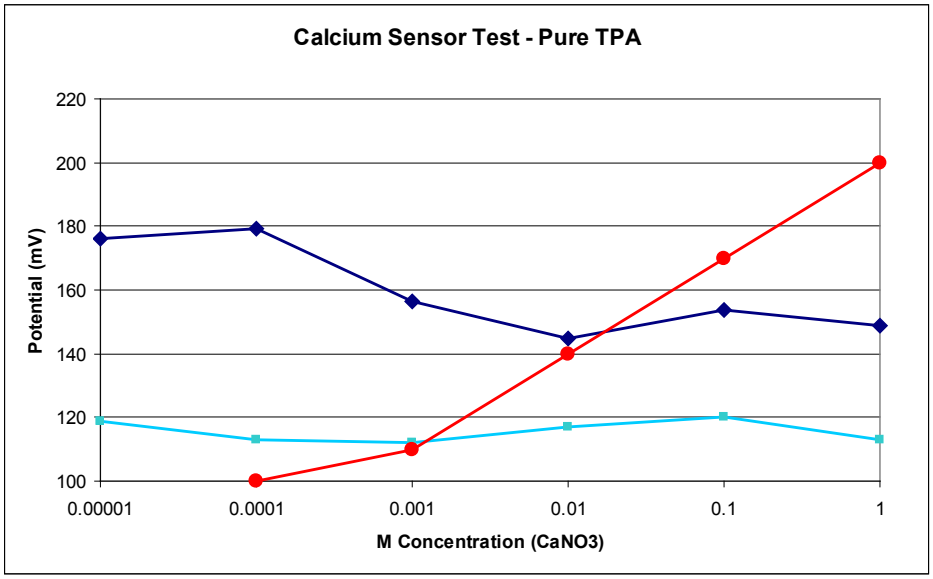

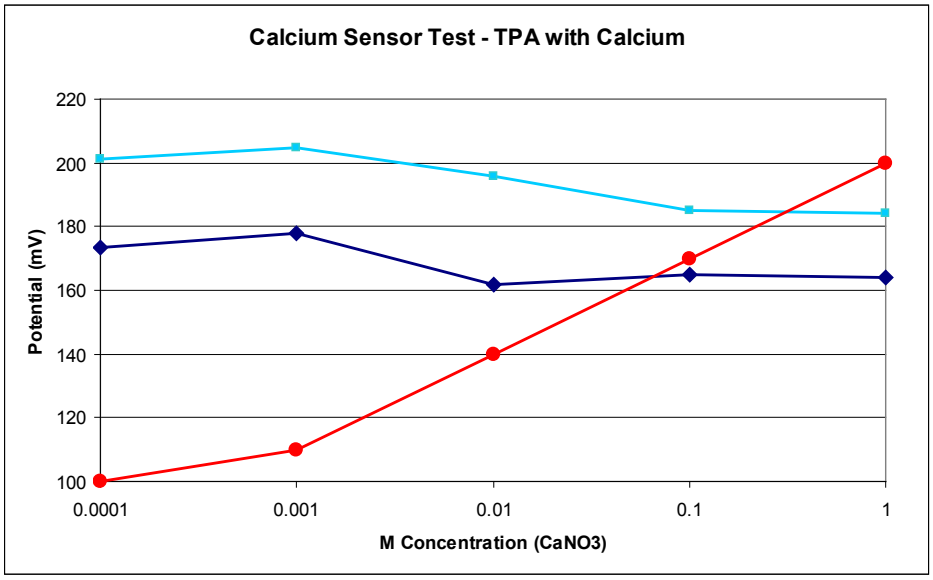

Figure 6. *Calibration tests to determine the electrodes success for the detection of calcium in solution. The dark blue line (with diamond) shows the test in pure CaNO3 solution, the light blue lines (with squares) shows the test in CaNO3 buffered to pH of 8 in with a borax buffer. The red line (with circles) shows the ideal (Nernstian) response to calcium concentration.*

Table 1. *List of the developed calcium electrodes. The electrode is named from the month and year of the polymerization of the electrode. The ionophore used for polymerization, TPA represents the ionophore developed in section 2.3, where as TPA+Ca is the ionophore developed in section 2.4. The conditioning periods list the length of the first (shortest) and subsequent conditioning periods for the electrodes. Conditioning was always conducted in* $Ca(NO_3)_2$ *solutions.*

Electrode	Ionophore polymerized	Conditioning Period	Conditioning Ca^{2+} Concentration
Ca0907a	TPA	1hr, 24hr	10^{-2}M, 10^{-1}M
Ca0907b	TPA	1hr, 36hr, 72hr	10^{-2}M, 10^{-1}M
Ca1007a	TPA	18hr, 24hr	10^{-4}M, 10^{-2}M
Ca1107a	TPA	24hr	1M
Ca0108a	TPA	1hr, 72hr	10^{-2}M, 10^{-1}M
Ca0208a	TPA+Ca	1hr, 24hr	10^{-3}M, 10^{-2}M, 10^{-1}M
Ca0208b	TPA+Ca	72hr	10^{-3}M
Ca0308a	TPA+Ca	2hr, 48hr	10^{-2}M
Ca0308b	TPA+Ca	2hr, 48hr	10^{-2}M
Ca0508a	TPA+Ca	3hr, 24hr, 48hr	10^{-2}M, 1M
Ca0508b	TPA	3hr, 24hr, 48hr	10^{-2}M, 1M

3.5 PVC based calcium sensors

The initial tests for the two calcium based sensors showed mixed results. Ca1PVC showed a very good response to changing calcium concentrations (in $Ca(NO_3)_2$), with a response of 27mV/decade, which is very close to an ideal Nernst response of 30mV/decade at 25°C (Fig. 7a). However, the second electrode, Ca2PVC did not perform as well, with a response of 15mV/decade. Both sensors had response range of approximately 4mg/l and as high as 4000mg/l (Fig. 7a). Ca1PVC was used in a continuous test in the laboratory for 30 days (Fig. 7b). The test showed a fairly stable signal with relatively constant drift (-3.1mV/day) over the first 14 days (through December 6), with an R^2 value of 0.97 and a standard deviation of 2.6mV. Given the pre-test calibration of 27mV/decade, this gives an accuracy of +/-10% from the drift. The sensor become more unstable during the second half of the test. The drift was lower (0.2mV/day) but much more unstable, with an R^2 value of 0.10, and a much higher standard deviation of 7.5mV. In addition, at the end of the test, the sensor was influenced by a unknown interference causing severe noise in the sensor's signal. It should be noted that between the two tests, the data-logger malfunctioned twice with a loss of data. It is not known how this

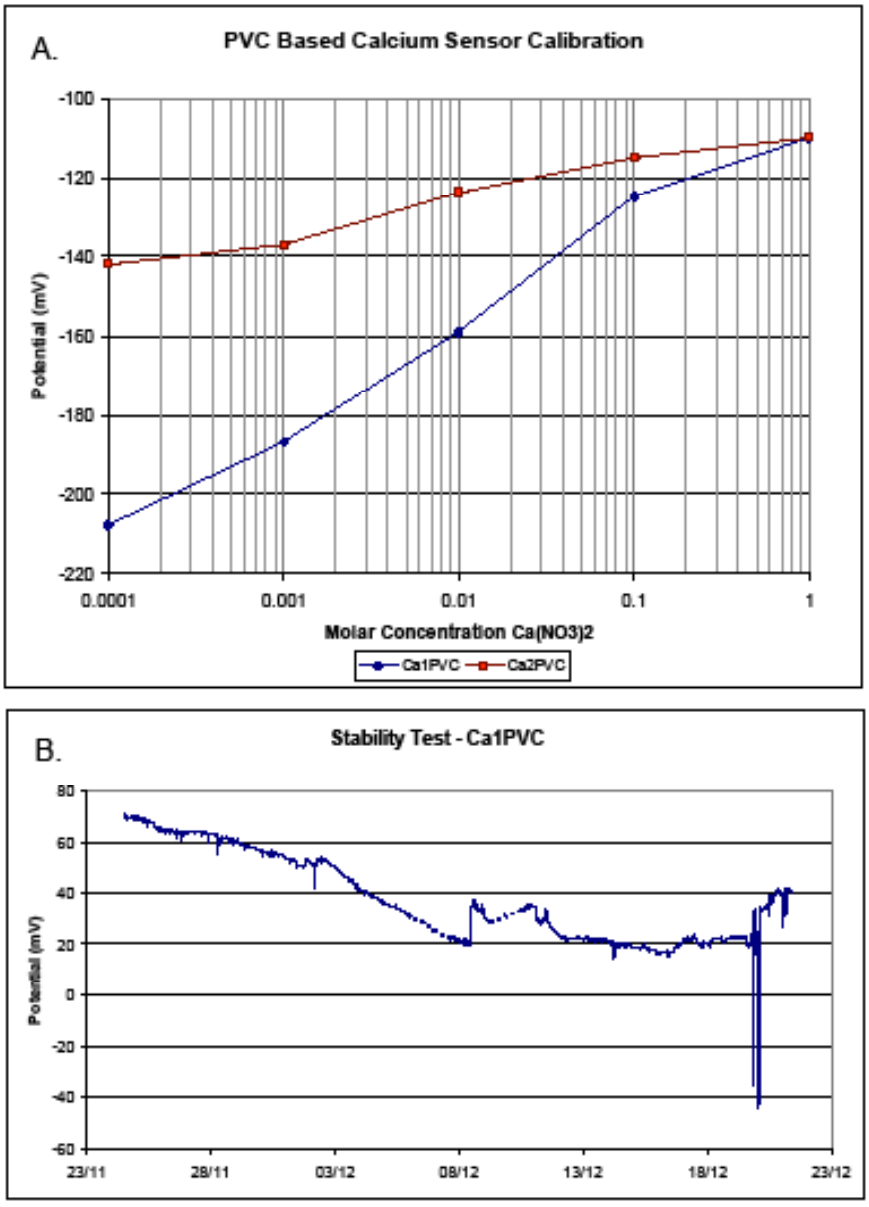

Figure 7. *Calibration of the PVC based calcium electrodes and sensor stability test (A). The lower plot shows the sensor stability test conducted in 0.01M Ca(NO3)2 solution (B). The dashed lines show the time periods (December 6-7 and December 9-10) where the data logger malfunctioned.*

affected the sensor signal after these events, but there is a definite difference in the quality of the signal (Fig. 7b). Calibration after the test showed a 20mV response between 10^{-3}M and 10^{-2}M and between 10^{-2}M and 10^{-1}M solutions of $Ca(NO_3)_2$.

4. DISCUSSION

Initial tests on the two PVC based sensors that were developed in this study showed that the calcium ionophore could be successfully incorporated into a PVC film to form a solid-state calcium sensor. In this case, both of the produced sensors responded to changing calcium concentrations after conditioning. However, there was still a significant difference in the response of the two calcium sensors, with one having a near-Nerstian response, and the other half of that. This inconsistency is also a trend which was observed to some degree in the PVC based for sodium sensors discussed in Chapter 4. The long term test also showed some promise, with the sensor initially having a consistent drift. However, the standard error of 20% will have to be improved upon. The second half of the test proved more troublesome with a much more unstable drift and a much higher standard error in the signal. Again, this is a similar trend that was observed with the sodium PVC based sensors. It needs to be stressed that only two PVC based sensors were produced in this study, and the results can only be considered very preliminary. More testing will need to be done in order to make a better evaluation on the sensors. Particular areas of concern that will need to be evaluated, and likely improved will be the longer-term stability of the sensors during continuous monitoring and reproducibility of a good, near Nernstian response of the sensors, particularly with respect to the fact that, in contrast to sodium and chloride, the ideal response is only 30mV/decade (at 25^{o}C), and any drift from this will quickly add error to the sensor reading.

The sensors produced in which the calcium ionophore (TPA) was attached directly to the gold surface proved to be unsuccessful. In this case, none of the sensors had any response to changing concentrations of calcium. It is not possible to determine exactly why the sensors did not work, as there are a number of possibilities that could have gone wrong. As noted above, the TPA ionophore was not fully soluble in the acetonitrile – lithium perchlorate solution, in which the polymerization was conducted in. Because the TPA was not fully soluble, it may not have been possible to attach the ionophore to the gold surface, with only thiophene attaching. However, the IR data suggests the presence of TPA on to the gold surface of the electrodes and not thiophene. Therefore it appears that there was enough of the TPA in solution to allow for the polymerization of TPA on to the gold surface.

A second possibility for the electrode not working is difficulties in getting a good binding attachment between the TPA ionophore and the gold surface. If there

is not a good connection between the TPA ionophore and the conducting gold surface, it will not be possible to measure the changes in potential registered by the ionophore. It is possible that the TPA ionophore is simply too large, with the size hindering the interaction between thiophene's sulfur and the gold surface (although no previous studies have been found reporting on size of the polymer affecting thiophene's ability to bind with gold). The large molecule could be getting in its own way as it tries to organize itself during the polymerization process. As stated above, if more than five voltammetric scans at 10mV/sec were used, then the film accrued on the gold electrode surface tended to become too thick, and broke off. This often would occur during rinsing of the electrode in water after polymerization or falling off during the conditioning period when it was soaked in $Ca(NO_3)_2$ solution. However, when five scans were used, the film would remain on the electrode surface during rinsing and conditioning. It could be possible that, even though the film remained on the electrode, the connection between the film and the gold electrode was not good enough to transmit the potential to the electrode and data logger.

There is, however, evidence that indicates that the connection between the film and the electrode is not a problem. When the potential is measured using a clean gold electrode, the potential reading is steady at 120mV +/-5mV. The electrodes with the TPA film had a potential of between 100 and 220mV, depending on the electrode. In one instance, one of the electrodes polymerized using 7 scans survived the rinsing and conditioning period, but the film subsequently fell off during the testing stage. During this test, the electrode registered a significant potential shift of approximately 50mV at the time that the film fell off, reverting to the potential of a gold electrode (121mV). If there was not a connection between the film and the electrode, then the potential should be in the zone for gold alone, which is not the case. Therefore, it appears that the lack of response in the electrodes is not due to a lack of connection between the TPA film and the gold electrode. However, it cannot be fully ruled out that, even though there is an apparent connection between the film and the electrode, that the signal might not be strong enough to register changes in potential due to changes in calcium concentration.

A third possibility for the lack of response in the electrode is that, during the synthesis of the TPA ionophore, the ion selective properties for calcium may have changed. Specifically, the ionophores ability to selectively bind the calcium ion is dependent upon the acidity of the phosphate in the polymer. The reduction

of Bis(4-nitrophenyl)phosphate in the first reaction may have created a situation where the newly created amine group on the ionophore takes electrons away from the phosphate group, reducing its acidity and ability to bind with calcium. However, it is thought that the addition of the thiophene group would negate this affect, with the phosphate group acidity its properties and ability to bind with calcium. Whether or not this occurs depends on the original ionophores acid dissociation constant (pKa value), which provides an indication on how resilient the phosphate group is to change; the lower the pKa value, the stronger the acid is, and the more likely the group is to retain their properties. Unfortunately, although a number of studies have looked at the pH range of operability of the sensors (i.e. Ruzicha et al. 1973, Brown et al. 1976, Keil et al. 1978) none of the studies measuring the pKa value for the phosphoric acid based calcium ionophores could be found. Since this was not within the scope of this project to determine the pKa values for the ionophores, a full assessment as to whether or not this is a full problem could not be made.

The final possibility is that the polymerized TPA film is not water soluble enough to allow water to diffuse into the membrane, allowing the potential from the calcium ions in solution to be measured. This would be similar to PVC, which is also impervious to water. PVC membranes containing ionophores have been previously used in ISE's (i.e. Kim and Amemiya 2008, Kumar et al. 2007, Sutter et al. 2004), however in these cases a plasticizer must be added to the film in order to soften up the PVC, allowing water to diffuse into and out of the membrane. The addition of thiophene on the BAP ionophore likely reduced its solubility in water. When polymerized on the gold electrode, it may have taken on properties similar to PVC, and became too hard for water to be able to diffuse into the membrane, and not allowing the Ca^{2+} ions to reach the ion selective sites. Without the Ca^{2+} ions cannot reach these sites, the ISE will not function properly.

One possible way to fix this problem is to incorporate a plasticizer into the polymerized film. The way this can be done is to polymerize a water soluble thiophene molecule together with the TPA on to the gold electrode. This could end up softening up the membrane up enough to allow water to diffuse into the membrane. One such possibility is the crown ether ionophore for potassium which was developed by Si et al. (2007). However, the main drawback would be that the signal would also incorporate a strong interference for potassium (and sodium) through the plasticizing ionophore. This would restrict the use of the developed

ISE in solutions where there would not be interference from potassium or sodium. The development of the calcium ISE was intended to be used to monitor changes in calcium within the groundwater, which often will have sodium present (and to a lesser extent, potassium), the interference was deemed to be too much in order to pursue this avenue. However, if an alternative, non ion specific plasticizing material that can be polymerized on to gold together with TPA can be found, then a successful calcium electrode using TPA could be developed (assuming that the other problems discussed above are not affecting the electrode).

5. CONCLUSION

Although the theory indicated that it is possible to develop a solid-state calcium ISE, with the sensing membrane polymerized directly on a gold electrode, in practice it was not possible. It was possible to take a known calcium ionophore, Bis(4-aminophenyl)phosphate and coble a thiophene group on the sides, forming a new ionophore, TPA. The IR scanning results also indicate that it was possible to electrochemically polymerize the ionophore on to a gold electrode. However, the polymerized electrode remained unresponsive to changes in calcium concentrations when tested in different concentrations of $Ca(NO_3)_2$solutions. The failure likely is a result of either the changing of the selectivity of the ionophore to calcium with the addition of the thiophene group on the ionophore, or to the molecule being too rigid to allow water to diffuse into the membrane. If the selectivity properties have changed, and the TPA molecule is no longer selective for calcium, an entirely new ionophore will need to be found in order to apply this technique. If the non-responsiveness is due to the insolubility of the membrane, then a technique in order to soften the membrane up to allow water to be able to enter the membrane, will need to be developed. Initial tests conducted on PVC based calcium electrodes did show some promise, but more studies need to be conducted in order to provide a sufficient evaluation of the sensors.

Mapping of the Geological Surface and Structure of the Maastrictian Chalk along Køge Bay

1. INTRODUCTION

Fractured Maastrictian chalk and Danian limestone just below the Quaternary glacial sediments compose the primary groundwater aquifer for the region around the coastline of Køge Bay, southwest of Copenhagen (Fig. 1). This aquifer supplies nearly 100% of the water supply for these coastal municipalities and is also an important part of the Copenhagen water supply. Given very low matrix hydraulic conductivities of both the chalk and limestone (measured at less than $5x10^{-8}$ m/sec), fractures are the primary source of hydraulic conductivity in the units (Frykman 2001, Larsen et al. 2006). Hydraulic conductivities are seen to vary throughout the area, ranging from $1x10^{-5}$to $1x10^{-4}$ m/sec in the chalk and $5x10^{-5}$to $5x10^{-4}$ m/sec in the limestone (Jensen et al. 2002, Larsen et al. 2006). The fractures are thought to have been developed from a combination of unloading from the erosion of sediments during the Neogene (Huuse et al. 2001, Japsen 1993, Japsen et al. 2007) and unloading after the retreat of the glacial ice which covered the area at different times during the Quaternary (Houmark-Nielsen 1987). Localized faulting and folding, however, can also have an influence on the fractures in the chalk and limestone, influencing fracture density, openness, and orientation. Particularly the presence of faults within the chalk and limestone could have significant localized effects on the hydrological properties. Thus a good, accurate mapping of the units and structure is important for the proper understanding and modeling of the groundwater aquifer in the area.

Previous studies in the area, dating as far back as 1925, have shown conflicting interpretations of the faulting in the limestone and chalk units near the coast of Køge Bay. Particularly contested is the existence of a major NE-SW trending fault parallel to (and approximately 2km from) the coastline. Rosenkrantz (1925)

was the first to map this structure based on well data, and was later supported by other prominent geologists, such as Ødum (1935). In fact, as can be seen from official letters and borehole log interpretations, Ødum, was very familiar with the geology in the Køge Bay area, being the geologist responsible for interpreting a large number of boreholes for the Karlstrup limestone quarry in the late 1940's (GEUS 2009). However, this interpretation of faulting was countered by Hansen (1941) who argued that the structure could be explained simply through gentle folding of the units. However, the Rosenkrantz interpretation has persisted, with official groundwater assessment reports as late as 1989 using the NE-SW trending fault with an off-set of over 30m (Hovedstadsrådet/Roskilde Amt 1989, Roskilde Amt 1987). Because the limestone and chalk is not exposed in the area, apart from in an old limestone quarry near the town of Karlstrup, these interpretations are based solely on data from well logs and very limited seismic sections. As the density of the boreholes has greatly increased since the original interpretations, a more detailed and accurate analysis should be possible. In fact Larsen (1998) conducted a study in the area within 3-4 km of the coastline from Solrød to Greve municipalities, where resistivity and gamma logs were used in combination with the borehole logs to map the structure of the top of the Maastrictian chalk. From the results, it was determined that there was otherwise only one small fault of limited extend about 1km north of the limestone quarry, where as there was absolutely no evidence for faults (Larsen 1998). However, this study was limited to the area immediately along the coast-line of Solrød and Greve munipalities. Analysis of wells further inland as well as to the north and south may also reveal more detail with regard to faulting and folding in the area.

According to the Geological Survey of Denmark and Greenland's borehole database, there are over 1000 wells present in the area around the NW coastline of Køge Bay area (GEUS 2009). The lithological descriptions of these wells provide an opportunity to map in detail the structure of the chalk and limestone aquifer. This study looks to build upon the results from Larsen (1998) by mapping in detail the Danian limestone and the Maastrictian chalk boundary in the area from the municipality of Roskilde in the west to Hvidovre in the east, along the NW coast of Køge Bay (Fig. 1). This is the region between the relatively well-known NNW-SSE trending Roskilde and Carlsberg faults. The area will be mapped by studying in detail the lithological logs from the wells in the region, while assessing the accuracy and quality of the logs. In addition, the pre-Quaternary surface will also be mapped from the well logs. This will be compared to the Danian/Maastrictian

boundary map in order to provide a detailed analysis of where the Danian limestone and Maastrictian chalk are exposed directly under the Quaternary sediments. Given the difference between the hydraulic conductivities of these two units, this information along with a detailed assessment of faulting in the area will provide an accurate geological model for the modeling of the primary aquifer in the area.

Figure 1. *Location of the study area in this area, showing the municipalities covered.*

2. GEOLOGICAL SETTING

The study area lies in the eastern margin of the Danish Basin, which extends from the Baltic Sea in the east to the Norwegian-Danish Basin in the North Sea (Fig. 2)(Clausen and Huuse 2002, Vejbæk 1997). The Danish Basin is bounded by Sorgenfrei-Tornquist fault zone to the north and the Ringkøbing-Fyn High to the south. The basin has a complex tectonic history. The basin originally formed during the Permian, as part of the rifting episode which formed the Zechstein sea (Ziegler 1990, Vejbæk 1997). Subsidence in the Danish Basin continued until the Albian age in the mid-Cretaceous. Tectonic inversion of the basin began thereafter,

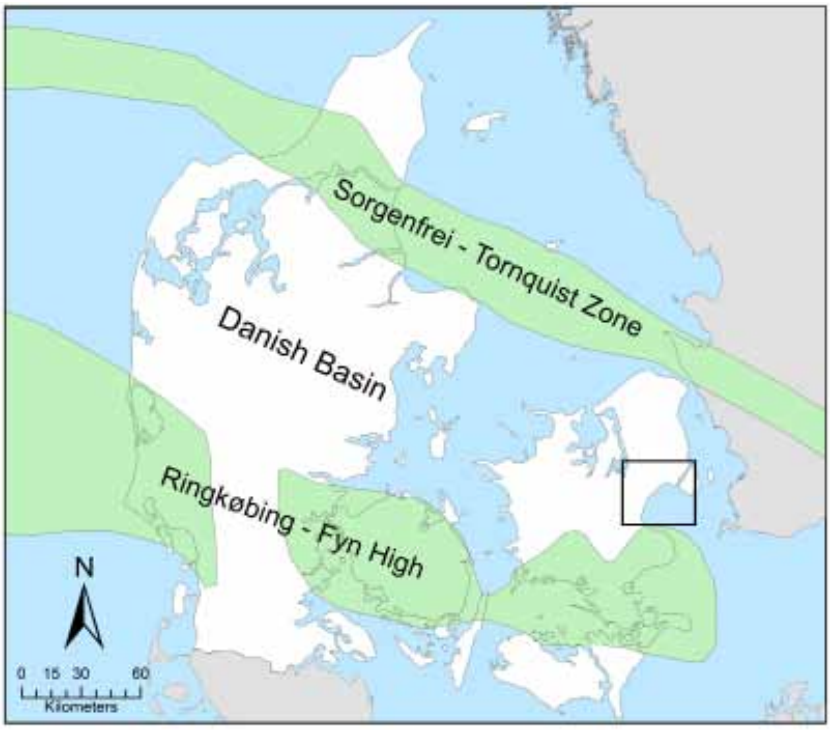

Figure 2. *Tectonic structure map over Denmark showing the location of the Sorgenfrei-Tornquist Zone and the Ringkøbing-Fyn High surrounding the Danish Basin. The study area is outlined in the black box (modified from Lykke-Andersen and Surlyk 2004).*

with the faults within the Sorgenfrei-Tornquist fault zone reactivated into high angle reverse faults, and culminated during the Santonian and Campanian age (Nielsen et al. 2005, Ziegler 1990). The basin remained submerged from the late Cretaceous and into the Paleocene where significant deposits of marine sediments accumulated. A second period of inversion began in the mid- to late Danian and continued throughout the remainder of the Paleocene (Nielsen et al. 2005, Ziegler 1990). The total thickness of the Paleocene sediments remains debated, with evidence of thicknesses of anywhere between 300m and 1000m (Huuse et al. 2001, Japsen et al. 2007, Surlyk et al. 2006). There are two well known faults which bracket the Køge Bay coastal area: Roskilde Fault to the west and Carlsberg fault to the east (Fig. 3) (Vejbæk 1997). These faults likely had their origins in the Permian, with reactivation throughout the Cretaceous and Tertiary (Huuse 2002, Vejbæk 1997). However, many of the faults within the greater Danish Basin are seen in the Lower Cretaceous, but die out within the Cretaceous strata, becoming simple monoclines in the top of the Maastrictian sediments (Ziegler 1990). Given the proximity of Greve to both the Roskilde and Carlsberg faults,

as well as the tectonic history of the area, there could be associated faults within the Maastrictian and Danian strata.

There are three primary units which underlie the Quaternary sediments in the area, and form the primary groundwater aquifer: the Maastrictian chalk, the Danian bryozoan limestone, and the Selandian greensands and marl. The oldest unit exposed under the Quaternary sediments is the Maastrictian chalk. The chalk was deposited in the relatively quiet late Cretaceous sea, which extended over a large portion of NW Europe (Frykman 2001, Hancock and Kauffman 1979). The chalk is a very fine-grained micritic limestone, composed primarily of cocolith skeletons and other pelagic nanno-fossils, interbedded with bands of black flint nodules (Anderskouv et al. 2007, Hancock 1976). The total thickness of the chalk in the area reaches as much as 1200m (Thomsen 1995).

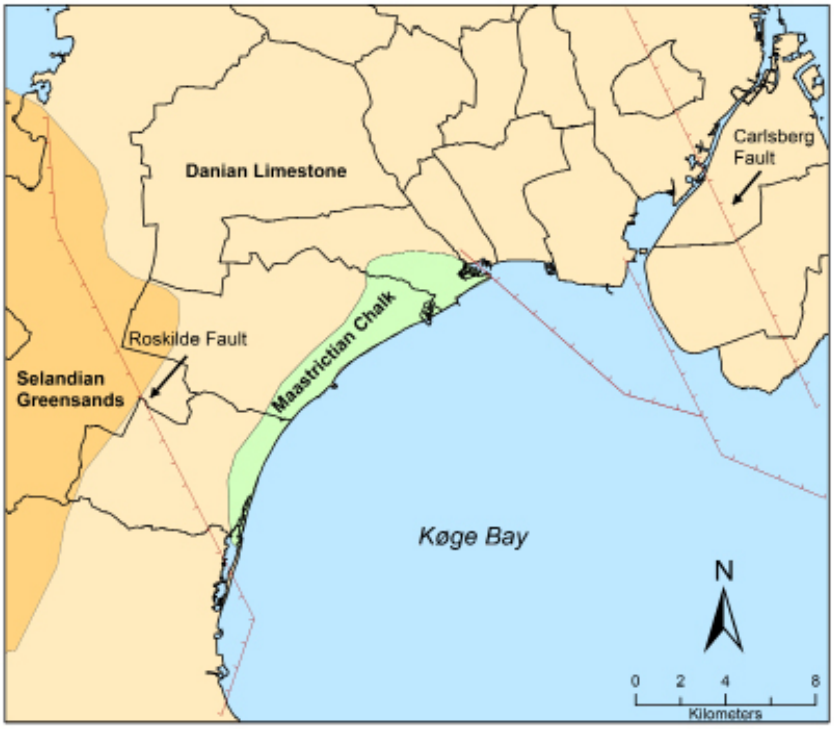

Figure 3. *Geological map of the pre-Quaternary units over the Køge Bay area, derived from Thomsen (1995), Larsen (1998) and Bidstrup and Klitten (2006). This map shows the geology before the interpretations from this study are included. Shown are the mapped locations of the Roskilde and Carlsberg faults, with the ticks indicating the down-thrown block.*

The second pre-Quaternary unit in the area is the Danian bryozoan limestone. It was deposited in the shallower seas which were present in the Danish Basin in the early Paleocene. The bryozoan limestone has a micritic matrix of calcareous nannofossils with bryozoan fossil fragments making up anywhere between 20% to 45% of the limestone (Clemmensen and Thomsen 2005, Thomsen 1995). Like the chalk, the Danian bryozoan limestone has bands of flint, often gray to dark gray in color (Thomsen 1995). Total thickness of the Danian bryozoan limestone in the area is 100m (Thomsen 1995).

The third unit, which was deposited on top of the Danian bryozoan limestone is the Selandian greensands and marl. The Selandian sediments are primarily clastic, with two different facies groups recognized in the study area (Clemmensen and Thomsen 2005). The first group is the Lellinge Greensand, which was deposited directly on top of the limestone. The greensands were deposited in shallow water depths under high energy conditions (Clausen and Huuse 2002). The sands are strongly calcareous and glauconitic, and are generally less than 10m thick (Clemmensen and Thomsen 2005). The Lellinge Greensands grade into the finer grained Kertminde Marl (Clemmensen and Thomsen 2005). The marl has a calcium carbonate content of 50-70%, with most of it composed of calcareous nannofossils. The thickness of the marl is unknown due to erosion, but it is estimated to have exceeded 100m (Clemmensen and Thomsen 2005).

3. METHODS

The Geological Survey of Denmark and Greenland (GEUS) maintains a public accessible on-line registry over all of the wells drilled in Denmark (GEUS 2009). This includes wells for groundwater abstraction, groundwater monitoring, geotechnical studies, mineral exploration and research. The registry includes documentation from the original lithological descriptions when the wells were drilled, foraminifera analyses conducted on samples taken from wells, and geophysical logging (gamma and resistivity) which has been conducted on a number of the wells (but not all). This available data was used to map out the Danian/Maastrictian boundary, analyzing the well logs and associated information from approximately 1000 wells over the study area.

The first step in the analysis of the well logs was to make an initial assessment of

the quality of information from each well. The quality of geological descriptions in the well-logs varied widely. Some of the logs used lithologic descriptors such as chalk and bryozoan limestone, or chronological descriptors such as Danian and Maastrictian. In these cases, the well logs were considered of good quality, with an absolute boundary elevation obtained for each well. Other well logs have merely vague descriptions the drill samples, such as undifferentiated limestone. In these cases, these wells were marked as questionable quality, even when the presence of a boundary was alluded to in the well log.

There were a large number of wells in the study area that did not penetrate the Danian/Maastrictian boundary. The wells that were only drilled into the Quaternary sediments were removed from the database. Wells that penetrated only either the Danian or Maastrictian were given a bracketing value, indicating that the boundary is either higher (in wells with only Maastrictian chalk) or lower (in wells with only Danian limestone). Wells that penetrated the boundary between the Selandian greensands/Danian limestone, which occurred in the western part of the study area, were also given absolute values for the Danian/Maastrictian boundary. As the Danian limestone is seen to be 100m in thickness (Thomsen 1995), this boundary was used as a proxy for the Danian/Maastrictian boundary by subtracting 100m from the elevation of the Selandian/Danian boundary.

The second step in the borehole evaluation process was the critical analysis of the boundary elevations obtained from the well logs. Each well's boundary elevation was analyzed with respect to its neighbors. In cases where there appeared to be discrepancies between wells, all of the available information in the database was examined. This included determining whether or not the registry borehole data, such as surface elevation of the borehole or location of the borehole, was entered correctly into the GEUS database. In cases where mistakes were observed, the data was either corrected (if there was sufficient evidence to do so), or the well was removed from the database. Accompanying information, including detailed geological sample descriptions, foraminifera studies, original borehole logs (often hand-written) as well as the geophysical well logs, was also looked at. In the cases where detailed geological and foraminifera data was present, the well is considered to be correct, and marked as such. If there appeared to be a question with respect to the quality of the geological descriptions, the wells were marked as questionable. In the cases where the conflicting data from two separate wells could not be reconciled, the well with the superior data (i.e. foraminifera data)

was considered correct and the well with the questionable well log was removed from consideration. In the cases where the wells each had descriptions of good quality, both wells were kept in the analysis in spite of the conflicting information.

After the detailed assessment of the quality of the individual well logs, the Danian/Maastrictian boundary elevation was constructed. A contour interval of 10m was used to map the boundary. Faults were interpreted in the locations where the elevation differences in the well logs could not be explained by gentle folding.

The elevation of the pre-Quaternary surface was mapped using borehole data from all of the wells in the area which extended into the Paleocene and Cretaceous sediments. A raster surface for the pre-Quaternary surface was generated in GIS (ArcMap) software, using the inverse distance weighting protocol. The elevation for each raster was calculated using the three nearest wells. Elevations for each well itself were not adjusted by the software.

A detailed pre-Quaternary geological map was subsequently produced by combining the mapped Danian/Maastrictian elevations with the pre-Quaternary surface elevation map. The Danian/Maastrictian surface elevation was simply subtracted from the pre-Quaternary surface elevation. The Danian/Maastrictian boundary was mapped out where the elevation difference between the surfaces was 0m, and the Selandian/Danian boundary was mapped out where the elevation difference was -100m (given a Danian thickness of 100m).

4. RESULTS

The analysis of the Danian/Maastrictian boundary shows an elevation range from just over sea level along the coast of Køge Bay, and decreasing in elevation towards the northwest (Fig. 4). The Roskilde Fault, trending roughly NNW-SSE, is observed on the western edge of the study area, a decrease in the boundary elevation of between 40 and 60 meters. The Carlsberg Fault on the eastern edge of the map is observed, also trending NNW-SSE and with a 60 meter decrease in elevation. However, the boundary is not seen to be sharp which would be typical for a fault, but rather seen to be a monocline fold. However, the fold is likely bounded by a fault deeper in the strata. There is interpreted a fold occurring in the middle of Ishøj municipality near the coast, gradually dying out towards the west (Fig. 4).

It is possible that this fold is bounded by a small fault on the NE side of the fold as illustrated by the dashed line in Figure 4. There are also small folds seen in the near-coast of Greve municipality, which also die off towards the west, however, there is no evidence for faults associated with these folds. In the SW part of the study area, there is one persistent fold structure which appears to split from the Roskilde Fault in Roskilde municipality, and then runs roughly parallel to the Roskilde Fault across western Greve and northern Solrød municipality (Fig. 4). It is possible that this structure is bounded by a small fault in the sediments with an off-set of no more than 10m.

The elevation of the pre-Quaternary surface shows that it is lowest along the coast, at elevations of below -35m, and then increasing towards the NW, being the highest at elevations of about 50m in the western part of the study area (Fig. 5). There is a significant Quaternary valley, resulting in a depression in the surface, observed in the north along the border of Ishøj and Greve. Combining this map with the Danian/Maastrictian boundary surface map, a detailed pre-Quaternary surface map was produced (Fig. 5). The Danian/Maastrictian boundary derived

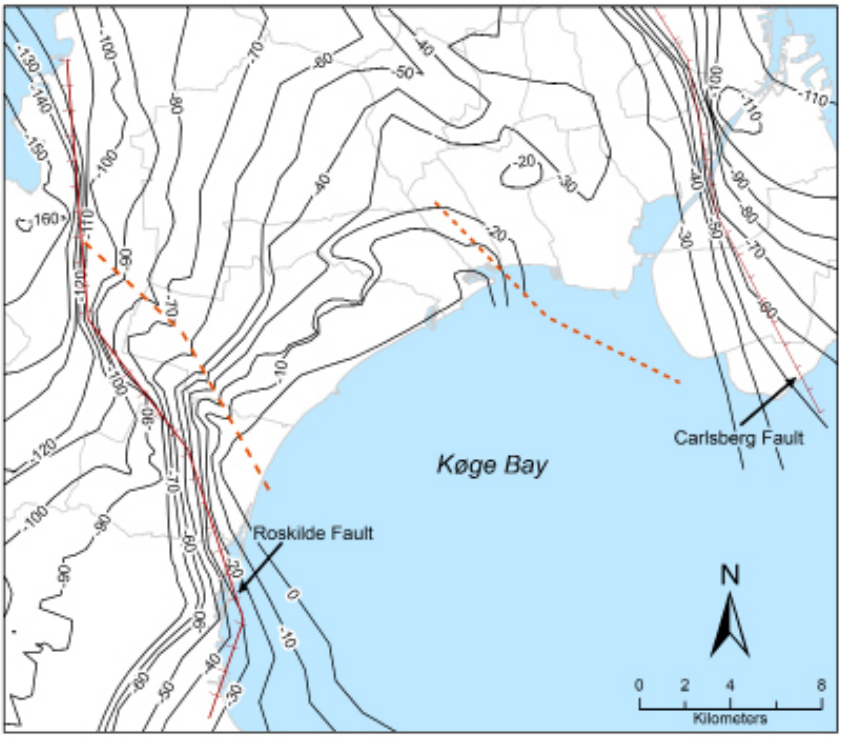

Figure 4. *Structural interpretation of the Danian/Maastrictian boundary for the study area. Both the Carlsberg and Roskilde faults can easily be seen as monocline folds. The dashed lines indicate the locations for possible minor faults, or folding with deeper faults.*

from this study (Fig. 5) was seen to correspond closely to that which was derived by Thomsen (1995), Larsen (1998) and Bidstrup and Klitten (2006) (see Fig. 3). The only difference is the detail in the boundary, specifically along the Quaternary valley incised into the pre-Quaternary sediments along the Ishøj/Greve municipal border. On the other hand, there was a significant difference in the location of the Selandian/Danian boundary. Here, Selandian sediments are seen to extend up to 1km further east in Solrød municipality, as well as extend north into Høje-Taastrup (Fig. 5)

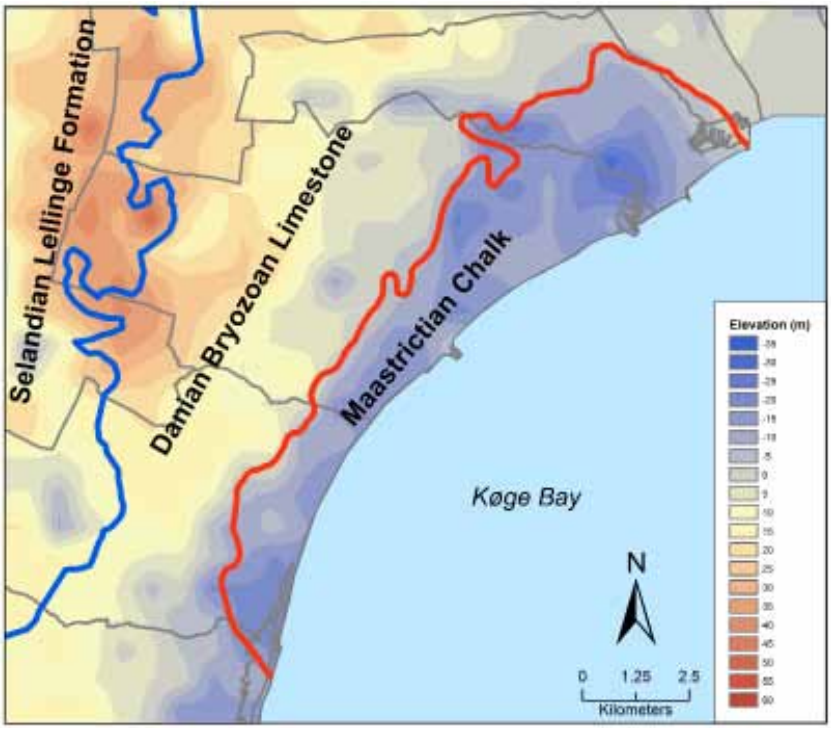

Figure 5. *Map showing the elevation of the pre-Quaternary surface, given in meters, and the interpreted pre-Quaternary geology for the coastal area. The thick red line shows the boundary between the Danian and Maastrictian, and the thick blue line shows the boundary between the Selandian and Danian, as calculated from the borehole data in this project.*

During the analysis of the well logs, a total of 42 wells were deemed to be incorrect and not used in the interpretation. Figure 6 shows the wells that were used for the analysis or discarded all together. The greatest portion of wells where the well logs were considered unreliable and not used were concentrated along the Danian/Maastrictian boundary, and most often discarded because of a poor or incorrect geological description of the borehole. There was a very high concentration of

discarded wells around the Karlstrup limestone quarry (Fig. 6). The reason for the disqualification of these wells is due to a misinterpretation of the boundary in the exploratory wells which were drilled before the limestone quarry came into operation. The quarry is the only place in the study area where the Danian/Maastrictian boundary is exposed, which is observed to be at an elevation of 0.2m in the northeastern corner of the quarry (Gravesen 1983) (Fig. 7). The interpreted boundary in all of the discarded wells were a full 8m lower than the observed boundary in quarry. There were, however, four wells in the quarry itself, where the geological interpretation fits the observations in the quarry outcrops, and thus not all of the wells associated with the quarry were incorrectly interpreted (Fig. 6).

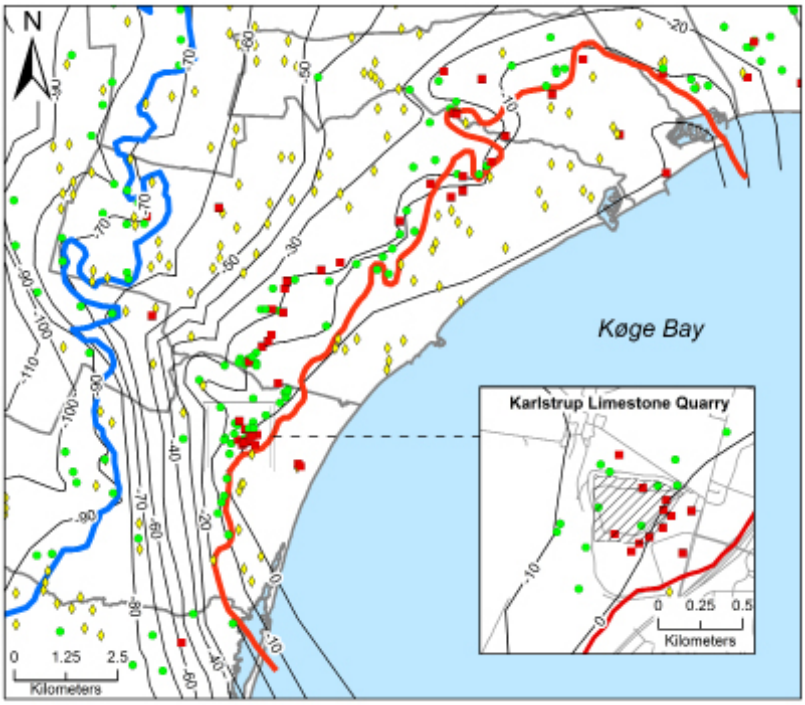

Figure 6. *Map showing the wells used for the interpretation in the study. The green circles show the wells with good well-log data. The yellow diamonds show the wells which do not cross the boundaries, and thus are used as bracketing values. The red squares show the wells with incorrect data, and were not used in the analysis. The inset map shows a close-up of the Karlstrup limestone quarry, with the extent shown in diagonal hashes.*

Figure 7. *Picture from the NE corner of Karlstrup limestone quarry showing the boundary between the Danian and the Maastrictian. The dashed yellow line shows the location of a 2cm thick clay layer which has been interpreted by Gravesen (1983) as the "Fish Clay" which occurs at the very end of the Cretaceous. The water level in the picture is precisely at an elevation of 0.0m, as measured using differential GPS.*

5. DISCUSSION AND CONCLUSION

The overall analysis of the Danian/Maastrictian boundary in the study area shows very little evidence for faulting. Even the well-known Roskilde and Carlsberg faults are seen as monoclines at the top of the Maastrictian chalk. This is backed up by seismic sections crossing the Carlsberg Fault, which also show a monocline at the Danian/Maastrictian boundary, turning into a fault further down in the strata (Bidstrup and Klitten 2006). The fold observed in Ishøj municipality is likely bounded by a fault further down in the strata, as is indicated by Bidstrup and Klitten (2006), however, there is no evidence for faulting at the surface, and is only interpreted as a fold at the top of the chalk.

The only structure that could be interpreted as a small fault is the NW-SE trending fold (?) structure that runs parallel to the Roskilde fault. This structure is seen both in the Selandian/Danian and Danian/Maastrictian boundary and continues for over 10km in length. The structure also corresponds with a small fault interpreted by Larsen (1998) 1.5km north of the Karlstrup limestone quarry. From

the borehole data, it is unclear whether or not this structure is a fold or a small fault, however, it is eviden that the off-set is less than 10m. Since this structure is seen in both of the boundaries, has a long linear extent, and runs parallel to the known Roskilde fault, it is considered to be of tectonic origin rather than a local depositional-related variation in the Danian/Maastrictian boundary.

The results from this study show no evidence for significant faulting in the area. This is in full agreement with the results from Larsen (1998) and Bidstrup and Klitten (2006) as well as the interpretation of Hansen (1941). This is particularly with reference to the NE/SW trending fault with an over 30m off-set, which has been previously interpreted by Rozenkrantz (1925), supported by Ødum (1935) and used in official management reports and by consulting firms conducting assessments of groundwater resources (Hovedstadsrådet/Roskilde Amt 1989, Roskilde Amt 1987). Even with the increased number of boreholes in the area, there is simply no evidence which supports the interpretation of significant faulting in the area.

The mapping of the Danian/Maastrictian boundary, however, can be problematic. The lithological transition from the Maastrictian chalk to the Danian bryozoan limestone in a borehole can be mistaken if careful control of the depth of the sampling and analysis of the samples themselves is not taken. Although the boundary is quite clear in outcrop, determining the boundary from the well cores can be difficult, as both units contain significant flint layers, as well as similar macro-fossils, specifically bryozoa (Gravesen 1983, Lykke-Andersen H. and Surlyk F. 2004, Surlyk et al. 2006). The best and most certain way to determine the boundary between the Danian and Maastrictian is through a foraminifera analysis of the samples. However, for this to be effective, close control over the depth from where the samples originated from must be maintained, otherwise the interpretation will be incorrect. This is very well illustrated in the Karlstrup limestone quarry, where expert geologists, including Ødum, had mis-interpreted the boundary as being 8m lower than it actually was (GEUS 2009, Gravesen 1983). One possible reason for the misinterpretation of this boundary by 8m could lie in the drilling method used for the boreholes. Although no records on the drilling methods used could be located, if a rotary drilling method was used in an open borehole, it is possible that drill chips from higher up in the borehole could have fallen down during the drilling process. Thus, chips of Danian limestone could have theoretically fallen into the borehole after the drilling had penetrated into

the Maastrictian. Thus, when the samples were collected, they showed Danian strata, when the well was actually in Maastrictian.

In the analysis of the structure of the boundary, particularly with respect to the interpretation of smaller faults, the natural depositional topography of the boundary must also be considered. Studies of the boundary at outcrops at Stevns along the coast 30km to the SE of the study site, shows the surface not to be flat, but rather undulating, varying as much as 3-5 meters over short distances (Lykke-Andersen H. and Surlyk F. 2004, Surlyk et al. 2006). This is enhanced by the natural structure of the bryozoan mounds deposited in the Danian, which can often reach heights of 9-11m (Surlyk et al. 2006). In these cases, it is seen that the boundary has a natural, depositional relief that is not related to faulting or folding of the units. It is not out of the question to see the relief giving a difference of 4-5m between wells only a short distance apart. In this case, the elevation difference may be interpreted as a fault, but in fact be just the natural depositional relief. In this study, a detailed map of the exposure of the Danian/Maastrictian boundary was produced, based upon the structure map. However, caution should be used on the detail of the boundary – the natural depositional relief of 4-5m will have an influence on the location of the boundary, possibly even varying up to one to two hundred meters depending on the pre-Quaternary relief.

In spite of both the potential problems with the interpretations of the borehole data and with the natural depositional relief on the Danian/Maastrictian boundary, the large database of borehole logs does provide a good structural map over the study area. No significant faulting was observed in the area. Therefore, when considering the construction of the conceptual geological model for the modeling of the groundwater system for the Køge Bay coastal area, it is apparent from this study that faults, apart from the bounding Roskilde fault, do not influence the hydraulic conductivity in the fractured chalk and limestone. Any preferential flow directions in the groundwater aquifers will be a result of the fractures in the rocks, formed from the later unloading of the sediments in the Neogene and ice in the Quaternary, rather than from faulting and folding in the Maastrictian and Danian.

Groundwater Salinity in Greve, Denmark: Determining the Source from Bulk Water Samples

1. INTRODUCTION

Groundwater exploitation near the coast comes with the inherent risk of saltwater intrusion. This is the case with the coastal community of Greve, approximately 25 km to the southwest of the Danish capital, Copenhagen (Fig.1). Since the 1960's, water supply companies have been abstracting groundwater within 2.5km of the Baltic Sea coast. Indeed, many of these groundwater wells have registered chloride concentrations above the 250 mg/l limit. Because of the proximity of the wells to the coast, it was generally thought that the source of the salinity observed in the wells was saltwater intrusion from the Baltic Sea. Throughout the 1980's and 90's the management of groundwater resources in Greve was conducted without a full understanding of how the fresh/saline groundwater interface changed once abstraction began. Depth of the wells, screened interval, well location and pumping rate were all observed to be important, however a full conceptual groundwater model that could explain the observed salinity was never realized. Thus, the response to the perceived threat of saltwater intrusion into the primary aquifer was to close down a number of the near coastal wells, with replacement wells located further inland.

In the late 1990's, the Geological Survey of Denmark and Greenland began a project that studied salinity in the chalk aquifers of the northeastern part of the Danish island of Zealand, which includes the municipality of Greve (Klitten et al. 2006). This study suggests a second source and transport mechanism for the observed salinity in the groundwater wells in the area: the diffusion of salt from connate formational waters (Bonnesen et al. 2009, Klitten et al. 2006). This recognition of a second source for the groundwater salinity has direct implication for the management of the groundwater resources for Greve. Seawater intrusion is a

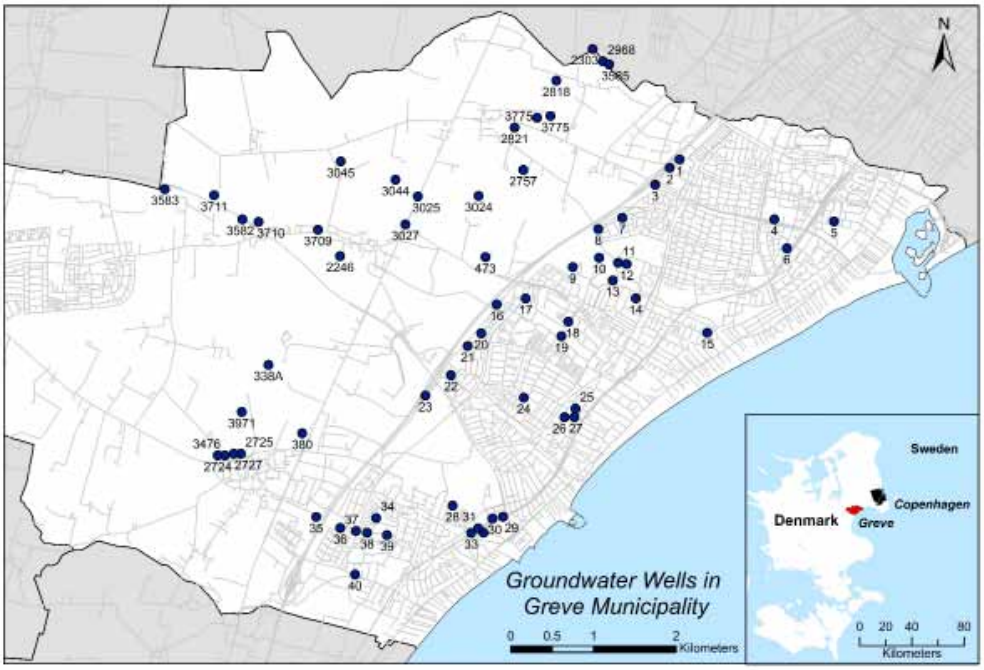

Figure 1. *Groundwater wells in the eastern half of Greve municipality, located approximately 25km SW of the Danish capital of Copenhagen. The three or four digit number corresponds to the Geological Survey of Denmark and Greenland's well identification number, where all have the prefix 207. The wells numbered from 1-40, all within 2.5km of the coast, correspond to the wells used in this study. The Geological Survey identification number for these wells is provided in Table 1.*

response to groundwater abstraction depressing the groundwater potential enough to initiate the flow of seawater inland. In the worst cases, salinities can reach levels as high as the parent seawater. This is in contrast to salinity from connate waters, from which salinity is restricted to the rate of diffusion and depth of groundwater abstraction, and will have a upper limit as to how saline the water can become, independent of abstraction rate or groundwater potential.

Geochemical data from groundwater wells can provide important information on the source and extent of groundwater salinity and saline intrusion. This article will illustrate how a detailed geochemical analysis can be used to determine the source of salinity, identify areas at risk for saline intrusion, and how this information can be used in the management of the groundwater resources. The municipality of Greve, Denmark will be used as the case example. The conceptual model will be based upon historical bulk groundwater chemistry data collected in the wells, combined with geological data from the well logs. Implications for current and future management of the groundwater resources will be discussed.

1.1 Study Area – Greve Municipality

Greve Municipality lies along the coast of the Baltic Sea, about 25km to the SW of the Danish capital of Copenhagen (Fig.1). Groundwater has historically been abstracted since the 1930's, with heavy abstraction beginning in the late 1960's and early 1970's. Figure 1 shows past and present wells that have been used for municipal groundwater abstraction, including water exported to the City of Copenhagen. The wells used in this study include 40 groundwater wells within the band 2.5km of the coast line, where elevated salinity has been recorded. For simplicity in presenting the geochemical data, the groundwater wells have been numbered 1-40 roughly from north to south (Fig. 1). These well numbers will be referred to in the tables and diagrams. Groundwater abstraction wells outside of the 2.5km band were not studied in detail.

1.2 Geological and Hydrogeological Setting

The near-surface geology (down to approximately 60m) of the municipality has been mapped using over 150 wells logs in the municipality. The depths of the wells range from 20m – 70m below the surface, with a few wells reaching deeper than 100m. Most of these wells penetrate the near-surface glacial deposits, reaching the pre-quaternary limestone and chalk deposits, which form the primary groundwater aquifer for the municipality. The well logs vary in quality of the geologic description, depending on the experience and thoroughness of the driller. In many cases, drilling samples have been kept and reviewed by geologists, providing better control on the well log data.

1.2.1 Pre-Quaternary Geological Units and Evolution

The pre-Quaternary units consists of late Cretaceous (Maastrictian) chalk and Paleocene (Danian) limestone. The Maastrictian chalk is present in the entire municipality, overlain directly by the glacial deposits in the eastern third and by the Danian limestone in the western two thirds of the municipality (Fig. 2). The Danian limestone has been eroded away in the eastern 1/3 of the municipality, and overlies the Maastrictian chalk in the western 2/3 (Fig. 2). The logs show an undulating chalk/limestone boundary dipping gently towards the west, with the thickness of the Danian limestone increasing so that most of the wells in the western half of the municipality do not reach the chalk (Fig. 3).

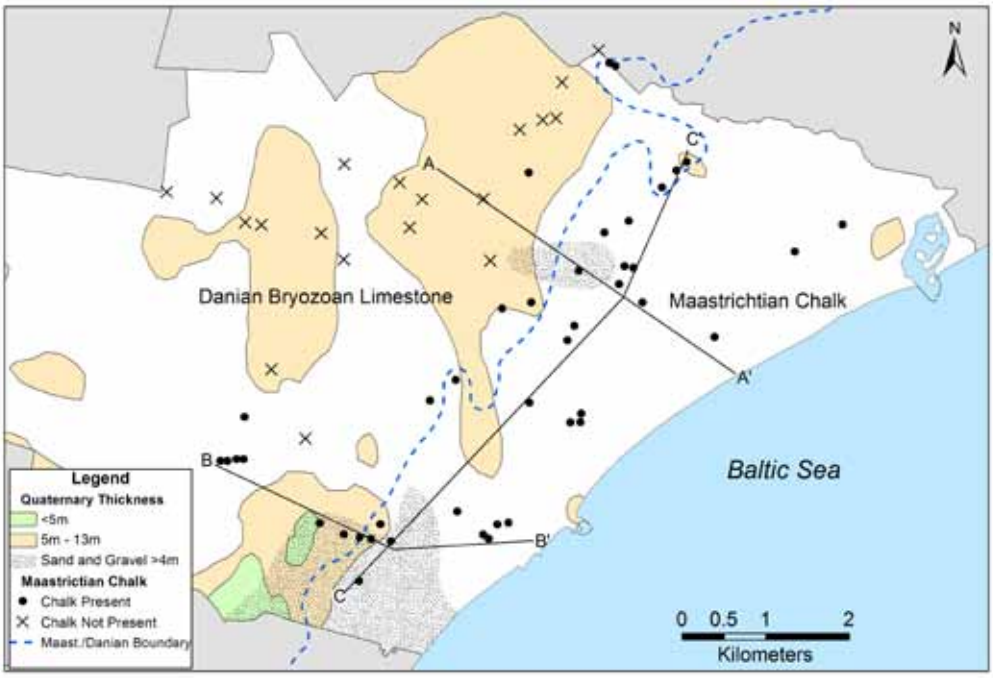

Figure 2. *Geological map of Greve Municipality showing the Pre-quaternary outcropping of the Danian limestone and Maastrictian chalk, with the boundary indicated by the blue dashed line. The map also shows the thickness of the Quaternary moraine and outwash sand and gravel deposits in the area. The stippled area is where outwash sands and gravels are greater than 2m thick. The black circles represent those wells which penetrate into Maastrictian chalk. The X's show the wells which only penetrate into the Danian limestone. The three lines indicate the placement of the three geologic cross-sections shown in Fig. 3.*

The Maastrictian chalk was deposited in the relatively quiet late Cretaceous sea which extended over a large portion of NW Europe, including most of England, northern France and Denmark (Frykman 2001, Hancock and Kauffman 1979). The chalk is a very fine-grained micritic limestone, composed primarily of coccolith skeletons and other pelagic nanno-fossils, interbedded with bands of black flint nodules (Anderskouv et al. 2007, Hancock 1976). More than 80% of the chalk has a particle size of less than 5 microns, where as less than 10% consists of fossils over 60 microns (Thomsen 1995). The total thickness of the chalk in the area reaches as much as 1200m (Thomsen 1995). The primary porosity of the chalk, measured at nearby outcrops, is shown to be high, ranging between 35 and 50% (Frykman 2001). In spite of the high porosity in the chalk, matrix hydraulic conductivity remains very low, reported at an average of $3.7x10^{-8}$ m/sec (Frykman 2001, Larsen et al. 2006).

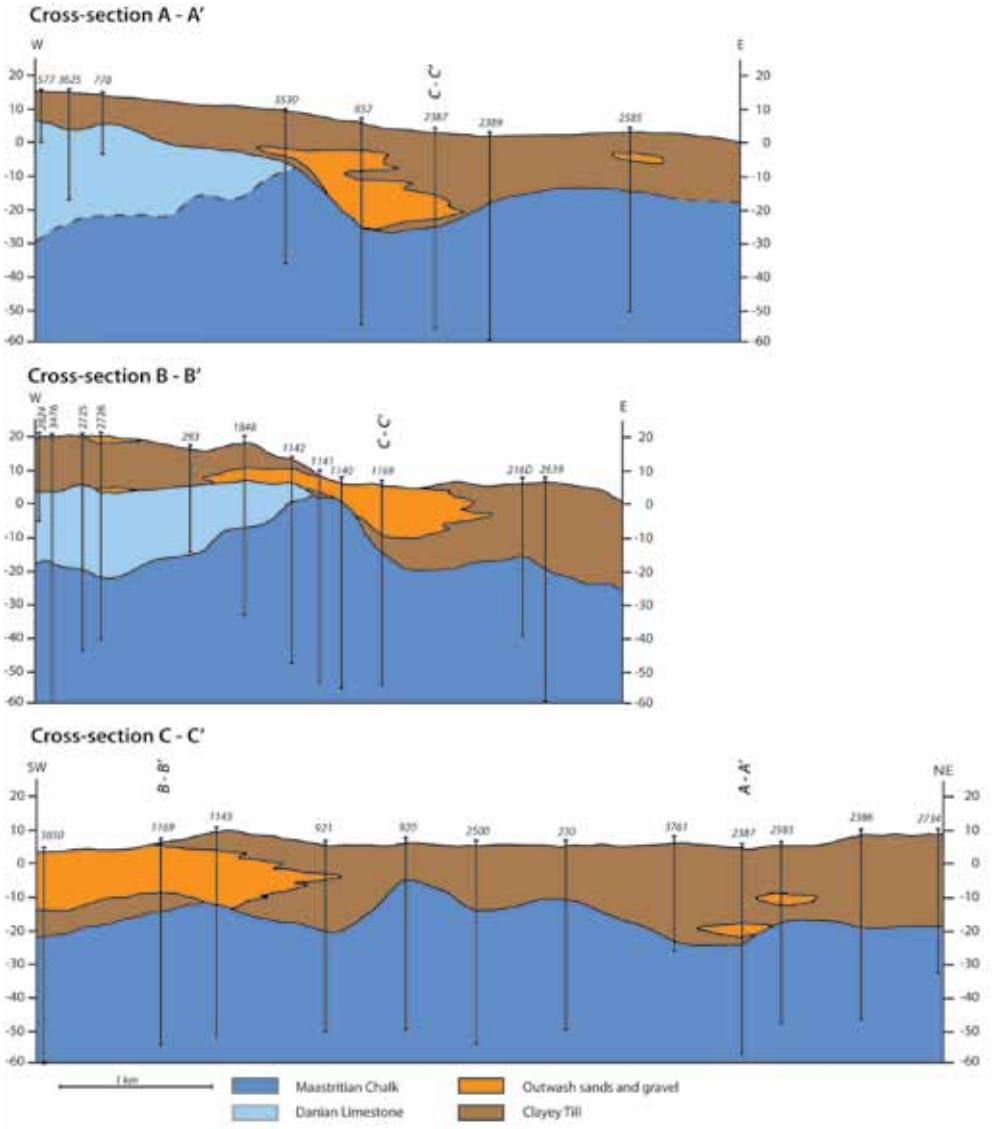

Figure 3. *Geological cross-sections across the Greve study area. The location for each cross-section is shown on Fig. 2.*

The Danian limestone was deposited in the shallower seas which were present in Denmark in the early Paleogene. The Danian limestone typically consists of bryozoan remains in a micritic matrix, giving the local name of bryozoan limestone (Thomsen 1995). Bryozoan fossil fragments make up from anywhere between 20 to 45%, and ranges between matrix supported and grain supported (biomicrite), where the bryozoan fossils form a self-supporting network (biosparite) (Thomsen 1995). Like the chalk, the Danian limestone also has bands of flint, often gray to

dark gray in color (Thomsen 1995). The primary porosity in the Danian limestone, has been measured at 30 to 40% (Frykman 2001). The matrix permeability is reported by Frykman (2001) to be about 10 times higher than that of the Maastrictian chalk, however Larsen et al. (2006) report a matrix hydraulic conductivity value of $4.5x10^{-8}$ m/sec, only slightly higher than the Maastrictian chalk matrix.

During the remainder of the Paleogene, the eastern part of the North Sea Basin, which includes the municipality of Greve, deposition of marine deposits continued. The amount sediments that were deposited during the remainder of the Paleogene is debated, with evidence that anywhere between 300m and 1000m of Paleogene sediments had been deposited on top of the Danian limestone (Huuse et al. 2001, Japsen 1993, Japsen et al. 2007). During the Neogene, there was regional uplift, and subsequent erosion of the Paleogene sediments (Huuse et al. 2001, Japsen et al. 2007). The unloading of these sediments is likely responsible for the formation of many of the vertical and horizontal fractures in the limestone and chalk, similar to the fractures observed in the Copenhagen limestone (upper Danien) approximately 20km to the NE of Greve (Jakobsen et al. 1999). The structure of the pre-Quaternary units in Greve includes gentle folds but no faults were observed, based on the interpretation of well-logs in the municipality.

1.2.2 Quaternary Geology

The Quaternary period for Greve included multiple glacial transgressions and regressions, with only deposits from the last two episodes preserved in the area (Houmark-Nielsen 1987). This has had a significant bearing on the hydrogeology of the area. The glacial transgression over the Maastrictian chalk and Danian limestone resulted in a brecciation of the upper 2-3m of the chalk and limestone, which is observed in the Karlstrup limestone quarry (Jakobsen et al. 1999). In addition, the ice loading and unloading cycles from the multiple glacial transgressions, and subsequent regressions, throughout the Quaternary also likely contributed to the fracturing of the limestone and chalk, in the same manner as in the Neogene (Houmark-Nielsen 1987). The fracturing from the brecciation and the Neogene/Quaternary unloading provides the permeability in the otherwise tight chalk and limestone units. Bulk hydraulic conductivities of the Maastrictian chalk and Danian limestone directly underlying the glacial sediments is $1.3x10^{-5}$ m/sec and $7.6x10^{-5}$ m/sec respectively (Larsen et al. 2006). The hydraulic conductivity is seen to decrease with depth, with the presumable closing of fracture aperture and decrease in fracture density (Bonnesen et al. 2009).

Well logs show the glacial deposits are predominately unsorted clayey tills, with lenses of outwash sands and gravels (Fig. 3). These sand and gravel lenses are, in general thin (less than 2m) and isolated, making correlation between wells difficult. There are two areas, however, with thicker deposits of sands and gravels; one in the central part of the municipality, and one in southern part of the municipality (Fig. 2). The southern lens is the most extensive, where the sands and gravels are thicker than the glacial till, and extends to the Baltic Sea. The clayey tills, with matrix hydraulic conductivity of between $1x10^{-9}$ m/sec to $1x10^{-11}$ m/sec act as the confining layer for the fractured limestone and chalk aquifers below (McKay et al. 1999, Nilsson et al. 2001). However, in the southern portion of the municipality the unconsolidated sands and gravels, with an estimated hydraulic conductivity of between $1x10^{-4}$ m/sec to $1x10^{-5}$ m/sec, likely allow the limestone and chalk aquifers to be in contact with the atmosphere.

The thickness of the quaternary deposits is highly variable across the area, and ranges from 3m to over 30m (Fig. 2). The thickness is important because recent studies on the clayey tills in the Copenhagen area have shown that these tills are highly fractured in the upper 5m, with oxidized fractures as far down as 13m (McKay et al. 1999, Mortensen et al. 2004, Nilsson et al. 2001). Bulk hydraulic conductivities in the upper 4m of clayey tills have been measured to $1\text{-}7x10^{-5}$m/sec, and as high as $1x10^{-7}$m/sec down to 13m (McKay et al. 1999, Nilsson et al. 2001). These fractures are important particularly in thinner clayey tills, as they provide a conduit to the chalk and limestone aquifer below.

1.3 Groundwater Abstraction in Greve

Groundwater abstraction for the communal water supply in Greve municipality began on a relatively small scale in the 1930's (Roskilde Amt 2004). In the coastal area, this water supplied primarily summerhouses. In the 1960's, the community began to grow quite quickly, particularly along the coast, changing from vacation to year-round residences as well as increased industrial activity. Subsequently groundwater abstraction, and the number of wells, increased. This continued throughout the 1970's, with total groundwater abstraction in the area exceeding 2 million m^3 per year by the 1980's (Roskilde Amt 2004). In the late 1970's and 1980's, as it became more evident of a groundwater salinity problem, many of the near-coastal wells were closed off, and replacement wells were established further

inland to make up for lost production(Roskilde Amt 2004). Figure 1 shows both the active and historic water wells in the municipality. The Current permits allow a maximum abstraction of about 3.8 million m^3 per year, with 1.4 million m^3 of that within 2km of the coast (Roskilde Amt 2004). According to the Geological Survey of Denmark and Greenland's (GEUS) on-line database (Jupiter), total abstraction in 2007 for the area was approximately 2.6 million m^3, with 790,000 m^3 taken within 2.5km of the coast (GEUS 2009). It should be noted that the current abstraction permits expire in 2010, and at the time of the writing of this manuscript, new abstraction permits have not yet been granted.

Groundwater abstraction in the study area has been occurred solely in the fractured Maastrictian chalk and Danian limestone aquifers. The water supply wells were generally drilled from 5m to 50m below the Quaternary/Pre-Quaternary boundary, with filters installed within 1-3m of the boundary to the bottom of the well. The aquifer is confined to semi-confined, depending on the thickness of the clayey tills, which act as the confining layer. Even in instances where the wells encountered a significant thickness of outwash sands and gravels, the wells were not screed over this interval.

According to information from the Greve Water Works archives and data from GEUS's database, the measured potential in 1900, before groundwater abstraction began, varied from 25m in the west, falling gradually and evenly to a level of 0m at the coast, showing a regular WNW to ESE flow pattern. After heavy groundwater abstraction began in the 1960's, depressions in groundwater potential of greater than -10m occurred at the wells nearest to the coast, with the uplands maintaining a potential of 23-24m. According to the archives, this continued to through the 1980's. The depressions lessened to around -6m in the 1990's when much of the abstraction was moved further inland, and the upland maintaining at about 24m. Figure 4 shows the groundwater potential from 2007.

1.4 Sources for Salinity

Given the proximity to the coast and the extended period the groundwater potential of several meters below sea level, seawater intrusion from the Baltic Sea is an obvious source for the measured salinity in the wells. Seawater salinity concentrations in the Baltic Sea near Copenhagen is seen to vary anywhere from 1 to

1.5 percent, depending on wind direction and storm events (Meier et al. 2006, Omstedt and Axell 1998). Therefore, from seawater intrusion from the Baltic Sea, chloride concentrations in the wells could theoretically reach as high as 5000mg/l.

Recently GEUS completed a study on connate formational waters in the Maastrictian chalk of NE Zealand, including all of Greve (Bonnesen et al. 2009, Klitten et al. 2006). They found that at a depth of about -250m, the porewaters had a salinity of modern seawater (chloride concentration of 15,000 mg/l). This decreases to 250mg/l at a depth of between -40 to -80m. This salinity concentration gradient is shown to be primarily via diffusion through the chalk's pore waters until advection in the near-surface aquifer takes over as the primary transport process (Bonnesen et al. 2009). This study is significant, because it now points to a second possible source of the salinity observed in the wells: diffusion of salts from deeper connate formational waters.

Differentiating between the two sources for salinity is important for management purposes. If the salinity results from advective flow from seawater intrusion, there is a risk of a significant level of salinity in the groundwater – up to 5000mg/l chloride in this case. This is in contrast to upward diffusion from saline porewaters, where the diffusion rate will be a limiting factor. In this case, chloride levels in the wells will be much less dependent on abstraction, but more dependent on the local hydrologic characteristics, including the local depth of advective flow through the fractures to the well and even the depth of the well.

It should be possible to use geochemical data from groundwater samples in order to determine the dominate source for salinity. As seawater moves through the sediments, particularly the clay minerals, sodium ions will be preferably held back, releasing calcium ions (Appelo and Postma 2005). This is in contrast to diffusion from the porewaters, where the aquifer is being "freshened" and calcium ions will be preferably adsorbed and sodium ions released (Appelo and Postma 2005). As chloride is a conservative ion in this process, wells influenced by saltwater intrusion should have low molecular sodium to chloride ratios, where as if diffusion is the primary process, the sodium to chloride ratio should be higher due to the preferential release of sodium ions. In addition, because diffusion rates are three to four factors of magnitude slower than the hydraulic conductivity, salinity via diffusion should be stable over time, where as seawater intrusion will show a significant increase in salinity over time as the saltwater front approaches, and intrudes into the well.

2. METHODS

The groundwater chemistry was assessed using historical bulk water sample data collected by the water supply companies from the individual wells. The data were collected over a long period of time, with the oldest from 1971. This occurred at irregular intervals through the 1970's, becoming more regular during the 1980's, and quarterly by the 1990's. Chloride was often the only ion analyzed for, with irregular sampling of the other ions (including Na, Mg, Ca, K, F, SO_4, HCO_3, heavy metals, and organic pollutants) before 2001. Beginning in 2001, quarterly sampling of the full array of ions became more common. The geochemical data used in this study was compiled off of the GEUS Jupiter web-accessible database (GEUS 2009), which contains both the geological and reported geochemical data for each well. The geochemical data was augmented with archival data from Greve Water Supply, which maintains data for over 45 current and past wells in the municipality. This data is more complete and used to fill in the gaps often found in the Jupiter database, particularly with the older measurements. The groundwater abstraction and potential data used in this study was received from Greve Municipality technical department and from Greve Water Supply.

The ions studied from the samples include chloride, sodium, calcium, magnesium, potassium, sulfate and bicarbonate. Chloride was analyzed with respect to amount and historical development in the individual borings. Sodium was looked at in the individual wells with respect to its ratio to chloride. This provides an indication on how the source of salinity may have changed over time. The remaining ions were analyzed together with sodium and chloride in a Piper plot (after Piper 1944), in order to evaluate the water type from the groundwater samples. The highest fluoride level is listed for each well, as fluoride is one of the factors which weighs into the management decisions made.

The samples for the geochemical analyses were collected by the individual water works, and sent to independent, certified laboratories in Denmark for analysis. For the older samples, it is unknown how they were collected. However, the recent samples from Greve Water Works were collected via a spigot at the well-head, during normal groundwater abstraction (Lydersen 2009). It is assumed that the earlier samples were also collected by this method; however, the authors could find no reference to the sampling methods in the data archives.

It needs to be stressed that the groundwater samples are bulk samples. Therefore, the geochemical signal provided is a sum of the entire length of the screened interval, and can also be subject to leaks from groundwater in the glacial deposits. Due to the complexity of fractured systems, it is not known the exact interval of water flow into the wells. In fact, in studies conducted with flow meters in new water wells drilled in Greve show that in one well, the water flow was seen to be restricted to the upper 2m of the screened interval, where as in another well just 100m away, the water was flowing in over the entire 20m screened interval (Jakobsen 2009). In spite of this problem, it is believed that the bulk groundwater samples can still be used as a representative sample from the wells, particularly with respect to ratio analysis of the ions.

3. RESULTS

The results of the bulk-water geochemical analysis will be presented with respect to its geographical extent, temporal development in the individual wells, depth of the groundwater wells, placement of the wells, the molecular ratio of sodium to chloride, bulk water geochemical analysis and with the presence/absence of fluoride in the wells. A summary of the geochemical data for the analyzed wells, numbered 1-40 (as shown in Figure 1), is presented in Table 1.

3.1 Geographical Extent of Bulk Groundwater Salinity

In this paper, groundwater salinity is represented by the concentration of chloride measured in the ground water wells. Wells with bulk water chloride measurements of under 50mg/l are considered to be purely fresh water. Using the drinking water limit of 250mg/l as a reference point, the extent of the salinity in each bulk water sample can be represented on a relative salinity scale, with values of 50-150mg/l being slightly elevated, 150-250mg/l being moderately elevated, 250-500mg/l being highly elevated, and over 500mg/l being very highly elevated.

Figure 4 shows the geographical extent of the salinity in Greve. From this map, it can be seen that the wells with elevated salinity are restricted to the area within 2.5km of the coast-line. The chloride measurements are from October 2007, or the last measurement in the wells where groundwater is no longer being abstracted.

Table 1 *Study area wells, listing the DGU ID number, well depth, abstraction rate, last measured fluoride, chloride levels and sodium/chloride molecular ratio. The renewed well depth gives the new depth for the wells after they were altered in 1981.*

Project Well ID	DGU ID Nr. (207)	Well Depth (msl)	Renewed Well Depth (msl)	Current Abstration (m3/hr)	Fluoride (mg/l)	Chloride (mg/l):				Na/Cl Ratio
						First	Max	Last	Ave	
1	2734	-32	NA	18.8	2.5	87	118	104	101	1.20
2	2733	-37	NA	20.0	2.5	136	254	246	224	1.14
3	2732	-33	NA	27.8	2.8	170	246	202	220	0.99
4	881	-38	-31	0	2.1	410	535	370	456	--
5	880	-57	-47	0	--	500	519	180	230	--
6	2586	-57	NA	0	2.1	233	293	226	250	--
7	2386	-52	NA	0	2.1	158	280	230	207	0.92
8	2385	-52	NA	0	2.6	292	292	236	244	1.16
9	852	-35	NA	26	2.9	71	490	240	320	1.13
10	2384	-59	NA	0	4.8	305	364	324	310	1.26
11	2582	-57	-32	16.3	2.4	277	348	116	136	1.10
12	2583[a]	-47	NA	10.5	2.6	308	370	241	237	1.23
13	2387	-56	NA	17.5	3.7	266	614	330	312	1.29
14	2389	-58	-47	0	3.3	313	454	390	300	0.97
15	234	-38	NA	0	2.4	320	424	325	353	1.07
16	2390	-51	NA	30	3.4	89	390	60	109	0.81
17	2388	-54	NA	19	3.7	118	329	134	120	0.95
18	2719	-39	NA	9.0	1.6	70	86	86	74	0.94
19	2720	-39	NA	15	2.0	103	196	102	105	1.06
20	2502	-51	NA	0	4.1	192	308	290	269	1.05
21	2501	-51	NA	0	3.1	31	130	120	107	0.97
22	2499	-54	NA	22	1.2	58	88	88	62	0.49
23	2313	-30	NA	10	1.2	53	94	60	55	0.68
24	2500	-56	-23	0	2.9	310	421	421	351	--
25	2581	-47	NA	0	2.7	180	180	143	150	1.04
26	2234	-59	-29	0	2.7	530	622	364	501	--
27	2580	-53	NA	0	--	210	210	192	191	--
28	708	-24	NA	5	1.3	28	31	27	27	0.90
29	2543	-70	NA	1	2.2	111	380	309	204	0.61
30	2662	-63	NA	1	2.2	61	730	524	397	0.74
31	2730	-49	NA	1	1.7	53	570	570	155	0.65
32	2639	-66	NA	1	1.6	116	1183	1183	595	0.64
33	216D	-40	NA	0	1.5	225	1100	1100	528	--
34	2735	-45	NA	8.0	0.7	34	106	100	64	0.51
35	1848	-36	NA	3.0	1.5	24	49	36	28	0.67
36	1142[b]	-47	-34	3.1	1.7	22	60	48	36	0.66
37	1141	-53	NA	5.1	1.5	38	162	148	94	0.53
38	1140[b]	-55	-16	4.4	1.2	44	180	180	112	0.47
39	1169	-55	NA	0	1.9	43	2200	2200	653	--
40	2964[c]	--	--	8.0	.85	52	127	120	83	0.63

[a] Filter begins in the glacial sediments. [b] Boreholes were reconditioned in 2007. [c] No borehole data exists for this well.

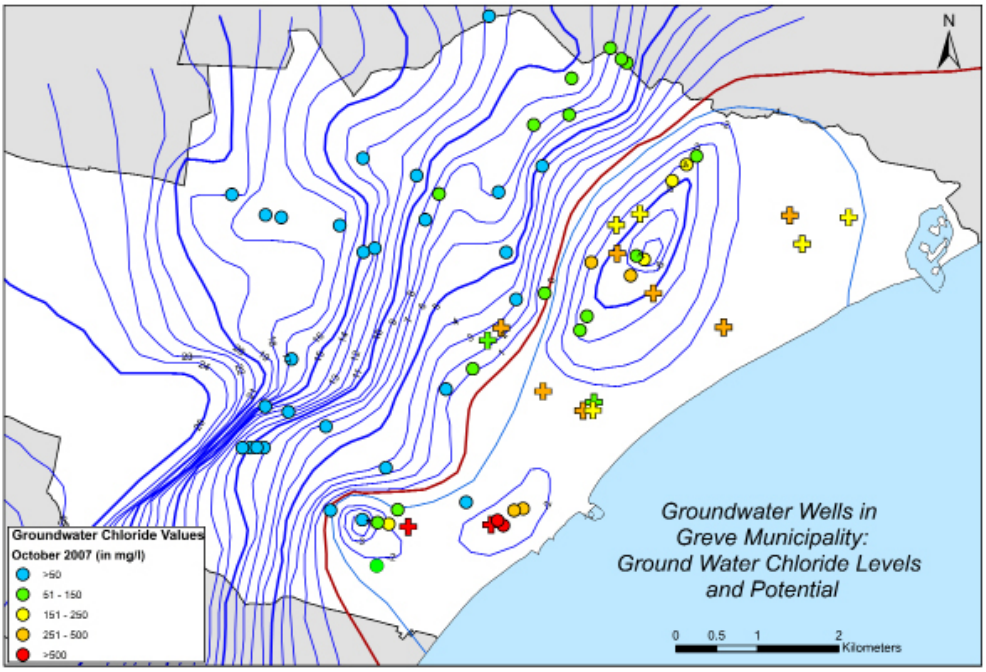

Figure 4. *The primary aquifer potential and chloride values for October 2007. The numbers inside the symbols indicate the well identification number. The crosses represent wells that are no longer used for groundwater abstraction. The chloride levels shown on the map for these wells is the last measurement taken. The red line represents a groundwater potential of 0m, and all of the contours to the east are below the mean annual sea level.*

The elevated salinity corresponds quite closely to the extent of the pre-Quaternary outcropping of Maastrictian chalk, or wells that penetrate into the chalk (Fig. 2). The only exception is a group of seven wells in the northern part of the municipality, which have slightly elevated salinity, but only three of the wells are deep enough to extend into the chalk. In every case, the chloride values in these seven wells is between 52 and 72 mg/l, and because this is so close to the 50mg/l threshold these wells were analyzed in further detail.

Nearly all of the wells with an elevated salinity within the 2.5km band (numbered 1-40 as shown in Fig. 1) from the coast have a groundwater potential below sea-level (Fig. 4). The only exceptions are well numbers 20 and 21, which have a potential of about 2m, where well 20 has a highly elevated salinity, and 21 is slightly elevated. Neither well is used any longer for abstraction. There are, however, wells with groundwater potential below sea level, which are fresh or have only slightly elevated salinity. For example, wells 36 and 37 are fresh and slightly elevated, respectively, in spite of a groundwater potential of 3m to 4m below sea level (Fig.

4). In the central part of the municipality, wells 18 and 19 have salinities only slightly elevated, where groundwater potential is 4m to 5m below sea level. The extent of the measured salinity is also seen to vary significantly over distances of just a few hundred meters. This is illustrated by wells 10 -12 and wells 25-27, where the salinities in each group range from slightly elevated to highly elevated (Fig.4).

3.2 Temporal Trends in Salinity

There are generally two types of temporal trends in chloride observed in the wells: chloride fluctuating around approximately the same level, and chloride which increases in an upward trend over time. The former is illustrated in wells 3, 9 and 20 (Fig. 5a). Well 3 has a starting value of just under 200mg/l in 1985 and this level then remains constant at just above 200mg/l through to 2007. Well 9 shows a very large initial increase between 1975 and 1981 from 71 mg/l to 400 mg/l, where as the measurements then stabilize to around 350mg/l until 2000, where there is seen a decrease to 250 mg/l over the last 10 years. Chloride in well 20 has varied constantly between 200mg/l and 300mg/l from 1971 until the well was shut down in 1992. This trend can also be observed in the summary data from Table 1 several of the wells across the area, where there is very little observed difference in the first, maximum, last and average measurement (wells 1, 4 and 6 are good examples).

The second observed trend is exemplified by wells 31, 32 and 33 (Fig. 5b). Here, all three wells can be seen to have a lower starting chloride concentration, then increasing over time to a significantly higher concentration. In wells 32 and 33, the increase occurs almost immediately after the first reported measurement, where as in well 31 there was an 8 year period before chloride began to increase (Fig. 5b). This trend is also seen in Table 1, where the first measurement is much lower than both the maximum and last measurement, with the average falling in the middle, as is illustrated by wells 34, 37 and 38.

The role the well's proximity to the coast and the temporal changes in the chloride is also important. If a saltwater wedge is intruding in from the coast, the wedge would logically be registered first in the wells closest to the coast, in addition to the wells closest to the coast would likely be recording the highest amount of salinity. This situation can be observed in wells 36-40 (Fig. 6a). Here well 39 is the closest

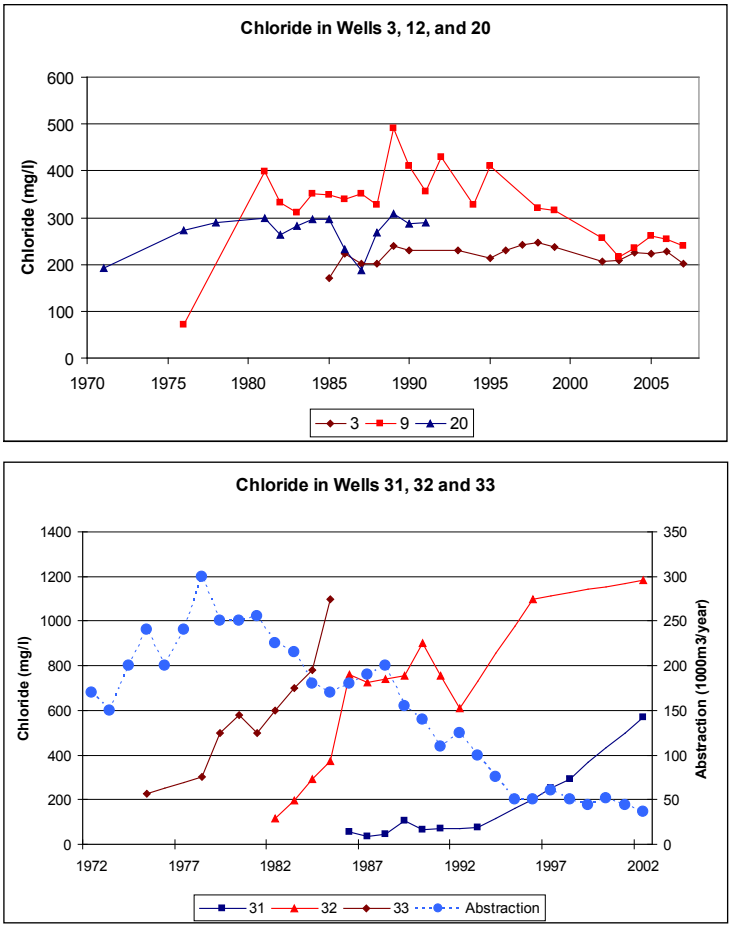

Figure 5. *Plots of the historical variation in chloride in representative wells. The upper plot (5a) illustrates wells which show no temporal trend in chloride through the years. The lower plot (5b) shows wells that have a positive temporal trend in chloride. Plot 5b also shows the total abstraction for the wells over time.*

to the coast, and has recorded a sharp rise in chloride starting in 1986, eventually reaching a value of over 2200mg/l. Wells 38 and 37, each respectively about 100m further inland, first started a steady, but slower rise in chloride beginning in 1988 and 1990 respectively (Fig. 6a). Well 36, the furthest in land has only a slight rise in salinity to 50mg/l in 1994, and has been steady since.

In other areas, proximity to the coast has not resulted in a higher chloride signal. Wells 25 and 26 are the same distance from the coast, but have significantly difference chloride levels, where as well 24, nearly 500m further inland has maintained chloride values between the levels of wells 25 and 26 (Fig. 6b). The same can be seen between wells 4 and 6, where the closest to the coast, well 6, has maintained a

significantly lower chloride level (Table 1). In the end, proximity to the coast appears to play a role in the chloride only in the southern part of Greve (wells 29-40) where as no observable role in the northern two thirds of the municipality (wells 1-28).

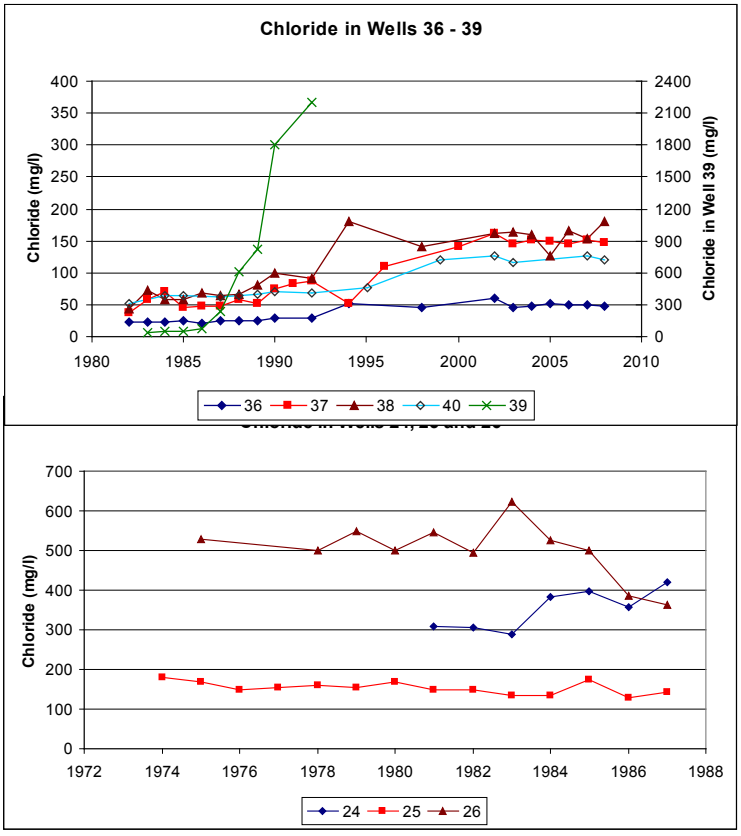

Figure 6. *Plots showing the temporal trends in chloride and proximity to the coast. The upper plot (6a) illustrates the arrival of seawater intrusion wedge to well 39 in 1986, to well 38 in approximately 1990 and to well 37 in 1994. Well 36 is the furthest from the coast, and has not seen the wedge yet. In the lower plot (6b), well 25, in spite of being the closest to the coast, has the lowest chloride levels, where as well 24, in spite of being the furthest from the coast. has the highest chloride values in 1987. All three wells were shut down for groundwater production in 1987.*

3.3 Relationship between well depth and salinity

The relationship between well depth and salinity has been casually observed by the water works and the municipal authorities since the 1970's but never thoroughly studied (Jakobsen 2009, Roskilde Amt 2004). They believed the deeper the well,

the higher the risk for salinity. According to Greve Water Works documents, a number of wells were partially filled in 1983 to reduce the depth (old and new depths shown in Table 1). In order to test this, the well depths were plotted against the last chloride measurements for all 40 wells (Fig. 7 left). There is a very weak positive statistical correlation between well depth and chloride levels (with an R^2 value of 0.07). However, the three wells with values over 1000mg/l (wells 32, 33 and 39) stand out from the other wells. When these wells are treated as outliers, there is no observable trend between well depth and chloride (Fig. 7 right).

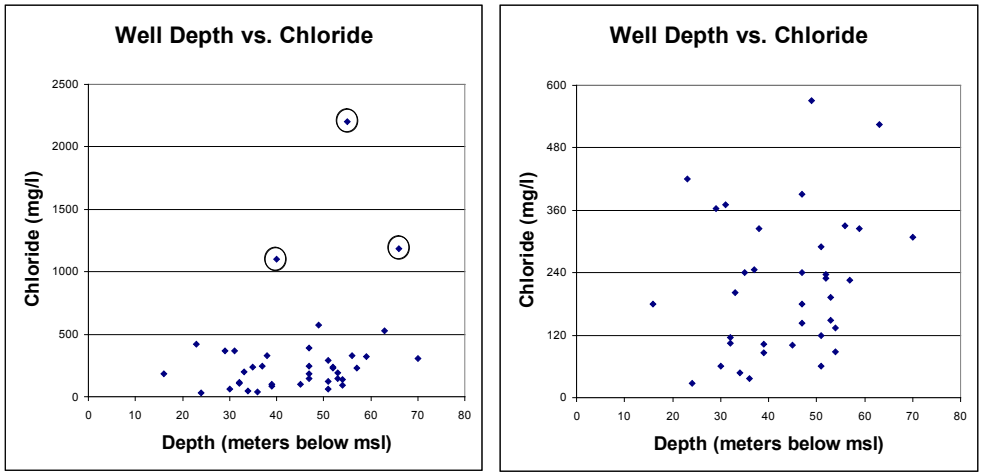

Figure 7. *Plots showing the relationship between each well's last measured chloride value and the well depth. The left-hand plot shows all wells in the study area, with the three wells circled being wells 34, 39 and 32 (from left to right). These three wells show the strongest signal for seawater intrusion. The right-hand shows the relationships after the three wells are removed. In this case, there is no observable correlation between well depth and chloride levels.*

The lack of correlation between salinity and well depth leads to the question; did the filling in the bottom of the wells in 1983 have an effect? To answer this, the chloride values both before and after the renewal of the wells were looked at. In wells 5 and 11, it appears that the filling in of the bottom of the wells had a significant effect, with a sharp drop of chloride observed immediately afterwards (Fig. 8). However, well 4 only had a small drop in chloride, and retained a significantly higher chloride value than well 5 in spite of having a much shallower bottom depth, -31 compared to -47m, and being further inland (Fig. 8 and Fig. 1). Well 14 actually shows an increase in chloride after becoming 11m shallower (Fig. 8). Well 24 also had no decrease in chloride after renewal, whereas well 26 had a drop, but remained over 350 mg/l (Table 1).

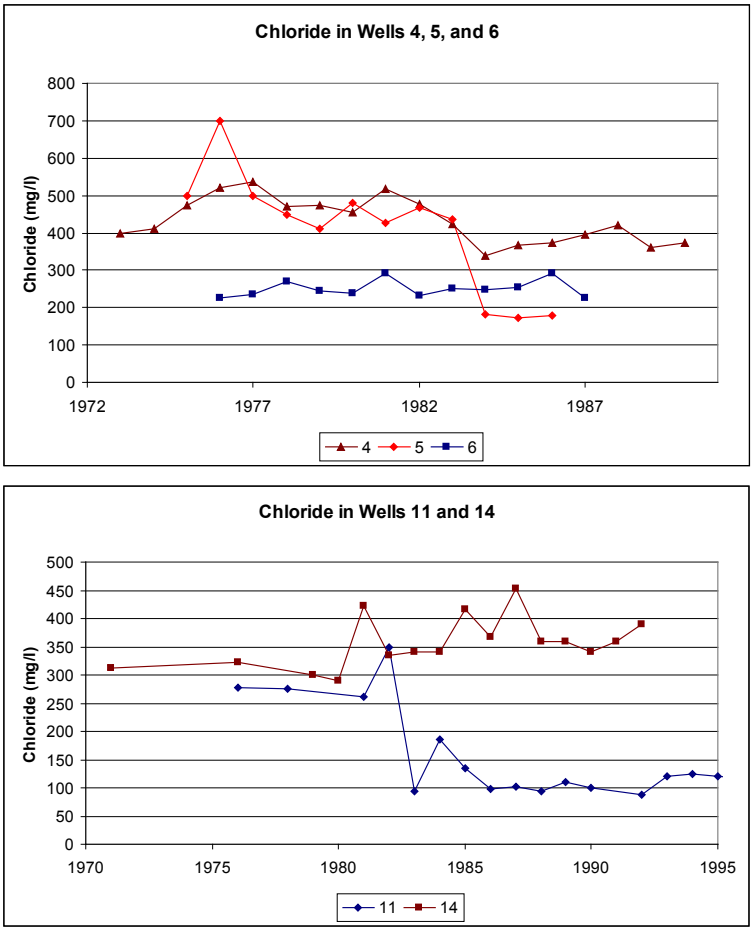

Figure 8. *Plots showing the effect of well renovation on the chloride. In the top plot (8a), well 4 shows only a slight response to the well renovation in 1983, where as well 5 shows a significant response. Well 6 was not renovated, and maintained the same chloride level throughout the observed period. In the bottom plot (8b), well 11 shows a significant decrease after renovation in 1983, where as well 14 shows no response to renovation.*

Geography also does not appear to play a role in how well depth compares to salinity. When comparing wells 1-3, all within 300m of each other, wells 1 and 3 have nearly the same depth, but well three has a significantly higher chloride value (Table 1). Well 2, in spite of being 4m deeper, has virtually the same chloride level as well 3. Wells 20 and 21, approximately 200m apart, also show a significant difference in chloride in spite of being the same depth (Table 1). Wells 25 and 26 are 100m apart, but well 25, in spite of being 18m deeper than well 26, has a significantly lower chloride level (Table 1). These examples illustrate the highly local variability with respect to bulk water salinity compared to well depth.

3.4 Groundwater Abstraction and Groundwater Salinity

There is no observable relationship between the well's groundwater abstraction rate and the chloride levels in any of the wells in the area. This is illustrated in the plot on well 4 from 1983 to 1990, where changes in abstraction rate did not have a significant, if any, impact on the chloride levels in the well (Fig. 9). Well 7 also shows no relationship, where it maintained a constant chloride level between 1983 and 1990 in spite of a general reduction in abstraction rate (Fig. 9). In fact, well 13 showed its highest chloride levels at a time when abstraction was the lowest, and afterwards chloride levels remained relatively constant at around 300mg/l despite fluctuating abstraction rates (Fig. 10). For wells 31, 32 and 33, chloride levels continued to steadily increase in spite of a 75% reduction in groundwater abstraction for the three wells (Fig. 5b). Therefore, it is apparent that changes in abstraction rates for the individual wells has played little, if any role in the measured groundwater salinity for the area.

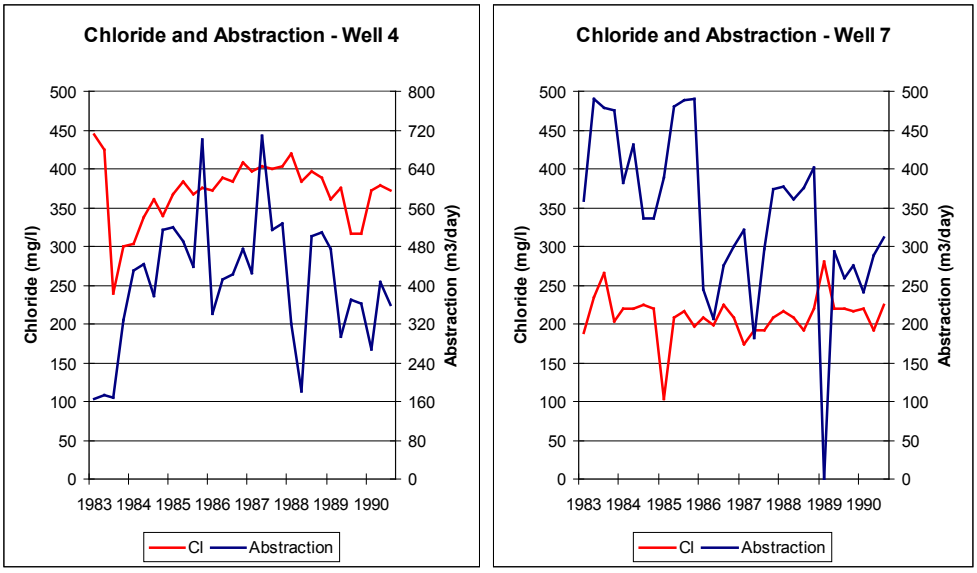

Figure 9. *Plots showing the chloride and groundwater abstraction rates for wells 4 and 7. Both wells show no discernable correlation between chloride level and abstraction rate. In well 7, it can be seen that the chloride level remains around 220mg/l in spite of a general trend of decreasing abstraction over the 10-year period.*

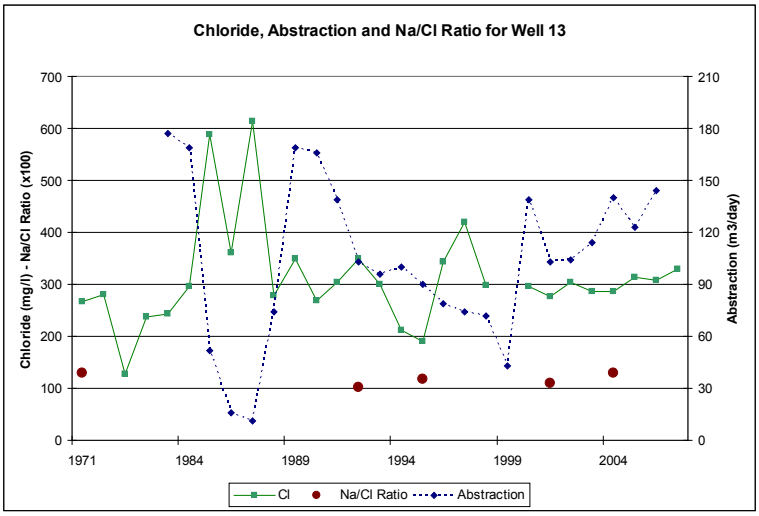

Figure 10. *Plot showing the groundwater abstraction rate and measured chloride for well 13. Note that there is no correlation between abstraction rate and measured chloride levels in the well. Also shown is the measured sodium/chloride molecular ratio, which remained constant between 1.0 and 1.1 over the entire time period.*

3.5 Analysis of the Sodium to Chloride Molecular Ratio

The sodium to chloride molecular ratio is an important indicator as to whether the source for salinity is from connate formational waters or from seawater intrusion. If the salinity is coming from seawater intrusion, the sodium/chloride ratios should be less than 1, where as if it comes from connate pore waters via diffusion, the ratios should be greater than 1 (Appelo and Postma 2005).

The sodium/chloride molecular ratio shows a distinct geographical relationship across the municipality. When comparing the wells within 2.5km of the coast, ratios over 1 occur in the northern third, with ratios around 1 occur in the central part, and ratios significantly lower than 1 occur in the south (Fig. 11, Table 1). The wells to the west of the 2.5km band show a distinctively low sodium/chloride ratio, with the exception of three wells in the southwest and one well in the north-central part of the municipality. Note that sodium has not been collected for nine of the wells in the study area (Fig. 11).

The data on sodium has not been sampled at the regular intervals like chloride, and therefore a temporal analysis of the sodium/chloride ratio is difficult. However,

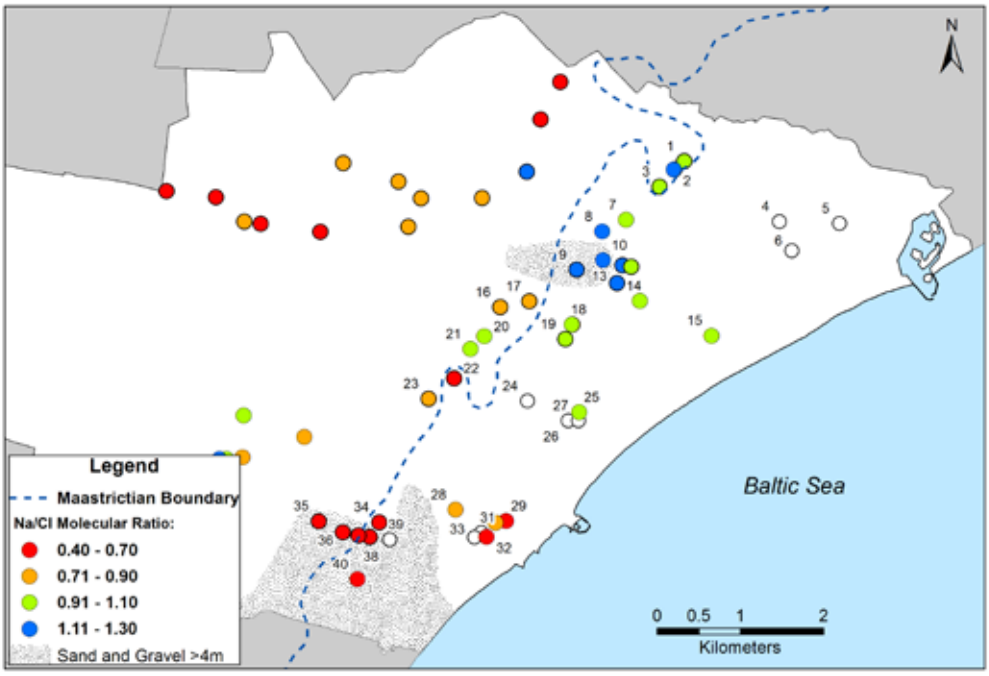

Figure 11. *Map over the last measured sodium/chloride ratio. The empty circles represent wells which there is no available data for sodium. Shaded area indicates significant sand layers. The dashed line represents the Danian-Maastrictian boundary.*

in the wells with more than one sodium sample, the ratio is seen to remain fairly constant through time. This is illustrated in well 13, where the ratio has remained just over 1 since 1971 (Fig. 10). The same trend is observed in well 37, where the ratio remained around 0.6 between 1982 and 2008 in spite of a tripling of the chloride level in the same time frame (Fig. 12).

3.6 Cation and Anion Exchange Analysis

A complete analysis of the cations sodium, potassium, magnesium and calcium along with the anions chloride, sulfate, carbonate and bi-carbonate, can also indicate whether the groundwater is undergoing a freshening process or seawater intrusion (Appelo and Postma 2005). A simple Piper plot on the bulk water samples where the data was available is shown in Figure 13. The wells were grouped into three different categories: group 1 includes wells with a chloride value under 100mg/l (squares on Fig. 13); group 2 includes wells which have a relatively stable chloride level higher than 100mg/l (triangles on Fig. 13); and group 3 includes wells

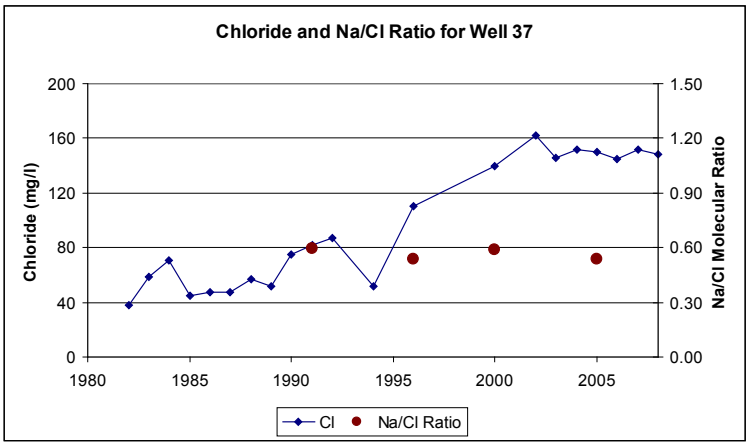

Figure 12. *Plot illustrating the chloride measurements and the sodium/chloride molecular ratio over time. Note that the sodium/chloride ratio has not changed, remaining around 0.6, in spite of a significant chloride increase (almost 3 times) between 1989 and 2001.*

which have an increasing chloride level, with the last measurement above 100mg/l (circles on Fig. 13). Group 2 includes the wells from the northern two thirds of the study area, group 3 includes wells from the southern third, and group one includes the wells from all parts of the study area with low chloride. On the plot, definite groupings of the wells can be seen. Group 1, as expected falls within the freshwater zone of the plot. Group 2 shows a relative enrichment to bi-carbonate and sodium with respect to sulphate and calcium and magnesium. This suggests that the wells in this group are freshening (Fig. 13). On the other hand, the wells in group 3 have a relatively higher sulfate and calcium and magnesium content. Thus the bulk water samples indicate mixed waters to seawater intrusion.

4. DISCUSSION

Before any analysis on the geochemical data for the municipality can be brought forward, the source of the geochemical data in this study must be discussed. The data has been collected by the water works, and represent bulk water samples from wells. Thus, the samples are representative of water from the entire screened interval, and any leaks within the well casing above the screened interval. In the case of this study, it was not possible to do an analysis of the depth and extent of the primary water bearing horizons or determine whether or not, or to what extent the casing is leaking. The primary aquifer for the municipality, from which

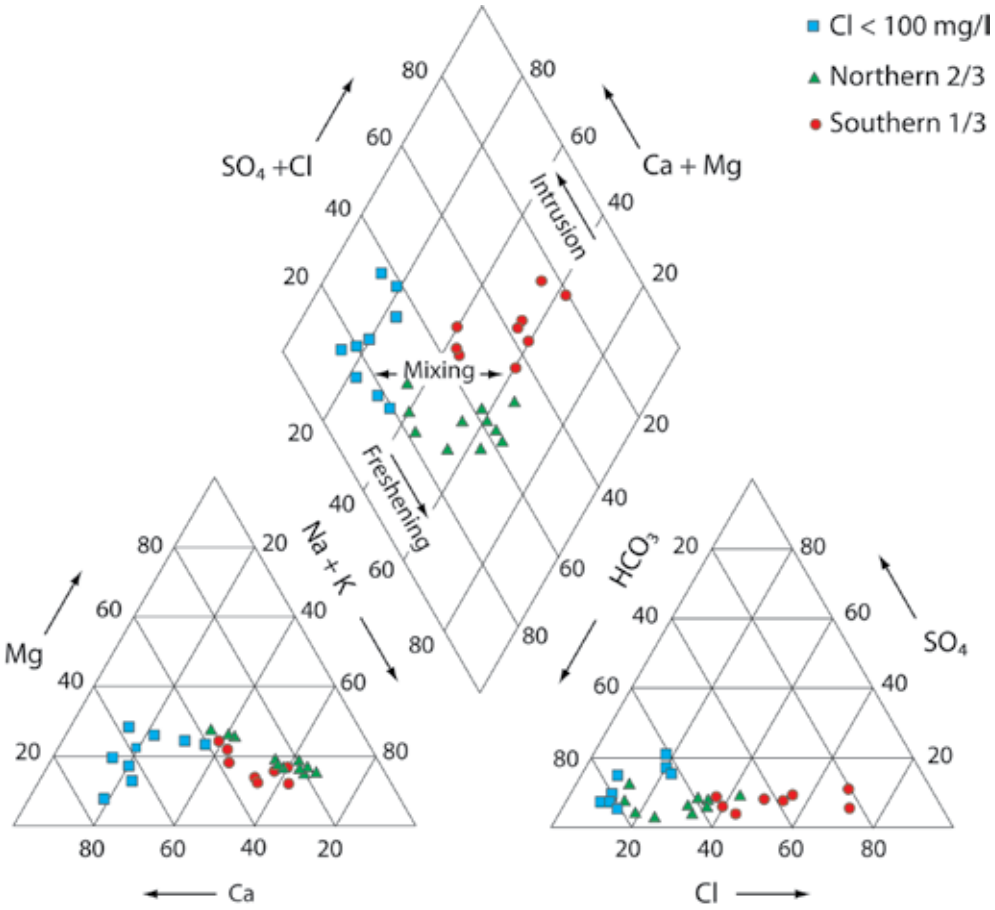

Figure 13. *Piper plot showing the chemical signatures from bulk water samples from the wells in the study area. Note that northern wells (green triangles), are more sodium and bicarbonate rich, and indicates groundwater freshening. On the other hand, the southern wells (red cirles) are relatively more calcium, magnesium and chloride rich, and indicates mixing to seawater intrusion in the groundwater.*

all the water wells take their water from, is fractured chalk and limestone. This creates a complex system which will vary from well to well, depending on how many fractures each well intersects, fracture aperture and interconnectivity. As mentioned before, flow analysis on new wells drilled inland from the study area have shown a high variability in the depth and extent of the water bearing units over a very short distance (Jakobsen 2009)That said, the authors believe that the geochemistry data can be used to identify the source of salinity for the area, and be used in management decisions.

4.1 The source of salinity

The temporal chloride trends observed in the wells reveal a great deal with regard to the source of the salinity. The connate pore waters in the Maastrictian chalk are currently undergoing the slow process of freshening via diffusion from depths of 200m up to between 40m and 70m below sea level, and has been undergoing this process for the last 900,000 years (Bonnesen et al. 2009). Therefore, it can be presumed that the system was in a steady-state when groundwater abstraction began, with the salinity measured in the well dependant upon the depth of the well and the local advection/diffusion interface depth. According to Fick's first law of diffusion, the flux of a specific ion is dependent on the ions diffusion coefficient and concentration gradient ($F = -D (\delta c/\delta x)$. When pumping commenced, the rate of groundwater flow in the area increased, removing the ions from the system at a faster pace. This, of course, changed the concentration gradient (δc) at the boundary between advective and diffusive flow, in essence delivering more ions across the boundary. However, according to Ficks law, if the salinity in the groundwater comes solely from diffusion from connate pore waters, then the concentration of the ions can never be higher than that of when pumping began (at steady state conditions). In essence, groundwater abstraction is increasing the freshening rate of the aquifer. The concentration should also be independent of abstraction rate. This is in contrast to salinity from seawater intrusion, where it would be expected a rise in chloride levels would be expected as the saltwater wedge approaches the well.

There is definite geographic difference in the observed temporal trends. The only wells that exhibit significantly of increasing chloride with time are 29-34 and 37-39; all located in the southern third of the study area (Figs. 6b and 7a, Table 1). These wells all started out with low chloride levels, increasing over time to levels of anywhere from 3 to 20 times the initial level. In addition, several of these wells, including 31, 37, 38 and 39 recorded no or low salinity in the samples for a period of 5-10 years, before the salinity began to increase. The point when salinity increases is interpreted to be the point when the saltwater/freshwater transition zone reaches the wells. The three wells in this area which do not exhibit this pattern (28, 35 and 36) have no salinity (Table 1). On the other hand, none of the wells which have recorded elevated salinity in the northern two-thirds of the study area have this increasing trend in chloride. Almost all wells which record elevated salinity have elevated chloride values from the start, and fluctuate around this level

no more than twice its original value, but generally +/- 50%. The only exceptions are well 9 (Fig. 5a) and well 16, where the initial recorded level is lower than the maximum value (Table 1). In well 9, it is only the very first measurement which is low, where after all the other measurements show no upward trend. For well 16, the difference is a brief spike in the chloride levels in 1999, where it returned to original levels. The reason for this spike is not known, however, the well lies in a zone where the tills are thinner (note Fig. 2), and it is possible that the chloride could have come to the well from a temporary surface pollution source via fractures in the clayey till. In spite of these two exceptions, the temporal trends in chloride suggest that the salinity in wells in the southern third of the study area is from seawater intrusion, where as the northern two-thirds is from diffusion.

The analysis of the other ions in the water samples supports the geographical difference observed in the temporal trends in the chloride. First of all, the sodium/chloride molecular ratios in the southern wells (29-40) are all very low. This suggests the preferential adsorption of sodium with respect to chloride, as seawater moves through the sediments. The wells in the northern two-thirds of the study area show exactly the opposite signal, with sodium/chloride ratios near or over one, as sodium is released from the sediments into the fresh groundwater moving through the aquifer. There are, however, four exceptions (wells 16, 17, 22 and 23) which have low ratios. In these four cases, the wells exhibit only a slightly elevated chloride level. In addition, the wells fall within the zone of thinner clayey tills (Fig. 2), and may have a greater influence of atmospheric waters on the chemical fingerprint. The analysis of calcium, magnesium, potassium, bicarbonate and sulfate from the water samples back this up as well. The Piper plot of the well water samples reveals a definite difference in chemical signature between the wells in the south and the wells in the northern two-thirds of the study area (Fig. 13). The southern wells are relatively calcium and sulfate rich and sodium and carbonate poor, and plot within the zone of mixing to seawater intrusion (Appelo and Postma 2005). The northern wells show the opposite signal, being sodium and carbonate rich and sulfate and calcium poor, and plot within the zone of groundwater freshening (Appelo and Postma 2005). Thus, the geochemical signals from the well water samples confirm the results from analysis of the temporal trends, being that the southern wells with high salinity are experiencing seawater intrusion, where as in the northern two-thirds, the source is from diffusion.

4.2 Groundwater Potential and Saltwater Intrusion

There have not been any significant changes in the groundwater potential for the chalk/limestone aquifer in Greve over the last 10 years. Almost the entire area within 2km of the coast line has maintained a potential under mean sea level, with significant depressions in both the north and south (Fig. 4). The depression in the north reaches as much as 7m below mean sea level, where the southern depression reaches just over 4m below mean sea level. Yet, in spite of the larger depression in the north, the geochemical evidence does not indicate intrusion from the Baltic Sea, where as there is intrusion in the southern depression. This leads directly to the question – what is the reason for this difference?

The answer to the posed question most likely lies in the thickness of the clayey tills as well as the presence of glacial outwash sands and gravels. In the northern two-thirds of the study area, the quaternary sediments are dominated by a thick deposit (>15m) of clayey tills (Figs. 2 and 3). The tills have a very low hydraulic conductivity, of between 10^{-10} to 10^{-11} m/sec (Nilsson et al. 2001). Fractures have been observed in the clayey tills down to about 12m (Mortensen et al. 2004, Nilsson et al. 2001), but the tills are thick enough that fractures do not penetrate through. Therefore the tills provide a buffer between the groundwater and the seawater. This prevents seawater intrusion in spite of the groundwater potential well below sea level. In contrast, the southern part of the municipality has a significant channel of outwash sands and gravels which overtake the clayey tills as the dominant quaternary sediment (Figs. 2 and 3). Here, the clayey tills are either completely absent or significantly reduced in thickness (less than 5m), allowing seawater to infiltrate through fractures in the till to the groundwater reservoir. Therefore, the sand and gravel channel acts as a preferential pathway for saltwater intrusion to occur in the southern part of the municipality. This situation is not without precedence, as paleochannels have been observed to act as preferential pathways for seawater intrusion (Han 1996, Mulligan et al. 2007). This evidence corresponds well with the geochemical data; the northern two-thirds of the study area is isolated from the sea by the clayey tills, and shows a salinity with a chemical signature indicating diffusion as a source, and the southern third, lacking this isolated layer, showing a chemical signature indicating seawater intrusion as the dominant source.

4.3 The Well Depth Problem

Salinity is seen to increase in the connate formational waters from a depth of -40m and deeper (Bonnesen et al. 2009, Klitten et al. 2006). Given that diffusion is the primary source of salinity in the northern two-thirds of the study area, it would be logical to presume that the deeper the well, the higher the salinity within the well waters will be. Indeed, a positive correlation between well depth and salinity can be observed in three of the wells, 5, 11 and 26, where there was a significant drop in salinity observed after the wells were renovated in 1983, when bottom portion of the wells were sealed. However, in wells 4, 14 and 24, there was no significant or sustained drop in salinity after renovation. This situation is backed up by the overall analysis of well depth versus salinity, where there is absolutely no correlation between well depth and the observable salinity (Fig. 8). This leads to the question, why do some wells exhibit a correlation between depth and salinity, where as others do not?

The author believes that the answer to this question lies within the complex nature of the fractured aquifers. There will likely be local variations in the density, aperture and depth of fractures as well as differences in the number of fractures that a specific well intersects. These anisotropies in the system are the most likely explanation for the differences in the measured salinity. For example, in the wells recorded a positive drop in salinity upon renewal, it is probable that the water bearing fractures at that locality extend to between the renovated and the original well depth. In that case, the pathway for diffusion is shut off, and the well salinity decreases. In the wells which had no response, the water bearing fractures intersected by the well likely extend well below, or were exclusively higher than the renovated well depth, allowing the elevated saline waters to continue to flow to the well. This local fracture anisotropy can also explain why two near-by wells of the same depth have significantly different salinity levels, as seen in wells 20 - 21, and 25 – 26 (Table 1).

A second possibility which could explain the lack of correlation between well depth and salinity could be younger, atmospheric water flowing into the wells. This could be via recharge through fractures in the moraine tills, or through leaks in the well casing. In the case of the former, the wells with a lower chloride level should be located in or near areas with quaternary deposits less than 13m in thickness – the depth to which fractures have been observed to penetrate the

clayey till (McKay et al. 1999, Mortensen et al. 2004). This could indeed be the case in wells 16, 22 and 23, which lie in thinner quaternary deposits, and have only a slightly elevated salinity value. However, this cannot explain the differences observed in, for example, wells 1-3, or wells 25-26 where all these wells lie in thick till deposits. With respect to leaks in the well casing, it is unknown what role this may indeed play, because this has not been investigated. However, the author believes that any leaks, should they occur, would only constitute a minor constituent of water to the bulk water sample, and will have negligible influence on the overall salinity measured in the well.

4.4 Management Implications

The source of the measured salinity is important for the management of the wells. When diffusion is from connate formational waters, the salinity does not significantly increase with time. In this case, if the salinity is higher than the allowed 250mg/l chloride, the water can be simply mixed with water from other wells with a lower salinity, so that the over-all distributed water maintains the

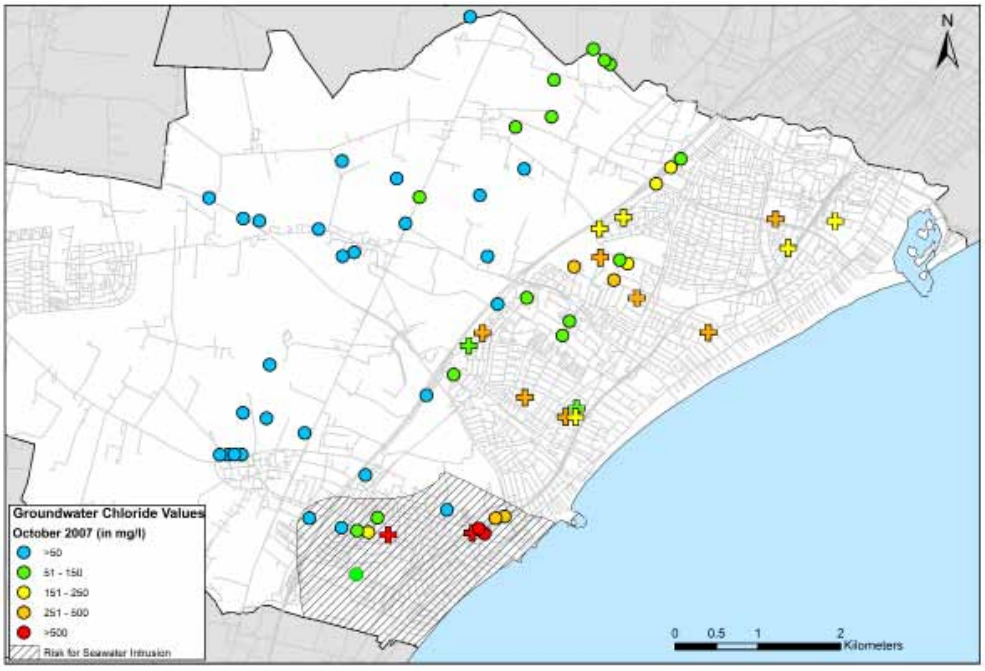

Figure 14. *Map showing the area with a risk for saltwater intrusion in Greve. The area with risk for seawater intrusion is shown in the cross-hatched section.*

quality requirements. This is, in fact, what the water works is doing for the wells that are still operating with an elevated chloride level (i.e. well 13). Because the diffusion rate is the delivering mechanism for the salinity, there is little risk for higher salinities. Increased pumping rates will have no influence on salinity, except for possibly decreasing it. This is in contrast to areas susceptible to seawater intrusion. Here, salinity can increase to very high levels, and relatively quickly, as illustrated in well 39, where chloride levels increased to 2200mg/l over just a few years, before the well was shut down. It is this area where the aquifer is the most vulnerable to salinity.

With respect to the salinity in Greve, it is the southern third of the study area which is the most vulnerable to salinity (Fig. 14). This is the area that has shown direct signs of seawater intrusion. In fact a saltwater wedge can be seen to have intruded progressively inland between wells 39 to 37, where, over the last 8-10 years, it appears to have reached a balance. However changes in precipitation and recharge or increased pumping, could upset this balance, allowing the wedge to push further inland. Monitoring of these wells is recommended. To the north, the elevated salinity from diffusion does not pose the same threat, and in fact salinities in these wells will only have a maximum of between 300-500mg/l depending on the local geohyrdrologic conditions. Therefore, the municipality and/or water works could consider increasing groundwater abstraction in the areas to the north where seawater intrusion is not a problem, taking some of the stress off of the southern wells. Alternatively, the water works could consider technical solutions, such as seawater intrusion barriers (either injection or pumping wells) between the coast and abstraction. In the past, the water works has closed down several wells in the northern two thirds of the study area due to the elevated salinity, and fear of seawater intrusion (note Fig. 4). In fact a total of seven wells were closed down in spite of chloride values below 250 mg/l, and two even below 150mg/l. Elevated fluoride levels, which is observed in the wells which penetrate into the chalk, played a role in the decision to close some of the wells (Jakobsen 2009). However there are examples where wells, such as nr. 13 continues as a producing well in spite of having significantly higher fluoride and chloride levels than wells 5-8, all of which have been shut down (Table 1). In the end, it can be argued that the wells in the northern two thirds of the study area were in no real danger for salinity and unnecessarily closed off.

5. CONCLUSION

Elevated salinity has been a problem in Greve in the area within 2.5km of the Baltic Sea coast ever since abstraction started at a large scale in the 1960's. Traditionally, it was thought that this salinity was of a result of seawater intrusion, but more recently diffusion from connate formational waters has been presented as a possible source. The geochemical signature of the bulk water samples indicate that both play a role in the elevated salinity in the area. In the northern two thirds of the study area, the geochemical signature suggests diffusion as the primary source, where as in the southern third of the area, it is from seawater intrusion. A thick layer of clayey till has prevented seawater intrusion in the north in spite of a significant depression below mean sea level in the groundwater potential. On the other hand, in the southern third of the study area, this protective layer is absent allowing seawater to intrude into the aquifer. Therefore, it is recommended that these wells be closely monitored for salinity. In addition, more abstraction could be conducted in the north without significant risk of elevated salinities above 300-500mg/l chloride.

Modeling of Seawater Intrusion in Greve, Denmark

1. INTRODUCTION

Elevated groundwater salinities (chloride levels of over 250mg/l) have been registered in several groundwater abstraction wells in the municipality Greve since large-scale groundwater abstraction began in the 1960's. The elevated salinity was restricted to in wells within 2-2.5km of the coast, and was traditionally thought to be a result of seawater intrusion. As a result, a number of wells were shut down. However, a recent study conducted by the Geological Survey of Denmark and Greenland (GEUS) suggests that the source of the salinity in the area could be a result of upward diffusion from saline connate pore waters within the fractured chalk aquifer (Bonnesen et al. 2009, Klitten et al. 2006). In Chapter 7, geochemical data from bulk water samples from the water wells in Greve were analyzed, revealing that the source of the salinity was from upward diffusion in the northern two-thirds of the municipality, where as seawater intrusion was the source in the southern one-third. This information, while important for the management of the aquifer, only shows what has occurred at the wells. There is no predictive information regarding whether or not a seawater wedge is approaching the wells that have not experienced seawater intrusion, or how the seawater wedge, in the areas with documented seawater intrusion, will continue in the future. This predictive ability is also important for the proper management and protection of the groundwater aquifer.

The numerical modeling of seawater intrusion has been problematic due to the density differences between saline and fresh waters. The freshwater-saltwater relationship was first described over 100 years ago by two separate groups, showing that the depth to the freshwater/saltwater interface, in a homogeneous, unconfined aquifer, with typical seawater salinity concentrations (3.5%, with a density of 1.025 g/cm^3), is 40 times the elevation of the groundwater head (Drabbe and

Badon-Ghyben 1888-1889, Herzberg 1901). This relationship, commonly called the "sharp interface" or Ghyben-Herzberg relation, can subsequently be applied to confined aquifers by using the aquifer's piezometric surface in the calculation (Todd and Mays 2005). The sharp interface has subsequently been applied in a number of groundwater models specifically for management of coastal groundwater resources (Mantoglou 2003, Mantoglou and Papantoniou 2008, Park and Aral 2004, Ranjan et al. 2006). The advantage for this, is that it provides a simple estimation of the saltwater/freshwater boundary, which can be incorporated into the coastal groundwater models in order to provide a prediction of seawater intrusion without creating a large computational burden (Mantoglou et al. 2004).

There are, however, inherent problems with using a sharp interface when modeling seawater intrusion. The sharp interface ignores the processes of molecular diffusion and dispersion which occur at the saltwater/freshwater interface, creating a transition zone between the two water bodies (Abarca et al. 2007b, Barazzuoli et al. 2008). Seawater intrusion itself will alter the density between the fluids, causing a variation of the seawater/freshwater relationship with space and time, as the concentration, temperature and pressure in the fluid changes (Barazzuoli et al. 2008). These processes directly influence the timing and concentration of seawater reaching a well. In order to account for this, a variable flow and transport modeling approaches have been developed, which allow for a more accurate modeling of seawater intrusion (Diersch and Kolditz 2002). The drawback for using variable flow and transport modeling techniques, however, is that they tend to be very computationally heavy (Langevin 2003). However, as computer computational power continues to increase, this becomes less of an issue.

The groundwater variable flow and transport model, FEFLOW, has the capacity to account for variable flow and transport for the modeling of seawater intrusion, both in 2-D and 3-D. A number of studies have successfully applied the code to model seawater intrusion. This has been done in different contexts and scales, including smaller scale site specific studies (i.e. Alberti 2006), kilometer-scale local studies (i.e. Barazzuoli et al. 2008) and large, regional scale studies (i.e. Kafri et al. 2007). The FEFLOW model has also been used in the variable density modeling influences on aquifer storage and recovery (Ward et al. 2008, Ward et al. 2009). This study uses FEFLOW to model the coastal zone in Greve, Denmark, in order to provide an assessment of the seawater intrusion as a response to past, present and future groundwater abstraction. The objective of the modeling is to provide

an assessment as to where seawater intrusion is most vulnerable, based upon and accurate conceptual geological model and actual groundwater abstraction data, and provide recommendations for the management of the coastal groundwater in Greve.

2. STUDY AREA

Greve Municipality lies along the coast of the Baltic Sea, approximately 25km to the southwest of the Danish capital of Copenhagen (Fig.1). Historically, groundwater abstraction began in the 1930's to provide water supply to the summer houses along the coast. Abstraction at this point was limited, and mostly during the summer season(Roskilde Amt 2004). In the 1960's saw a high growth of full-time residents in the area, resulting in a large increase in the groundwater abstraction. Parallel to increased growth of the area, abstraction continued to increase until the early 1990's, when water quality problems, particularly salinity, forced the closure of a number of wells, and a reduction in the overall groundwater abstraction rate (Roskilde Amt 2004). Since 1992, there has been a slight decrease in overall groundwater abstraction in the coastal area, with the replacement abstraction being located further inland.

The study is focused on the area in Greve Municipality which falls within approximately 2.5km of the Baltic Sea coast, and also includes a small portion of

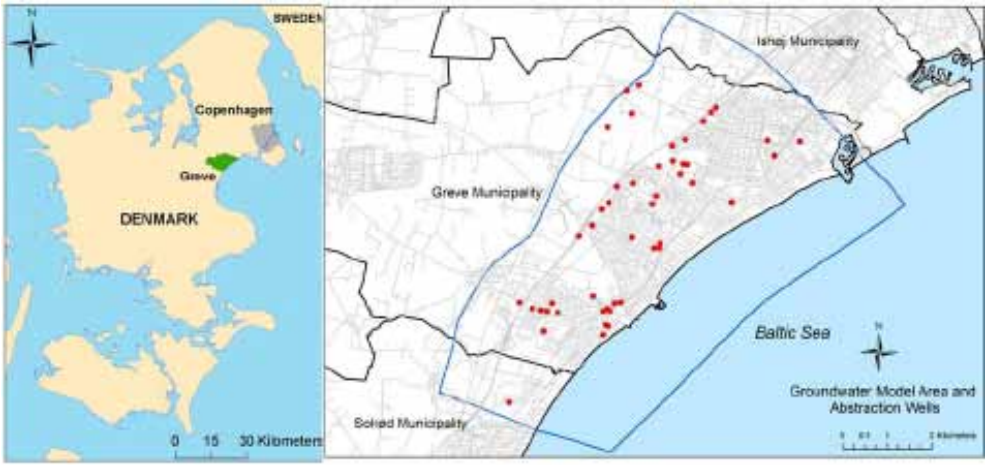

Figure 1. *Map showing the location of Greve Municipality, Denmark (left). The right map shows the model area (outlined in blue) and the groundwater abstraction wells within the boundaries of the model.*

Solrød Municipality to the south and Ishøj Municipality to the north (Fig. 1). In total, there were 49 groundwater abstraction wells in operation at various times between 1965 and 2009 (Fig. 1).

2.1 Geological Setting

The near-surface geology consists of Danian (Paleogene) bryozoan limestone and Maastrictian (Upper Cretaceous) chalk overlain by between 3 and 30m of Quaternary deposits, consisting primarily of clayey tills with lenses of outwash sands and gravels (Fig. 2 and Fig. 3) (Larsen 1998). A full description of the geological units and their evolution is provided in section 1.2 in Chapter 7. However, important aspects of the geological setting with significance to the modeling will be summarized in this section.

The fractured Danian limestone and fractured Maastrictian chalk comprises the primary groundwater aquifer in the area, with all municipal groundwater wells

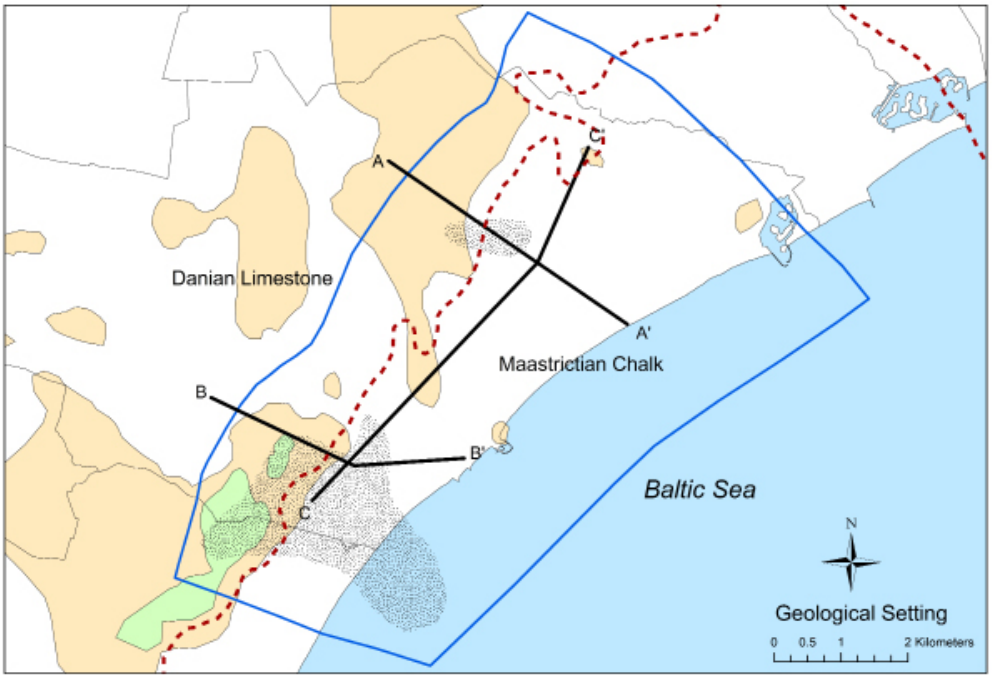

Figure 2. *Geological setting in Greve. The red dashed line shows the pre-quaternary boundary between the Tertiary Danian Limestone and the Cretaceous Maastrictian Chalk. The Quaternary units less than 13m thick are shown in orange, and where it is less than 5m thick is shown in green. Stippled area shows where the dominant quaternary unit is glacial outwash sands and gravels. Otherwise, the dominant quaternary unit is clayey till.*

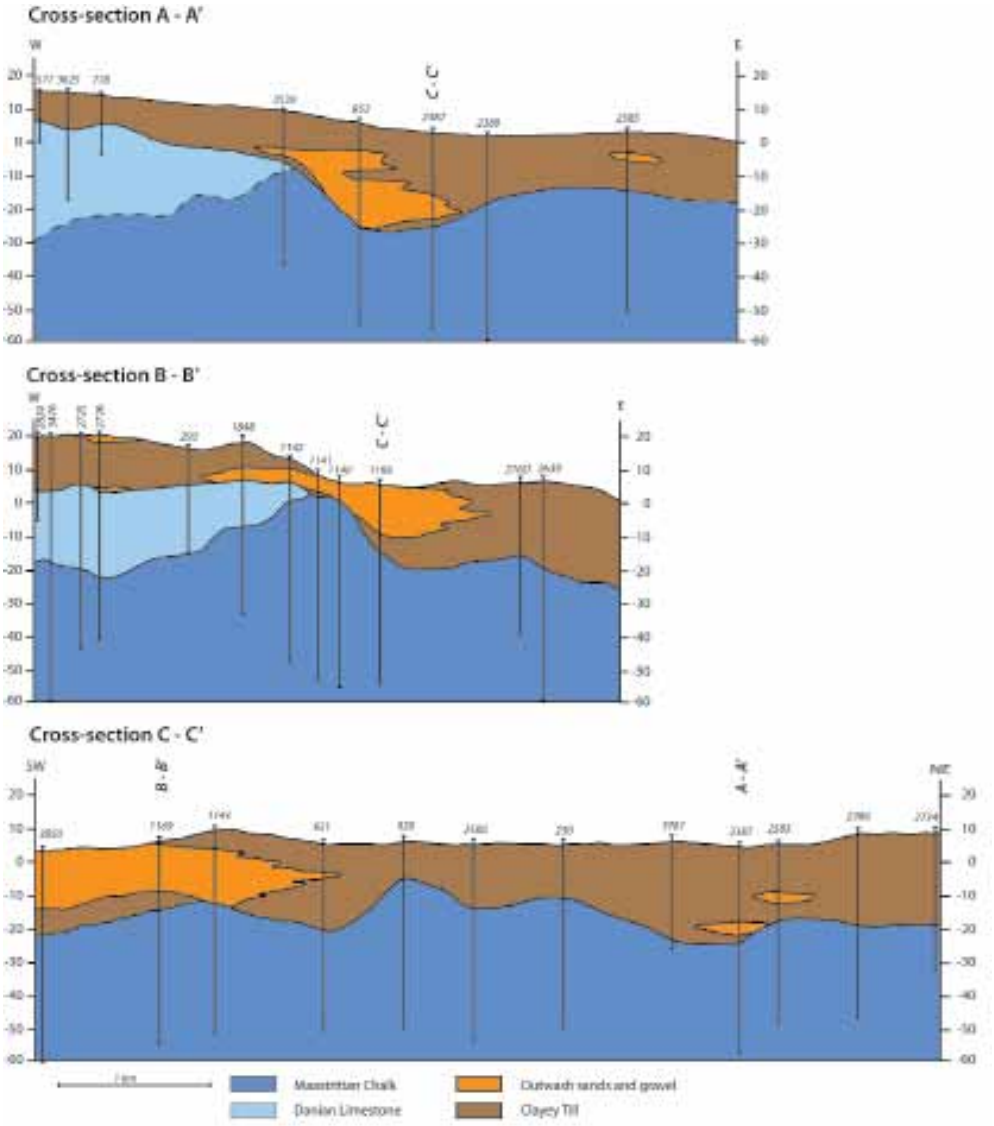

Figure 3. *Geological cross-sections over the model area. The location of the cross-sections is shown on the map in Figure 2. Note the irregular erosion surface between the older limestone/chalk and the Quaternary deposits.*

screened exclusively in the limestone and chalk. The matrix porosity of both the limestone and chalk is over 30%, however matrix hydraulic conductivity remains low, from 3-4 x10^{-8} m/sec (Frykman 2001, Larsen et al. 2006). The dominant hydraulic conductivity in the limestone and chalk comes from the fractures. Hydraulic conductivity from the fractures in the limestone and chalk ranges from 7.6x10^{-5} and 1.3x10^{-5} m/sec (Larsen et al. 2006). It is generally thought that most of the conductivity occurs in the upper 10m of the units, where as below this level

the fractures become closed off, and tight (Jensen, et al. 2002). However, observations from well flow measurements conducted in the water wells have shown that the water conducting layers varies widely from well to well, with anywhere from the only the upper meter to even more than the upper 15 meters (Jakobsen 2009, Klitten et al. 2006). No direct documentation on well-flow studies could be located, but highly variable well specific capacities (measured in m^3/hr/m screen) measured by the water works seem to confirm this observation. This is important because differences in the thickness of the water bearing fractures suggest that there will also be a high variability in transmissivity in the aquifer across the study area.

The surface of the chalk and limestone, as interpolated from the borehole logs, generally goes from approximately -20m along the coast to as high as 20m in the southwest part of the study area (Fig. 4). Therefore, it is seen that the elevation of the fractured aquifer increases inland towards the northwest. However, it is important to note that this surface is not even, with holes particularly occurring in the middle and northern part of the study area (Fig. 3 and Fig. 4).

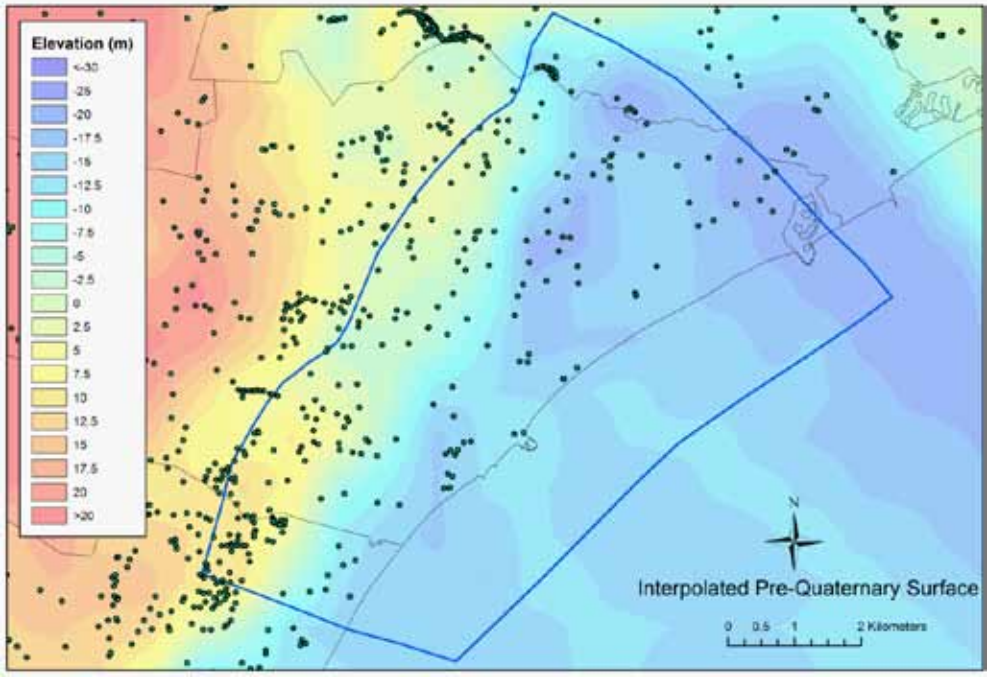

Figure 4. *Elevation of the pre-Quaternary surface over the model area. This represents the elevation of the top of the aquifer. Note how the aquifer is lowest towards the sea, and highest inland. There are also a couple of depressions in the north-central part of the model area.*

The Quaternary glacial sediments are predominately composed of clayey till with lenses of outwash sand and gravels. The clayey till, with hydraulic conductivities of under $1x10^{-9}$ m/sec act as the confining unit over the limestone and chalk aquifer (McKay et al. 1999, Nilsson et al. 2001). The outwash sands and gravels, however, are more permeable, with hydraulic conductivities of as high as $1x10^{-4}$ m/sec (Nilsson et al. 2001), and can provide an avenue for both recharge and seawater infiltration. The outwash sands and gravels are predominately located in the southern part of the study area, where they dominate the Quaternary deposits (Fig. 2 and Fig. 3). The thickness of the clayey till also plays an important role in the hydrological properties in the study area. The clayey tills have been observed to be fractured in the area, with the fractures extending as deep as 13m (McKay et al. 1999, Nilsson et al. 2001). This has altered the hydraulic conductivity through the clayey till, reaching as high as $3x10^{-4}$m/s down to a depth of 4m, and $1x10^{-7}$m/s at 13m (McKay et al. 1999, Nilsson et al. 2001). These fractures provide a preferential pathway not only for recharge, but also for seawater to intrude into the aquifer. In the study area, the thinner Quaternary deposits lie predominately in the southwestern and northwestern part of the study area, and are over 13m in thickness at the seashore (and presumably also under the seabed) (Fig. 2). Therefore, looking at the quaternary deposits, the thick clayey tills will provide a buffer against seawater intrusion in the area, apart from the southeastern part of the study area (Fig. 2). Here, the outwash sands and gravels are the dominant Quaternary deposit, providing a conductive pathway for seawater to infiltrate into the primary aquifer.

2.2 Hydraulic Head and Salinity in Greve

Hydraulic head from the primary aquifer (fractured limestone and chalk) before heavy groundwater abstraction began in the 1960's was shown to be as high as 28-30m in the western part of the municipality and decreasing regularly, as expected, to a potential of 0m at the coast (Roskilde Amt 2004). Upon the start of significant groundwater abstraction in 1965, two depressions in the groundwater potential near the coast were created, with the potential decreasing to as low as -20m in the north-central part of the study area. After the decrease in groundwater abstraction in the 1980's and 90's, the aquifer has recovered significantly. As of 2007, the groundwater potential in a significant portion of the study area remains below sea-level, with two depressions reaching -8m in the north-central, and -5m

in the south-central part of the study area (Fig. 5). According to the data from the municipality, the potential in the western portion of the municipality has remained relatively unchanged at between 24m and 26m since 1975 (Roskilde Amt 2004).

Groundwater salinity in the study area, as represented by chloride, varies from as low as 20mg/l to as high as 2200 mg/l (Fig. 5). The chloride is measured from bulk water samples taken from the abstraction wells by the water works, as part of the water quality monitoring program. Over the study area, the chloride can be, in general, seen to increase towards the coast. However, as discussed in Chapter 7, the salinity in the northern 2/3 of the study area is due to diffusion from connate pore waters in the chalk, resulting in a more irregular pattern. The salinity in the southern 1/3 of the study area, on the other hand, shows a more traditional pattern of seawater intrusion.

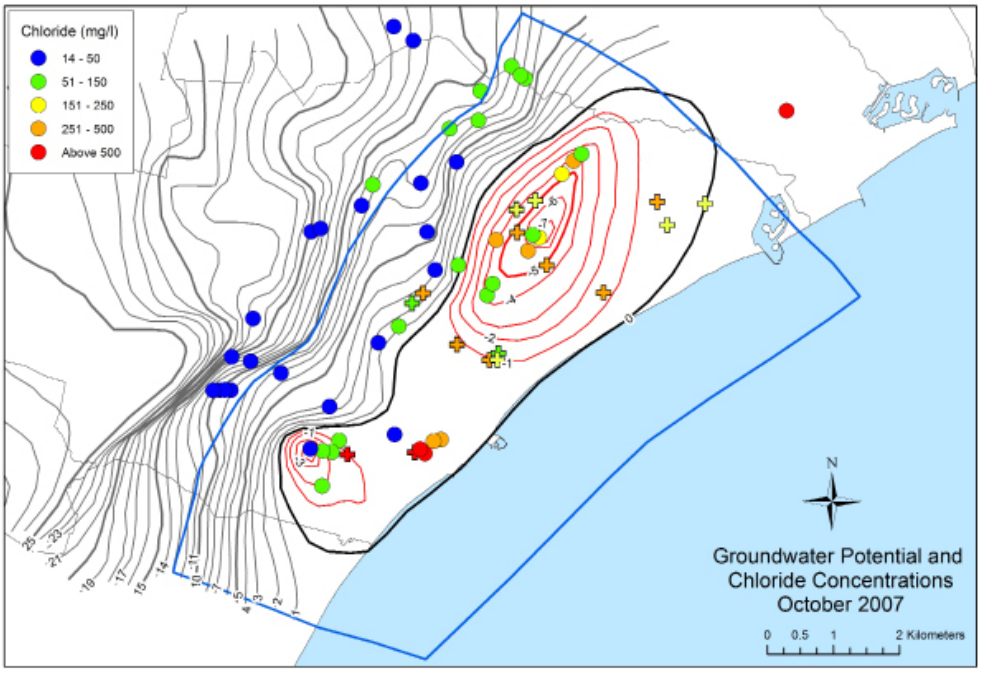

Figure 5. *Map of the groundwater potential, as measured by Greve Municipality in October 2007. The red contours show the area with groundwater potential below mean sea level. Also shown are the measured chloride concentrations in active wells in 2007 (circles) or the last chloride concentration measured before the wells were closed down (crosses).*

3. NUMERICAL MODELING

3.1 FEFLOW

The numerical modeling for this study was conducted using FEFLOW, version 5.3, which is a model that allows for the subsurface modeling of fluid flow and transport of dissolved constituents (Diersch 2006). This code can do both 2D and 3D finite element modeling with density-coupled flow and transport, under both steady-state and transient conditions. It is not within the context of this study to provide an analysis of the governing equations used within the FEFLOW code, and will not be presented here. For the theoretical and practical information and the mathematical basis for the code is thoroughly presented by Diersch (2006).

The FEFLOW software was chosen because of its ability to incorporate the necessary parameters to model saltwater intrusion under transient conditions. Modeling of seawater intrusion is sensitive to a number of issues. First of all seawater intrusion is very sensitive to anisotropy in hydraulic conductivity, and the presence of preferential flow paths (Abarca et al. 2007b, Mulligan et al. 2007). Secondly, diffusion and dispersion affect the saltwater/freshwater interface, producing a transition zone rather than a sharp interface (Diersch and Kolditz 2002, Barazzuoli et al. 2008). Thirdly, head measurements are affected by differences in the freshwater and seawater density, which will also affect the groundwater movement within the aquifer (Diersch 2005, Post et al. 2007). By utilizing the finite element method, FEFLOW has the capacity to account for the spatial differences in hydraulic conductivity from changing geological conditions as well as directional anisotropy as is often observed in fractured or karst aquifers (Diersch 2006). The model code takes direct consideration diffusion and dispersion, allowing for the modeling of the transition zone in both 2D and 3D (Diersch 2006). The software also allows for nodal grid refinement around points or lines for more accurate modeling around, for example, abstraction wells, monitoring wells or the coastline.

3.2 Modeling Dimension

For the purpose of this study, a 2-D numerical model was chosen. It is recognized the advantages in 3-D modeling with respect to density driven groundwater flow problems such as seawater intrusion. This is particularly with respect to changes in

salinity with depth in the aquifer, as well as the ability to model seawater intrusion in a multi-layered aquifer system. However, 3-D models are more computationally intensive and require a greater amount of detailed input into the model parameters in order to produce a robust model. 2-D models, on the other hand, are simpler and less computationally burdensome, and quicker to set-up and run. In certain cases, the models can be just as reliable in the prediction of seawater intrusion as 3-D models, and would be the better choice.

A 2-D model was chosen for Greve for the following reasons:

1) The geology in Greve is relatively straight forward, with the groundwater aquifer being fractured chalk and limestone overlain by clayey till or outwash sands and gravels. There are not multiple aquifers which need to be accounted for.
2) As described in section 2.1, the actual thickness of the open, water bearing fractures in the chalk and limestone aquifer is extremely variable, anywhere from 1m to over 10m. The problem is that it is impossible to map (and characterize) this change in aquifer thickness due to a lack of data. Therefore a 3-D model would generalize the aquifer to being a uniform thickness. This is precisely what a 2-D model would do anyway.
3) All of the wells in the study area extend more then 10m (some even greater than 40m) into the limestone and chalk aquifers and are thus likely to be fully penetrating. Thus any water intake will be an average over the entire screened interval. Therefore upward coning of saltwater is not an issue in this case. FEFLOW averages the concentration for the entire thickness of the aquifer, and thus is representative of the salinity which would be measured by a fully penetrating well.
4) FEFLOW's 2-D model can accommodate for the different hydrogeological properties of the overlying Quaternary sediments by setting the mass and flow transfer rates from the top into the model. This allows us to accommodate for differences in recharge and connection to the sea through the Quaternary sediments.
5) Considering the size of the study area and computational times for the model, using a 2-D model allowed the use of a much finer mesh, with greater enrichment around the coast and wells possible. This provided for a finer simulation of seawater intrusion along the horizontal plane.

3.3 Discretization and boundary conditions

The model area used for the study runs from approximately the 8m groundwater head level, as mapped in 2002 by Greve Municipality, and extending approximately 2km beyond the coast line in order to simulate the part of the aquifer beneath the Baltic Sea (Fig. 5). The aquifer was discretized using a triangular mesh containing 18,046 elements and 9,149 nodes (Fig. 6). A high degree of refinement was conducted around the abstraction wells and the coastline. Size of the elements ranged from 25m to 150m, with a total area of 50.3 km^2. A constant head of 8m was assigned on the upper boundary, and a saltwater compensated head of 0.30m was assigned to the seaside side of the model. Saltwater head was compensated using the equations outlined by Diersch (2005, p. 133), which takes into account the density difference between freshwater (assumed at 1.0kg/l) and seawater from the Baltic Sea (set at 1.01kg/l for a total dissolved solid (TDS) concentration of 12,000mg/l), and an average aquifer depth of 30m. Seawater transfer rates into the model from the area of the model beneath the Baltic Sea were set with respect to the geological properties. In the areas where the Quaternary deposits

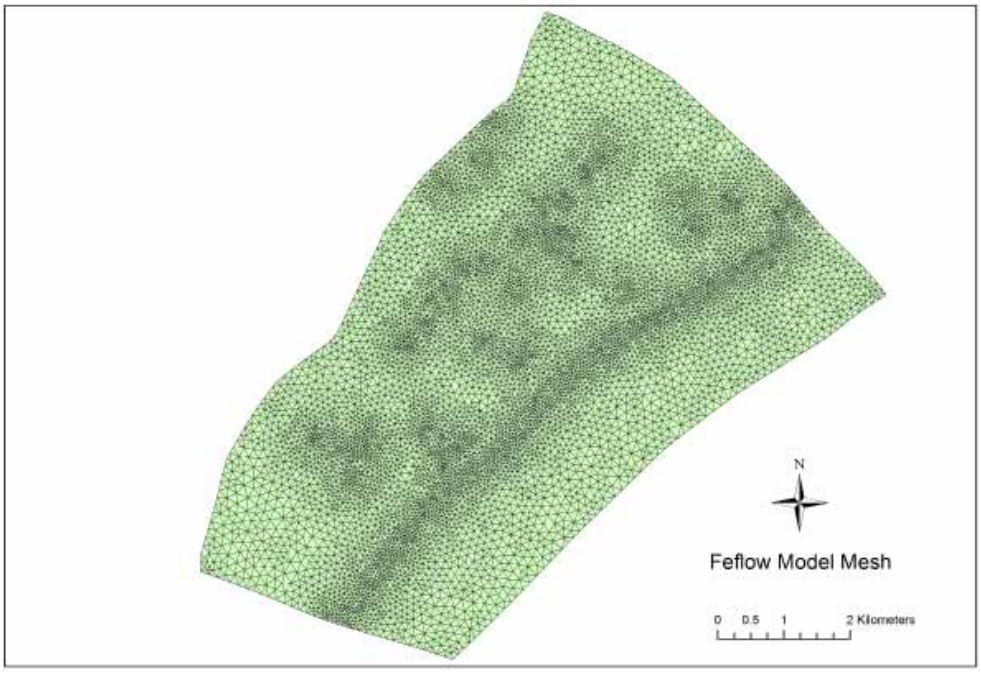

Figure 6. *Diagram showing the triangulated mesh used in the Feflow model. The model contains 18,100 triangles, and been refined around the abstraction wells and coast-line.*

are primarily outwash sands and gravels (stippled area in Fig. 2), a transfer rate of 0.0514m/d was used. The remaining area, which is dominated by the thick clayey till deposits, the transfer rate was set to $1x10^{-5}$m/d. These rates were calculated from the different hydraulic conductivities of the two units. Recharge was set to 36mm/year in the model area with greater than 13m of clayey till overlaying the aquifer, and to 100mm/year in the area under the sands or with less than 13m of till (Fig. 2). This is based on recharge potential in the area, accounting for average precipitation minus evapotranspiration potential and surface run-off (Roskilde Amt 2004) and hydraulic conductivity of the clayey till. Initial mass transport values for the model had the following conditions: 12,000mg/l total dissolved solids (TDS) for the seaward edge of the model and top infiltration beneath the sea, initial value of 250mg/l TDS for the aquifer, and 100 mg/l TDS (fresh water) for recharge and inflow into the model from the groundwater upland (above the 8m head boundary). Default mass transport diffusion rates of $1x10^{-9}m^2$/sec, and longitudinal and transverse dispersivity were 5m and 0.5m respectively.

3.4 Model Calibration

The primary objective of the model calibration is to obtain hydraulic heads in the abstraction wells as close to the observed results as possible. August 2002 was chosen for calibration, using the abstraction rates for each well from the period 1992-2002 (Table 1). This period was chosen for calibration because the municipality measured all of the current abstraction wells and three monitoring wells within a two day period (Roskilde Amt 2004). This provided the most detailed and accurate measurement of the groundwater potential in the primary aquifer because the head measurements were concentrated within a two-day period, rather than spread out over a longer period of time. Hydraulic heads from the calibrated model were then verified using data on the wells from October 2007, where the municipality conducted a similar two-day monitoring program in the same manner as in August 2002. During this period, groundwater abstraction was reduced, resulting in a rebound in measured hydraulic heads from 2002.

Calibration of the model was conducted within the FEFLOW software. Two parameters, recharge and transmissivity were considered for calibration. As a starting point, recharge was set to 100mm/year in the areas with less than 13m of clayey till and 36mm a year over the rest of the model area above sea-level. Transmissivity

Table 1. *List of the groundwater abstraction rates (m^3/day) used in the groundwater model. Location of the individual wells can be seen on Figure 7.*

Project Well ID	DGU ID Nr. (207.-)	1965 -1969	1969 -1975	1975 -1982	1983 -1987	1988 -1989	1990 -2002	2002 -2009
1	2734	0	0	0	165	294	135	99
2	2733	0	0	0	135	273	155	116
3	2732	0	0	0	167	283	194	138
4	881	0	0	192	176	76	0	0
5	880	0	0	0	0	0	0	0
6	2586	0	0	192	176	0	0	0
7	2386	0	0	176	88	99	0	0
8	2385	0	0	176	90	90	0	0
9	852	137	137	176	251	214	240	118
10	2384	0	0	176	100	100	0	0
11	2582	137	137	176	146	144	110	94
12	2583	137	137	176	159	171	110	66
13	2387	0	0	176	85	122	117	130
14	2389	0	0	176	122	190	0	0
15	234	137	137	410	0	0	0	0
16	2390	0	0	176	314	325	130	35
17	2388	0	0	176	256	337	300	323
18	2719	0	0	0	173	267	102	108
19	2720	0	0	0	197	280	205	149
20	2502	0	0	176	100	90	0	0
21	2501	0	0	176	100	90	0	0
22	2499	0	0	176	434	390	396	349
23	2313	0	0	176	191	202	159	127
24	2500	0	0	258	267	208	0	0
25	2581	137	137	258	267	208	0	0
26	2234	65	65	258	267	208	0	0
27	2580	0	0	258	267	208	0	0
28	708	194	194	249	237	240	190	171
29	2543	0	0	0	79	136	48	34
30	2662	0	0	0	79	136	48	34
31	2730	0	0	0	79	136	48	34
32	2639	0	0	0	79	136	48	34
33	216D	95	95	95	0	0	0	0
34	2735	0	0	0	207	199	221	260
35	1848	0	246	246	207	199	221	260
36	1142	0	246	246	207	199	221	260

(Continued on next page)

(Continued from page 203)

Project Well ID	DGU ID Nr. (207.-)	1965 -1969	1969 -1975	1975 -1982	1983 -1987	1988 -1989	1990 -2002	2002 -2009
37	1141	0	246	246	207	199	221	260
38	1140	0	246	246	207	199	221	260
39	1169	0	246	246	207	199	0	0
40	2964	194	194	249	237	240	190	171
41	2757	0	0	0	0	0	153	153
42	2821	0	0	0	0	0	680	680
43	3775	0	0	0	0	0	0	191
44	3024	0	0	0	0	0	284	284
45	216A	95	95	95	0	0	0	0
46	216C	95	95	95	0	0	0	0
47	2295	95	95	95	79	0	0	0

was set to $4.0x10^{-4}$ m^2/sec. This was chosen as the starting tranmissivity because it is the same used in non-density dependent groundwater flow models previously applied water flow and balance models for the area (Roskilde Amt 2004), and is in line with recorded fractured hydraulic conductivities, assuming an aquifer thickness of 10m.

Hydraulic heads calculated in the model using the initial recharge and transmissivity values were unsatisfactory, with modeled head differences of up to 6m. Subsequent, alterations in recharge rates had very little effect on the head measurements. Recharge rates were not allowed to be adjusted to values higher than 150mm/year or lower than 36mm/year in the model area, as it was deemed that values outside of this are unrealistic.

Hydraulic heads, on the other hand, were seen to be much more sensitive to variations in transmissivity. Transmissivity was altered in distinct regions in the model, varying from $1x10^{-4}$ to $1x10^{-3}$ m^2/sec (Fig. 7). Four wells, nr. 16, 17, 35 and 36 (Fig. 7) proved difficult to calibrate. Close examination of the parameters from wells 16 and 17 showed that they had high abstraction rates with little recorded drawdown, and thus the model continually over estimated hydraulic head. According to Greve Water Works data, these two wells had very high specific capacities (measured in m^3/hr/m screen) with respect to the other wells (Fig. 8). Therefore a transmissivity of $1x10^{-3}$ m^2/sec was used around these wells. The opposite was true for wells 35 and 36, which had the lowest measured specific capacity, and

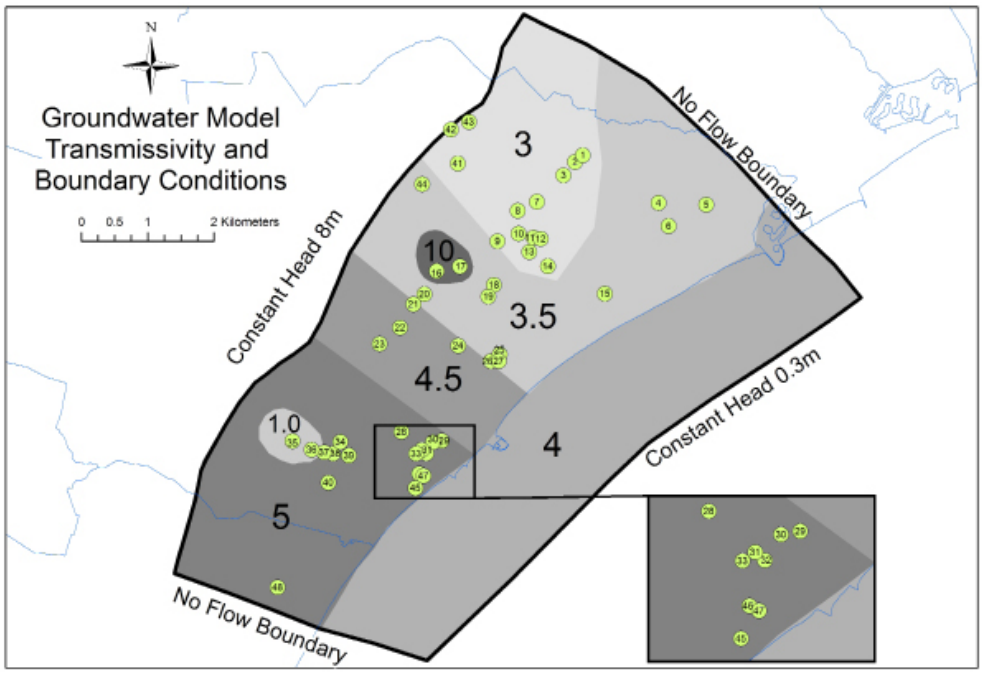

Figure 7. *Calibrated model transmissivity values (in 10-4 m2/sec). The circles show the locations of the abstraction wells in the model, with the well numbers correlating to the abstraction data listed in Table 1. The model edge boundary conditions used are shown.*

thus drawdown was continually under estimated in these two wells. Transmissivity around these wells was therefore set to $1x10^{-4}$ m^2/sec to accommodate for this. The calibrated hydraulic head for the model area is shown in Figure 8. The calibration plot shows a good correlation with the measured heads, with the average variance from the measured values being 0.7m, with the largest variation being 2.5m (from well 16)(Fig. 9). Validation of the model for 2007 shows still a relatively good correlation, with average difference of 1.2m, but a maximum difference of 3.3m (Fig. 9). In general for 2007, the model underestimated the drawdown, particularly in wells 9, 11, 12, and 13, all in the north-central part of the model area (Fig. 7), where all four wells have measured drawdown of 5.5-6.5m, but calculated drawdown of about 3.5m. In spite of this, the model is considered to be in the acceptable range for calibration.

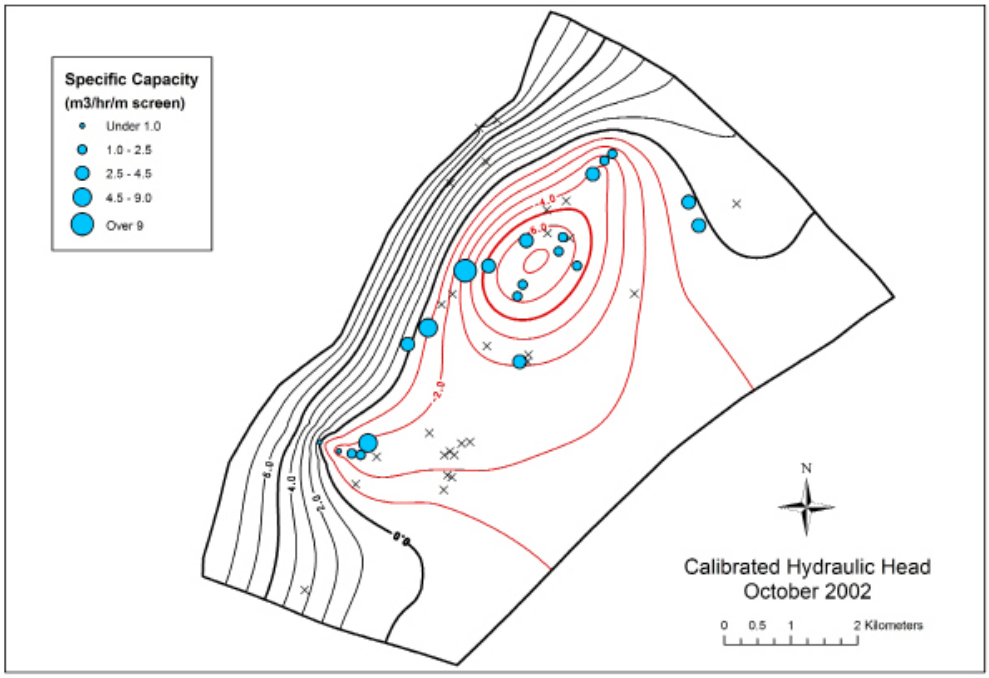

Figure 8. *Calibrated hydraulic head over the model area. Contour interval is 1m, with the red contours representing heads below sea level. The circles on the map show the relative specific capacity for each well (in units m3/hour/m screen). The x's mark the wells where no specific capacity data was available.*

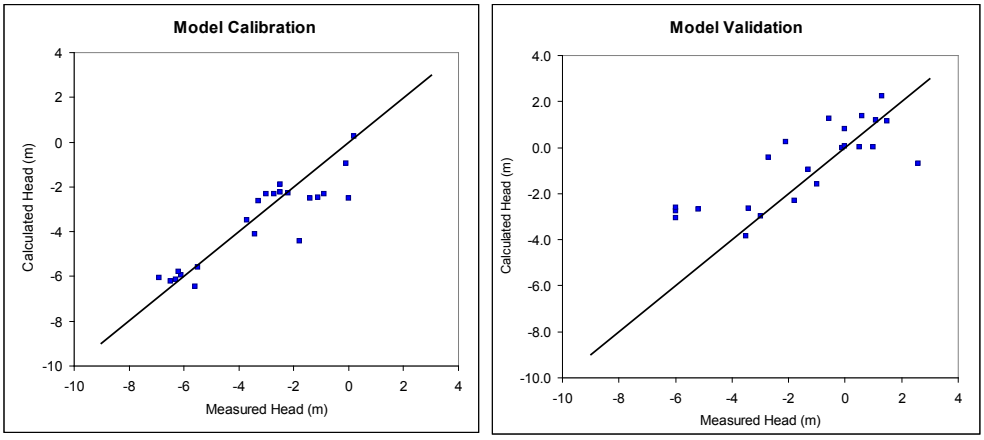

Figure 9. *Model calibration and validation plots.*

4. MODEL RESULTS

The calibrated model was run to simulate seawater intrusion in the past, as well as future projections. Past projections were conducted using actual groundwater abstraction totals for the period 1965-2009, as listed in Table 1. Unfortunately, abstraction data was not always reported for individual wells, but rather for groups of wells. In these cases, the total abstraction for the specific group was evenly divided among the wells within the group. This, of course, adds to a certain amount of error in the model, specifically with respect to model calibration (as drawdown is a function of abstraction rates). The model was first run assuming that 1965 was steady-state conditions, with no significant abstraction occurring before this data. The model was then run during the subsequent stages where groundwater abstraction rates changed. The future projections were run to 20 years into the future under current 2009 abstraction rates, increased abstraction in the north only, and increased abstraction in the south only.

4.1 Simulation of past abstraction

The model was run first to simulate steady-state conditions before groundwater abstraction began. The model showed that the freshwater extended up to 750m beyond the coastline under the Baltic Sea in the areas where the sea is protected by the clayey till (Fig. 10). However, in the area where the sands and gravels are the predominant quaternary sediment, the conduit between the sea and aquifer is opened up, and saline water extends almost the entire way to the coast line. By 1982, after 17 years of increased groundwater abstraction, a significant wedge of seawater intrusion can be observed in the southern portion of the study area, with the near coastal wells registering significant salinity, specifically wells 45, 46 and 47, with a small amount of salinity reaching well 33, which is 200m further inland (Fig. 10). In the mid and northern portion of the study area, the seawater is slowly intruding landward, but has not reached the coastline, with near coastal wells 5, 6, 16 and 27 remaining free of salinity from seawater intrusion (Fig. 10). At this time (1982), wells 45-47 were shut down due to high salinity, and abstraction was moved 300m inland (to the north) to wells 29-32.

By 1987, the intrusion wedge in the southern part of the study area intrudes further inland, reaching wells 30, 31, 32, and 33, and approaching wells 28 and 39 (Fig.

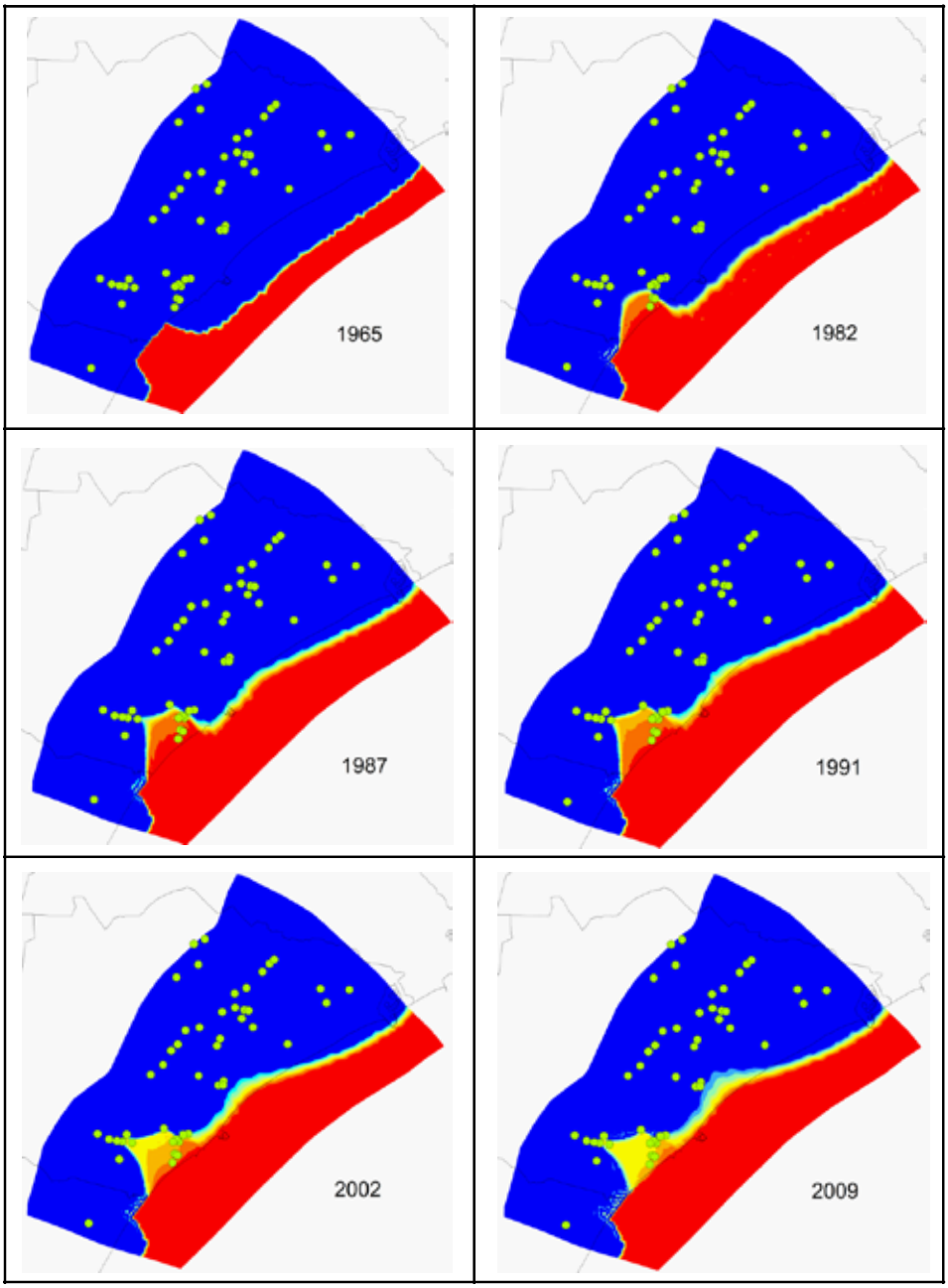

Figure 10. *Modelled saltwater intrusion from 1968 to 2009. The bright red color shows TDS concentrations of 12,000 mg/l, and the dark blue shows TDS below 250 mg/l. The boundary between the light green and yellow colors represents the 500mg/l TDS, the water quality limit for salinity.*

10). Well 33 was shut down for abstraction in 1987. In the mid and northern part of the study area, the salinity in the groundwater continues to approach the coastline, but still is not close to the wells. Between 1987 and 1991, the seawater intrusion wedge in the south continues to strengthen and move further inland, with strong salinity reaching wells 28 and 39 by 1991 (Fig. 10). In the mid and northern portion, the wedge continues to move inland, now at the coastline. Between 1991 and 2002, there was a significant reduction in groundwater abstraction, with well 39 being shut down in 1991, in addition to wells 24, 25, 26 and 27 in the middle of the study area ceasing abstraction in 1989 (Table 1). This led to a weakening of the seawater wedge in the south, however, the salinity continued to move further inland reaching wells 37 and 38 (Fig. 10). The seawater concentrations in the southern part of the study area continued to weaken between 2002 and 2009 in the south. Over this period, however, the seawater intrusion wedge continued to move inland, passing the coast line, but still not reaching any of the groundwater wells.

Actual groundwater salinity measurements from the bulk-water samples taken from the wells provide a reference to evaluate the effectiveness of the model's prediction. As discussed in Chapter 7, the wells in the middle and northern portion of the study area showed no seawater intrusion. This is also the case in the model simulations. In the southern third of the study area, water quality samples in the near-coastal wells showed that when there was a higher salinity, it was as a result of seawater intrusion. A comparison of the water quality samples with the model results shows a good correlation between the two. Wells 36, 37, 38 and 39 show a similar response between show a good correlation, both in timing and concentration between the model and samples. Here the seawater wedge first reached well 39 in 1987, and continued to increase until the well was shut down in 1991 (Fig. 11). Afterwards, seawater intrusion reached wells 37 and 38 by the mid 1990's, where after the chloride levels stabilized out at 150mg/l (Fig. 11), just as predicted by the model. Wells 29, 30, 32 and 33 also show a signal of seawater intrusion similar to the timings predicted by the model (Fig. 11). However, the model over estimated the amount of salinity reaching wells, particularly in well 32, where salinities over three times the observed concentrations of about 1000 mg/l in the 1990's were predicted. The simulation of the model, however, diverges from the water quality data for wells 28, 31 and 40. In the case of well 28, the model simulates seawater intrusion similar in timing and concentration to that of well 39, but water quality data show that chloride never reaches above 50mg/l in the

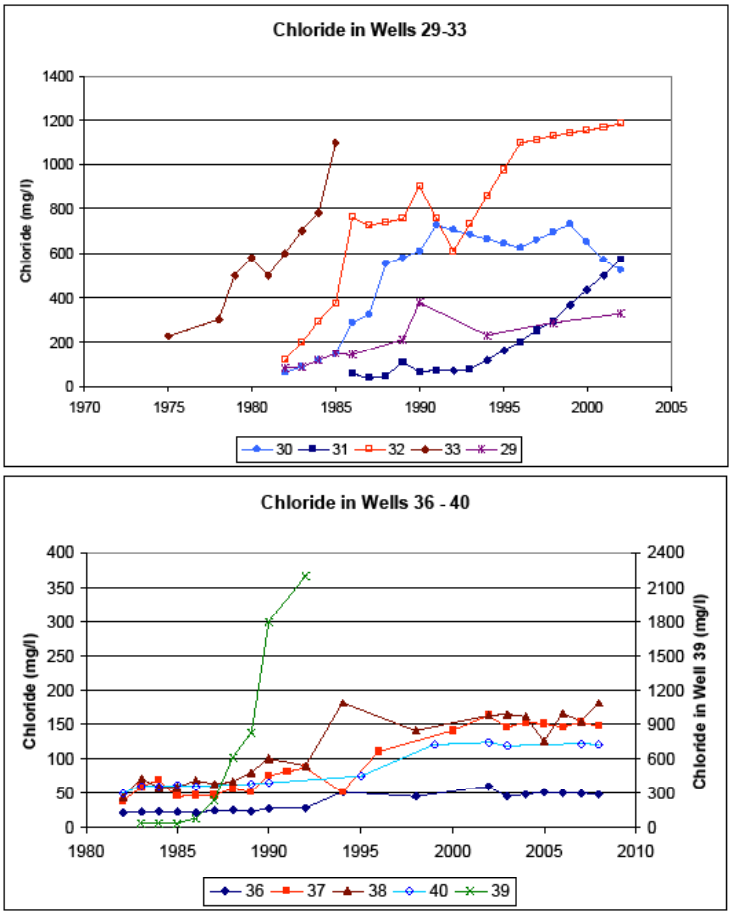

Figure 11. *Groundwater salinity history for groundwater model wells 29-33 and 36-40. Note that well 39 has a different scale (right side) from the other wells.*

well - the well has remained completely fresh. For well 31, the model predicts the salinities to begin to increase between 1982 and 1987 (Fig. 10), but the chloride measured in the well does not increase until 1993, where after it shows the typical signal for seawater intrusion (Fig. 11). Data from well 40 also shows a difference between the model simulation and measured results, where between 1995 and 2000, the samples in the well measured a slight increase in salinity; however the model simulation has no salinity approaching the well during this period. The groundwater sample data from all of the active wells, except for 31, also show a leveling off of chloride levels, indicating that seawater is no longer intruding in, and that it is residual seawater now entering into the wells. This is the same as the model predictions. Unfortunately there is no chloride data from wells 45-47, the wells closest to the coast, to compare with the model results.

The water balance in 2002 for the model is as follows: model inflow included 2971m^3/d entering in the model's upper boundary, and 125m^3/d of seawater entering in the model from the lower boundary, recharge providing an additional 2183m^3/d, and infiltration of seawater predominately through the outwash sand and gravel provided 184m^3/d. Model outflow included 5222m^3/d in groundwater abstraction and 241m^3/d in submarine discharge of freshwater out of the model. Here it can be seen that, according to the model, abstraction is taking all of the available freshwater in 2002, with only a minor component being discharged into the sea. The model also shows that most of the submarine discharge is occurring through the outwash sands and gravels in the southern part of the layer, where as most seawater intrusion is occurring on the northern boundary of the sand and gravel deposit (Fig. 12).

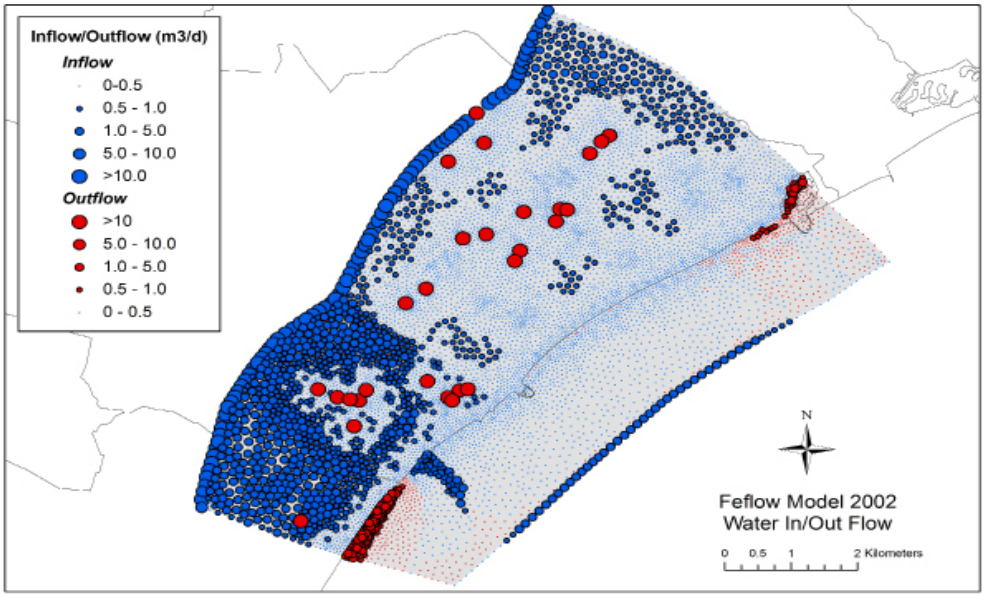

Figure 12. *Calculated inflow/outflow for the model in 2002. Red indicates water leaving the model area, where as blue indicates the nodes where water is entering the model. The largest red circles show the location of the active abstraction wells, where as the smaller red circles show where there is submarine discharge.*

4.2 Simulation of future seawater intrusion

Simulation of seawater in the study area was first conducted using 2009 abstraction rates (no change from the status quo) 20 years forward to 2030. The simulation shows a continued weakening of the seawater intrusion in the southern portion of the study area. In the middle section, a seawater intrusion wedge is infiltrating all the way in to wells 18 and 19, though remaining quite weak and diffuse (Fig. 13). The inflow/outflow analysis from the model shows that, during this time, there is no longer seawater intrusion occurring through the sand and gravel, with a large amount of submarine freshwater discharge occurring along the coast in the southern and northern thirds of the study area (Fig. 13). Seawater inflow into the model, both through the clayey till and at the lower boundary is negligible.

An alternative scenario of increased abstraction in the wells in the northern 2/3 of the study area was run. In this scenario, all operating wells (as of 2009) numbered between 1 and 27 abstraction was increased to 150m^3/d. The wells that produced more than this amount, and the wells numbered between 28-48 were left the same. The results from this simulation were virtually the same as the simulation of the status quo, with only a slight strengthening of the seawater intrusion wedge around well 18 observed (Fig. 14). The wedge in the south continued to weaken under this scenario.

A second scenario, increasing the abstraction in the south was also conducted. This case, abstraction rates for wells 34-40 were increased to a rate of 150m^3/d, where as all other wells retained the 2009 levels. The results of this simulation were identical to the simulation of the status quo to 2030 (Fig. 13 and Fig. 14). The increased abstraction in these wells did not reinitiate seawater intrusion through the sands and gravels in the south, nor did it result in any increase in salinities in the wells.

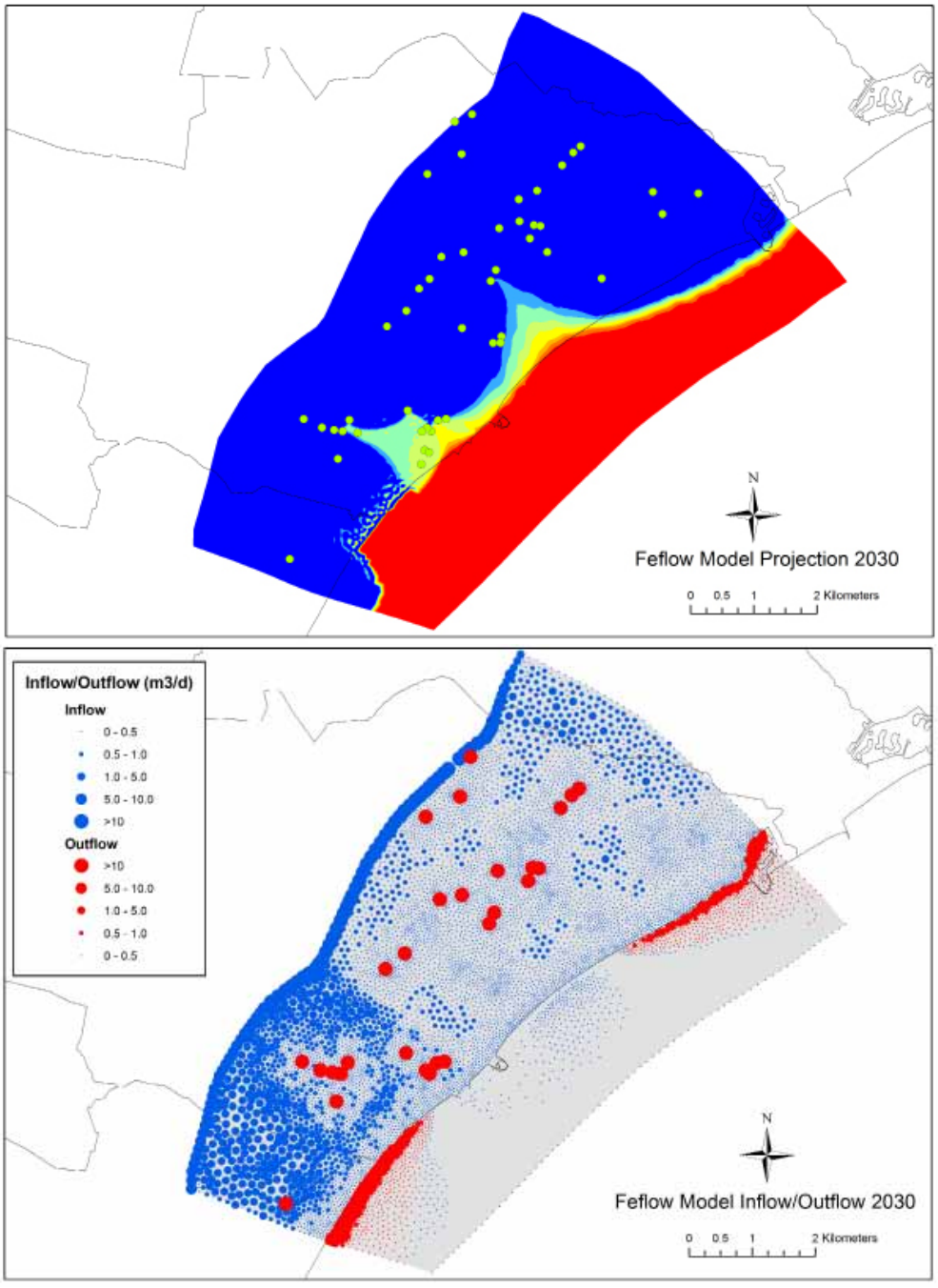

Figure 13. *Feflow model projection for Greve, under current (2009) groundwater abstraction rates. The lower map shows the model inflow and outflow, where the red is water exiting the model and blue is where it is entering.*

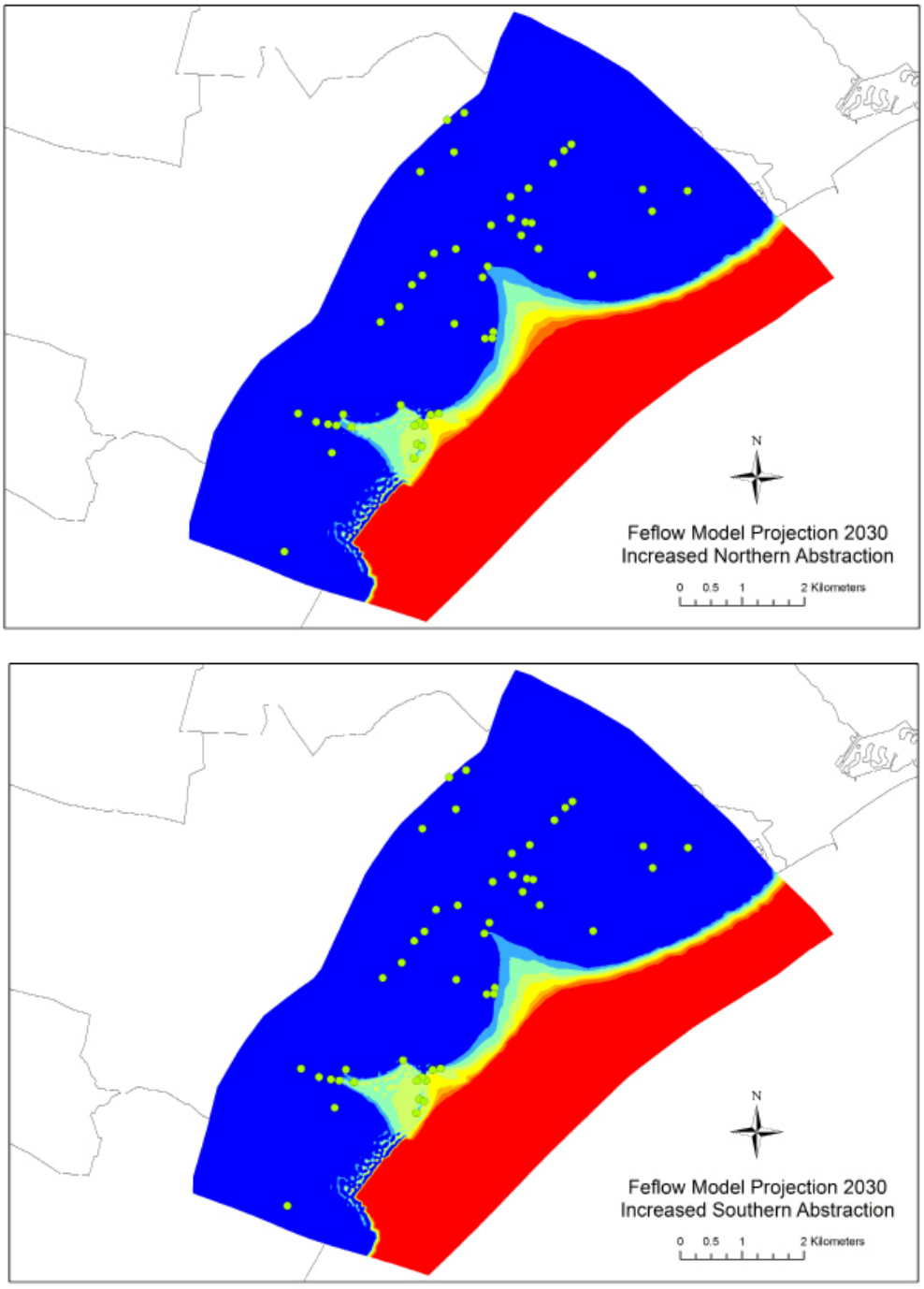

Figure 14. *Seawater intrusion projections with increase abstraction in the north (upper diagram) and increased abstraction in the south (lower diagram). The lower map shows the model inflow and outflow, where the red is water exiting the model and blue is where it is entering.*

5. DISCUSSION

The primary purpose of the study was to develop a model for seawater intrusion in Greve using accurate and realistic geologic, hydrologic and abstraction data. The model is then compared with the observed water quality data to evaluate its effectiveness. Groundwater data from the abstraction wells, as discussed in Chapter 7, has shown that there is a chemical signal of seawater intrusion in the southern part of the coastal zone in Greve municipality. On the other hand, the middle and northern coastal zone, has no chemical signal for seawater intrusion in the samples; the increased salinity measured in these areas comes from diffusion into the aquifer from connate pore waters from the Maastrictian chalk, as described by Bonnesen, et al. (2010). The difference in the source of the salinity has a direct impact on the management of the coastal groundwaters, where if the salinity is coming from diffusion from the pore waters, the salinity measured in the wells is restricted by diffusion rates from the chalk, and will not increase with higher levels of groundwater abstraction. However, increased rates of groundwater abstraction can induce seawater intrusion, which is a much greater threat to the water quality in the aquifer, as here salinities can reach as high as the levels measured in the Baltic Sea. A successful seawater intrusion model can be then applied to evaluate the threat of seawater intrusion in the future.

A comparison of the water quality data collected from the wells with the model results, shows that the model was fairly successful in the simulation of the past seawater intrusion. Model simulation showed that no wells in the northern or middle part of the study area had seawater intrusion, which was confirmed by the groundwater chemistry data from the wells. The model simulation showed seawater intrusion into a number of wells in the southern part, in which the timing and concentrations were fairly close to that of most of the wells. The model did have some problems with simulating the details of the seawater intrusion, particularly with respect to an overestimation of the salinity in wells 29-33, as well as intrusion reaching well 28, when none was observed. However, over-all the model was relatively reliable with respect to the observed data.

As good as the model results were, caution need to be used when interpreting the results. The model was calibrated with regard to hydraulic heads measured from the primary aquifer. Even though the calibration was relatively good, with modeled heads within 0.7m of the measured, in order to calibrate the model, the

transmissivities around four wells needed to be significantly tweeked in order to produce computed heads close to the measured heads. This can be in part justified by looking at the specific capacity of the wells that were adjusted. The specific capacities of the wells that were adjusted to a very low transmissivity (wells 35 and 36) were the lowest in the entire study area, and indicated tight formation around those wells (Fig. 7 and 8). On the other hand, the specific capacities of wells 16 and 17, which were adjusted to be higher, were seen to be very high compared to the other wells in the study area (Fig. 7 and 8). Experiences from the water works also confirm that both the hydraulic conductivity and thickness of the fractured aquifer is variable (Jakobsen 2009). The tweeking of the aquifer transmissivities, though justified, is still an artificial adjustment, and the transmissivities are still only a best-guess estimation of a complex system. This is likely part of the explanation as to why, in the validation of the model, the model tended to under-estimate the drawdown.

The model showed that the saltwater intrusion in Greve Municipality is sensitive to the geology of the area. The model showed that the thicker clayey tills provided the protection from seawater intrusion in the areas where the thickness was greater than 13m. On the other hand, in the southern part of the municipality, seawater intrusion was seen to move through the outwash sands and gravels. In other studies, seawater intrusion is seen to be sensitive to heterogeneity in hydraulic conductivities, providing preferencial flow paths (such as paleochannels) for the seawater to move through (Mulligan et al. 2007, Carrera et al. 2010). This just emphasizes the importance of a good conceptual geological model when modeling seawater intrusion. In Greve, the relatively high density of wells, allowed for a fairly accurate mapping of the geology. However, with a less dense system of wells, the outwash sands and gravel lens in the south could have been missed, leading to an incorrect modeling of the seawater intrusion.

The model for Greve did show some weaknesses in its predictability. This is specifically with reference to well 28, which does not have the salinities which the simulation showed the well should have and to well 40, which did not simulate the salinity increase between 1995 and 2000 which were observed in the groundwater data. This illustrates that the seawater intrusion wedge is further south than it was simulated. This is likely due to smaller scale variations in the hydraulic conductivity in the area – specifically differences in the fracture flow. In higher, Danian limestone units near Copenhagen, water-bearing vertical fractures are seen

to have a distinct preferred orientation at 30°NW (Jakobsen et al. 1999), which could provide preferential groundwater movement, affecting the location of the seawater intrusion. However, the aquifer in Greve lies below the Quaternary sediments, and with a lack of outcrops in the area to measure the fracture orientation and, it was not possible analyze fracture orientation, which could subsequently be incorporated into the model.

The model simulations also resulted in an over-estimation of the salinities in the near-coastal wells 29-33, particularly in wells 31 and 32. This is most likely a function of local variations in the depth of the penetration of the fractures in the chalk aquifer. It has been pointed out in other studies that aquifer bathymetry (the elevation of the aquifer) will influence the location of seawater intrusion and the transition zone (Abarca et al. 2007a, Carrera et al. 2010). In the case in Greve, the water bearing layers in the fractured chalk are observed to vary well to well, from only the top meter to as much as 15-25m conducting water to the well (Jakobsen 2009, Klitten et al. 2006) and observed to vary over distances of less than 200m (Jakobsen 2009). Local variations in the depth of the open vertical fracture penetration will have a direct influence on thickness of the aquifer, and thus the effective bottom of the aquifer. The model used an aquifer thickness of 10m in order to simulate the transition zone. The salinities simulated in the model are averages of the salinity in the total column, accounting for density flow and the transition zone. This corresponds to the salinities which would be pumped out of a fully penetrating well, which is the case in the abstraction wells in Greve. However, if the water-bearing strata are restricted to the top meter or two, then the groundwater from the well would only come from the higher strata with the lower salinities, with the higher salinities flowing around the well in the deeper fractures. The model assumes a depth of water-bearing fractures to be 10m; if the depth is actually less, the model will over-estimate the salinity in the well.

The depth of the fractures could also conceptually explain the salinity observation in well 31, which did not register any increase in chloride until 1993, where all of the wells around it (wells 29, 30, and 32) already from their start in 1982 (Fig. 11). If the screen from well 31 only intercepts the water-bearing fractures in the top meter, then it could create a situation where the saline seawater simply flowed around the well in the deeper fractures, until the point where the saline wedge moved far enough inland so that the salinity began to increase. Unfortunately there is no data on the depth of the water bearing strata within any of these wells

to confirm or refute whether or not this is the case. This also illustrates the impossibility for incorporating this detailed data into the model.

The role of the well-construction also cannot be ignored with regard to the specific water concentrations. Carrera et al. (2010) pointed out that well construction will also affect actual measured salinities. Thus, if there are leaks in the well casing from higher, pure freshwater aquifers, this will dilute the sample, and thus the well will not be representative of the actual salinities in the aquifer being modelled. In this case, it is possible that leaks from a higher aquifer in the Quaternary sediments (i.e. fractured tills or an outwash sand and gravel lens) or even through the disturbed sediments around the well casing, could also be a conduit for freshwater to enter the well, and thus diluting the measured salinity. The model simulation, not accounting for this, will then overestimate the salinity in the wells.

Incorporating the local anisotropies in the aquifer in detail for a model of this scale, covering 50km^2, is virtually impossible. This would require very detailed studies on the aquifer properties in all of the pumping and monitoring wells in the area. This would be very time consuming and expensive. In addition, information would also be required in the areas between the wells, which is virtually impossible to collect. Therefore, model simulations showing the specific detail (i.e. specific salinity concentrations in the individual wells) is not possible. What the model can do, however, is provide a general indication as to where seawater intrusion is a threat, and a time frame in which seawater could be expected under certain abstraction conditions. Regular monitoring will still be required in order to confirm or refute the model predictions, and allow for adjustments in the model itself.

This model was successful in showing how seawater intrusion has occurred and changed over time with actual groundwater abstraction. Results generally confirmed the groundwater data collected from the wells, showing seawater intrusion in the southern part until about 1992, where after the seawater wedge began to weaken, and that there was no seawater reaching the wells in the northern and middle portion of the study area. Future predictions from the model could therefore be used by water managers to see how the seawater intrusion will change. The model shows that even moderate increase in groundwater abstraction in the active wells in either the north or south, and even the staus quo, will not result in a re-initiation of the seawater intrusion in the south or the north. However, a final word of caution with regard to the model set-up needs to be accounted for. The

upper boundary of the model was set at a constant head of 8m. This, of course is an arbitrary boundary, which is subject to changes in recharge and abstraction both within and outside of the model boundaries. The groundwater potential maps made by the municipality at various times between 1955 and 2007 show only minor variation of up to 3m from this boundary at different times. These maps, of course are themselves an interpretation of head measurements, but they indicate that the 8m boundary head has been relatively consistent. However, should significant groundwater abstraction begin upland of the model boundary, then the conditions will change, with less water reaching the model area. Therefore, when predicting seawater intrusion into the future, abstraction both within and outside of the model boundaries must be considered.

6. SUMMARY/CONCLUSION

The numerical groundwater model FEFLOW was used to simulate seawater intrusion in Greve Denmark from 1965 to the present, and 20 years into the future under different groundwater abstraction scenarios. Due to the simple geological situation and advantages in computational time and high model discretion, a 2D model was used for the simulations. A good calibration for the model heads was achieved through varying the transmissivity of the aquifer across the area. Comparing the model simulations with actual groundwater data, the model is seen to accurately predict the seawater intrusion. The model showed that seawater intrusion occurred in the southern part of the municipality, using the outwash sands and gravels as a preferential path-way through to the fractured chalk aquifer. In the northern and middle part of the municipality, the simulation confirmed that the thick layer of clayey tills provided a protective layer, preventing seawater from intruding into the aquifer in significant quantities, with no seawater reaching the wells in this part of the municipality. This was confirmed in the water quality data collected from these wells. The model was able to simulate the timing of the seawater intrusion in the south, however, tended to overestimate the salt concentrations in the wells. This is likely a function of the anisotropy in the fractured chalk aquifer, with local variations in the fracture depth and frequency, which will affect the seawater movement through the aquifer and into the wells. The model showed that it was successful in simulating the general trend in seawater intrusion. However, continued monitoring of the groundwater salinity is required.

Overall Conclusions and Final Remarks

The ability to continuously monitor groundwater salinity can be a very important tool in the management of coastal aquifers. Reliable, continuous data can be incorporated to refine groundwater models and obtain a better understanding of the saltwater/freshwater interaction at an individual well-filed or site. Continuous monitoring can also provide well field managers with an early warning system, sounding the alarm in the event of increasing salinity, allowing a response before the water quality in the aquifer is completely compromised. A monitoring system could also be used in conjunction with systems such as aquifer storage and recovery and seawater intrusion barriers in order to assure their maintenance and even make the systems run more efficiently and economically. There is currently well established technology for sensors which could be used for continuous monitoring. However, they have several draw-backs which have prevented their use, particularly cost, but also size and a lack of information on their durability, life-span and signal noise and drift for continual, in-situ use. The technology of using ionophores which can be electrochemically polymerised directly on to a gold electrode in order to produce an ion specific sensor showed promise to fill this gap. Utilizing this technology, small solid-state sensors for sodium and calcium are able to be produced at a fraction of the cost of the commercially available sensors. When these sensors are combined with the chloride sensors made from a small oxidized silver rod, one can assemble a small, flexible, inexpensive, solid-state sensor array, which could be used for the continuous monitoring of groundwater salinity. However, since this is a new technology, these sensors have not been applied for such a purpose, and therefore there is no information on the sensors life-span, signal reliability, noise, or drift. Therefore it is the purpose of this study to work on the development of these sensors, and test them for continuous monitoring and make an assessment as to whether or not the sensors can be used for this purpose and ultimately integrated into a real-time well field management system.

The chloride sensor showed very good promise for continuous monitoring. The sensor proved to be very robust, where as long as fouling of the sensing surface was not an issue, was seen to last several months, if not longer. Drift was observed in the signal during the testing, seen to be as high as 2.3mV/day, but most often around 0.6mV/day. The drift was also seen to be regular, which makes it much easier to correct for. When the chloride sensor was adjusted for drift, the error was always seen to be less than 10%, and often even under 5%, which was observed in the Wickford monitoring well tests. The Wickford monitoring test also illustrated the value of the chloride sensor, where the sensor still responded to actual changes in chloride at concentrations below 100mg/l, where as the conductivity probe did not register changes at such a low concentration. Fouling of the sensor surface was seen to affect the chloride sensors ability to maintain an accurate response, specifically with respect to the Greve monitoring well test, and any deployment of the sensor, the possibility of fouling should be reduced as much as possible. However, given the simplicity of the technology and the extremely low costs involved, the chloride sensors have shown very good possibilities to be employed in a continuous monitoring system. The only draw-back from this is that periodic (every 14-28 days, depending on the situation) sampling of the water is needed in order to re-calibrate the sensors with regard to drift.

The new technology used to produce the solid-state sensors for sodium showed good promise. This includes both the cases when the ionophore was directly (and successfully) polymerized on to the gold electrode, and when the ionophore was incorporated into a plasticized PVC film on the gold electrode. In both of these cases, the sensors had a good response to changing sodium concentrations during the calibration initially after the construction of the sensors. Laboratory tests showed that they had a similar drift to that of chloride, and had relatively stable signals for the long term tests. However, these sensors showed difficulties in application for continuous in-situ measurements. In the applications in the field, the sensors were not stable, with irregular drift as well as noise, and were susceptible to fouling. The accuracy of the sensors was much less when compared to that of the chloride sensors, with errors of over 50%. In addition, it was seen that the life span of the sensors was less than 3-4 days. Although the initial results showed promise for the technology, more work needs to be done in order to try to extend the life-span of the sensors and improve upon the drift and stability when applied in the field.

The calcium sensors proved difficult to produce. The calcium ionophore, when it was incorporated into a plasticized PVC film on the gold electrode, showed a response to the changes in calcium concentration. Testing on sensors developed with this technology was limited to only two sensors, and more thorough testing needs to be done. The results, however, do show that the ionophore is able to successfully bind to calcium. In contrast, the when the ionophore is synthesized with a thiophene group attached so that it can be polymerized directly on to the gold electrode surface, there was no response to calcium. Both IR and NMR results show that there was successful synthesis of the ionophore as well as polymerization on to the gold electrode. However, the ionophore would simply not work when polymerized directly on to the gold electrode. Therefore it is apparent that much more work needs to be done in order to develop a stable and functional calcium sensor.

The coastal area of Greve, with elevated groundwater salinities observed in several wells, was chosen to be a test study area for the application of the sensors in an actual case of seawater intrusion. Therefore, a geochemical analysis of the groundwater salinity for Greve was conducted along with the development of a groundwater model on the seawater intrusion. Through the geochemical analysis, it was shown that the elevated salinity for the northern two thirds of the near-coast aquifer was from diffusion from formational pore waters and not the result of seawater intrusion, as was thought by the municipal authorities. The data from the southern third, however, showed that the elevated salinities were indeed from seawater intrusion, with seawater likely infiltrating down to the primary aquifer through a large outwash sand and gravel lens. This lens occurred only in the southern part of the municipality, where as in the central and northern part, the aquifer was isolated from the sea by a thick layer of impervious outwash sands and gravels. The groundwater model for the area, conducted using the FEFLOW code, also showed only seawater intrusion occurring in the southern third of the municipality. However, the model also showed that where seawater intrusion had occurred, the reduction in abstraction since 1992 had reversed the trend, where salinity concentrations in the aquifer no longer increasing. This result is confirmed by the groundwater wells, where salinities have maintained a stable level since 2000. Since the salinities have been stable over the last 10-years, incorporating the sensor data into a proactive well-field management system for the time-frame of one year was not possible. However, the data and model did illustrate that using the sensors for monitoring around the production wells could provide an

early-warning system for re-activation of seawater intrusion, should abstraction and/or recharge conditions change. This could include a conscious decision by the groundwater managers to again increase groundwater abstraction in this area.

This project provided a good start on the development and analysis of sensors for the monitoring of groundwater salinity and application for well-field optimization (and protection). In order to truly test the sensor's ability and application in a well-field optimization model, the sensors need to be tested in a situation where there are active changes in groundwater salinities with respect to abstraction, recharge and/or flooding. Since the sensors require periodic re-calibration, they will be most effective and useful in situations where the groundwater salinity is rapidly changing. This can include studies or management of coastal karst aquifers, where there can be salinity changes in a mater of hours with respect to a heavy precipitation event. It could also include studies of the seawater/freshwater relation and the effects of tides, storm surges, or flooding events on it. In such situations where groundwater salinity is seen to rapidly change, the application of the sensors can provide very useful information to help us understand the freshwater/salt water interaction and help to manage these freshwater resources.

References

Abarca E, Vazquez-Sune E, Carrera J (2006) Optimal design of measures to correct seawater intrusion. Water Resour Res 42

Abarca E, Carrera J, Sanchez-Vila X (2007a) Quasi-horizontal circulation cells in 3D seawater intrusion. J Hydrol (Amst) 339:118-129

Abarca E, Carrera J, Sanchez-Vila X (2007b) Anisotropic dispersive Henry problem. Adv Water Resour 30:913-926

Alberti L (2006) Hydrogeologic parameters and human activities influence on sea water intrusion at a refinery site. International FEFLOW User Conference,:207-216

Anderskouv K, Damholt T, Surlyk F (2007) Late Maastrichtian chalk mounds, Stevns Klint, Denmark - Combined physical and biogenic structures. Sediment Geol 200:57-72

Appelo CAJ, Postma D (2005) Geochemistry, Groundwater and Polution, 2nd Edition. A.A. Balkema, Leiden, The Netherlands

Barazzuoli P, Nocchi M, Rigati R (2008) A conceptual and numerical model for groundwater management: a case study on a coastal aquifer in southern Tuscany, Italy. Hydrogeology Journal 16:1557-1576

Barlow PM (2003) Ground water in freshwater-saltwater environments of the Atlantic coast. United States Geological Survey Circular 1262:1-113

Bidstrup T, Klitten K (2006) Kortlægning af Danienkalk-Skrivekridt grænsen samt forkastninger i denne - Delrapport 1 (in Danish) 2006/16:1-13

Bonnesen EP, Larsen F, Sonnenborg TO (2009) Deep saltwater in Chalk of North-West Europe: origin, interface characteristics and development over geological time. Hydrogeol J 17:1643-1663

Brown H, Pemberton J, Owen J (1976) Calcium-sensitive microelectrode suitable for intracullular measurement of calcium(II) activity. Anal Chim Acta 85:261-276

Buck RP, Lindner E (1994) Recommendations for nomenclature of ion-selective electrodes. Pure and Applied Chemistry 66:2527-2536

Bühlmann P, Pretsch E, Bakker E (1998) Carrier-based ion-selective electrodes and bulk optodes: Ionophores for potentiometric and optical sensors. Chemical Review 98:1593-1687

Carrera J, Hidalgo JJ, Slooten LJ (2010) Computational and conceptual issues in the calibration of seawater intrusion models. Hydrogeology Journal 18:131-145

Cammann K, Schroeder A (1979) Working with Ion-Selective Electrodes. Springer Verlag, New York, USA

Chaniotakis N, Sofikiti N (2008) Novel semiconductor materials for the development of chemical sensors and biosensors: a review. Analytica chimica acta 615:1-9

Clausen OR, Huuse M (2002) Mid-Paleocene palaeogeography of the Danish area. Bulletin of the Geological Society of Denmark 49:171-186

Clemmensen A, Thomsen E (2005) Palaeoenvironmental changes across the Danian-Selandian boundary in the North Sea Basin. Palaeogeogr , Palaeoclimatol , Palaeoecol 219:351-394

Dale L (2004) Electricity Price and Southern California's Water Supply Options. Resources, Conservation, and Recycling 42:337 p

Dawoud MA (2005) The role of desalination in augmentation of water supply in GCC countries. Desalination 186:187-198

Diersch H-G (2006) FEFLOW 5.3 User's Manual. WASY GmbH, Institute for Water Resources Planning and Systems Research, Berlin, Germany

Diersch H-G (2005) Variable-density flow and transport in porous media: approaches and challenges. FEFLOW White Papers Vol. I. WASY GmbH, Institute for Water Resources Planning and Systems Research, Berlin, Germany

Diersch H-G, Kolditz O (2002) Variable-density flow and transport in porous media: approaches and challenges. Adv Water Resour 25:899-944

DOE (1994) Handbook of methods for the analysis of the various parameters of the carbon dioxide system in sea water; version 2.13; Chapter 5: Physical and thermodynamic data ORNL/CDIAC-74:10-12

Drabbe J, Badon-Ghyben W (1888-1889) Nota i verband met de voorgenomen putboring nabij Amsterdam. Tijdschrift van het Koninklijk Instituut van Ingenieurs:8-22

Dreizin Y (2006) Ashkelon seawater desalination project ; off-taker's self costs, supplied water costs, total costs and benefits. Desalination 190:104-116

Esbensen K, Kirsanov D, Legin A (2004) Fermentation monitoring using multisensor systems: feasibility study of the electronic tongue. Anal Bioanal Chem 378:391-395

Edwards BD, Evans K (2005) Saltwater intrusion in Los Angeles area coastal aquifers - the marine connection. United States Geological Survey Fact Sheet 030-02:1-2

Feeney R, Kounaves SP (2002) Voltammetric measurement of arsenic in natural waters. Talanta 58:23-31

Frykman P (2001) Spatial variability in petrophysical properties in Upper Maastrichtian chalk outcrops at Stevns Klint, Denmark. Mar Pet Geol 18:1041-1062

GEUS (2009) Jupiter Well Log Database. In: . Geological Survey of Denmark and Greenland. http://www.geus.dk/jupiter/data-dk.htm 2009

Goff T, Braven J, Ebdon L (2003) Automatic continuous river monitoring of nitrate using a novel ion-selective electrode. J Environ Monit 5:353-358

Gokel GW, Leevy WM, Weber ME (2004) Crown ethers: sensors for ions and molecular scaffolds for materials and biological models. Chemical reviews 104:2723-2750

Gravesen P (1983) Maastrichtien/Danien - grænsen i Karlstrup Kalkgrav (Østsjælland)(in Danish). Dansk Geologisk Forening, Årskrift for 1982:47-58

Groves W, Grey A, O'Shaughnessy P (2006) Surface acoustic wave (SAW) microsensor array for measuring VOCs in drinking water. J Environ Monit 8:932-941

Guo J, Amemiya S (2006) Voltammetric heparin-selective electrode based on thin liquid membrane with conducting polymer-modified solid support. Analytical chemistry 78:6893-6902

Han M (1996) Realationship between the seawater intrusion and landforms in Laizhou Bay Area. Oceanol Limnol Sin /Haiyang Yu Huzhao 27:414-420

Hancock JM, Kauffman EG (1979) The great transgressions of the Late Cretaceous. J Geol Soc 136:175-186

Hancock JM (1976) Petrology of the chalk. Proceeding of the Geologists' Association 86:499-535

Hansen K (1941) Tektoniske retningslinier paa Sjælland (in Danish). Meddelser fra Dansk Geologisk Forening 10:9-16

Harris DC (1996) Quantitative Chemical Analysis, 4. Edition. W.H. Freeman, New York

Herzberg B (1901) Die Wasserversorgung einiger Nordseebader. Journal Gasbeleuchtung und Wasserversorgung 44:819

Hiscock K (2005) Hydrogeology Principles and Practice. Blackwell Publishing, Oxford, United Kingdom

Hobby P, Moody G, Thomas J (1983) Calcium ion-selective electrode studies: Covalent bonding of organic phosphates and phosphonates to polymer matrices. Analyst 108:581-590

Houmark-Nielsen M (1987) Pleistocene stratigraphy and glacial history of the central part of Denmark. Bulletin of the Geological Society of Denmark 36:1-189

Hovedstadsrådet/Roskilde Amt (1989) Vandressourceundersøgelse i Køge Bugt: Kommunerne, Fase 1 Status Billede (in Danish):1-90

Huuse M (2002) Late Cenozoic paleogeography of the eastern North Sea Basin: climate vs. tectonic forcing of basin margin uplift and deltaic progradation. Bulletin of the Geological Society of Denmark 49:145-169

Huuse M, Lykke-Andersen H, Michelsen O (2001) Cenozoic evolution of the eastern Danish North Sea. Mar Geol 177:243-269

Jakobsen J (2009) Personal communication, Director, Greve Water Works

Jakobsen PR, Klitten K, Jakobsen PR (1999) Fracture systems and groundwater flow in the Kobenhavn Limestone Formation. Nordic Hydrol 30:301-316

Japsen P, Green PF, Nielsen LH (2007) Mesozoic-Cenozoic exhumation events in the eastern North Sea Basin: a multi-disciplinary study based on palaeothermal, palaeoburial, stratigraphic and seismic data. Basin Res 19:451-490

Japsen P (1993) Influence of lithology and neogene uplift on seismic velocities in Denmark: Implications for depth conversion of maps. Am Assoc Pet Geol Bull 77:194-211

Jensen S, Wernberg T, Krom T (2002) Groundwater Model for Roskilde Amt (in Danish). Model developed by Water Tech A/S for Roskilde Amt:1-208

Johnson KE, Marks LY (1959) Ground-water map, Wickford quadrangle, Rhode Island 1:24,000

Kafri U, Goldman M, Lyakhovsky V (2007) The configuration of the fresh-saline groundwater interface within the regional Judea Group carbonate aquifer in northern Israel between the Mediterranean and the Dead Sea base levels as delineated by deep geoelectromagnetic soundings. J Hydrol (Amst) 344:123-134

Katsifarakis K, Petala Z (2006) Combining genetic algorithms and boundary elements to optimize coastal aquifers' management. Journal of Hydrology 327:200-207

Khalil S, Moody G, Thomas J (1985) Studies of calcium ion-selective electrodes in the presence of biochemical materials. Analyst 110:353-358

Klitten K, Larsen F, Sonnenborg T (2006) Saltvandsgrænsen i kalkmagasinerne i Nordøstsjælland, hovedrapport (in Danish) 2006/15:1-44

Keil L, Moody G, Thomas J (1978) Evaluation of PVC matrix membrane calcium-selective electrodes based on nitrated (octylphenyl) phosphate sensors and phosphonate mediators. Anal Chim Acta 96:171-175

Kim Y, Amemiya S (2008) Stripping Analysis of Nanomolar Perchlorate in Drinking Water with a Voltammetric Ion-Selective Electrode Based on Thin-Layer Liquid Membrane. Anal Chem (Wash) 80:6056-6065

Kristiansen SM, Christensen FD, Hansen B (2010) Evaluation of Danish groundwater aquifers sensitivity to road salt (in Danish). GEUS Special Report

Kumar KG, Poduval R, John S (2007) A PVC plasticized membrane sensor for nickel ions. Microchim Acta 156:283-287

Kume T, Umetsu C, Palanisami K (2009) Impact of the December 2004 tsunami on soil, groundwater and vegetation in the Nagapattinam District, India. Journal of environmental management 90:3147-3154

Langevin C (2003) Simulation of Submarine Ground Water Discharge to a Marine Estuary: Biscayne Bay, Florida. Ground Water 41:758-771

Larsen F, Sonnenborg T, Madsen P (2006) Saltvandsgrænsen i kalkmagasinerne i Nordøstsjælland, delrapport 6 (in Danish) 2006/21:1-103

Larsen O (1998) Mapping of the Maastrictian-Danian boundary in the coastal area of Køge Bugt by gamma- and resistivity logging. Bulletin of the Geological Society of Denmark 44:101-113

Levine IN (1995) Physical Chemistry, 4th Edition. McGraw-Hill, Inc., New York

Lydersen H (2009) Personal communication, Head Technician, Greve Waterworks

Lykke-Andersen H., Surlyk F. (2004) The Cretaceous-Palaeogene boundary at Stevns Klint, Denmark: inversion tectonics or sea-floor topography?. J Geol Soc 161:343-352

Manahan SE (2001) Fundamentals of Environmental Chemistry, Second Edition. Lewis Publishers, New York

Mantoglou A, Papantoniou M (2008) Optimal design of pumping networks in coastal aquifers using sharp interface models. J Hydrol (Amst) 361:52-63

Mantoglou A, Papantoniou M, Giannoulopoulos P (2004) Management of coastal aquifers based on nonlinear optimization and evolutionary algorithms. J Hydrol (Amst) 297:209-228

Mantoglou A (2003) Pumping management of coastal aquifers using analytical models of saltwater intrusion. Water Resour Res 39

McKay L, Lenczewski M, Fredericia J (1999) Spatial variability of contaminant transport in a fractured till, Avedore Denmark. Nordic Hydrol 30:333-360

Meier HEM, Kjellstroem E, Graham LP (2006) Estimating uncertainties of projected Baltic Sea salinity in the late 21st century. Geophys Res Lett 33

Michael HA, Mulligan AE, Harvey CF (2005) Seasonal oscillations in water exchange between aquifers and the coastal ocean. Nature 436:1145-1148

Morris L, Caruana DJ, Williams DE (2002) Simple system for part-per-billion-level volatile organic compound analysis in groundwater and urban air. Measurement Scientific Technology 13:603-612

Mortensen A, Jensen K, Nilsson B & Juhler R (2004) Multiple tracing experiments in unsaturated fractured clayey till. Vadose Zone Journal 3:634-644.

Mulligan AE, Evans RL, Lizarralde D (2007) The role of paleochannels in groundwater/seawater exchange. J Hydrol (Amst) 335:313-329

Nielsen SB, Thomsen E, Hansen DL (2005) Plate-wide stress relaxation explains European Palaeocene basin inversions. Nature 435:195-198

Nilsson B, Sidle RC, Klint KE (2001) Mass transport and scale-dependent hydraulic tests in a heterogeneous glacial till-sandy aquifer system. J Hydrol (Amst) 243:162-179

Noh J, Coetzee P (2007) Evaluation of the potentiometric determination of trace fluoride in natural and drinking water with a fluoride ISE. Water S A 33:519-529

Ødum H (1935) Træk af den prækvartære undergrunds geologi paa Sjælland m.v. (in Danish). Meddelser fra Dansk Geologisk Forening 8:516-524

Okeke B, Ma G, Cheng Q (2007) Development of a perchlorate reductase-based biosensor for real time analysis of perchlorate in water. J Microbiol Methods 68:69-75 Mortensen AP, Jensen KH, Nilsson B et al (2004) Multiple Tracing Experiments in Unsaturated Fractured Clayey Till. Vadose Zone J 3:634-644

Omstedt A, Axell LB (1998) Modelling the seasonal, interannual, and long-term variations of salinity and temperature in the Baltic proper. Tellus A 50:637-652

Park C, Aral M (2004) Multi-objective optimization of pumping rates and well placement in coastal aquifers. J Hydrol (Amst) 290:80-99

Parra EJ, Crespo GA, Riu J (2009) Ion-selective electrodes using multi-walled carbon nanotubes as ion-to-electron transducers for the detection of perchlorate. The Analyst 134:1905-1910

Parra V, Arrieta AA, Fernandez-Escudero J (2006) Electronic tongue based on chemically modified electrodes and voltammetry for the detection of adulterations in wines. Sensors and Actuators B 118:448-453

Patra GK, Goldberg I (2003) Synthesis and crystal structures of copper and silver complexes with new imine ligands - air-stable, photoluminescent Cu(I)N4 chromophores. European Journal of Inorganic Chemistry:969-977

Pawlak E, Palys B, Biesiada K (2008) Covalent binding of sensor phases - a recipe for stable potentials of solid-state ion-selective sensors. Anal Chim Acta 625:137-144

Piper AM (1944) A graphic procedure in the geochemical interpretation of water analysis. Trans American Geophysical Union 25:914-923

Post V, Kooi H, Simmons C (2007) Using Hydraulic Head Measurements in Variable-Density Ground Water Flow Analyses. Ground Water 45:664-671

Ruzicka J, Hansen E, Tjell J (1973) Selectrode - the Universal Ion-Selective Electrode. Part Vi. the Calcium (Ii) Selectrode Employing a New Ion Exchanger in a Nonporous Membrane and a Solid-State Reference System. Anal Chim Acta P 155-178:39 REF.

Ranjan S, Kazama S, Sawamoto M (2006) Effects of climate and land use changes on groundwater resources in coastal aquifers. J Environ Manage 80:25-35

Reichard EG, Johnson TA (2005) Assessment of regional management strategies for controlling seawater intrusion. Journal of Water Resources Planning and Management 131:280-291

Rosenkrantz A (1925) Undergrundens tektoniske forhold i København og nærmeste omegn (in Danish). Meddelser fra Dansk Geologisk Forening 6:3-17

Roskilde Amt (1987) Saltvandsproblemer på kildepladser i Køge Bugt område (in Danish):1-160

Roskilde Amt (2004) Indsatsplan for grundvandsbeskyttelse, Greve området (in Danish):1-76

Rudnitskaya A, Ehlert A, Legin A (2001) Multisensor system on the basis of an array of non-specific chemical sensors and artificial neural networks for the determination of inorganic pollutants in a model groundwater. Talanta 55:425-431

Sakaguchi H, Matsumura H, Gong H (2005) Direct Visualization of the Formation of Single-Molecule Conjugated Copolymers. Science (Wash) 310:1002-1006

Sherif MM, Hamza KI (2001) Mitigation of seawater intrusion by pumping brackish water. Transport in Porous Media 43:29-44

Shoemaker WB (2004) Important observations and parameters for a salt water intrusion model. Ground Water 42:829-840

Si P, Chi Q, Li Z (2007) Functional polythiophene nanoparticles: size-controlled electropolymerization and ion selective response. Journal of the American Chemical Society 129:3888-3896

Sotiropoulos P, Tzanis A, Sideris G (2007) Watertool: An automated system for hydrological investigations with application at the area of Kato Souli (NE Attica, Greece). Bulletin of the Geological Society of Greece 40:548-559

Sutter J, Radu A, Peper S (2004) Solid-contact polymeric membrane electrodes with detection limits in the subnanomolar range. Analytica Chimica Acta 523:53-59

Surlyk F, Damholt T, Bjerager M (2006) Stevns Klint, Denmark: Uppermost Maastrichtian chalk, Cretaceous–Tertiary boundary, and lower Danian bryozoan mound complex. Bulletin of the Geological Society of Denmark 54:1-48

Takakusa H, Kikuchi K, Urano Y (2002) Design and synthesis of an enzyme-cleavable sensor molecule for phosphodiesterase activity based on fluorescence resonance energy transfer. Journal of the American Chemical Society 124:1653-1657

Tercier-Waeber M, Buffle J, Confalonieri F (1999) Submersible voltammetric probes for in situ real-time trace element measurements in surface water, groundwater and sediment-water interface. Measurement Scientific Technology 10:1202-1213

Thomsen E (1995) Kalk og kridt i den Danske undergrund (in Danish). In: Nielsen OB (ed) Danmarks Geologi fra Kridt til i Dag. Aarhus University, Aarhus, Denmark, pp 31-67

Thorn P, Conallin C (2007) RHYHABSIM as a stream management toll: Case study in the River Kornerup catchment, Denmark. Journal of Transdisciplinary Environmental Studies 5:1-18

Timms WA, Timms WA, Timms WA (2004) Real-time analysis of small volume samples with micro ion-selective electrodes. Ground Water Monit Remediat 24:67-72

Todd DK, Mays LW (2005) Groundwater Hydrology, Third Edition:636

Tran TK, Oçafrain M, Karpe S (2008) Structural control of the horizontal double fixation of oligothiophenes on gold. Chemistry (Weinheim an der Bergstrasse, Germany) 14:6237-6246

Urish DW (2009) Personal communication, Professor Emeritus, University of Rhode Island

Urish DW, McKenna TE (2004) Tidal Effects on Ground Water Discharge Through a Sandy Marine Beach . Ground Water 42: 971- 982

Vejbæk OV (1997) Dybe strukturer i danske sedimentære bassiner (in Danish). Geologisk Tidsskrift 1997:1-31

Violette S, Boulicot G, Gorelick S (2009) Tsunami-induced groundwater salinization in south-eastern India. C R Geosci 341:339-346

Ward J, Simmons C, Dillon P (2009) Integrated assessment of lateral flow, density effects and dispersion in aquifer storage and recovery. J Hydrol (Amst) 370:83-99

Ward J, Simmons C, Dillon P (2008) Variable-density modelling of multiple-cycle aquifer storage and recovery (ASR): Importance of anisotropy and layered heterogeneity in brackish aquifers. J Hydrol (Amst) 356:93-105

Werner A, Gallagher M (2006) Characterisation of sea-water intrusion in the Pioneer Valley, Australia using hydrochemistry and three-dimensional numerical modelling. Hydrogeology Journal 14:1452-1469

Winkler S, Rieger L, Saracevic E (2004) Application of ion-sensitive sensors in water quality monitoring. IWA Publishing, Alliance House 12 Caxton Street London SW1H 0QS UK

Wu J, Liu J, Fu M (2005) Classification of Chinese yellow wines by chemometric analysis of cyclic voltammogram of copper electrodes. Sensors 5:529-536

Zhou X, Chen M, Liang C (2003) Zhou, X., Chen, M. & Liang, C., Environmental Geology 43:978-985

Ziegler PA (1990) Geological Atlas of Western and Central Europe. Shell International Petroleum Maatschappij B.V., The Netherlands

Zou Z, Jang A, MacKnight E (2008) Environmentally friendly disposable sensors with microfabricated on-chip planar bismuth electrode for in situ heavy metal ions measurement. Sensors Actuators B: Chem 134:18-24